AN ALGORITHM FOR SKIN LESION DIAGNOSIS AND CLASSIFICATION USING DEEP LEARNING WITH IMPROVED ACCURACY

Thesis Submitted for the Award of the Degree of

DOCTOR OF PHILOSOPHY

in

Electronics and Communication Engineering

By

DOMA MURALI KRISHNA

Registration Number: 41800957

Supervised By

Dr. Sanjay Kumar Sahu (23393)

School of EEE (Professor)

Lovely Professional University

Co-Supervised by

Dr.G.R.L.V.N.Srinivasa Raju (402)

ECE (Professor)

Shri Vishnu Engineering College for Women

LOVELY PROFESSIONAL UNIVERSITY, PUNJAB

2025

DECLARATION

I, hereby declared that the presented work in the thesis entitled "**An Algorithm for Skin Lesion Diagnosis and Classification using Deep Learning with improved Accuracy**" in fulfilment of degree of **Doctor of Philosophy (Ph. D.)** is outcome of research work carried out by me under the supervision of Dr.Sanjay Kumar Sahu, working as Professor, in the School of Electronics and Electrical Engineering of Lovely Professional University, Punjab, India and the Co-Supervision of Dr.G.R.L.V.N.Srinivasa Raju, working as Professor in Department of ECE in Shri Vishnu Engineering College for Women(A), Bhimavaram, India. In keeping with general practice of reporting scientific observations, due acknowledgements have been made whenever work described here has been based on findings of other investigator. This work has not been submitted in part or full to any other University or Institute for the award of any degree.

(Signature of Scholar)

Name of the scholar: DOMA MURALI KRISHNA

Registration No.: 41800957

Department/school: School of Electronics and Electrical Engineering

Lovely Professional University,

Punjab, India

CERTIFICATE

This is to certify that the work reported in the Ph. D. thesis entitled "**An Algorithm for Skin Lesion Diagnosis and Classification using Deep Learning with improved Accuracy**" submitted in fulfillment of the requirement for the award of degree of **Doctor of Philosophy (Ph.D.)** in the School of Electronics and Electrical Engineering, is a research work carried out by DOMA MURALI KRISHNA, 41800957, is bonafide record of his original work carried out under my supervision and that no part of thesis has been submitted for any other degree, diploma or equivalent course.

(Signature of Supervisor)	**(Signature of Co-Supervisor)**
Name of Supervisor: Dr.Sanjay Kumar Sahu	Co-Supervisor: Dr.GRLVNSRaju
Designation: Professor	Designation: Professor
Department/school: SEEE	Department : ECE
University: Lovely Professional University	College: SVECW(A)

ABSTRACT

(Keywords: Skin Lesion Segmentation, Deep Learning(DL), Multi-Layer Residual Convolutional Neural Network, ISIC-2019 Dataset, Convolutional Neural Network(CNN), Deep Convolutional Inverse Graphics Network(DCIGN))

Skin cancer is a growing global health issue associated with rising incidence rates and significant mortality risks. Early and precise detection of skin lesions is pivotal for timely intervention and improved patient outcomes. Over the past few years, Deep Learning (DL) has surfaced as a revolutionary innovation within the realm of medical imaging, particularly for advancing the precision of skin cancer detection and categorization systems. This thesis embarks on an in-depth exploration of a groundbreaking approach, showcasing the development and implementation of a state-of-the-art skin cancer recognition and categorization system, emphasizing the pivotal role of DL in achieving unprecedented accuracy. The proposed system harnesses advanced DL algorithms, particularly CNNs, to examine dermoscopic images, enabling automated identification and classification of skin lesions. Its innovation lies in its ability to significantly boost accuracy and reliability, thus diminishing the risk of misdiagnosis and unnecessary medical procedures.

The system's performance is rigorously assessed through techniques such as cross-validation, confusion matrix evaluation and other performance metrics. The results unequivocally illustrate the supremacy of the proposed DL-based skin cancer detection and classification system when compared to conventional methods. Notably, the system's accuracy, sensitivity, and specificity surpass established benchmarks. Furthermore, the practical implications of this innovation are vast. It serves as a critical tool for dermatologists, general practitioners, and patients, enabling early skin cancer detection and facilitating timely medical interventions. Its incorporation into mobile applications and telemedicine platforms extends its utility, enabling individuals to conduct self-examinations and receive prompt feedback.

In conclusion, this thesis underscores the transformative potential of DL in advancing skin cancer detection and classification. The integration of extensive datasets, data augmentation, feature extraction, and classification approaches represents a significant leap in accuracy and dependability. The system signifies a critical stride toward enhanced skin cancer diagnosis, emphasizing the paramount importance of

early detection and its capacity to save lives while reducing the economic burden on healthcare systems. As technology continues to advance, maintaining a pioneering role in the fight against skin cancer remains paramount. This thesis holds the promise of significantly contributing to that mission.

Consequently, this thesis endeavors to present and scrutinize three DL-driven models designed for the detection and classification of skin lesions. These models have been meticulously simulated and analyzed, employing the extensive ISIC-2019 dataset, which boasts 25,331 dermoscopy images across eight distinct categories of skin diseases.

Segmenting skin lesions presents a formidable challenge owing to indistinct boundaries, uneven color distribution, and irregular shapes. Existing DL models have limitations in achieving optimal segmentation performance and reducing artifacts and noises. The first DL model addresses these issues by introducing the Hybrid Gaussian Guided Image Filter (HGGIF) for noise removal and Multilayer Ressidual Network (MLRNet) for segmentation. The suggested approach comprises two primary phases: preprocessing using the HGGIF filter and segmentation using MLRNet. The HGGIF filter effectively removes noises and artifacts, improving color illuminations and making the disease-affected regions of the skin lesion more visible. MLRNet, a residual analysis-based segmentation technique, accurately segments the skin lesion. Later the effectiveness of the suggested MLRNet method is compared with conventional segmentation approaches using the ISIC-2019 and PH2 datasets. MLRNet outperforms on other methods in terms of performance metrics of accuracy, sensitivity, F-score, precision, recall and specificity achieving superior segmentation performance. The proposed first DL based model effectively addresses the challenges of indistinct boundaries, uneven color distribution, and irregular shapes in skin lesions. The demonstration of experimental results of MLRNet surpasses conventional segmentation approaches interms of performance metrics.

Skin lesions pose a challenge in diagnosis due to their diversity in size, position, form, and color. Existing image processing-based feature extractors are limited in their ability to extract detailed features from large datasets. The proposed second DL model based on DTLNet, have shown promise in extracting spectral, texture, color and spatial features from segmented images, enabling accurate classification of skin

lesions. The DTLNet framework composed of several steps, including preprocessing, segmentation, feature extraction and classification. Preprocessing involves enhancing the images and removing noise using the Hybrid Gaussian Weiner Filter (HGWF) algorithm. The segmentation process is executed utilizing the AlexNet algorithm, while feature extraction is carried out using a DL convolutional neural network (DLCNN). The features extracted then classified using a SoftMax classifier for multi-class classification task. The efficacy of the DTLNet is evaluated using both subjective and objective analysis. Regarding the segmentation performance, the suggested AlexNet based model outperforms existing methods. In this, the novel design of the DTLNet, which combines preprocessing, segmentation, feature extraction and classification, contributes to its outstanding performance. The proposed DTLNet demonstrates promising results in the detection of skin lesions. By leveraging DTL techniques, the network achieves accurate segmentation & classification of skin lesions into eight disease categories. The DTLNet Outperforms existing techniques in regards to both segmentation and classification performance, making it an important CAD system for dermatologists in the diagnosis of skin diseases.

The third proposed DL based model is the development of a novel approach for AI-driven skin cancer diagnosis. The aim is to optimize diagnostic accuracy, particularly in early-stage detection, and overcome the challenges associated with imbalanced datasets. The suggested method is geared towards augmenting the potential of AI-powered diagnostic systems, aiming to elevate early detection rates and thereby positively impacting the survival rates of skin cancer patients. The proposed approach involves the use of various models and techniques. The deep convolutional inverse graphics network (DGCIN) model utilizes pixel relativity extraction to identify the cancer-affected area, while the hybrid deep kohonen network (HDKN) model identifies the probabilistic Kohonen characteristics of the segmented image to determine the link between different types of skin cancer. The swarm-based pelican optimization algorithm (SPOA) model is developed for feature selection, and the deep echo network machine (DENM) model is used In the context of multi-class skin cancer categorization. Finally the Hybrid Optimized DL Approach for Skin Cancer Classification Using Pelican-Optimized Deep Kohonen Features and Echo State

Networks (HOS-Net) surpassed state-of-the-art methods in simulated scenarios for the detection, segmentation, and classification of skin lesions. In this context, the effectiveness of the suggested method was assessed by employing performance metrics on an independent test dataset. The segmentation and classification performance of the HOS-Net, the model was juxtaposed with other models utilizing the identical ISIC-2019 dataset. It addresses the limitations of conventional methods in AI-driven skin cancer diagnosis. By optimizing diagnostic accuracy and overcoming challenges associated with imbalanced datasets, the approach aims to improve early diagnosis rates and contribute to the improvement of skin cancer patient's survival rates. The HOS-Net model surpassed state-of-the-art methods in simulations for detection, segmentation of effected region, and classifying caner images. Further, the research and investigations are needed to explore the potential of this approach and its future scope.

ACKNOWLEDGEMENT

The work presented in this thesis entitled **"An Algorithm for Skin Lesion Diagnosis and Classification using Deep Learning with improved Accuracy"** couldn't have happened without my tight relationships with several people who were always there for me when I needed them most. I would want to use this opportunity to thank them and express my thanks for making this Ph.D. thesis possible. I am deeply thankful for the encouragement and support provided during my dissertation by my supervisor **Dr.Sanjay Kumar Sahu** and co-supervisor **Dr.GRLVNSrinivasa Raju** for their patience, inspiration, and vast expertise, as well as for their continuous encouragement of my research. Their unwavering direction, collaboration, and encouragement have always enabled me to succeed. I really thank them for their assistance in every manner.

I take it as highly esteemed privilege in expressing my sincere gratitude to Committee members, for their insightful comments and encouragement that motivated me to do my research from various perspectives during the progress of the thesis. I want to express my heartfelt gratitude to my colleagues **Dr.Kishore Kumar Gundugolau, Dr.Prema Kumar M, Dr.M.V.Ganeswara Rao** and **Dr. M.V.Subba Rao** for their timely support in all the ways. I want to express my gratitude in particular to my mother **Mrs. Siva Parvathi,** my father **Mr. Mastan Rao** and my wife **Mrs Chandra Kala** for believing in me and allowing me the freedom to do as I pleased. Having a family who supports and loves me unconditionally makes me feel like the luckiest person alive.

I would also want to thank **Dr.K.Padma Vasavi, HoD-ECE**, and management of **Shri Vishnu Engineering College for Women**, **Bhimavaram** and **Lovely Professional University**, **Punjab** for their constant support in the utilisation of resources. I am very grateful to Almighty God for giving me the power, health, and knowledge to conduct this research and for seeing it through to completion.

Thank you all very much!!!

DOMA MURALI KRISHNA

CONTENTS

List of Tables i

List of Figures ii

Abbreviations iv

CHAPTER 1: INTRODUCTION

1.1 Introduction 1

1.2 Skin Composition 2

1.3 Skin cancer overview 4

1.3.1 Melanoma 5

1.3.2 Melanocytic Nevus 5

1.3.3 Basal Cell Carcinoma 5

1.3.4 Actinic Keratoses 6

1.3.5 Benign Keratosis 6

1.3.6 Dermatofibromas 7

1.3.7 Vascular Lesions 7

1.3.8 Squamous Cell Carcinoma 8

1.4 Skin cancer problems and necessity or early detection 8

1.5 Skin Imaging Techniques 11

1.6 CAD System for Skin Disease Diagnosis 15

1.7 Convolutional Neural Network Architecture 16

1.7.1 Convolution Layer 18

1.7.2 ReLU 19

1.7.3 Batch Normalization 19

1.7.4 Pooling Layer 19

1.7.5 Dropout Layer 20

1.7.6 Fully Connected Layer 20

1.7.7 Activation Functions 21

1.8 DL Techniques 21

1.9 Performance Metrics used in the Research 23
1.10 Motivation of the Research 24
1.11 Major Contributions of the Research work 25
1.12 Organization of the Thesis 27
1.13 Summary 28

CHAPTER 2 : REVIEW OF LITERATURE

2.1 Skin Lesion Segmentation 29
2.2 Hybrid Gaussian Guided Image Filter 33
2.3 Multi-Layer Residual Convolutional Neural Networks 34
2.4 Deep Transfer Learning Network 35
2.5 Advancements in Skin Lesion Diagnosis 46
2.6 Research Gaps 56
2.7 Problem Statement 57
2.8 Research Objectives 58
2.9 Research Scope and Significance 60
2.10 Summary 61

CHAPTER 3 : SKIN LESION SEGMENTATION USING HYBRID GAUSSIAN GUIDED IMAGE FILTER WITH CNN

3.1 Introduction 63
3.2 Proposed Skin Lesion Segmentation 64
3.2.1 HGGIF Filtering 65
3.2.2 HGGIF Algorithm 67
3.3 Proposed MLRNet for Segmentation of Skin Lesion 69
3.4 Results 79
3.5 Summary 79

CHAPTER 4 : DEEP TRANSFER LEARNING-BASED HYBRID MODEL FOR SKIN LESION DETECTION AND CLASSIFICATION

4.1 Introduction 81

4.2 Proposed DTLNet Algorithm 84

4.2.1 Process of Training 84

4.2.2 Testing Process 85

4.2.3 Proposed DTLNet Framework 86

4.3 Gaussian Filter 90

4.4 Wiener Filter 92

4.5 Hybrid Gaussian-Wiener Kernel Function 93

4.6 Proposed Segmentation Using Alexnet 94

4.6.1 Advantages of Transfer learning models adaption 96

4.6.2 ALEXNET for Skin Lesion Segmentation 97

4.7 Feature Extraction And Classification 98

4.8 Results 101

4.9 Summary 101

CHAPTER 5 : ENHANCED SKIN CANCER CLASSIFICATION THROUGH A HYBRID OPTIMIZED APPROACH

5.1 Introduction 103

5.2 Dataset Augmentation 106

5.3 DCIGN Segmentation 107

5.3.1 Convolutional Autoencoder 108

5.3.2 Inverse Graphics Module 110

5.3.3 The segmentation algorithm of DCIGN 111

5.4 HDKN Feature Extraction 114

5.5 SPOA Feature Selection 118

5.6 DENM Classifier 123

5.7 Results 128

5.8 Summary 128

CHAPTER 6 : RESULTS AND ANALYSIS

6.1	Introduction		130
6.2	Comprehensive overview of the ISIC-2019 Dataset for Skin Lesion Diagnosis and Research		131
	6.2.1	Setting the Stage: Experimental Configuration for the ISIC-2019 Dataset	133
6.3	Comprehensive Experimental Setup		135
6.4	Outcome Analysis: Assessing MLRNet's Performance		146
6.5	Outcome Analysis: Assessing DTLNet's Performance		155
6.6	Outcome Analysis: Assessing HOS-Net's Performance		164
6.7	Performance comparison of all the proposed Models		177
6.8	Estimation of Computational Time		179
6.9	Summary		182

CHAPTER 7 : DISCUSSIONS AND CONCLUSIONS

7.1	Introduction		183
7.2	MLRNet’s Outshines Its Peers In Lesion Diagnosis And Classification		183
	7.2.1	MLRNet’s Superiority in Skin Lesion Diagnosis and Classification	184
	7.2.2	MLRNet's Superiority In Skin Lesion Diagnosis And Classification On The PH2 Dataset	185
73	Comprehensive Analysis of Lesion Diagnosis and Classification		185
	7.3.1	Segmentation Performance Analysis in Lesion Diagnosis and Classification	186
	7.3.2	Assessing Classification Performance in Skin Lesion Diagnosis and Categorization	186
7.4	HOS-NET: Superior Lesion Segmentation		187
	7.4.1	Advancing Dermatology With HOS-Net: Exceptional Skin Lesion Segmentation And Classification	188
7.5	Computational Time Estimation in Skin Lesion Diagnosis		189
7.6	Conclusion		190
7.7	Future Scope of the Research		191
7.8	Summary		192

BIBILOGRAPHY

List of Journal Publications

List of Conference Publications

LIST OF TABLES

Table No.	Table Name	Page Number
3.1	HGGIF algorithm	68
4.1	Proposed HGWF algorithm	86
5.1	Data augmentation with parameters	106
5.2	Optimal parameter tuning of DCIGN	113
5.3	Optimal parameter tuning of SPOA	121
5.4	Optimal parameter tuning of DENM	124
5.5	Skin cancer classification algorithm of DENM	126
5.6	Optimal parameter tuning of DENM	128
6.1	Performance comparison with ISIC challenge participated teams	148
6.2	Performance comparison with conventional segmentation approaches with ISIC-2019 dataset	150
6.3	Performance comparison various segmentation approaches	158
6.4	Classification performance comparison of various SLDC methods	162
6.5	Segmentation performance estimation of various methods	166
6.6	Percentage of improvements of Table 6.5	169
6.7	Classification performance estimation of various methods	174
6.8	Percentage of improvements of Table 4.7	175
6.9	Computational time (seconds) of various segmentation methods	179
6.10	Computational time (seconds) of various classification methods	180

LIST OF FIGURES

Fig. No.	Figure Name	Page Number
1.1	Skin Structure	2
1.2	Different Images of Melanoma	5
1.3	Different Images of Melanocytic Nevus	5
1.4	Different Images of Basal Cell Carcinoma	6
1.5	Different Images of Actinic Keratoses	6
1.6	Different Images of Benign Keratosis	7
1.7	Different Images of Dermatofibromas	7
1.8	Different Images of Vascular Lesions	8
1.9	Different Images of Squamous Cell Carcinoma	8
1.10	Skin Imaging Techniques	12
1.11	Skin Scope	13
1.12	Computer Aided Diagnosis System	15
1.13	Deep Neural Network	16
1.14	Convolutional Neural Network	18
1.15	Convolution Layer	18
1.16	ReLU Layer Output	19
1.17	2*2 Max Pool Layer	20
1.18	Dropout Layer	20
1.19	Fully Connected Layer	20
3.1	HGGIF in DWT domain	66
3.2	Proposed MLRNet for skin lesion segmentation	71
4.1	Proposed DTLNet framework	86
4.2	HGWF based skin lesion preprocessing	91
4.3	AlexNet architecture for skin lesion segmentation	97
4.4	DLCNN Feature Extraction and Classifier	99
5.1	HOS-Net Overview	104
5.2	DCIGN architecture for skin lesion segmentation	108
5.3	The architecture of the HDKN for feature extraction	114
5.4	Optimal feature selection process using SPOA	119
5.5	Classification Model of DENM	125

6.1	Graphical representation of Performance comparison	148
6.2	Graphical representation of Conventional Segmentation Approaches	151
6.3	Graphical representation of performance comparison of conventional segmentation with PH2 dataset	153
6.4	Results from Performance Comparison of Various Segmentation Approaches	160
6.5	Graphical representation of performance comparison of various SLDC methods	163
6.6	Diagrammatical representation of performance estimation of various methods	167
6.7	Graphical representation of Percentage of improvements	170
6.8	AUC-RoC curves of various methods	173
6.9	Classification Performance Analysis with Proposed HOS-Net	174
6.10	Improvement of Parameters	176
6.11	Computational time (seconds) of various segmentation methods	180
6.12	Computational time (seconds) of various classification methods	181

ABBREVIATIONS

ABCDE: Asymmetry, Border, Colour, Diameter, and Edge.

ANN: Artificial Neural Network

ASR: Age-Standardized Rate

ATL: Attention Transfer Learning

AUC-ROC: Area under the receiver operating characteristic curve

AuDNN: Augmented Intelligence enabled Deep Neural Networking

BCC: Basal Cell Carcinoma

BCN: Basal Cell Carcinoma Nevus.

CAD: Computer-Aided Diagnosis

CDNN: Convolutional Deep Neural Network

CNN: Convolutional Neural Network

CSLM: Confocal Scanning Laser Microscopy

CT: Computer Tomography

DENM : Densely-Connected Echo State Network

DL: Deep Learning.

DLCNN: Deep Learning Convolutional Neural Network

DTLNet: Deep Transfer Learning Network

DWT: Discrete Wavelet Transform

EDC: Extracted Data Clusters.

ESRGAN: Enhanced Super-Resolution Generative Adversarial Networks

FC: Fully Connected.

FCRN: Fully Convolutional Residual Network

FPA: Feature Pyramid Attention

Fuzzy U-net: Fuzzy U-network

GAN: Generative Adversarial Network, a machine learning model

GIF: Guided Image Filtering

GPU: Graphics Processing Unit.

HAM: Human Against Machine.

HCNN: Hybrid Convolutional Neural Network

HDKN: Hybrid Deep Kohonen Network.

HGGIF: Hybrid Gaussian Guided Filter

HGWF: Hybrid Gaussian-Wiener Kernel Function

IDFT: Inverse Discrete Fourier Transform

ISIC: International Skin Imaging Collaboration.

ISIC-2019: International Skin Imaging Collaboration 2019 dataset

KSOM: Kohonen Self-Organizing Map.

MEL: Melanoma

MISO: Multiple-Input Single-Output

ML: Machine Learning.

MLRNet: Multi-Layer Residual Convolutional Neural Networks

MRI: Magnetic Resonance Image

MuSClD: Multi-Site Cross-Organ Calibration based Deep Learning

NLP: Natural Language Processing

NN: Neural Network

NSGA II: Non-dominated Sorting Genetic Algorithm II

OCT: Optical Coherence Tomography

ORACM: Object-Relationship Aware Co-attention Model

PSPNet: Pyramid Scene Parsing Network

ReLU: Rectified Linear Unit

ResNet: Residual Network

RNN: Recurrent Neural Network

ROC curves: Receiver Operating Characteristic curves

SACC: Segmentation Accuracy

SCC: Squamous Cell Carcinoma

SCDNet: Skin Cancer Diagnosis Network

SF1: Segmentation F1-Score

SGD: Stochastic Gradient Descent

SLDC: Skin Lesion Diagnosis and Classification

SPOA: Social Pelican Optimization Algorithm

SPF: Sun Protection Factor

SPR: Segmentation Precision

SRE: Segmentation Recall

SSEN: Segmentation Sensitivity

SSPE: Segmentation Specificity

U-RP-Net: U-Net with Aquila Whale Optimization

UV: Ultraviolet

VGG16: Visual Geometry Group 16

ViT: Vision Transformer.

WHO: World Health Organization

WSI: Whole Slide Images

CHAPTER 1

INTRODUCTION

In this chapter we will see the introduction to skin cancer and structure of skin followed by different types of skin cancers, traditional methods used for detection, need of CAD and organization of thesis

1.1 INTRODUCTION

The human skin acts as a protective barrier that separates the body from the external environment. Comprising water, proteins, fats, and minerals, it is a significant component of the person body. Nerves in the skin enable the perception of sensations such as heat and cold. The integumentary system establishes a shield between the body and the surroundings, effectively isolating the body from external factors. The primary functions of the integumentary system encompass safeguarding, sensory perception, temperature regulation, vitamin D synthesis, and waste excretion. The skin serves as a defense against abrasion and UV radiation, as well as a barrier that prevents the entry of bacteria and limits water loss to prevent dehydration.

The sensory function of the skin allows us to perceive pain, touch, heat, pressure, and cold. Body temperature is regulated through the activity of sweat glands and the control of blood flow within the skin. Exposure to UV radiation prompts the skin to produce a molecule that can be converted into vitamin D. Both the farthest layer of the person skin (epidermis) and gland secretions contribute to the elimination of small amounts of waste. Skin conditions and disorders encompass various issues, including allergies like contact dermatitis, the formation of blisters, and infections such as cellulitis. Skin disorders also encompass conditions like acne, psoriasis, eczema, and vitiligo, while injuries, burns, and scars fall within the category of skin-related conditions.

As individuals age, they may experience a reduction in the levels of collagen and elastin in their skin. This depletion leads to a thinning of the dermis layer, potentially causing sagging skin and the development of wrinkles. To preserve the health of the skin, it is advisable to use sunscreen with a minimum SPF of 30. Regular skin examinations are important for an early detection of skin diseases. It's worth noting that nicotine and the chemicals found in cigarettes accelerate the aging process of the

skin. Skin infections can be instigated by a diverse array of bacteria, encompassing a spectrum of severity from mild to severe. Medical professionals, including doctors and specialists, harness various technological advancements in the realm of medicine to swiftly identify and treat skin ailments. Advanced CAD systems have become essential tools in the identification and diagnosis of skin disorders. This chapter presents a comprehensive exploration of dermoscopy skin images and introduces a platform for comprehensive detection of skin lesions through the utilization of dermoscopy images. This platform facilitates the CAD system, enabling healthcare providers to conduct rapid assessments of lesions.

1.2 SKIN COMPOSITION

The prime organ of human body is skin, plays a crucial role in shielding us from various diseases [10]. Skin tumors are well-known for their abnormal growth and structural deficiencies. Lesions can manifest in a variety of forms, including swelling, cysts, rashes, discolorations, pus-filled sacs, and blisters. Depending on their extent, these lesions may or may not pose harm or risk to one's health. In the realm of medical diagnostics, ongoing research aims to alleviate the challenges faced by dermatologists when it comes to the screening and diagnosis of lesions, particularly in the context of melanoma, utilizing digital images for diagnosis. The structure of ski we can see in the Figurel.1

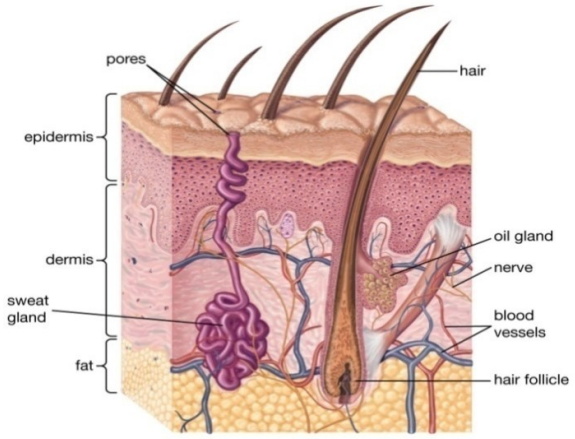

Figure l.l Skin Structure

Skin diseases typically originate in the epidermis, the outermost layer of the skin. Within this layer, there are three primary cell types: squamous cells, basal cells, and melanocytes. Squamous cells, also known as flat cells, form the surface of the

epidermis. The basal cell layer, located at the epidermis's bottommost part, consists of basal cells. Melanocytes are responsible for producing the brown pigment called melanin. These cells can develop into melanoma, a condition that gives the skin a tan or brown appearance. Additionally, melanin pigment is an important role in safeguarding the skin's deeper layers from harmful elements.

Epidermis

The epidermis, which is the skin's farthest layer, acts as barrier of protection against various external factors, including those stemming from natural disasters. Among its important functions, the epidermis guards against infection by preventing bacteria and germs from entering the body and bloodstream . Additionally, it shields the skin from the sun, rain, and other environmental elements. The epidermis is continuously generating new skin cells. The pigment responsible for skin coloration is called melanin, and its levels in the body determine skin texture and color. Individuals with higher melanin production tend to have darker skin and are more prone to sunburn.

Dermis

Dermis is a skin layer situated between the epidermis and the subcutaneous tissue. It is composed of dense irregular connective tissue, which serves to protect the body from pressure and stress. Within dermis, collagen is a fundamental protein that provides the skin with strength and resilience. Elastin contributes to skin flexibility and aids in restoring strained skin. Nerves within the dermis serve as sensors, alerting the body to sensations such as excessive heat, discomfort, or gentle touches, while also playing a role in pain perception. This layer also produces oils, and it houses sweat glands responsible for sweat production.

Hypodermis

Within vertebrates, the hypodermis constitutes the lowest layer of the integumentary system, containing fibroblasts, adipose cells, and macrophages as its principal cell types. These components are located beneath the epidermis and within the dermis, and they primarily serve as a reservoir for storing fat. The hypodermis is the fatty layer responsible for regulating body temperature by preventing excessive cooling or overheating. In cases of accidents, the fat within the hypodermis provides protection for muscles and bones.

1.3 SKIN CANCER OVERVIEW

Skin cancer is a pervasive and escalating global health concern that impacts millions of individuals every year. As per thr World Health Organization (WHO), skin cancer is diagnosed in over two million people globally each year, establishing it as one of the most widespread cancer types worldwide. This alarming prevalence underscores the urgent need for effective diagnostic and preventive measures.

Skin cancer encompasses various types, with the most common forms being basal cell melanoma, SCC and BCC. BCC, constituting the majority of skin cancer cases, usually initiates in the basal cells of the epidermis. It is generally localized and has a lower propensity to metastasize. Squamous cell carcinoma, which arises in the squamous cells of the skin, can be more invasive than BCC. While it has a lower risk of metastasis than melanoma, early recognition and treatment are critical for optimal outcomes. Melanoma, which is the most. lethal type of skin cancer, emerges from melanocytes, the cells accountable for melanin production. Melanoma exhibits a heightened risk of metastasis, emphasizing the utmost significance of timely diagnosis and intervention, as stated by the American Cancer Society. The primary risk factors for skin cancer is UV radiation exposure. Extended exposure to UV radiation, whether originating from natural sources such as the sun or artificial sources like tanning beds, markedly amplifies the susceptibility to skin cancer [106]. Alterations in the environment, including ozone layer depletion, can exacerbate UV radiation exposure and contribute to the escalating occurrence of skin cancer [88]. Skin type plays a crucial role, with individuals possessing fair skin, light hair, and light eyes being more susceptible to skin cancer due to lower levels of melanin, which provides some protection against UV radiation [88]. A family history of skin cancer is allied with an enlarged individual risk, and weakened immune systems of individuals, such as organ transplanted human beings, face elevated susceptibility [99]. The significance of identifying skin cancer early is complex and varied. Studies have consistently demonstrated that early diagnosis leads to higher survival rates [22]. Furthermore, early diagnosis often allows for less invasive and less complex treatments, reducing patient discomfort and healthcare costs [12]. Perhaps most critically, early detection can prevent the spread of malicious cells across the body parts, significantly impacting patient outcomes [15].

Skin diseases encompass all issues that irritate, obstruct, or negatively impact the skin. These problems can either be inherited or acquired. Common signs of different

skin conditions include itchiness, acne, and rashes. Fortunately, many skin issues can be managed through medications, proper skincare routines, and lifestyle adjustments. Some notable skin diseases include Melanoma (MEL), Melanocytic Nevus (NV). Basal Cell Carcinoma (BCC), Actinic Keratosis (AKIEC), Benign Keratosis (BKL), Dermatofibromas (DF), Vascular Lesions (VASC), Squamous Cell Carcinoma (SCC)

1.3.1 Melanoma

It is one kind of cancer that originates from cells responsible for producing melanin, responsible for skin coloration. This type of cancer is the most deadly among skin cancers and can also develop in the eyes, nose, or throat. While the particular root of all melanomas remains unclear, being uncovered to sun UV radiation substantially elevates the threat of developing this cancer. Reducing skin exposure to UV light, as depicted in Figure 1.2, can help lower the risk of melanoma

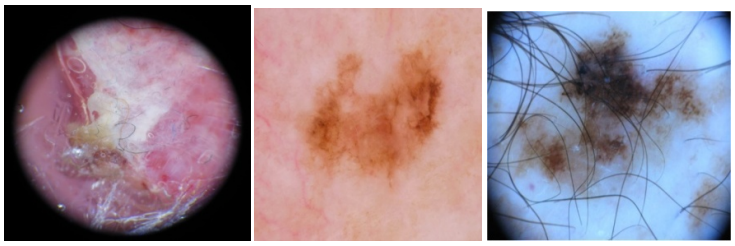

Fig. 1.2: Different Images of Melanoma

1.3.2 Melanocytic Nevus

Melanocytic nevi are non-cancerous growths composed of melanocytes, which are cells responsible for producing pigment. These melanocytes typically extend into the epidermis, as depicted in Figure 1.3. The majority of acquired melanocytic nevi are regarded as benign tumors. While this condition can be found in various mammals, it is most commonly observed in humans, dogs, and horses.

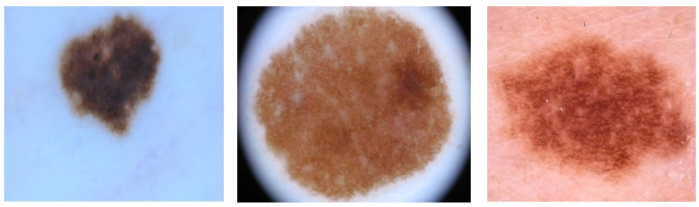

Fig. 1.3: Different Images of Melanocytic Nevus

1.3.3 Basal Cell Carcinoma

This kind of cancer originate in a particular layer called basal cover of skin and leads to the production of new skin cells following the demise of the old ones. It typically

presents as a skin-colored, translucent, shiny bump, as depicted in Figure 1.4. In individuals with brown or black skin, this bump may appear dark or glossy black.

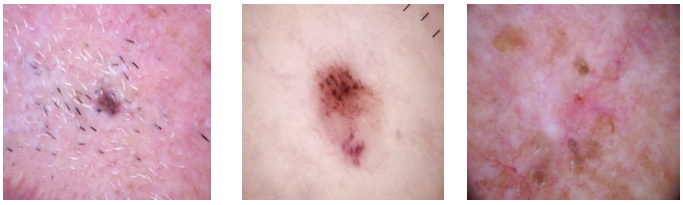

Fig. 1.4: Different Images of Basal Cell Carcinoma

In such cases, tiny blood vessels may be visible, although they can be difficult to discern. There is a possibility that the bump may bleed and form a scab. At times, it can resemble a lesion with dark spots or exhibit a brown, black, or blue hue, or it may manifest as a scaly patch with a flat, scaly elevated border.

1.3.4 Actinic Keratoses

An actinic keratosis, often referred to as Bowen's disease or solar keratosis, is a rough, scaly patch of skin that typically develops after exposure to sunlight. These patches are commonly found on the forearms, lips, neck, cheeks, ears, scalp, and backs of the

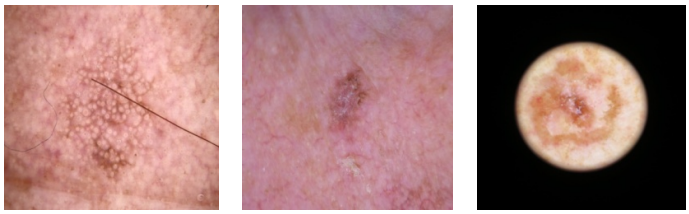

Fig. 1.5: Different Images of Actinic Keratoses

hands. They can appear as scratchy, dry, or scaly areas on the skin, usually with a diameter of less than 1 inch (2.5 cm). In some cases, they may have a rough, warty texture and can exhibit various colors like pink, red, or brown, as illustrated in Figure 1.5. Additionally, actinic keratosis can lead to itching, burning, bleeding, or the formation of crusts on the skin.

1.3.5 Benign Keratosis

BKL is a common benign skin growth that often occurs as people age. These growths can be brown, black, or light tan in color. It is essential to emphasize that seborrheic keratosis is not contagious and does not pose any health risks. They do not necessarily require treatment but can be removed if they become bothersome due to their interaction with clothing or if someone wishes to remove them for cosmetic reasons.

Seborrheic keratosis typically presents as a waxy or rough bump on the face, chest, shoulders, or back, often exhibiting a round or oval shape, as depicted in Figure 1.6.

Fig. 1.6: Different Images of Benign Keratosis

These growths can vary in size, ranging from very small to over 1 inch (2.5 cm) in diameter. They can appear as a single growth or in multiple numbers, ranging from a few to many. In individuals with black or brown skin, it's common to see small clustered growths around the eyes, referred to as flesh moles

1.3.6 Dermatofibromas

Dermatofibromas are a prevalent skin condition with an unknown cause, predominantly observed in women. They typically appear on the extremities and are often without symptoms, although they can occasionally lead to sensations of burning and discomfort, as illustrated in Figure 1.7.

Fig. 1.7: Different Images of Dermatofibromas

Dermatofibromas are the most common type of bothersome skin condition. They exhibit distinct histological characteristics. Treatment for malignancy is usually unnecessary unless there is significant uncertainty about the diagnosis or the symptoms become exceedingly troublesome.

1.3.7 Vascular Lesions

Vascular lesions encompass a wide range of skin conditions, including those that are acquired later in life and which are present by birth & develop shortly thereafter, vascular birthmarks, as illustrated in Figure 1.8. These lesions can either be Vascular lesions encompass a broad range of skin conditions, together with that are acquired

later in life and which are present by birth & develop shortly thereafter, known as vascular birthmarks, as illustrated in Figure 1.8. These lesions can either be

Fig. 1.8: Different Images of Vascular Lesions

benign or malignant. Laser therapy is often the preferred treatment option for addressing this category of skin disorders.

1.3.8 Squamous Cell Carcinoma

It is also one kind of cancer that originates from the squamous cells found in the outermost skin layer called epidermis. It is most familiar types of skin cancer, often arising due to cumulative sun exposure over the years as show in Figure 1.9. SCC tends to develop in areas frequently exposed to the sun, such as the face, ears, etc.,

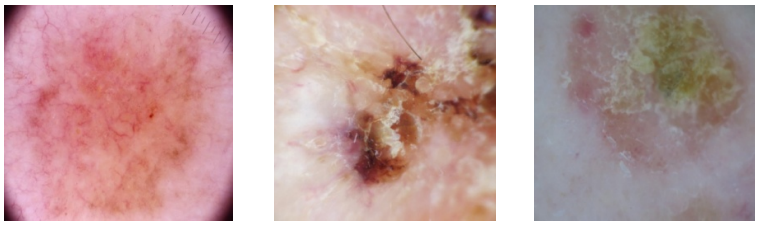

Fig. 1.9: Different Images of Squamous Cell Carcinoma

1.4 SKIN CANCER PROBLEMS AND NECESSITY OF EARLY DETECTION

Skin cancer is an important public health concern with several implications for both individuals and healthcare systems. This chapter delves into the various aspects of skin cancer, including its prevalence, causes, risk factors, mortality rates, and the crucial importance of early detection in addressing this global issue. Skin cancer ranks among the most frequently diagnosed cancers worldwide, covering various forms such as BCC, MEL, and SCC. Its incidence varies regionally, with areas of high sun exposure reporting higher rates. According to the World Cancer Research Fund, the worldwide occurrence of skin cancer is on the rise, and projections indicate an alarming surge in melanoma cases by [41]. Overexposure to UV rays, from both the sun stands as the primary cause of skin cancer. UV radiation damages DNA, leading to genetic mutations that can initiate cancer development. Genetic predisposition and environmental factors also influence

susceptibility. Key risk factors encompass fair skin, history of sunburn, tanning bed usage, and a family history of the disease [129].

Advanced skin cancer, especially melanoma, significantly impacts mortality rates. While melanoma is less common than other skin cancers, it contributes substantially to skin cancer-related deaths. In 2022, approximately 7,400 deaths in the US were attributed to melanoma. The consequences of skin cancer extend beyond mortality, encompassing physical, emotional, and financial burdens on individuals and their families. Moreover, the disease places a considerable burden on healthcare systems due to the costs associated with diagnosis, treatment, and ongoing care [15]. Early detection is paramount in improving the prognosis and saving lives in the case of skin cancer. When diagnosed at an earlier stage, skin cancer is highly treatable, often requiring minimally invasive interventions. Prompt and precise skin lesion segmentation is crucial for early detection. It not only enhances treatment outcomes but also reduces the need for more aggressive and costly therapeutic measures. Therefore, public awareness campaigns and regular skin screenings by healthcare professionals are crucial for promoting early detection and prevention [36]. The field of medicine has undergone a significant transformation with the application of image analysis techniques. These technologies, driven by rapid technological advancements, have become indispensable tools for modern healthcare. They extract valuable information from a variety of medical images, for instance CT scans, MRIs, X-rays, and dermatological images, facilitating precise diagnosis, treatment monitoring, and research across multiple medical domains, including radiology, pathology, and dermatology [82].

Image analysis plays a dynamic role in this transformation, providing non-invasive, efficient, and highly informative solutions in medicine. It is particularly relevant in the context of dermatology, where it aids in the precise segmentation of skin lesions, contributing significantly to the early detection of skin cancer. Experts in dermatology, such as [39] have focused on feature recognition and diagnosis accuracy using reflectance confocal microscopy (RCM). Advanced imaging modalities like dermoscopy and RCM have revolutionized dermatology by providing deeper insights into skin structures and lesion characteristics, enhancing diagnostic accuracy and patient care [94]. However, the field of medical image analysis is not without its challenges. The vast amount of data generated by medical imaging requires sophisticated algorithms for efficient processing and analysis. Image quality, noise, and artifacts can also affect the accuracy of automated

analysis, making specialized algorithms and approaches crucial, especially in dermatology, where image quality can be highly variable due to factors like lighting, skin tones, and image artifacts [114]. The applications of image analysis in dermatology have gained prominence, particularly in skin lesion analysis. Researchers like [114] have developed automated systems to identify and categorize skin ailments, including psoriasis. Their work demonstrates the potential of image analysis in accurately identifying skin conditions, aiding in early diagnosis and treatment. Additionally, CAD systems created to aid skin doctors in the before time detection of skin cancer. These systems employ image analysis techniques to partition skin lesions, evaluate their features, and offer diagnostic assistance, as demonstrated by the research of [39].

First and foremost, raising awareness about skin diseases is of utmost importance. A clinical diagnosis should be conducted, and strategies can be developed to minimize delays and obstacles, ensuring that patients receive timely treatment. It is crucial to prevent skin conditions from progressing to skin cancer. To achieve this, two complementary preventive measures for skin diseases are applying sunscreen before sun exposure and avoiding outdoor activities during high-temperature periods. Additionally, wearing protective clothing can help shield the skin from direct sunlight. Dermatologists often assess various aspects of the skin, including its texture, shape, and color, to find weather the lesion of skin is benign or malignant. Over recent years, incidence of skin melanoma has been rapidly increasing. Although melanoma is a unsafe form of skin cancer, it will be successfully treated when detected at an early stage [50]. Given the rising incidence of melanoma, research in this field has gained momentum. Diagnosis involve a physical inspection of skin and may include a skin biopsy. Certainly, epiluminescence microscopy, also known as dermoscopy, is a valuable procedure in diagnosing skin conditions. This procedure employs various equipment to assess the pigment and blood vessel patterns of a mole without removing it. It provides crucial insights for medical professionals to make accurate assessments. Several common skin tests are conducted for diagnostic purposes. Patch tests are employed to diagnose skin allergies. In this procedure, potential allergens are applied to the skin, and any reactions are observed. Skin biopsies are instrumental in diagnosing skin cancer and other benign skin conditions. During a skin biopsy, a portion of the skin is removed (after local anesthesia) and sent to a laboratory for

analysis. Different tools such as a scalpel, razor blade, or a cylindrical punch biopsy tool can be used to extract the skin, and stitches may be employed to close the wound afterward. These diagnostic techniques are crucial for accurate and timely identification of various skin ailments.

Cultures are diagnostic tests employed to identify the specific microorganism responsible for an infection, whether it's a bacterium, fungus, or virus. These cultures can be collected from several of sources, including the skin (including surface scrapings, biopsies, and the contents of pus, pimples, and blisters), hair, or nails.

In addition to cultures, the ABCDE rule is utilized for detecting skin diseases. The acronym ABCDE stands for Asymmetry, Border, Color, Diameter, and Evolution. This rule helps in assessing potential skin abnormalities. Melanomas, for instance, often exhibit asymmetrical shapes, unlike non-cancerous moles that are typically symmetrical. The borders of melanomas tend to be irregular in shape, and they can have multiple colors. Melanoma growths are often larger than 6mm in diameter, and they can change in characteristics such as size, shape, and color over time. This rule serves as a useful guideline for identifying suspicious skin conditions that may require further evaluation.

1.5. SKIN IMAGING TECHNIQUES

Indeed, imaging techniques in dermatology are invaluable for identifying and diagnosing various skin diseases. The term "medical imaging" has significantly streamlined this process over the past century. These techniques enable the generation of images from different areas of the skin, aiding in diagnosis, monitoring, and treatment planning. As technology advances, an array of imaging technologies is continually developed and utilized, enhancing our understanding and diagnosis of skin conditions. Various strategies in this field are continuously evolving To offer medical professionals with more precise and comprehensive information

Tele-dermoscopy

Tele-dermoscopy is gaining popularity due to its capacity to offer patients consistent, convenient, and accessible care. This is particularly crucial in regions like Canada, where a shortage of dermatologists has led to extended wait times for skin assessments. Tele-dermoscopy programs enable clinical specialists to provide accessible care, enhance patient engagement, reduce unnecessary in-person visits,

shorten patient wait times, and promptly generate comprehensive reports [60]. Figure 1.10 (a) displays an image obtained through tele-dermoscopy.

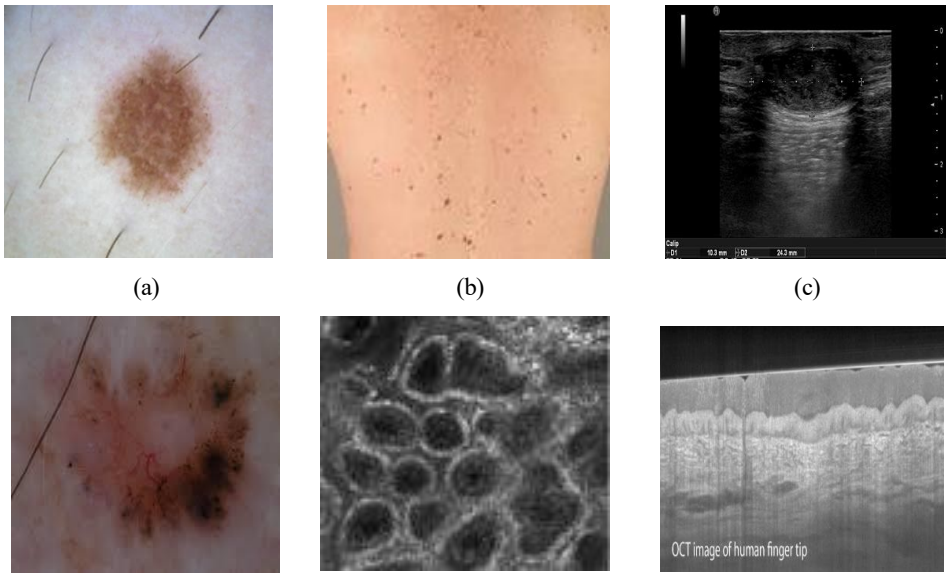

(a) (b) (c)

(d) (e) (f)

Fig. 1.10: Skin Imaging Techniques (a) Tele-dermoscopy, (b) Total Body Photography, (c) Ultrasonography, (d) Dermoscopy, (e) Confocal Microscopy, (f) Optical Coherence Tomography

Total Body Photography

Full body screening, also referred to as absolute body photography or body imaging, enables dermatologists to conduct regular monitoring of high-risk patients by capturing images of their skin on a recurring basis. This involves the acquisition of a series of high-quality photographs of various areas of the patient's body for the purpose of tracking and monitoring skin lesions. This advancement holds great promise in aiding physicians in the early detection of skin malignancies, as it allows for the rapid and accurate assessment of existing skin spots on patients. An example of total body photography is illustrated in Figure 1.10(b).

Ultrasonography

This diagnostic tool, which has been previously used, serves as a valuable resource for evaluating skin thickness in various medical fields. Its key advantages include non-invasiveness, safety, and cost-effectiveness, making it a favored choice. The image resolution improves as the ultrasonic frequency increases. The process involves the detection of reflected sound waves as they pass through tissues with varying

acoustic properties. Figure 1.10(c) displays an ultrasonography image as an example of its application.

Dermoscopy

Digital dermoscopy is a non-invasive technique employed for evaluation of pigmented skin lesions. This method employs a handheld device known as a dermatoscope, functioning as a visual aid. This tool can be utilized by professionals or non-experts to inspect and diagnose skin lesions and diseases, including melanoma. Additionally, it is useful for examining the scalp, hair, and nails.

Fig. 1.11: Skin Scope

Figure 1.10(d) displays an example of a dermoscopy image, showcasing its application in dermatological diagnosis. Dermatoscopes utilize light and magnification to improve the visibility of a effected skin, as illustrated in Figure 1.11. By employing dermatoscopes, clinicians can observe intricate details in the outer layer of the skin that might be indiscernible to the naked eye. This advanced technology represents the most contemporary method for evaluating pigmented skin lesions, significantly increasing physicians' confidence in clinical diagnoses. These devices are specifically designed to visualize structures beneath the skin's surface and epidermis, which are not easily observable to the naked eye. Moreover, the images can be digitally recorded and stored for sequential analysis and further examination of the lesions in digital mode. This digital capability enables in-depth scrutiny and facilitates accurate assessments for dermatological conditions. Dermoscopic image analysis has proven to be a highly useful tool, achieving an enhanced diagnostic accuracy of 5-30% by eliminating the need for biopsies in both precancerous and malignant tumors. In recent dermoscopy, non-polarized light sources are exclusively used to illuminate the skin. This approach requires the use of a liquid interface to

optimize the interaction between the lens and the skin, reducing the amount of light that is reflected, refracted, and diffracted from the skin's surface. Consequently, this technique enables observers to visualize structures located beneath the stratum corneum, the outermost layer of the skin.

In contrast, polarized light dermoscopy can visualize deeper skin features without the use of a liquid interface. Dual-mode dermoscopy combines both technologies, allowing for the imaging of superficial structures and blood vessels in the skin, as well as a comprehensive examination of the various components within the skin.

Confocal Microscopy

Confocal Scanning Laser Microscopy (CSLM) is a valuable technique for evaluating skin lesions, providing high-resolution tissue images that are comparable to histopathological images. In CSLM, a low-power laser beam is precisely directed onto a specific point of the skin through a lens. The light redirected from that focal point is detected using a confocal pinhole filter, and the resulting image can be seen in Figure 1.10(e). Subsequently, the collected light is converted into an electrical signal and displayed on a computer for analysis.

CSLM allows for the examination of lesions at an integral level, enabling the detection of irregularities and details that may not be apparent through other imaging methods. This technique enhances our ability to assess and understand skin lesions, aiding in their accurate diagnosis and evaluation.

Optical Coherence Tomography

OCT is a macro-optical technology that generates images using light tissue communication, as demonstrated in Figure 1.10(f). This non-invasive technique creates high-resolution real-time skin images by conducting a cross-sectional observation to a depth of up to 2 mm beneath the skin's surface. Due to the light scattering effect caused by pigment, OCT dermatology is particularly effective for monitoring Non-Melanocytic Skin Malignancies (NMSC). However, when dealing with pigmented lesions, additional information is often required for accurate analysis.

In the case of NMSC, OCT images focus on the architectural abnormalities within the epidermis, providing unique insights that aid in the diagnosis and evaluation of skin conditions. This technology offers a valuable tool for dermatologists in the assessment and monitoring of various skin malignancies and abnormalities.

1.6. CAD SYSTEM FOR SKIN DISEASE DIAGNOSIS

Skin diseases come in various forms and can result from factors such as sunlight exposure, viral infections, immunological suppression, and genetic abnormalities. Melanoma, a type of skin cancer, is typically treated with surgery, often being the primary recommended treatment at this stage. Over time, several alternative approaches for treating skin diseases have been suggested. These methods include biopsy (to diagnose and evaluate skin conditions), broad excision (to remove abnormal tissue), and chemotherapy (using drugs to kill or slow down the growth of cancer cells). Traditionally, unaided clinical examinations have been the primary method for diagnosing skin diseases. Nonetheless, there is an increasing inclination towards visual examination conducted by specialists for the early detection of diseases. Nevertheless, this approach faces challenges due to disparities in assessments among different experts. While dermoscopy has enhanced the diagnostic proficiency of seasoned physicians, acquiring this skill remains daunting, and even with training, the analysis still remains subjective.

Given these challenges, there is a rising demand for the computerized, automated analysis of images of skin lesions. This approach offers capable avenues for skin disease detection through Computer-Aided Diagnosis (CAD), providing a more objectives and accurate assessment of skin conditions. The block diagram of CAD system is shown in Fig 1.12.

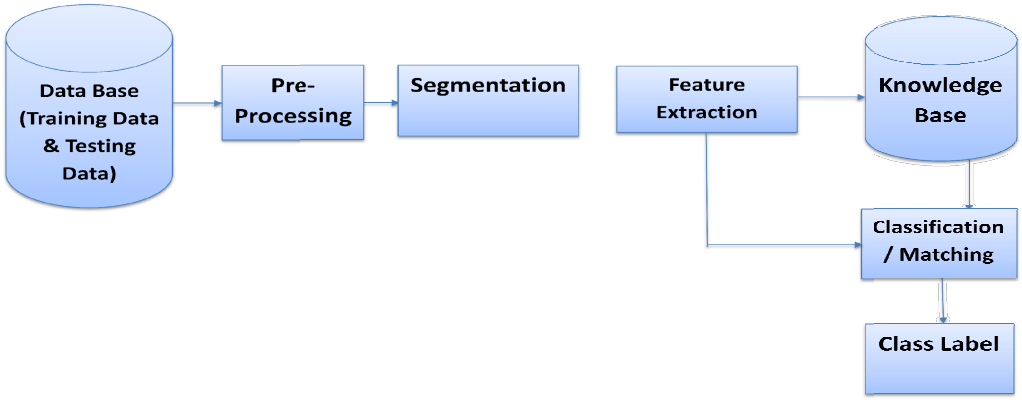

Fig. 1.12: CAD System

CAD technologies have a critical role in recognizing and diagnosing melanoma, leading to the survival of hundreds and thousands of patients. Image pre-processing is very important step in this process. It involves enhancing the image's intensity (lesion)

while simultaneously minimizing undesired distortions and reducing noise. These processed images are then used for the segmentation of the nodule region, allowing for a more accurate and effective analysis of skin lesions and aiding in early detection of melanoma. Image segmentation refers to a process of dividing image regions and isolating objects from the background. In the context of dermoscopy images, this technique is used to separate the lesion (abnormal skin area) from the surrounding healthy tissue. This segmentation step is crucial in determining whether the identified nodule is malignant or benign. Once the lesion is segmented, image classification techniques are employed. These techniques encompass various approaches to categorize skin diseases depicted in dermoscopy images. By utilizing sophisticated classification methods, medical professionals can accurately identify and diagnose different skin conditions relying on the visual data extracted from the images. These advancements in image analysis and classification significantly contribute to enhancing the precision and effectiveness of diagnosing skin disorders

1.7 CONVOLUTIONAL NEURAL NETWORK ARCHITECTURE

ANN is numerous interconnected elements known as neurons. These neurons are arranged in a succession of layers, and each neuron generates real-value activations in a sequential manner. This network architecture draws inspiration from the arrangement of biological neurons in a brain of human and is applied across a range of ML and DL applications. It is employed to model intricate relationships and execute tasks like pattern recognition and classification

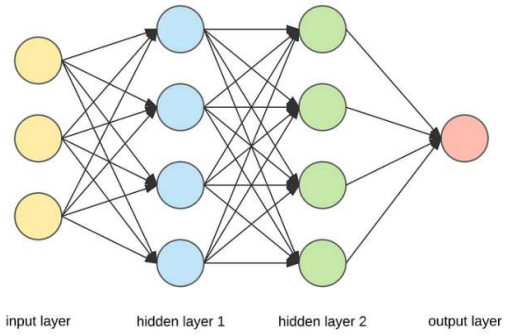

Fig. 1.13: Deep Neural Network

Within an ANN, a portion of neurons functions as inputs, gathering diverse data from the surrounding environment. Further neurons in the hidden layer become active through weighted connections. These interconnections constitute the hidden layer, as

demonstrated in Figure 1.13. The output neuron, positioned at the network's output, offers insights into how effectively the network has acquired knowledge from the training data it received. The operation of a neuron comprises the calculation of the weighted sum of all inputs and their associated connection weights. Subsequently, this summation is processed through an activation function to generate the neuron's output. The activation function introduces non-linearity to the neuron's response, enabling neural networks to capture intricate data relationships and glean insights from patterns. In an artificial neural network, weights assigned to neurons are determined during the learning process. The idea is to optimize the network's ability to solve the assigned task efficiently, often with the assistance of a technique called backpropagation. In a typical artificial neural network, all neurons are fully connected, meaning that each neuron in one layer is linked to every neuron in the next hidden layer. Deeper neural networks, with many layers, offer advantages because they can represent more complex functions with fewer neurons in each hidden layer and appropriate weights assigned to them. This depth allows neural networks to capture complex patterns and associations in data. Additionally, various neural network architectures are developed to excel in specific tasks, making them highly adaptable and suitable for a broad range of applications. CNNs are widely used DL architectures specifically designed for tasks related to recognition and classification. They are particularly effective for image and spatial data analysis because of their unique ability to learn automatically and extract hierarchical features from data. CNNs have a significant impact on computer vision, image analysis, and various other fields where pattern recognition and classification are essential. They have proven to be highly successful in tasks such as image classification., object detection., and image seg.mentation, among others. In the proposed research, a CNN has been developed for the detection and classification of skin diseases. The CNN architecture has several types of layers, which includes convolutional layers, an activation function layer (typically ReLU), batch normalization layers, max-pooling layers, and a fully connected layer, as depicted in Figure 1.14.

Here's a breakdown of how these layers work:

1. Convolutional Layers
2. Max Pooling Layer
3. Batch Normalization Layer
4. Activation Function Layer (ReLU Layer)

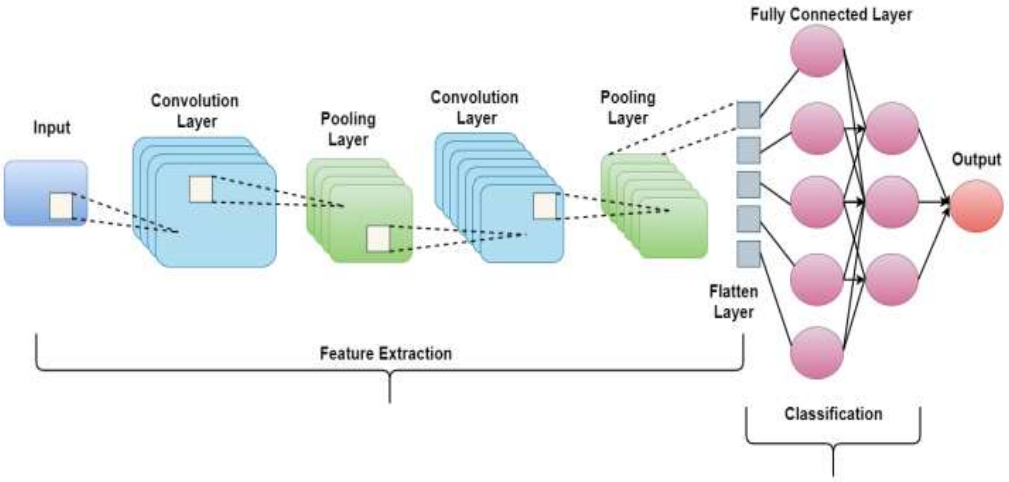

Fig. 1.14: Convolutional Neural Network

These layers work together in the CNN to automatically acquire and discern pertinent attributes from the input data, rendering it exceptionally proficient in the categorization of skin ailments. The process continues with additional layers, eventually leading to the fully connected layer for the final classification.

1.7.1 Convolution Layer

Convolution layer is the first layer in CNN and this layer consists of filters that are

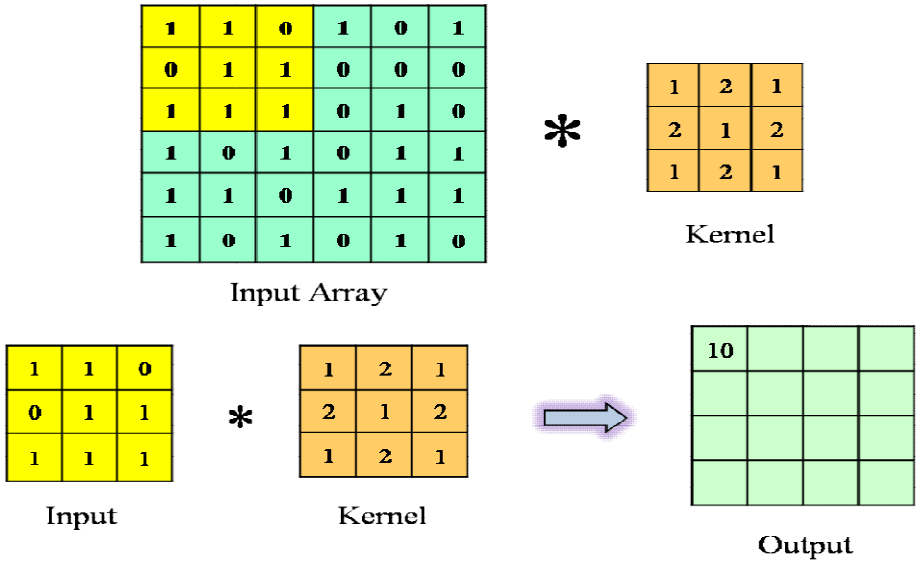

learnable as shown in fig. 1.15

Fig. 1.15: Convolution Layer

The calculation of output parameters in the convolution layer is done by Eq. (1.1). Here 'm' is width, 'n' h.eight of filter and 'K' denotes no. of filters.

$$Number\ of\ output\ parameters = \big((m * n * a) + 1\big) * K \tag{1.1}$$

The value of 'a' is determined by the input image dimension: if the image is 2D, then 'a' equals 2, and in the case of a 3D image, 'a' is set to 3.

1.7.2 ReLu

It replaces all values with negative sign from the filtered input image by zeros and it keepts the values with positive sign as it is. Equation (1.2) demonstrates that any values that are either negative or zero are substituted with zeros. The response f(x) of ReLU is shown in fig. 1.16.

$$f(x) = \begin{cases} 0\ for\ x < 0 \\ x\ for\ x\ \geq 0 \end{cases} \tag{1.2}$$

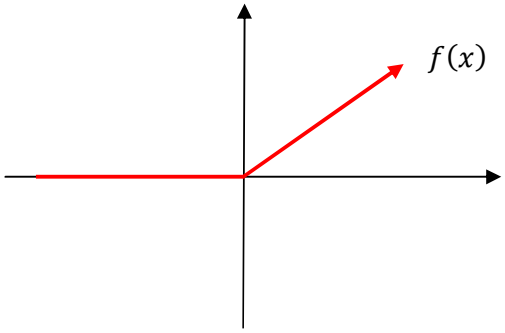

Fig. 1.16: ReLU Layer Output

1.7.3 Batch Normalization

This layer is employed to normalize the sizes of varying images and is incorporated to fine-tune the weights for the output layers. To get the output we have to use an equation which computes the output parameter provided in Equation (1.3).

$$Parameter = z * 4 \tag{1.3}$$

Here, 'z' is the dimension of previous layer response. For instance, if the input image for the batch normalization layer has dimensions of 3 * 3 * 64, then 'z' would equal 64.

1.7.4 Pooling Layer

In this layer, the image stack is shrinked into a smaller size. In the max pooling method, the highest value is picked and rest values are discarded as

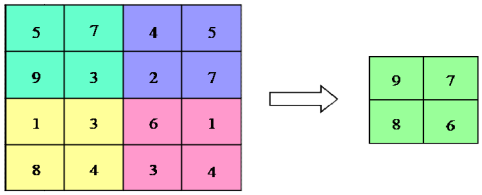

Fig. 1.17: 2x2 Max Pool Layer

shown in fig. 1.15. Whereas, in average pooling method, the mean. of the values is calculated. After pooling, image is provided for flattening in the next layer.

1.7.5 Dropout Layer

The dropout layer assumes a pivotal role in mitigating the problem of overfitting in neural networks, preventing the network from becoming overly specialized for the training and testing datasets, as depicted in Figure 1.16. Its principal function entails deactivating a randomly selected subset of neurons within a layer by setting their values to zero.

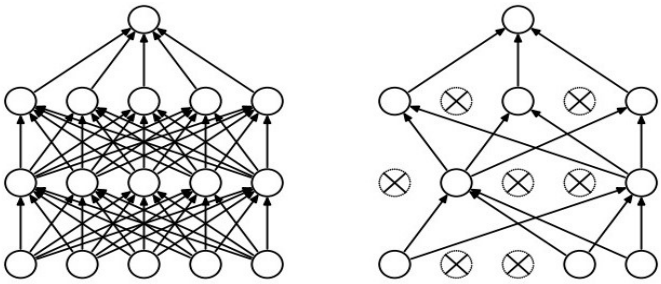

Fig. 1.18: Dropout Layer

1.7.6 Fully. Connected Layer

A Fully Connected .layer allows for the scrutiny of nonlinear patterns portrayed by the output from the convolutional layer, as illustrated in the figure 1.19 below.

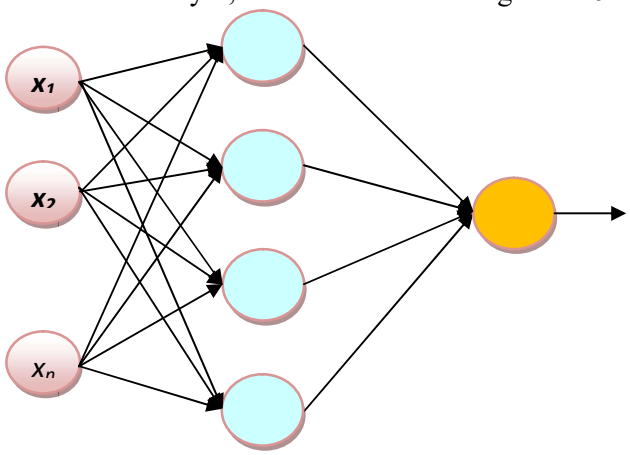

Fig. 1.19: Fully Connected Layer

1.7.7 Activation Functions

A basic neural network comprises a single neuron, serving as the fundamental computational unit of the neural network. In a neural network, each layer consists of numerous neurons that operate in parallel, with each neuron representing a function in vector-to-scalar form. Typically, these units are designated to accept an input vector 'x' and perform a transformation, as illustrated in Equation (1.4)

$$z = W^T x + b \tag{1.4}$$

In this context, the 'W' matrix represents the mapping from input vector 'x' to output vector 'z' along with the bias 'b,' which is applied during the transformation process. Subsequently, the output 'z' undergoes a nonlinear transformation denoted as *'g(z)'* applied element-wise, which is commonly referred as the activation function.. The sigmoid fn., is utilized to represent the probability distribution function for binary variables. The Softmax activation fn., is an extension of the logistic fn., for multiple dimensions

1.8. DL TECHNIQUE

DL, a subset of AI, has rapidly arisen as a transformative force in area of medicine. This literature review explores the applications of DL in medical diagnostics, patient care, and research, highlighting its impact on healthcare outcomes. DL, a subset of ML, involves the use of ANNs to examine and interpret data. It has gained prominence in medicine because of their efficiency to process enormous amounts of complex medical data, ranging from medical images to electronic health records. DL models, particularly CNNs and RNNs, have demonstrated remarkable capabilities in pattern. recognition, classification, and. prediction tasks [76]. One of the most prominent applications of DL in medicine is in medical imaging. CNNs have proven highly effective in tasks such as image segmentation, lesion detection and disease classification. For instance, researchers have developed DL models for diagnosing conditions like diabetic retinopathy, skin cancer, and lung diseases based on medical images. The work of [48] showcases the potential of DL in automating the interpretation of retinal images for diabetic retinopathy diagnosis, with a performance on par with human experts. DL models have also shown promise in predictive analytics for patient outcomes. Recurrent neural networks, with their capability of analyzing sequential data, are being employed to forecast patient deterioration and disease progression. Studies by [102] demonstrate the use of DL for

predicting in-hospital mortality and patient readmissions, aiding healthcare providers in timely interventions and resource allocation.

In addition to image analysis, DL plays a noteworthy role in natural language processing (NLP) applications in healthcare. NLP models are capable of extracting valuable. information from clinical notes, electronic health records, and medical literature. This is exemplified in the work of [81], which demonstrates how DL models can capture and interpret clinical narratives, potentially facilitating improved patient care and research by tapping into the wealth of unstructured clinical data.

Image Processing and DL

This section delivers an in-depth examination of the pivotal role of image processing and DL in the context of skin cancer diagnosis and classification.

Image Processing in Medical Imaging

Image processing is a fundamental component of medical imaging, and its significance in dermatology and skin cancer diagnosis cannot be overstated. It encompasses a range of techniques aimed at improving the quality, clarity, and interpretability of medical images, including those of skin lesions. Preparing medical images, like those of skin lesions is necessary to mitigate the impact of factors like noise, artifacts, and inconsistent lighting conditions [128]. Pre-processing steps often include noise reduction to enhance the quality of input data. Noise in medical images can obscure crucial details and affect the accuracy of diagnostic algorithms [35]. Furthermore, artifacts, such as those caused by camera imperfections, can distort the appearance of skin lesions, making their analysis challenging. Pre-processing techniques, including filtering and contrast adjustment, are critical to addressing these issues [39].

DL in Medical Imaging

DL, particularly CNNs, has revolutionized the area of health imaging, including the diagnosis of skin cancer. DL methods can automatically learn intricate patterns and features from images, making them highly suited to the complex and diverse nature of skin lesions. One of the most notable achievements of DL in dermatology is its capacity to discriminate malignant & benign skin lesions with remarkable accuracy. Studies have demonstrated that DL models can outperform human dermatologists in this regard [36]. DL models often follow a two-step process. First, the algorithm undergoes training using a vast collection of labeled skin lesion photos. During training, the model learns to identify distinguishing features that separate benign from malignant lesions.

Subsequently, the model is examined on new, unknown data to evaluate its performance. This testing phase is crucial for ensuring the model's generalizability to a variety of cases [55]. Moreover, DL models can contribute to the localization of disease-affected regions within skin lesion images. Localization is essential for accurate diagnosis, as it pinpoints the area of concern within the image, allowing for focused analysis [84].

Recent advancements have also witnessed the application of transfer. learning, a DL technique; where a model trained on one task is repurposed for another, to develop the efficiency of skin cancer categorization models. Transfer learning can considerably reduce the need for extensive labeled data for training and fine-tuning [126].

1.9 PERFORMANCE METRICS USED IN THE RESEARCH

To evaluate the effectiveness of the proposed deep learning models for skin cancer detection and classification, several standard performance metrics were employed. These metrics provide a comprehensive understanding of how well the models performed in distinguishing between different classes of skin lesions. The following are the key metrics used in this research:

1. Accuracy

Accuracy is the most commonly used metric and represents the proportion of correctly classified instances (both positive and negative) among the total number of predictions. It is calculated as:

$$\text{Accuracy} = (TP + TN) / (TP + TN + FP + FN)$$

Where: TP = True Positives, TN = True Negatives, FP = False Positives, FN = False Negatives.

2. Precision

Precision measures the proportion of true positive predictions among all instances predicted as positive. It is crucial in medical diagnosis to minimize false positives.

$$\text{Precision} = TP / (TP + FP)$$

3. Recall

Recall indicates the ability of the model to correctly identify all actual positive cases. This refers to the correct identification of malignant lesions.

$$\text{Recall} = TP / (TP + FN)$$

4. F1-Score

The F1-score is the harmonic mean of precision and recall. It provides a balance

between the two and is useful when dealing with imbalanced datasets.

$$\text{F1-score} = 2 * (\text{Precision} * \text{Recall}) / (\text{Precision} + \text{Recall})$$

5. Specificity

Specificity measures the ability of a model to correctly identify negative cases. In other words, it quantifies how well the model avoids false alarms by correctly identifying healthy (non-cancer) cases.

$$\text{Specificity} = TN / (TN + FP)$$

The use of these performance metrics ensured a rigorous and multi-dimensional evaluation of the proposed CNN, MLRNet, and DTLNet models.

1.10 MOTIVATION OF THE RESEARCH

The incidence of skin cancer is continuously increasing due to factors like increased exposure to ultraviolet (UV) radiation and changes in climatic circumstances, making it a significant global health concern. Improving patient outcomes and survival rates requires early detection and precise classification of skin cancer, especially malignant melanoma. The current diagnostic procedure, however, mostly depends on the knowledge of dermatologists, who evaluate skin lesions by visual inspection and then histological analysis. This conventional diagnostic approach is useful in many situations, but it has a number of built-in drawbacks that highlight the necessity for automated solutions. Subjectivity is one of the main problems with manual diagnosis. Due to variations in training, experience, and judgment, different dermatologists may interpret the same lesion differently. Inconsistent diagnoses and possibly ineffective or delayed therapy may result from this. Furthermore, visually examining and evaluating skin lesions takes a lot of time and effort, particularly in clinical settings with a large patient volume or restricted access to specialists. The shortage of qualified dermatologists in areas with limited resources makes it more difficult to diagnose skin malignancies promptly and accurately, which raises the risk of missed or incorrectly diagnosed cases. The possibility of misdiagnosis is another serious issue, especially when lesions have unusual characteristics or resemble benign illnesses. It can be challenging for even skilled medical professionals to distinguish between benign and malignant lesions based only on visual cues. Delays in receiving biopsy findings in certain situations may have a negative impact on the course of treatment. These drawbacks underscore the pressing need for scalable, accurate, and

automated diagnostic tools that can assist physicians and improve the diagnosis process. New avenues for medical image analysis have been made possible by developments in deep learning (DL), a branch of artificial intelligence (AI). Deep learning models are very good at identifying intricate patterns and structures because they can automatically learn hierarchical features from vast amounts of picture data. This is especially true with convolutional neural networks (CNNs). Deep learning models may directly extract and enhance pertinent features from raw images, increasing accuracy and generalization in contrast to typical machine learning techniques that rely on manually created features. Moreover, real-time picture processing and analysis capabilities of deep learning-based systems provide the possibility of quick and reliable evaluations despite resource or location constraints. These models can perform on par with highly skilled dermatologists when trained on a variety of well-annotated datasets. As a result, they are a crucial instrument for lowering diagnostic variability, accelerating the decision-making process, and expanding access to high-quality care, especially in underprivileged or isolated locations. The need to create a deep learning-based framework for skin cancer detection and classification that is precise, dependable, and flexible enough to be used in actual clinical settings is what drives our research in light of these potential and challenges. The objective is to use deep learning's advantages to support and improve dermatological practice by bridging the gap between the demand for diagnostics and the supply of healthcare.

1.11 MAJOR CONTRIBUTIONS OF THE RESEARCH WORK

This research presents a comprehensive and innovative framework for the early detection and accurate classification of skin cancer using advanced deep learning techniques. The significant contributions of the study are as follows:

1. **Development of an End-to-End Deep Learning Pipeline**

   A complete deep learning-based system was designed and implemented for skin lesion analysis, encompassing image preprocessing, segmentation, feature extraction, and classification. This pipeline enables the automation of skin cancer diagnosis with improved precision and reduced human dependency.

2. **Implementation of a CNN-Based Diagnostic Model**

   A customized Convolutional Neural Network (CNN) architecture was developed

specifically for the classification of dermoscopic skin lesions. This model was optimized with key architectural enhancements such as batch normalization, ReLU activation, dropout layers, and max pooling to improve generalization and mitigate overfitting.

3. **Utilization of the ISIC Dataset for Multiclass Classification**
   The model was trained and evaluated using the publicly available ISIC dataset, focusing on the classification of multiple types of skin lesions, including melanoma, basal cell carcinoma, squamous cell carcinoma, and other common skin conditions. The study effectively addresses the multiclass nature of the dataset, which is a known challenge in dermatological image analysis.
4. **Introduction of Effective Preprocessing and Segmentation Techniques**
   Advanced preprocessing techniques were used to enhance lesion features while reducing noise and artifacts in dermoscopic images. The study also applied segmentation approaches that improved the delineation of lesion boundaries, aiding more accurate feature extraction and classification.
5. **Integration of Hybrid Filtering Methods**
   A Hybrid Gaussian Guided Image Filter (HGGIF) was employed for noise removal and image enhancement, enabling clearer visualization of skin lesions and supporting the CNN model in learning discriminative features more effectively.
6. **Proposal of a Multi-Layer Residual Convolutional Network (MLRNet)**
   A novel MLRNet model was designed to achieve improved segmentation performance for early-stage melanoma. This deep architecture incorporates residual learning and advanced image filtering techniques, demonstrating competitive accuracy compared to traditional segmentation models.
7. **Use of Deep Transfer Learning Network (DTLNet)**
   The research integrated transfer learning by utilizing pre-trained models such as ResNet and DenseNet to enhance classification accuracy with limited training data. This approach reduced training time and improved the model's ability to generalize across different lesion types.
8. **Performance Validation Using Robust Metrics**
   The proposed models were evaluated using standard performance metrics such as accuracy, precision, recall, F1-score, and AUC. The experimental results

demonstrated the superiority of the developed methods over existing techniques in terms of both accuracy and computational efficiency.

9. **Contribution to Clinical Decision Support**

   By providing an automated, accurate, and reliable skin lesion classification system, this research contributes to clinical decision-making, particularly in regions lacking access to expert dermatological care. The work has the potential to reduce diagnostic delays and improve patient outcomes through early intervention.

1.12 ORGANIZATION OF THE THESIS

The objective of this work is to employ effective detection and classification methods to identify skin cancer diseases in combination with DL techniques. The following is a list of the chapters that have been developed for this research.

Chapter 1 provided a comprehensive introduction covering topics such as the anatomy of the skin, the various layers of the skin, types of skin diseases, computer-aided diagnosis systems, the motivation behind the research, and the thesis organization.

In Chapter 2, we presented an extensive exploration of the current body of research in the field of skin cancer .detection & classification. This chapter provides an overview of the wealth of knowledge accumulated in this domain, highlighting the advancements, methodologies, and key findings of previous studies. Furthermore, we will identify critical gaps in the literature, underscoring the necessity for further research and objectives of our research work. By delving into the state of the art, we lay the foundation for the significance of our research in advancing the field of dermatology.

In Chapter 3, we delve into the actual work done in our research, providing an in-depth understanding of the objectives and the methodology employed. The primary focus here is on our DL model, specifically the CNN used for skin cancer detection. We elucidate intricacies of this approach, explaining how the model was designed, trained, and validated. This chapter works as a guide for readers to understand the technical underpinnings of our research.

In Chapter 4, we presented and analysed the research findings. We discussed the datasets used, the pre-processing techniques applied, and delve into the performance of the DL. models in the diagnosis of skin cancer. This segment offers a detailed

inspection of the outcomes, showcasing the performance metrics of model's and potential clinical implications. It is here that we translate data into insights, demonstrating how DL can revolutionize the field of skin cancer detection.

Chapter 5, serves as a culmination of our research journey. We summarize results and their implications for healthcare, emphasizing the significance of our findings in the context of skin cancer diagnosis. Moreover, we offer valuable recommendations for future research, outlining the paths that researchers can explore to further advance this critical field. This chapter underscores the transformative. potential of DL in dermatology and the bright prospects it holds for improving patient outcomes and healthcare efficiency.

1.13 SUMMARY

This chapter provides a comprehensive introduction, covering the anatomy of the skin, various types of skin diseases, methods for diagnosing skin diseases, skin imaging techniques, and CAD systems for skin disease diagnosis. Additionally, it briefly introduces CNNs, which play a essential role in design of the skin disease diagnosis model presented in this research. To establish the foundational understanding of the research, the chapter outlines the research's objectives and the structure of the subsequent chapters in the thesis. In the upcoming chapters, the work of previous researchers in the field of detecting skin diseases in dermoscopy images will be discussed.

CHAPTER 2

REVIEW OF LITERATURE

In the previous chapter we have discussed about various types of skin diseases, methods for diagnosing skin diseases, skin imaging techniques, and CAD systems for skin disease diagnosis and also CNNs. In this chapter we presented a comprehensive insight into the extensive reservoir of expertise amassed within this particular domain. It accentuates the progress, methodologies, and pivotal discoveries from prior research endeavors. Moreover, we will pinpoint significant voids in the existing body of literature, thereby emphasizing the compelling requirement for further investigations. By thoroughly exploring the most cutting-edge knowledge, we establish the bedrock for the importance of our research in propelling the area of dermatology forward.

2.1. SKIN LESION SEGMENTATION

Skin lesion segmentation is a vital aspect of dermatology and computer based diagnosis, particularly for the early detection of skin cancer. This review explores the methods and techniques involved, focusing on the transformative role of DL, as demonstrated by [36]. Accurate skin lesion segmentation is essential for early diagnosis and appropriate treatment. Traditionally, this process relied on manual delineation by medical experts, a time-consuming and subjective approach. However, the subjectivity and variability associated with manual segmentation methods led to the exploration of computer-aided techniques, such as thresholding, edge detection, and region-based algorithms. These automated methods aimed to streamline the process and reduce inter-observer variability, though they faced challenges due to variations in lesion appearance, lighting conditions, and lesion complexity. The emergence of DL, particularly CNNs, has revolutionized skin lesion segmentation. CNNs have demonstrated their effectiveness in learning and representing complex patterns, making them well-suited for the diverse appearances of skin lesions. Researchers have developed DL models that accurately segment skin lesions in medical images, offering both speed and reliability, as showcased in the work of [51]. Large datasets; such as the International Skin Imaging. Collaboration (ISIC) dataset and the HAMl0000 dataset, have significantly advanced skin lesion segmentation.

These datasets, containing thousands of labeled images, have been instrumental in training and evaluating segmentation models. Benchmarking challenges, like the ISIC Skin Lesion Analysis Competition, have driven innovation and the creation of cutting-edge segmentation algorithms, exemplified by the research of [126].

Accurate skin lesion segmentation is instrumental in the early detection of skin cancer. Precise delineation of lesions allows for the analysis of their characteristics and features, aiding dermatologists in diagnosing skin conditions. CAD Systems, integrated with accurate segmentation algorithms, assist in distinguishing between malignant and benign lesions. This can possibly decrease the count of unneeded biopsies and improve patient outcomes, as demonstrated in [36] study in 2017.

Comprehensive survey on segmentation methods

This comprehensive survey on segmentation methods examines the profound impact of DL approaches across various applications, with a particular focus on Skin Lesion Diagnosis and Classification (SLDC) models [57]. In an in-depth analysis involving 19 research studies dedicated to skin lesion categorization, the authors adopted a CNN-based classifier and conducted a comparative evaluation of its performance against that of clinical practitioners [53]. Another study reviewed an automated skin cancer finding, emphasizing the role of image analysis and ML for skin cancer identification and avoidance [104]. A compelling investigation integrated patient health parameters into SLDC using CNN [61]. Additionally, a separate study explored skin lesion categorization through DLCNN architectures [111].

Comparative studies leveraging various CNN models for melanoma detection were meticulously conducted, effectively highlighting the advantages of DL in the domain of skin cancer diagnosis [66]. The pioneering task of deep convolutional neural networks in image classification, including the analysis of skin lesions, was established, notably contributing to the field [72]. Furthermore, research in skin lesion analysis with a specific focus on melanoma detection using DL networks was at the core of the exploration [78]. Notably, DL was also applied to skin cancer diagnosis through hierarchical architectures, offering valuable insights and potential solutions [17].

Various DL models, including fully convolutional-deconvolutional networks, were systematically applied for the skin lesion segmentation, as demonstrated in the work

of [135]. Furthermore, the automatic analysis of skin lesions using large-scale dermoscopy. images and deep. residual networks significantly advanced the state of the art [19]. Ensembles of DL methods proved to be pivotal in the context of segmentation of lesions in skin followed by analysis, and classification, exemplified by remarkable performance at the ISIC Challenge 2018.

Noteworthy is the introduction of a novel DL architecture for segmentation named the Pyramid Scene Parsing Network (PSPNet) [139]. However, it is essential to mention that the segmentation accuracy was primarily assessed over a limited number of training epochs. Building upon this foundation, an extension was developed that incorporated advanced transfer learning for segmentation, featuring ResNet50, MobileNet, and DenseNet-121 [54]. Despite its potential, this approach encountered challenges related to model synchronization and optimization. Furthermore, U-Net was thoughtfully implemented for skin lesion segmentation, integrating the Tversky index for loss optimization [1]. However, it's worth noting that the difficulty of this approach grew as the number of layers expanded, which introduced certain limitations.

Lastly, the multi-layer residual convolutional neural network (MLRNet) emerged as a formidable approach for skin lesion segmentation, incorporating modified Gaussian and also guided image filters for noise removal [31]. Notably, MLRNet surpassed other methods in terms of performance and results.

These seminal contributions exemplify a diverse array of approaches to skin lesion segmentation, highlighting the dynamic evolution and innovation within the domain of DL for analysis of medical images.

Advancements in DT Learning for Skin Lesion Classification

In the area of DL-based transfer learning for classification tasks, several noteworthy studies have made significant advancements in achieving exceptional accuracy while simultaneously reducing the reliance on extensive datasets.

One remarkable example comes from the research conducted by researcher [43], which focused on the detection of MEL skin cancer. By harnessing ML techniques and image biomarker cues, their approach achieved an remarkable accuracy rate of 77%. This achievement underscores the potential of transfer learning in dermatological applications, especially in the context of skin lesion classification.

Another significant contribution to the field was made by scholars [105]. In their study, they employed pixel based fusion and multilayer feature lessening during the tests conducted on the ISIC-2017 and ISBI-2016 datasets. Their meticulous approach resulted in an outstanding accuracy of 94.9% for the classification of MEL. This work highlights the critical role of feature engineering and data reduction techniques in improving classification accuracy, lessening false positives, and enhancing the overall performance of DL model's. In an innovative approach to skin lesion classification, researchers [98] demonstrated the potential of feature extraction from skin lesions. Their methodology aimed to categorize different types of MEL while mitigating false positives. Notably, they experimented with various classifiers and found that the random. forest classifier exhibited the highest levels of accuracy and precision. This approach highlights the effectiveness of combining feature engineering with robust classifier selection in the context of dermatological applications.

Similarly, scholars [100] harnessed transfer learning by employing models based on AlexNet for skin lesion classification. Their approach yielded an remarkable accuracy rate of 85.8%. This result underscores the power of transfer learning with established neural network architectures to enhance classification tasks. In another significant study by [140], deep CNNs were trained using the ISIC-2016 dataset, ultimately achieving an F-score of 94%. This research emphasized the importance of considering data distribution-based inter-class differences when applying DL techniques to skin lesion classification.

Several other studies, exemplified by the work of [3], have leveraged the potential of transfer learning for classification tasks using datasets such as HAM1000. These studies often involved the utilization of models like AlexNet and VGG-16 to extract features, with support vector machines employed for the subsequent classification process. Collectively, these investigations serve as a testament to the versatility and potential of transfer learning, showcasing its effectiveness across diverse datasets, including ISIC and HAM10000, and its ability to progress the accuracy and effectiveness of skin lesion classification.

Advancing Skin Lesion Diagnosis with Ensemble 1earning and Deep Models

Recent research work in the area of dermoscopic lesion analysis has been particularly focused on leveraging ensemble learning-based techniques to achieve higher

accuracy. Ensembling, which involves combining multiple models, has demonstrated its effectiveness in improving the overall accuracy of various applications. In the context of SLDC, researchers have employed ensembles of DNN models, such as GoogleNet, VGGNet, and AlexNet. DL techniques have played a pivotal role in this domain, with various approaches like ANN, backpropagated-ANN, DenseNet 201, CNN-DG, DLCNN, and Hybrid CNN (HCNN) being extensively used. For instance, Nozdryn-Plotnicki and colleagues achieved remarkable success in the ISIC2018 sub challenge by implementing Ensembling CNN (ECNN) for SLDC. Additionally, transfer learning techniques using architectures like DenseNet, ResNet, and SENet were integrated, accompanied by loss optimization mechanisms. The complication of this work is notably heightened due to synchronization challenges that can arise when combining various models. Nevertheless, this approach has certain limitations, particularly in its ability to identify only a limited number of skin circumstances. Increasing the no. of layers in the models intensifies computing complexity, leading to higher loss and extended training times.

This comprehensive overview underscores the importance of ensemble learning-based techniques in dermoscopic lesion analysis. It highlights the role of DL methodologies, as well as the specific models and approaches employed to improve performance metrics of skin lesion diagnosis and classification.

2.2. HYBRID GAUSSIAN GUIDED FILTER

The Hybrid Gaussian Guided Filter (HGGIF) is a novel image filtering technique that combines Gaussian filtering and guided filtering, for image enhancement and noise lessening. This literature review explores the significance of HGGIF, its underlying principles, and its applications in image processing.

HGGIF is an image enhancement technique that leverages both Gaussian filtering and guided filtering [57]. The purpose of this design is to address challenges related to noise reduction and image enhancement across various applications, including tasks like image denoising, contrast enhancement, and preserving edge details.. The principles of HGGIF involve combining the smoothing properties of Gaussian filters with the guidance of the guided filter. The Gaussian filter serves as a preliminary step to reduce noise, while the guided filter refines the output by preserving the image's structural information, resulting in enhanced images with improved clarity and

reduced noise artifacts. HGGIF finds applications in diverse domains, from medical image processing to computer vision. In medical imaging, HGGIF can be employed for enhancing the quality of MRI or CT scans, improving the visualization of anatomical structures while reducing noise [70]. In computer vision, HGGIF can enhance the clarity of images for object detection and recognition tasks. One of the notable advantages of HGGIF is its ability to outperform traditional filtering methods in terms of noise reduction and image enhancement [132]. Comparative studies have shown that HGGIF yields better results, particularly in scenarios where preserving fine details and structures is crucial.

Despite its effectiveness, HGGIF is not without its challenges. The choice of appropriate parameters, such as the window size and regularization parameter, can impact the filter's performance. Ongoing research aims to develop automated methods for parameter selection and to adapt HGGIF to specific applications, ensuring optimal results.

2.3. MULTI-LAYER RESIDUAL CONVOLUTIONAL NEURAL NETWORKS

Segmenting skin lesions plays a crucial role in the early identification and discovery of skin cancer. Achieving precise delineation of skin lesion borders is a complicated task, prompting the investigation of different segmentation approaches. Initially, thresholding techniques, encompassing methods like Otsu, fundamental, global, adaptive and multi-level thresholding[101], were commonly utilized. Nonetheless, these approaches frequently encountered challenges in accurately defining the boundaries of skin lesions.

A significant breakthrough in the field came with the introduction of a morphological approach by Zortea and colleagues in 2017. While effective, this approach came with a downside: it required extensive initialization time and exhibited high computational complexity. Subsequently, researchers delved into clustering-based techniques. For instance, contributors in [131] employed the k-means clustering algorithm for skin lesion identification, but challenges arose due to the improper selection of k-neighbors, leading to suboptimal lesion localization. Similarly, scholars [97] utilized Fuzzy C Means (FCM) clustering, but sensitivity to noise and initialization difficulties resulted in imperfect segmentation. A promising alternative was found in DL-based segmentation approaches. In the study by [135], deep convolutional-deconvolutional

NN (CDNN) was used to achieve impressive results in skin lesion segmentation. Yet, this approach had a shortcoming—it did not consider training loss, thus limiting the network's performance and potentially eliminating crucial skin lesion features.

Researchers [78] introduced FCRN for skin lesion segmentation, securing a high rank in the ISIC2017 challenge. This method primarily focused on getting low level features for the task of segmentation. In another study by [19], Deep Residual Networks (ResNet) were utilized, resulting in a third-place rank in the same challenge. However, a limitation of this procedure is the absence of training loss calculation and optimization.

The research landscape primarily centered around the ISIC 2017 challenge initially, but there was a notable shift towards the ISIC-2018 challenge. In these studies, various DL architectures and models, including PSPNet, MobileNet, DenseNet-121, ResNet50, and U-Net, were explored. Conventional segmentation methods faced a series of challenges, including inaccurate segmentation of lesion, lower accuracy; higher computational complexity, and limited applicability to specific skin lesion classes. Moreover, these methods lacked effective pre-processing approaches, resulting in the ineffective removal of noise and lesion artifacts, thus diminishing segmentation performance.

2.4. DEEP TRANSFER LEARNING NETWORK

In recent years, the field of dermatology has witnessed a transformative shift driven by advancements in DL, particularly CNNs, which have been applied to skin lesion analysis with remarkable success [36]. These neural networks have proven effective in both to identify and categorize skin ailments, offering the potential for early diagnosis and treatment [51]. This literature review explores the application of DTLNet, a DTL based hybrid model, in this context.

Transfer learning is a key component of DTLNet, which capitalizes on pre-trained models to enhance its performance. By utilizing models trained on extensive datasets like ImageNet, DTLNet can be fine tuned for analysis of skin lesion, reducing the amount of data required for training and improving its ability to generalize [84]. This approach addresses a significant challenge in the field, where obtaining large and high-quality dermatological datasets can be a cumbersome process [126]. Hybrid models, as exemplified by DTLNet, present a promising path forward for skin lesion

analysis. These models combine various neural network architectures and techniques, aiming to leverage; the strengths of several DL approaches. In the case of DTLNet, this fusion involves transfer learning in combination with other techniques, such attention mechanisms [121]. The synergy achieved through hybridization contributes to enhanced performance and adaptability. Advanced models, including Inception, DenseNet, and ResNet, have laid the foundation for transfer learning in DTLNet [28]. These models have been instrumental in boosting the accuracy of skin lesion classification. However, they also present unique challenges, such as model interpretability and the potential for biases in training data. The literature should investigate how DTLNet addresses these challenges and whether it introduces new limitations in the context of skin lesion analysis [38]. Effective data augmentation and preprocessing are vital to the success of skin lesion analysis. DTLNet likely incorporates strategies to enhance its performance by generating diverse training examples. These techniques, when coupled with transfer learning, result in a more robust model capable of accurate diagnosis and classification [50].

Furthermore, the clinical implications of DTLNet in real-world scenarios are of paramount importance. It is crucial to assess how the performance of model compares to the dermatologists' proficiency in making precise and suitable diagnoses. DTLNet's potential to guide healthcare professionals in the field is a key consideration, and the literature should explore this dimension to gauge its practical utility [36].

Howver, DTLNet, as a deep transfer learning-based hybrid model, represents a significant development in dermatology. Its synthesis of DL, transfer learning, and hybridization offers the potential to advance the diagnosis and treatment of skin diseases. However, further research and clinical validation are necessary to fully understand its capabilities and limitations [121].

Skin Lesion Diagnosis and Classification (SLDC) segmentation methods

This section delves into the extensive array of methodologies developed by researchers within the area of segmentation of skin lesion and classification. In doing so, it not only highlights these innovative approaches but also comprehensively addresses the challenges and limitations that every method encounters. These methodologies cover a spectrum of techniques, ranging from conventional image processing methods to cutting-edge DL algorithms, reflecting the dynamic landscape

of research in this domain. The overarching objective of this survey is to meticulously examine and assess the current body of research dedicated to segmentation of skin lesion and classification methodologies. This exploration includes a detailed analysis of various techniques, meticulously scrutinizing their respective strengths., limitations., and their performance in the realm of handling different skin lesion images. By undertaking this review, researchers aim to unearth frequent trends, pioneering advancements, and critical gaps within the existing landscape of skin lesion diagnosis methodologies. The insights garnered from this extensive survey extend beyond mere documentation. They serve to identify fertile ground for future research and development. By addressing the limitations and shortcomings of existing methods, this survey contributes to the blueprint for the creation of more robust, reliable, and efficient CAD systems for the diagnosis of skin 1esions. In essence, this survey is cornerstone in the continual evolution of diagnostic tools and holds the promise of advancing patient care in dermatology.

Skin Lesion Diagnosis and Classification (SLDC) segmentation methods are a critical area of research in dermatology, with far-reaching implications for the exact recognition and categorization of skin lesions. Within the domain of dermatology, early diag.nosis and classification of skin lesions are vital for the timely treatment of diseases, particularly skin cancers like melanoma. Researchers have developed various methods to address this challenge, incorporating a diverse range of techniques, from conventional image processing methods to cutting-edge DL algorithms. Recent advancements in DL have significantly influenced the landscape of SLDC segmentation methods. In particular, CNNs have demonstrated substantial promise in enhancing the accurateness segmentation of skin lesion and classification. For example, scholar [43] leveraged ML techniques and image biomarker cues to attain an remarkable accuracy of 77% in identifying MEL skin cancer. Additionally, researcher [105] employed pixel based fusion and multilayer feature reduction on datasets such as ISIC-2017 and ISBI-2016, resulting in a remarkable 95% accuracy for MEL classification. These studies underscore the power of DL techniques in improving segmentation accuracy. However, SLDC segmentation methods encounter their fair share of challenges and limitations. Skin lesions vary greatly in terms of size, shape, color, and texture. Moreover, issues like poor lighting or image artifacts

can complicate the segmentation process. These challenges emphasize the ongoing need for research to develop more robust and versatile segmentation methods. Contributor [140] highlighted the importance of considering data distribution-based inter-class differences, further emphasizing the complex nature of segmentation in the field of dermatology.

SLDC segmentation methods are not isolated techniques; rather, they often form integral components of CAD Systems. These CAD systems assist dermatologists and healthcare providers in rendering more precise and swift diagnoses. Consequently, the precision of lesion segmentation directly influences the efficacy of these systems in clinical practice. Moreover, the potential for further research and innovation in SLDC segmentation methods is vast. Researchers are continually exploring novel techniques and tools to enhance segmentation accuracy and address the multifaceted challenges posed by real-world clinical images.

Advancements in DL-Based Skin Cancer Classification: A Comprehensive Review of Recent Studies

In 2021, researchers [30] conducted research that introduced "MLRNet," a DL-based approach for automating the segmentation of early-stage melanoma within dermoscopic images. This study marks a significant stride in the domain segmentation of skin lesion, mainly focusing on the vital area of early melanoma detection.

Krishan and his team leveraged CNNs, known for their prowess in image segmentation tasks. By utilizing DL, they sought to streamline the process of identifying and delineating early-stage melanoma within dermoscopic images. The transition from conventional, rule-based systems to data-driven DL methodologies is noteworthy in itself, as it represents a shift towards more advanced and automated approaches. Their findings underline the substantial potential of DL techniques in achieving precise and automated skin lesion segmentation, particularly for early melanoma detection. Such automation is instrumental in expediting the diagnostic process, enabling healthcare providers to make timely and precise interventions. However, it's worth noting that the study lacks a comparative analysis with other existing segmentation methods. While MLRNet exhibits its capabilities, the absence of such comparisons leaves room for further exploration and validation. Comparative evaluations against other methodologies play a crucial role in understanding

MLRNet's relative strengths and weaknesses, contributing to a more comprehensive assessment of its performance. In 2021, scholars [30] conducted research that introduced "MLRNet," a DL-based approach for automating the segmentation of early-stage melanoma within dermoscopic images. This study marks a significant stride in area of skin lesion segmentation, mostly focusing on the vital area of early melanoma detection.

Krishna and his team leveraged CNNs, known for their prowess in image segmentation tasks. By utilizing DL, they sought to streamline the process of identifying and delineating early-stage melanoma within dermoscopic images. The transition from conventional, rule-based systems to data-driven DL methodologies is noteworthy in itself, as it represents a shift towards more advanced and automated approaches. Their findings underscore the substantial potential of DL techniques in achieving accurate and automated skin lesion segmentation, particularly for early melanoma detection. Such automation is instrumental in expediting the diagnostic process, enabling healthcare providers to make timely and precise interventions. However, it's worth noting that the study lacks a comparative analysis with other existing segmentation methods. While MLRNet exhibits its capabilities, the absence of such comparisons leaves room for further exploration and validation. Comparative evaluations against other methodologies play a crucial role in understanding MLRNet's relative strengths and weaknesses, contributing to a more comprehensive assessment of its performance.

In 2022, researchers [18] and their fellow researchers introduced an intriguing study and their primary aim was to create a sturdy system adept at distinguishing between benign & malignant skin lesions. To achieve this, the research harnessed the power of a hybrid DL approach, underpinned by various ML techniques. The study unveiled a promising fusion of ML methods that effectively addressed the challenging task of differentiating skin lesions based on their malignancy. By embracing a hybrid approach, the researchers harnessed the strengths of diverse methodologies, contributing to the overall effectiveness of their classification model. Their work highlighted the versatility of ML techniques when applied to the domain of dermatology. However, it is crucial to acknowledge one limitation that emerged from their study. The research presented a somewhat limited explanation of feature

selection and extraction processes incorporated into their model. While the model's effectiveness was evident, a more comprehensive elucidation of these feature selection and extraction methods would greatly enhance the interpretability of their model. This deeper understanding of the inner workings of their approach could offer insights into how the model makes its classifications, contributing to its transparency and trustworthiness in clinical applications.

In 2022, researchers [13] and his colleagues made a significant contribution with their research. In their study was dedicated to tackling the intricate task of classifying various complex types of skin cancer. To achieve this, they developed an intelligent system based on a two-stream deep neural network, which incorporated the fusion of different data streams and harnessed the power of Multi-Objective Firefly Optimization (MFO) for optimization. Their work marked a remarkable endeavor to address the challenges posed by complex skin cancer types. By employing a two-stream deep neural network, they effectively integrated multiple sources of information and leveraged optimization techniques to enhance the model's performance. This innovative approach was aimed at improving the classification accuracy of diverse skin cancer types, potentially offering a valuable contribution to the field of dermatology. Despite the evident strengths of their approach, one limitation of their study should be considered. The research did not provide a direct comparison with other fusion approaches for skin cancer classification. While their fusion and MFO optimization techniques showed promise, a comparative analysis with alternative fusion methods would have added further depth to their work. Such a comparison could have shed light on the specific advantages of their proposed fusion method and how it performs in relation to other existing techniques, ultimately contributing to a more comprehensive understanding of their intelligent system's capabilities.

In 2022, a notable contribution to the area diagnosis of skin lesion and classification was made by Puneet Thapar and their research team. Their study, titled "A innovative combined DL method for skin lesion segmentation and categorization," centered on the critical task of separating the region of interest in dermoscopy images. To achieve this, they devised a novel hybrid DL approach, integrating advanced techniques for both segmentation and classification, which reflects the complex nature of the task.

Their work showcased the potential of DL in enhancing the accuracy of skin lesion segmentation. Moreover, they incorporated efficient loss optimization techniques, which can significantly contribute to the reliability and precision of the segmentation process. By focusing on the region of interest, they aimed to facilitate a more targeted analysis of dermoscopy images, a crucial aspect of dermatological practice. However, it's important to make a note that the study had a limitation. While they successfully utilized the Grasshopper Optimization Algorithm (GOA) for efficient loss optimization, the research did not provide a detailed explanation of the parameter settings for GOA. This omission represents a gap in the study, as a clear understanding of parameter tuning is vital for replicability and broader applicability of their approach. Addressing this limitation by offering insights into the parameter settings for GOA would not only enhance the transparency of their methodology but also enable other researchers to implement and build upon their work with more ease and accuracy.

In 2022, A scholar [112] made research concentrated on the implementation and application of stacked ensemble models in the context of early melanoma detection. One of the notable aspects of this work was its commitment to creating an ensemble model that not only enhanced accuracy but also promoted transparency and explainability. To achieve this, the study incorporated transfer learning techniques and explainable CNNs. These innovations contributed to a more interpretable and understandable approach to melanoma detection, which is essential for building. trust and confidence in the medical field. Nonetheless, it's essential to acknowledge a limitation in this research. While the study successfully introduced an ensemble model for improved melanoma detection, it fell short in providing an in-depth analysis of the ensemble model's performance. To fully appreciate the advantages and potential of the ensemble approach, a more extensive evaluation is needed. Such an evaluation could elucidate the ensemble model's strengths, which are particularly valuable in medical contexts, where transparency and performance are paramount. By addressing this limitation, future work can provide a a deeper insight into the effectiveness of this explainable stacked ensemble model for melanoma skin cancer detection.

In 2022, researcher [106] and her team made a noteworthy contribution to the domain detection of skin cancer and segmentation with their study. This research was primarily focused on the critical task of distinguishing between skin lesions. One of the strengths of their work was the utilization of transfer learning-based feature extraction. By leveraging established features extracted from pre-trained models, their approach demonstrated promise in enhancing the accuracy and reliability of skin lesion classification, a pivotal task in dermatology and healthcare. However, it's crucial to acknowledge a limitation in this study. While the research successfully introduced a deep convo1utional approach for detection of skin cancer, it offered a partial discussion on feature optimization, specifically using the Grasshopper Optimization Algorithm (GOA). Feature optimization is a fundamental component of improving classification accuracy and model performance. Therefore, a more comprehensive exploration and insight into feature optimization using GOA could provide a valuable enhancement to their methodology.

By addressing this limitation, future work can refine the feature extraction process and potentially uncover additional features that contribute to more accurate and reliable skin cancer detection. This further exploration could lead to advancements in the field of dermatology and ultimately benefit patients by improving the precision of skin lesion diagnosis.

In 2022, an academic [2] and their colleagues introduced a research study and their work was dedicated to developing an innovative hierarchica1 framework for segmentation of skin lesion, which included a 3 step super pixel process of segmentation. One of the commendable aspects of their research was the introduction of a structured and hierarchical approach to skin lesion segmentation. This framework offered a promising method for effectively distinguishing between different regions of interest within dermoscopy images, which is a critical aspect of skin lesion analysis. However, it's essential to acknowledge a limitation in their study. While their hierarchical three-step super pixel segmentation process showcased effectiveness, the research did not include a comparative analysis with other existing segmentation approaches. Comparative analysis is valuable for assessing the relative advantages of a new methodology, and its absence in this study leaves room for a additional inclusive understanding of the framework's performance. Incorporating comparative

evaluations with other segmentation approaches could give precious insights of strengths and weaknesses of the proposed hierarchical framework. This comparison might highlight its unique contributions and help scholars and professionals in dermatology make informed decisions about the most suitable segmentation methods for their specific needs.

In 2022, researcher [10] and their research team carried out a study titled "Melanoma Detection Using DL-Based Classifications." Their research focused to improve the accuracy and precision of melanoma lesion identification by focusing on precise lesion zone removal. They employed an innovative approach that incorporated ESRGAN, which stands for improved Super-Resolution GANs. One of the notable strengths of their work was the application of DL techniques, particularly ESRGAN, to enhance the resolution and clarity of dermoscopy images for precise lesion zone removal. This approach held the potential to provide detailed and precise analysis of skin lesions, which is crucial in dermatology practice. on the other hand, it is essential to admit a limitation within their study. The research did not encompass a comprehensive validation process on diverse skin lesion images. Dermoscopy images can vary significantly due to differences in skin types, ethnicities, and lesion characteristics. Therefore, a more extensive validation process involving a broader range of skin types and lesion variations is important to confirm the robustness and consistency of their model in real-world clinical scenarios.

Broader validation would enable researchers and healthcare practitioners to have greater confidence in the effectiveness of their approach, as it would demonstrate its ability to perform consistently across diverse patient populations. Additionally, it could highlight the adaptability of their methodology to various clinical settings, ultimately improving its clinical utility in the finding and managing of skin lesions.

In 2023, researchers [20] conducted a study titled "Segmentation of skin cancer using fuzzy U-network via DL." Their research was dedicated to the crucial task of accurately segmenting afflicted regions in skin cancer images, a fundamental aspect of skin lesion diagnosis and treatment planning. To achieve this, they employed the innovative Fuzzy U-net, a DL model, and harnessed the May Fly Optimizer as part of their methodology.

Their work represents a notable advancement in the domain analysis of skin cancer images. The application of DL models, like the Fuzzy U-net, offers a powerful and efficient approach to segmenting afflicted regions within skin cancer images. This has the capacity to markedly improve the precision of diagnosis and facilitate more effective treatments for patients. Despite these strengths, it's important to acknowledge a limitation within their study. The research did not provide an extensive comparison with other optimization methods commonly used in the area of healthcare. Comparative analysis plays a pivotal part in ascertaining the advantages and disadvantages of specific optimization techniques. By omitting a more detailed comparative evaluation, the study missed an opportunity to highlight the strengths and distinctiveness of their chosen May Fly Optimizer and provide valuable insights for the research community. Further comparative analysis involving a broader range of optimization techniques would shed light on whether the May Fly Optimizer is indeed superior to other approaches or under what specific circumstances it excels. This additional information could help researchers make informed choices when selecting optimization methods for their own projects and contribute to the ongoing enhancement of skin cancer segmentation techniques.

In the study by researcher [93], the researchers aimed to create an advanced framework, SCDNet, for the multiclassification of skin cancer. This framework, which combined Vgg16 and CNN architectures, was designed to handle both segmentation and classification tasks for skin cancer lesions.

The major goal of their investigation was to implement a complete solution for accurate labeling of various skin cancer types based on dermoscopy images. Vgg16, a well-known DL architecture, was integrated with CNNs to improve the model's ability to analyze these images effectively. Despite demonstrating significant potential, one limitation of the study is the need for more extensive validation on larger and more diverse datasets. This expansion in the validation process would ensure that the SCDNet framework can effectively handle the full spectrum of skin cancer cases encountered in real clinical practice. In summary, academic [93] research represents a notable advancement in the field of skin cancer diagnosis, offering a promising framework for multiclassification. The model's combination of Vgg16 and

CNNs holds potential for improving diagnostic accuracy, but broader validation on different datasets is essential to authenticate its consistency in clinical scenarios.

In their study, conducted by scholar [74] , the researchers set out to address the critical issue of skin cancer detection. Their proposed solution, the U-RP-Net, leveraged the U-Net architecture in combination with Aquila Whale Optimization as an optimization strategy. The main objective of their work was to implement a model that could effectively detect skin cancer, contributing to earlier diagnosis and treatment of disease. The combination of the U-Net architecture with Aquila Whale Optimization represents an innovative approach to improving model's segmentation capabilities, thereby improving the overall detection accuracy. Despite the promise shown by their approach, one limitation of the study is the relatively limited comparison with other optimization techniques. To get a more complete thoughtful of the effectiveness of their chosen optimization approach, it is essential to conduct comparative analyses with other optimization methods commonly employed in the field. Such analyses would shed light on the advantages and potential areas for improvement in their proposed U-RP-Net.

In summary, researcher [74] explained a innovative approach to detection of skin cancer through the U-RP-Net, combining the U-Net with Aquila Whale Optimization. While their approach holds promise, further comparative analysis with other optimization techniques is required to provide a more comprehensive assessment of its effectiveness in enhancing skin cancer detection accuracy.

The studies discussed collectively make significant contributions to the field lesion diagnosis of skin, specifically within the context of DL methodologies. These research endeavors encompass a variety of approaches, each offering unique strengths and revealing certain limitations. While the individual studies have advanced our understanding of skin cancer diagnosis, there is a need for further research and comparative analyses to address some of the limitations highlighted in these studies. Such efforts are crucial for improving the correctness and reliability in diagnosis of skin cancer tools, ultimately helpful for patients and healthcare providers in the field of dermatology.

2.5 ADVANCEMENTS IN SKIN LESION DIAGNOSIS

This section provides an encompassing view of the work related to skin lesion diagnosis, highlighting significant studies and contributions in the field. The historical perspective of this domain can be traced back to the late 20th century when image analysis and ML started making their way into dermatology. In the initial stages, the focus was on rule-based systems and feature extraction techniques aimed at distinguishing benign from malignant lesions. Although these early endeavors were groundbreaking, they lacked the robustness and generalizability that modern DL methods offer (Bosserhoff et al. 1997).

A significant turning point in the field was the introduction of DL techniques in skin lesion diagnosis. Contributor [36] made a pioneering contribution by developing a DL model capable of classifying skin cancer with dermatologist-level accuracy. Their model, trained on a extensive dataset of skin lesion images, showcased the potential of DL to provide precise and reliable diagnoses. The study even indicated that DL had the potential to outperform human dermatologists in distinguishing between benign and malignant lesions. Building on researcher [36] work, subsequent research explored the utilization of transfer learning in dermatology. Scholar [126] introduced the HAMl0000 dataset, a vast group of dermatoscopic images, and harnessed transfer learning techniques to adapt DL models for skin lesion classification. This approach significantly reduced the necessity for extensive labeled data by reusing pre-trained models, making DL more accessible to smaller dermatology clinics and research teams.

In addition to classification, accurately localizing disease-affected regions within skin lesion images is a pivotal aspect of diagnosis. Academic [84] introduced DL techniques for lesion segmentation and localization. Their work highlighted the potential of DL in pinpointing areas of concern within images, which can greatly aid dermatologists in focused analysis and diagnosis. The development of these localization methods has notably improved the overall diagnostic process. While DL has made remarkable progress in skin lesion diagnosis, certain challenges persist. These challenges encompass the requirement for huge and different datasets to enhance model generalizability and the need to address interpretability issues associated with DL models. Future research activities are anticipated to tackle these

challenges and explore innovative techniques to further enhance diagnostic accuracy and efficiency.

To summarize, the integration of DL methods has brought about a transformative shift in the field of skin lesion diagnosis. Seminal studies by [36], [126], and [84] have laid the foundation for advanced diagnostic tools. The ongoing pursuit of extensive and diverse datasets, along with the refinement of DL algorithms, holds promise for achieving even more precise and well-organized skin lesion diagnosis in the future.

Exploring DL in Skin Lesion Diagnosis

In 2022, contributors [4], and their research team conducted a study and their primary focus was on ASRGS-OEN for melanoma detection. To achieve this, they employed an EfficientNet model and fine-tuned it with FPA (Feature Pyramid Attention) to enhance classification efficiency. This research demonstrated the promise of their model as an efficient tool for classification of skin cancer, addressing the common issue of imbalanced datasets in dermatological diagnostics. By using DL techniques and feature augmentation, they aimed to progress the accuracy and consistency of the classification process. However, the study revealed a specific limitation that requires consideration. The validation of their model, while showing positive results, was somewhat restricted in its scope. This limitation pertained to the extent of dataset diversity involved in the validation process. The research could benefit from more extensive validation across a broader range of datasets. A comprehensive validation process would not only reinforce the credibility of their findings but also provide insights into the generalizability of their classification system. The working of the model across diverse datasets is important in determining its real-world applicability and practicality.

In summary, the work by contributors [4], and their research team introduced an innovative DL-based approach to skin cancer classification, with a specific focus on imbalanced datasets. Their utilization of ASRGS-OEN and FPA fine-tuning in conjunction with the EfficientNet model displayed potential for improving melanoma detection. Nevertheless, the study's limited validation on a variety of datasets suggests an opportunity for more extensive exploration, enabling a more wide-ranging understanding of the model adaptability to several clinical scenarios.

In 2022, researchers [83] and their research team delved into the field of skin cancer diagnosis with their study. The central aim of their research was to determine the most effective approach for staging skin cancer using hyperspectral microscopic imaging. In doing so, they brought Augmented Intelligence enabled Deep Neural Networking (AuDNN) into the spotlight, a technique that surpassed traditional CNNs for the analysis of dermoscopy images. Their research provided valuable insights into the performance of AuDNN, indicating its superiority over CNNs in this specific context. This approach had the potential to revolutionize the staging of skin cancer, bringing more accuracy and reliability to the diagnostic process. Nonetheless, one noteworthy limitation surfaced in their study. While they demonstrated the effectiveness of AuDNN in comparison to traditional CNNs, they did not explore or compare it with other advanced CNN architectures. The absence of comparative analysis with alternative advanced CNN models left a gap in understanding the distinctive advantages of AuDNN in comparison to other advanced techniques. In conclusion, researchers [83] and their research team made significant contributions in the area of skin cancer staging through the utilization of hyperspectral microscopic imaging and the introduction of AuDNN. Their study revealed the superior performance of AuDNN in comparison to conventional CNNs for dermoscopy image analysis. However, for a more comprehensive perspective on the strengths of their approach, a future direction may include conducting comparative analyses against other advanced CNN architectures, enabling the broader dermatological community to appreciate the distinct advantages of their innovative method. In 2022, scholars [103] and their research team delved into the field of skin cancer detection with their study. Their research introduced a novel approach known as Multi-Site Cross-Organ Calibration based DL (MuSClD) for recognition of melanoma.

Their research introduced a promising procedure for improving the recognition of melanoma, a critical aspect of early cancer diagnosis. MuSClD leveraged the power of transfer learning to improve the accuracy and consistency of skin cancer detection. It represented an important step forward in utilizing DL methodologies for this purpose.

However, one noteworthy limitation surfaced in their study. While they introduced the innovative concept of Multi-Site Cross-Organ Calibration, the study provided a

limited explanation of this specific process. The absence of detailed information about the cross-organ calibration process left gaps in understanding their methodology. To fully appreciate the advantages and inner workings of MuSClD, a more comprehensive explanation of the cross-organ calibration process would be invaluable. In conclusion, scholars [103], and their research team made a notable contribution to skin cancer detection with the introduction of MuSClD, a technique based on transfer learning. Their innovative approach showed significant promise in improving the detection of melanoma. To enhance the broader understanding of their methodology, future research endeavors may focus on providing further details and insights into the cross-organ calibration process, thereby enabling the dermatological community to fully grasp the potential of this novel technique.

In 2022, researchers [68], and their team of researchers conducted a study. Their research aimed to enhance the classification of melanoma, a critical aspect of skin lesion diagnosis. Their study introduced an innovative approach in the form of a novel DCNN, which they applied to the HAM10000 database. Additionally, they utilized an Improved Super-Resolution GAN preprocessing technique to improve the resolution of dermoscopic images, further enhancing the quality of their input data. However, one notable limitation became apparent in their research. While they introduced novel methodologies and preprocessing techniques, their study lacked a detailed evaluation of the classification performance. A thorough evaluation is essential to gain insights into the model's effectiveness, its capability to correctly categorize melanoma, and its potential for practical application in clinical settings. In summary, researchers [68], and their research team made a notable advancement in the realm of melanoma categorization with their innovative ESRGAN preprocessing. The potential benefits of their approach are evident; however, to fully comprehend its strengths and weaknesses, further research efforts should concentrate on conducting an extensive evaluation of the classification performance. This comprehensive evaluation is pivotal for the eventual adoption of their model in real-world dermatological practice.

In 2023, contributors [118] undertook a research project titled "Automated Skin 1esion Diagnosis and Classification Using 1earning Algorithms." Their study focused on utilizing DL (DL) techniques for the purpose of melanoma detection in whole slide images. An integral component of their research involved the recognition and

classification of skin lesions using whole slide images (WSI). Their study represented a noteworthy endeavor in the field of dermatology, demonstrating the potential of DL methods to contribute to more efficient and accurate melanoma detection. By applying DL to whole slide images, they aimed to enhance the capabilities of automated skin lesion diagnosis. However, one limitation of their research emerged. While their work showcased the effectiveness of DL-based melanoma detection and classification using WSI, the study had a limitation in terms of limited benchmarking against other approaches that utilize whole slide images. A more comprehensive comparative analysis involving other WSI-based methodologies would provide valuable insights into the unique advantages of their chosen approach. In conclusion, contributors [118] research represents a valuable contribution to the domain of automated diagnosis of skin lesion and c1assification. Their innovative use of DL for detection of melanoma and subsequent c1assification using WSI has promising implications for dermatological practice. However, to gain a more holistic understanding of their approach, further research should focus on comparative analysis to elucidate the specific strengths and advantages of their chosen methodology within the context of whole slide image-based skin lesion diagnosis.

In 2023, scholar [73] and their team conducted an innovative study and the research primarily centered around the development of an automatic method for melanoma detection, a critical aspect of skin cancer diagnosis. To achieve this, they harnessed the capabilities of a pre trained deep CNN model and introduced a hierarchy of c1assifiers.

Their study represented a important stride in the area of skin lesion diagnosis, especially in automating the process of melanoma detection. The integration of DL techniques, such as a pre-trained CNN model, is a promising approach to achieving accurate and efficient classification of skin cancer. However, a limitation in their research emerged. While their work showcased the potential of AuDNN for skin cancer classification, it had a limitation in providing a detailed clarification of the tree of c1assifiers and its efficacy within the proposed framework. Further insights into the internal workings of this aspect of their methodology would enhance the transparency and interpretability of their model.

In conclusion, contributors [73] represent a helpful contribution to skin cancer classification and prediction. Their pioneering strategy involving the utilization of a pre trained deep CNN model and the creation of the AuDNN framework holds the promise of making a substantial mark in the domain of dermatology. Nevertheless, to further advance their research, a more comprehensive understanding of the tree of classifiers and its role within their framework is needed to ensure that it is an effective component in the automated melanoma detection process.

In 2023, scholars [6] embarked on a significant research endeavor and their study is positioned at the forefront of the field, striving to attain accuracy of dermatologist-level in the classification of skin cancer, particularly melanoma. To accomplish this challenging task, they introduced a DL system with residue connections, an innovative approach within the domain of dermatology. The use of residue connections in their DL model represents an advancement in the quest for accurate melanoma identification from dermoscopy images. Residue connections, also known as residual connections, have proven to be successful in enhancing the training and performance of DNNs. By implementing this architecture in their model, [6] to enhance the robustness and accuracy of melanoma classification. However, their research does have a limitation. The study primarily focused on a specific network architecture that incorporates residue connections, but it had a limitation in the limited exploration of different network architectures. Exploring alternative architectures and comparing their performance with the one used in their study could offer precious insights in to the comparative advantages and disadvantages of different DL models. Such a comparative analysis could lead to further improvements and a better understanding of which architecture is best suited for dermatologist-level skin cancer classification.

In summary, scholars [6] research signifies a notable milestone in the field of dermatology by striving to attain dermatologist-level skin cancer classification. Their use of residue connections in a DL model showcases innovative thinking. Nevertheless, for further enhancement and a deeper understanding of model performance, future investigations should encompass an exploration of various network architectures and a comparative ana1ysis to determine the efficient approach for skin cancer classification.

In the year 2023, a group of researchers and their collaborators, as documented in reference [137], undertook pioneering investigations under the title "Multi-site cross-organ calibrated DL (MuSClD):" Their research constitutes a notable advancement in the automated finding of non-melanoma cancer, placing specific emphasis on the identification of multi-stage melanoma through dermoscopy image analysis.

One of the notable strengths of their research lies in the introduction of a practical preprocessing method for de-noising dermoscopy images. Dermoscopy images are often affected by noise, which can hinder the accuracy of automated diagnosis. [137] recognized the significance of image quality and employed an effective de-noising technique. This innovative preprocessing step is a valuable addition to the field, as it contributes to more reliable and precise automated diagnosis. Nonetheless, their study does have a limitation. While the research demonstrates the effectiveness of their approach, it was conducted with a relatively limited scope of validation. The study had a limitation in the insufficient comprehensive validation across various identification stages. Broadening the validation procedure to include a range of skin lesion identification stages would yield a more holistic insight into the strengths and limitations of their MuSClD methodology. Thorough validation is pivotal for assessing the model's adaptability and resilience across different medical scenarios and non me1anoma skin cancer identification stages.

In conclusion, researchers [137] research in the field of automated Detection and Diagnosis of Non-Me1anoma Cancer presents a promising approach. Their method of preprocessing for removing noise in dermoscopy images is a significant contribution to improving the accuracy of diagnosis. However, future work should include more extensive justification on various steps of identification to enhance the understanding of their MuSClD approach and its applicability across a broader spectrum of clinical scenarios.

In 2023, scholars [65] and their team conducted an extensive study and their research addressed the critical task of extracting the Area of Interest using the ORACM (Object-Relationship Aware Co-attention Model) and achieved highly favorable results by employing the NSGA II for mu1ti-objective optimization. A notable strength of their research lies in their innovative approach to addressing melanoma detection and localization within histopathological whole slide images. The ORACM

represents a cutting-edge model that allows for the precise extraction of the Area of Interest, enhancing the efficien.cy and effectiveness of melanoma diagnosis. Furthermore, the employment of NSGA II for multi-objective optimization indicates a commitment to achieving the best possible results when it comes to localization and detection tasks.

However, their study does have a limitation, while they have demonstrated the efficacy of their method in.terms of achieving favorable results; the research lacks a detailed evaluation specifically focused on the effectiveness of the ORACM. A more thorough analysis of the performance, strengths, and weaknesses of this component of their approach is necessary to give a complete understanding of its impact on the overall melanoma detection and localization system.

In summary, scholars [65], and their team have made a noteworthy part to the area of melanoma detection and localization in histopathological whole slide images. Their utilization of the ORACM and NSGA II for multi-objective optimization showcases the potential for more accurate and reliable diagnosis of melanoma. However, further work should include a detailed evaluation of the ORACM to assess its specific impact and effectiveness within the context of melanoma detection and localization.

In 2023, researchers [65], and their team conducted an extensive study and, in their research, addressed the critical task of extracting the Area of Interest using the ORACM (Object-Relationship Aware Co-attention Model) and achieved highly favorable results by employing the NSGA II. A notable strength of their research lies in their innovative approach to addressing melanoma detection and localization within histopathological whole slide images. The ORACM represents a cutting-edge model that allows for the precise extraction of the Area of Interest, enhancing the efficacy and usefulness of melanoma diagnosis. Furthermore, the utilization of NSGA II for multi-objective optimization indicates a commitment to achieving the best possible results when it comes to localization and detection tasks. However, their study does have a limitation. While they have demonstrated the helpfulness of their method in terms of achieving favorable results, the research lacks a detailed evaluation specifically focused on the effectiveness of the ORACM. A more thorough analysis of the performance, strengths, and weaknesses of this component of their approach is

necessary to provide a comprehensive understanding of its impact on the overall melanoma detection and localization system.

In summary, academic [65] and their team have made a noteworthy part in the area of melanoma detection and localization in histopathological whole slide images. Their utilization of the ORACM and NSGA II for multi-objective optimization showcases the potential for more accurate and reliable diagnosis of melanoma. However, further work should include a detailed evaluation of the ORACM to assess its specific impact and effectiveness within the context of melanoma detection and localization.

In 2023, scholars [69] presented their study and in their research was focused on implementing a VisionTransformer (ViT) network classification model, which stands out as a distinct alternative to conventional CNNs for categorizing skin lesions into multiple classes. The study's innovative approach in adopting the ViT model is a notable aspect of their research. It demonstrates a commitment to exploring novel methods that can potentially enhance the accuracy and effectiveness of skin lesion classification. However, the research has a particular limitation that warrants attention. The research does not offer a comprehensive justification of how well the Stochastic Gradient Descent (SGD) optimization approach was employed in their work. A detailed elucidation of the application of SGD optimization is essential for transparency and reproducibility, enabling other researchers to replicate and build upon their methodology effectively.

In conclusion, the work by scholars [69] in 2023 offers a promising approach to multi class c1assification of skin lesions through the utilization of the VisionTransformer (ViT) model. The research's exploration of unconventional models is commendable. To further enhance its impact, providing a comprehensive explanation of the SGD optimization approach is recommended to facilitate a clearer understanding and successful replication of their methodology by the scientific community.

In 2023, academics [8] conducted a study and their research introduced a hybrid model that combined EfficientNets and metadata for fine-tuned Artificial Neural Network (ANN) classification using the Multiple-Input Single-Output (MISO) model. The study's innovative approach in utilizing wavelet transforms, deep residual neural networks, and the ReLU based Extreme 1earning machine is a notable contribution to the area of skin lesion c1assification. It showcases their dedication to enhancing the

correctness and efficacy of classification models for skin lesions. However, the research does have a particular limitation that deserves attention. The study does not provide a comprehensive validation of the effect of every input in the combined model. Understanding how each component contributes to the model's performance is crucial for further refining and optimizing the classification model. A more in-depth analysis of the individual impact of EfficientNets, metadata, and the MISO model could provide valuable insights for future research.

In conclusion, researchers [8] work in 2023 introduces a promising combined model for skin lesion classification that combines various techniques and components. Their research paves the way for more advanced classification models. To enhance the study's impact, it is recommended to conduct a thorough validation of the individual contributions of each input in the hybrid model, enabling a clearer understanding of their respective roles in achieving accurate skin lesion classification.

In 2022, scholars [30] presented their research aimed to leverage a deep transfer 1earning model by combining modified AlexNet and DLCNN to enhance the detection and c1assification of skin lesions. While their work is a noteworthy involvement to the area of skin lesion diagnosis, it is important to note a particular limitation in their research. The study encountered challenges in capturing disease-specific features, which subsequently resulted in low classification accuracy. Moreover, the classification accuracy appeared to be heavily dependent on the specific disease, suggesting that the model's performance may not be consistent across different skin conditions. This limitation highlights an essential area for future research and development. Improving the model's capability to seperate disease-specific parameters and ensuring consistent accuracy across various skin conditions is crucial for its practical applicability in clinical settings.

In summary, contributors [30] study in 2022 introduces a DL model for skin disease classification. While the model shows promise, addressing the challenge of capturing disease-specific features and enhancing classification accuracy, particularly for various skin conditions, is essential to realize its full potential as a diagnostic tool.

Collectively, the review contributed considerably in the area of skin lesion diagnosis by leveraging diverse DL techniques and methodologies. They suggest important insights in to artificial intelligence potential in improving diagnostic accuracy and

efficiency for skin cancer and melanoma. However, it is crucial to recognize that these studies also exhibit certain limitations that can guide future research and development. While these studies have demonstrated the effectiveness of their proposed methods, it's important to emphasize that research in the field of skin lesion diagnosis using DL is still evolving. The limitations mentioned in each study, such as the need for more extensive validation, better interpretability, and additional comparative analyses, highlight areas for further investigation. These limitations should be considered opportunities for future research to refine and enhance the proposed methodologies. By addressing these challenges, researchers can work towards developing more robust, accurate, and widely applicable diagnostic tools for dermatology.

In conclusion, these studies collectively contribute to the ongoing transformation of skin lesion diagnosis by leveraging DL techniques. They serve as stepping stones for further research work and innovation in the field, ultimately advancing the accuracy, reliability, and accessibility of skin cancer diagnostic tools.

2.6 RESEARCH GAPS

In the realm of skin lesion diagnosis using DL, certain research gaps have come to light that can significantly influence the direction of future investigations. These gaps not only align with the study's primary objectives but also provide a roadmap for addressing critical challenges in the field.

The first research gap revolves around the issue of

- Limited validation and generalizability

Previous studies have often fallen short in conducting comprehensive validation on diverse datasets. This research gap corresponds to the need for developing a robust pre-processing and segmentation approach capable of effectively handling a broader spectrum of skin lesion datasets. This initiative seeks to bolster the generalizability and adaptability of the proposed algorithm, ensuring its consistent performance across a wide array of clinical scenarios and disease stages.

Another salient research gap involves the

- Absence of comparative analyses

The lack of these comparative assessments hampers the ability to thoroughly evaluate the performance of novel classifiers. To bridge this gap, the research should

emphasize conducting in-depth comparative analyses that align with the overarching objective of assessing the proposed classifier's performance. These comparative evaluations will shed light on the strengths and weaknesses of the DL-based classifier, ultimately offering invaluable insights into its effectiveness and competitiveness.

Another critical research gap in this field is

- Transparency and interpretability constitute

Prior studies have often faltered in providing comprehensive explanations for essential components of their algorithms, impairing the overall understanding and replicability of these solutions. To address this gap, the research should place a heightened focus on delivering detailed and transparent explanations of the algorithm's inner workings, which should include a comprehensive overview of the optimization approaches employed. This enhanced transparency is paramount to facilitate the successful application of the solution within clinical settings.

The other research gap is

- Inconsistent accuracy across different skin conditions

It is an evidenced by previous research, is a compelling challenge to surmount. To address this specific research gap, it is essential to design the algorithm with a clear emphasis on effectively capturing disease-specific features. This approach will not only ensure consistent accuracy in the classification of skin lesions but also enable the practical applicability of the classifier within real-world clinical scenarios. This gap underscores the significance of achieving a high degree of accuracy and reliability in skin lesion diagnosis.

2.7 PROBLEM STATEMENT

The problem at hand involves the diagnosis and classification of skin lesions, with a particular focus on the application of DL-based techniques. However, several research gaps have been identified in this domain that pose significant challenges to the development of accurate and reliable solutions. One key research gap is the limited validation and generalizability of existing studies. Previous research often lacks comprehensive validation on diverse datasets, limiting the adaptability of algorithms to a broad range of skin conditions and clinical scenarios. Addressing this gap requires the development of a robust pre-processing and segmentation technique that can be universally applied to enhance the generalizability of proposed algorithms.

Comparative analyses represent another critical research gap. The absence of such comparisons in prior research hinders the thorough evaluation of novel classifiers. Conducting in-depth comparative assessments is essential for understanding the strengths and weaknesses of DL-based classifiers and assessing their effectiveness and competitiveness. Transparency and interpretability in explaining algorithm components constitute a significant research gap. Many previous studies have been deficient in providing detailed explanations of their inner workings, including optimization approaches. This lack of transparency impedes the understanding and replicability of proposed solutions, posing challenges to their effective application in clinical settings.

Lastly, the inconsistency in accuracy across different skin conditions is a pressing issue. This research gap emphasizes the need to design algorithms that can effectively capture disease-specific features. Ensuring consistent accuracy in skin lesion classification is crucial for practical applicability in real clinical scenarios. Thus, achieving a high degree of accuracy and reliability in skin lesion diagnosis remains a paramount challenge.

2.8 RESEARCH OBJECTIVES

This research encompasses three primary objectives that collectively aim to advance the area of skin lesion diagnosis through the application of DL. Each objective is rooted in the need to enhance accuracy, efficiency, and reliability in the diagnostic process, backed by literature evidence and supported by the motivation provided in the previous section:

Objective 1: ***To Achieve Pre-processing and Segmentation of the Skin Lesion Data for Input to a DL-Based Classifier***

The first objective of this research work is to develop a robust pre-processing and segmentation pipeline for skin lesion data, preparing it for input to a DL-based classifier. Skin lesion images often exhibit variations in lighting, noise, and artifacts, which can affect the performance of subsequent classification algorithms. Moreover, accurate segmentation is a fundamental step in isolating the region of interest within an image, allowing for more focused analysis. Numerous studies in the literature highlight the significance of pre-processing and segmentation in medical image analysis. For instance, a paper by Litjens et al. (2017) discusses the critical role of

pre-processing and segmentation in the context of prostate histology image analysis. The authors emphasize that proper pre-processing and segmentation techniques are essential for ensuring accurate classification results, and this principle can be applied to the domain of skin lesion diagnosis.

Objective 2: ***To Propose an Algorithm for Skin Lesion Diagnosis and Classification Using DL***

The second objective involves the development of an innovative DL-based algorithm for skin 1esion diagnosis and c1assification. DL has demonstrated substantial potential in various medical imaging tasks, with CNNs being at the forefront of these advancements. The proposed algorithm will leverage the power of DL to automatically learn discriminative features from the segmented skin lesion data and make accurate diagnostic decisions. Numerous studies in the literature have showcased the application of DL in medical image analysis, further emphasizing its efficacy in diagnosing skin lesions. For instance, a study by [36] demonstrated the superiority of DL models in classifying skin lesions, specifically melanoma. Their research provides compelling evidence of the capabilities of DL in addressing the complexity of skin lesion diagnosis.

Objective 3*: To Evaluate the performance of the Proposed Classifier against the State-of-the-Art Solutions by Means of Quality Metric Parameters*

The third objective involves the comprehensive evaluation of the proposed DL-based classifier. This evaluation will be conducted using state-of-the-art solutions as benchmarks and will employ quality metric parameters to assess its performance rigorously. Quality metrics are generally used in the literature to gauge the effectiveness of medical image c1assification models.

Numerous studies have utilized these quality metrics to estimate the performance of skin lesion c1assification models. For example, the International Skin Imaging Collaboration (ISIC) has organized challenges, such as ISIC-2019, where participants employ quality metrics to assess the efficacy of their skin lesion classification algorithms. These challenges have become standard benchmarks in the field and exemplify the importance of rigorous evaluation using quality metric parameters.

In summary, the research objectives presented here are anchored in the need to address the complexities and challenges in skin lesion diagnosis through advanced DL

techniques. The use of quality metrics and benchmarks from the literature underscores the rigorous evaluation and validation process that the proposed algorithm will undergo, ensuring its reliability and effectiveness in clinical applications.

2.9 RESEARCH SCOPE AND SIGNIFICANCE

- **DL Techniques for Skin Lesion Diagnosis**: This research primarily focuses on the application of advanced DL techniques, specifically CNNs, for skin lesion diagnosis. The scope encompasses the development of algorithms that can automatically analyze skin lesion images and make accurate diagnostic decisions. These methods leverage the capacity of DL to recognize intricate patterns and features within images, making them highly suited to the complex and diverse nature of skin lesions.
- **Pre-processing and Segmentation**: A critical aspect of this research is the pre-processing and segmentation of skin lesion data. Pre-processing methods aim to improve the quality of input data by addressing issues such as noise, artifacts, and variations in lighting conditions. Accurate segmentation is essential for isolating the region of interest within an image, allowing for precise analysis. The research will explore and develop methods for efficient pre-processing and segmentation that can enhance the overall performance of the diagnostic system.
- **Algorithm Development**: The study seeks to propose novel algorithms for skin lesion diagnosis and classification using DL. These algorithms will be tailored to address the specific challenges posed by skin lesion images, including the segregation of benign& malignant lesions. The development of these algorithms will involve extensive experimentation and optimization to ensure their effectiveness.
- **Performance Evaluation**: The research emphasizes a rigorous performance evaluation of the proposed algorithms. This evaluation will employ a comprehensive set of quality metric parameters and the AUC-ROC. Benchmarking against existing state-of-the-art solutions and large-scale datasets, such as ISIC-2019 and PH2, will be conducted to assess the algorithm's efficacy.
- **Clinical Implications**: Beyond the technical aspects, the research will explore the clinical implications of the developed algorithms. This includes an investigation into how these tools can be integrated into the workflow of healthcare professionals, such as dermatologists. The study will assess the potential for improved diagnostic accuracy, reduced subjectivity, and enhanced efficiency in clinical practice.

Significance

1. **Enhanced Accuracy in Diagnosis**: The profound importance of this research lies in its potential to substantially improve the accuracy of skin lesion diagnosis. The application of advanced DL techniques can enable early and accurate detection of skin cancer, leading to improved patient outcomes and, in some cases, life-saving interventions. The impact on individual patients and public health is substantial.
2. **Automation and Efficiency**: The development of automated tools for diagnosis of skin cancer offers the promise of streamlining the diagnostic process. By providing healthcare professionals with powerful diagnostic aids, dermatologists and clinicians can make more efficient, data-driven decisions. This can reduce the time required for diagnosis and, in turn, improve the speed at which patients receive appropriate care.
3. **Reduced Subjectivity and Error**: Transitioning from subjective visual examination to data-driven DL models minimizes the inherent subjectivity and potential for error in traditional diagnostic methods. This shift can contribute to more consistent and reliable diagnoses, reducing the uncertainty often associated with visual examinations.
4. **Transforming Dermatology**: The potential to revolutionize the field of dermatology is one of the most notable aspects of this research's significance. It has the capacity to introduce a new paradigm in skin cancer diagnosis and classification. By merging cutting-edge technology with clinical practice, it can reshape the way skin cancer is diagnosed and managed.
5. **Global Health Implications**: The global health impact of skin cancer is substantial, with increasing diagnosis rates, particularly in regions with high UV radiation exposure. The outcomes of this research can make a significant contribution to public health by enabling earlier interventions and ultimately saving lives. This is particularly relevant in regions where access to dermatologists may be limited.

2.10 SUMMARY

In this chapter we have seen an extensive literature survey on the existing methods for the various tasks pre-processing., segmentation., feature extraction and c1assification. Research gaps are identified alogn with the scope of the research and it’s significance.

Finally the research objectives are framed to bridge the gaps identified in the literature review. In the next chapter we will discuss about the detailed research methodology proposed to achieve the above mentioned objectives for skin lesion detection and classification with improved accuracy

CHAPTER-3

SKIN LESION SEGMENTATION USING HYBRID GAUSSIAN GUIDED FILTER WITH CNN

In the prior chapter we have gone through the extensive literature survey, gaps identified and objectives framed for improvement of accuracy in diagnosis. In this chapter we provided the information about one of the proposed model for skin lesion segmentation by using guassian and guided filter together with the help of multilayer residual network detail to implement the novel ideas and effective algorithms to segment the skin cancer images with improved accuracy

3.1. INTRODUCTION

Skin cancer has become a significant cause for concern in recent years, mainly due to the increasing emphasis on the significance of early recognition and effective treatment [14]. Within the realm of skin cancer, it can be categorized into 2 types: benign and ma1ignant. Among these, me1anoma stands out as the most life-threatening form, especially when compared to non-melanoma skin cancers. The growing incidence of melanoma underlines the critical significance of early diagnosis for the survival of patients [14]. Dermatologists, drawing upon their specialized knowledge, have turned to computer-assisted techniques for the early identification of melanoma. However, achieving high accuracy in this endeavor has proven to be a formidable challenge, leading to complications in the classification process [47]. In the pursuit of improving early skin cancer detection, several researchers have explored the application of image preprocessing techniques, which allow for the identification of skin cancer at its initial stages, subsequently leading to more effective therapeutic interventions [96]. To extend the scope and effectiveness of diagnostic procedures, it is crucial to establish robust frameworks for categorizing different skin diseases [14]. Multiple studies have been conducted about skin cancer recognition and classification, and these efforts have been furthered by the initiation of challenges by the ISIC since 2016. These challenges serve to officially verify the performance of participating teams and provide standardized datasets [50]. In response to these challenges, various authors have displayed a strong interest in developing new DL and ML architectures aimed at enhancing the accuracy of

segmentation and classification processes (Goyal et al., 2020). Hospitals around the world have begun to implement these advanced methods, which have been inspired and refined by the ISIC challenges, to improve the chances of individual patient survival (Gutman et al., 2016).

The efficacy of segmentation algorithms in the perspective of malignancy diagnosis is contingent on the specific segmentation method that's employed and the unique facets of medical images (Jagadesh et al., 2020). These segmentation algorithms fall into two broad categories: region and edge based. For algorithms based on region to perform accurate segmentation, the regions of interest in the image need to have a significant degree of similarity or homogeneity in their visual characteristics, while edge-based methods depend on the presence of strong edges for precise results (Jagadesh et al., 2020). Developing accurate segmentation algorithms for medical images, as well as images with issues like intensity inhomogeneity or weak edges, can pose significant difficulties. These challenges arise due to variations in image characteristics and the need to adapt segmentation techniques to address these issues effectively. In skin cancer diagnosis, skin cancer segmentation is an important task because skin lesions frequently exhibit unclear boundaries, uneven colour distribution, and irregular shapes [14]. Skin lesion segmentation requires advanced NN architectures and techniques to handle the variability and complexity of skin lesions effectively. Traditional DL models, though available, have faced limitations in achieving the maximum level of segmentation performance and have often resulted in increased computational complexity. To address these limitations, this work introduces the HGGIF filter, which is designed to eliminate noise, artifacts, and enhance color illumination [14]. Additionally, this work employs MLRNet for skin lesion segmentation, incorporating residual analysis into the process.

3.2. PROPOSED SKIN LESION SEGMENTATION

The HGGIF filtering step and the subsequent MLRNet segmentation stage are the two separate phases of the skin lesion segmentation model proposed in this study. In the initial phase, test skin lesion images serve as the input for HGGIF filtering. This filtering step serves a dual purpose, effectively removing noise and various artifacts while concurrently improving the color illuminations within the images. Following this pre-processing, the resulting filtered image is then passed through the MLRNet

model, which is specifically designed for the segmentation of skin lesions.

3.2.1. HGGIF Filtering

Gaussian filtering is a widely used image processing technique for noise removal and smoothing. It plays a crucial role in medical image preprocessing, particularly in enhancing skin lesion images for further analysis and segmentation. The fundamental idea behind Gaussian filtering is to blur the image using a Gaussian function, which helps in reducing high-frequency noise while preserving important image features such as edges and textures. In the context of skin cancer detection, Gaussian filtering is essential for improving the quality of dermoscopic images. Skin lesion images often contain artifacts, hair, and varying illumination, which can obscure important lesion boundaries. Applying Gaussian filtering helps in smoothing out these imperfections, enhancing the visibility of lesion regions and preparing the image for accurate segmentation.

Gaussian filtering uses a Gaussian kernel to convolve with the input image. The kernel is defined by the Gaussian function:

$$G(x, y) = (1 / (2\pi\sigma^2)) * \exp(-(x^2 + y^2) / (2\sigma^2))$$

where (x, y) are the coordinates of the pixel

σ is the standard deviation of the Gaussian distribution.

The filter assigns weights to the neighboring pixels such that the central pixel has the highest weight and the weights decrease with distance, following a bell-shaped curve.

In this research, Gaussian filtering is applied within the Discrete Wavelet Transform (DWT) domain on the LL (low-low) band coefficients of skin lesion images. This step specifically targets low-frequency noise and enhances the spectral domain of the image. By doing so, the filter improves image smoothness while retaining important lesion structures. The filtered image is later reconstructed into the spatial domain using the Inverse DWT and further refined using Guided Image Filtering (GIF).

The initial step in the proposed skin lesion seperation process is the HGGIF Filtering, which focuses on denoising skin lesion images within the Discrete Wavelet Transform (DWT) domain. This technique is visually depicted in Figure 3.1 and described. The DWT is an integral component in this phase, as it facilitates the decomposition of the input image into multiple bands using various directions, a method commonly found in image processing [26] [119]. As part of this

decomposition, directional coefficients are generated, a practice widely adopted to mitigate various forms of noise, including both spatial and spectral noise. This application of DWT in noise reduction is well-established in the literature [116] [23]. However, to further refine the denoising process, the Hybrid Gaussian Guided Image Filtering (HGGIF) is introduced. Its primary focus is to target the low-level noise reduction primarily found in the skin lesion image on the texture region. By systematically addressing these smaller noise sources, the outcome is not only rendered cleaner but also exhibits enhanced robustness and efficiency here by achieving superior outcomes compared to the best and most widely accepted methods or techniques currently available. [24] [87].

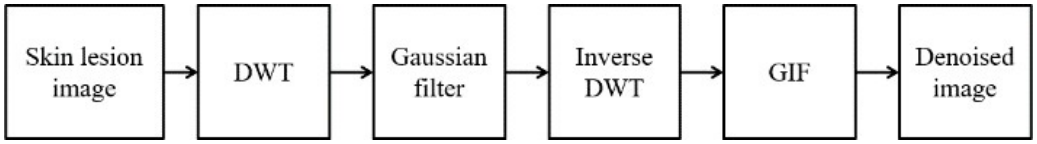

Figure 3.1 HGGIF in DWT domain

Skin Lesion Image: The process starts with a skin lesion image, which may contain various forms of noise and imperfections.

DWT: The first step is to apply the DWT to the skin lesion image. DWT decomposes the image into multiple bands or levels, capturing both high and low-frequency components in various directions. This transformation helps represent the image in a more structured and analysable form.

Gaussian Filter: In the DWT domain, the image undergoes a Gaussian filtering step. The Gaussian filter is used to smooth and denoise the image. Gaussian filters are popular in image processing for their ability to reduce noise while preserving image features. The goal of this phase is to eliminate any undesired noise artifacts from the DWT-transformed image.

Inverse DFT (Discrete Fourier Transform): After the Gaussian filtering, an Inverse Discrete Fourier Transform (IDFT) is applied on filtered image. This task is crucial as it transforms filtered image back to spatial domain, restoring it to its original form. The IDFT reconstructs the filtered image by reversing the DFT applied during the Gaussian filtering process.

GIF (Guided Image Filtering): Following the IDFT, the image is subjected to Guided Image Filtering (GIF). GIF is an image processing method that improves and polishes an image while preserving its edges and structure. It helps further denoise the image and can improve its overall appearance.

Algorithm

Guided Image Filtering (GIF) is an edge-preserving smoothing technique that enhances image quality by removing noise while retaining important structural features such as edges. Unlike standard filters that blur edges along with noise, GIF performs selective filtering guided by a reference image—often the input image itself.

The core idea behind GIF is to compute a locally linear model between the guide image (**I**) and the filtering input image (**P**). The result is a filtered output **Q** that preserves the edges of **I** while smoothing the noise in **P**.

For a pixel '*i'*, the filtering output q_i is modeled as:

$$q_i = a_k I_i + b_k \qquad \forall \quad \mathrm{i} \; \forall \mathbf{i} \in \mathrm{w_k}$$

Where:

- q_i: Output at pixel *i*
- I_i: Guidance image pixel
- $q_i = a_k I_i + b_k$: Linear coefficients in window $\mathrm{w_k}$

Denoised Image: The outcome of these steps is a denoised image. This final image is cleaner and more robust than the initial skin lesion image, with various noise sources eliminated. The denoised image is now better suited for further analysis and segmentation, as it presents a clearer representation of the skin lesion.

By applying these processes within the DWT domain, the method effectively targets and reduces noise in skin lesion images, ultimately improving the photos' quality and usefulness for upcoming diagnostic or segmentation tasks. The combination of Gaussian filtering, Inverse DFT, and GIF within the DWT framework helps to provide a comprehensive approach to denoising and enhancing skin lesion images.

3.2.2 HGGIF Algorithm

The Hybrid Gaussian Guided Image Filtering (HGGIF) procedure listed in Table 3.1 offers a thorough explanation of the advanced image processing method used to improve image quality and reduce noise in various types of images, including medical

images like skin lesion photographs. HGGIF combines the strengths of Gaussian filtering and Guided Image Filtering (GIF) within the DWT domain, creating a powerful tool for image denoising and enhancement. By utilizing DWT for decomposition, Gaussian filtering for noise reduction, Inverse Discrete Fourier Transform (IDFT) for image reconstruction, and GIF for guided smoothing, HGGIF achieves notable improvements in image quality and clarity. This algorithm is particularly valuable in medical image analysis, where precise and noise-free images are crucial for accurate diagnosis and further processing.

Input: Medical image of a skin lesion that requires analysis or processing.

Output: Result of applying pre-processing steps or techniques to the input image.

Table 3.1 HGGIF algorithm

Step 1: Loading the skin lesion image that is affected by noise This initial step involves importing noisy skin lesion image, which may contain various forms of noise and imperfections.
Step 2: Applying the DWT to divide the images with noise into various frequency components which are created using the filter banks such as LL, LH, HL and HH. In this, we employ the DWT to decompose a noisy skin lesion image into multiple bands. The DWT breaks down an image or signal into different frequency components at multiple scales, known as wavelet coefficients. The DWT achieves this by using filter banks such as LL, LH, HL, and HH. Each of these bands captures different frequency components and details within the image. Importantly, Non-sub-sampled directional filter banks is a method that is used here by DWT for multi-dimensional decomposition of the test image. This results in a more structured representation of the image.
Step 3: Gaussian filtering is used specifically on the LL (low-low) band coefficients. Now, Gaussian filtering is used specifically on the LL (low-low) band coefficients. LL band coefficients, which contain low-frequency information and often constitute the smoother areas of the image. Here, we apply Gaussian filtering to these LL coefficients. Gaussian filtering helps enhance the spectral domain of the image.

This step serves to reduce noise in the lower frequency components while preserving essential image features.
Step 4: Minimize the main Noises in Spectral Region. Following the Gaussian filtering, the resultant coefficients in the LL band now contain different region properties with the reduction of significant noise sources within the spectral region. This step is critical for improving the whole quality of the image and preparing it for further processing.
Step 5: Using the IDWT to combine the coefficients back into a single spectral band To recover a single spectral band from the filtered coefficients, we apply the Inverse DWT (IDWT). The IDWT reconstructs the filtered outcome, effectively transforming it back to the original spatial domain. This step is pivotal in restoring the image to its familiar format while retaining the benefits of noise reduction obtained in the spectral domain.
Step 6: The GIF (Guided Image Filtering) algorithm is applied to remove both high-level and low-level noise in the texture and spatial regions of the image High-level and low-level noise sources in the image texture and spatial areas are removed using GIF. This procedure improves the image's quality and makes a substantial contribution to denoising. GIF is a flexible method that successfully reduces image noise while preserving edges and fine details.

The result of these sequential steps is the preprocessed outcome, which is notably cleaner, more noise-free, and suitable for further analysis, segmentation, or diagnostic tasks. The HGGIF algorithm, with its combination of DWT, Gaussian filtering, IDWT, and GIF, is a valuable tool for enhancing image quality, particularly in medical image analysis, where accuracy and clarity are paramount.

3.3 PROPOSED MLRNet FOR SEGMENTATION OF SKIN LESION

In the field of medical imaging, precise skin lesions segmentation plays a key role in the timely detection, and subsequent treatment of any skin diseases, most notably skin cancer. Over recent years, by applying DL techniques to medical image analysis resulted in notable advancements in the accuracy and efficiency of disease detection. Among these innovations, the Multi-Level Residual Network (MLRNet) has emerged

as a noteworthy solution, tailored specifically for the meticulous segmentation of skin lesions. At the core of MLRNet's functionality, it is a DCNN architecture enhanced by the principles of residual learning. By allowing the training of extremely deep neural networks while addressing the vanishing gradient issue, residual learning made popular by researcher [58] has completely changed the field of deep learning. As a result, the integration of residual learning into MLRNet has elevated its performance, making it a innovatory tool in the skin lesion segmentation domain [58]. MLRNet is not just an isolated innovation but a product of extensive research and development aimed at tackling the challenges inherent in skin lesion analysis. This network's capacity for highly accurate segmentation has drawn substantial attention from researchers, healthcare professionals, and technology developers alike, thanks to its capacity to improve the accuracy and dependability of diagnostic procedures.

The significance of accurate skin lesion segmentation cannot be understated. By providing clear and precise delineations of skin lesions within medical images, MLRNet can expedite the identification and classification of skin diseases. This has the potential to significantly increase the effectiveness of dermatological diagnostics, which would lead to earlier interventions and improved patient outcomes. The method presented in this study employs MLRNet for the segmentation of skin lesion over conventional CNN and RNN methods traditionally are used for this task. MLRNet works well for processing 1-D time sequences, but it takes a particular method to adapt to the context of 2D skin lesion images. The 2D skin lesion photos are first scanned in the following directions: left to right, top to bottom, bottom to up, and right to left. This scanning procedure generates four distinct sequences. These sequences are then subjected to multi-layer processing to extract spatial dependencies and features. The outcome of every layer is summed, and the result is processed using a softmax classifier for the accurate segmentation of skin lesions. This technique makes good use of MLRNet's capabilities to increase skin lesion segmentation accuracy, especially when applied to 2D pictures.

Architecture

The proposed MLRNet is composed of a structured architecture that includes 18 convolutional layers, 1 recurrent layer, 4 layers of max pooling, 4 concatenation layers, and a sigmoid activation function, as visualized in Figure 3.2. These

components are organized into a total of 9 blocks. When a test input image is fed into MLRNet, it undergoes a series of processing steps within the convolutional layers. These layers serve the crucial role of extracting deep features from the test images. This feat is achieved through the application of many filters with varied kernel sizes. Specifically, 3 × 3 sized kernels are employed in the convolutional layers, while 2 × 2 kernels are utilized in the MaxPooling and dropout layers Furthermore, the network employs filters of varying dimensions, with 32, 64, 128, 256, and 512 filters being used in different layers. The structure of MLRNet can be further divided into two major components: up-sampling encoders and down-sampling decoders. Together, these elements enhance the network's ability to interpret and evaluate the input data, enabling efficient skin lesion segmentation.

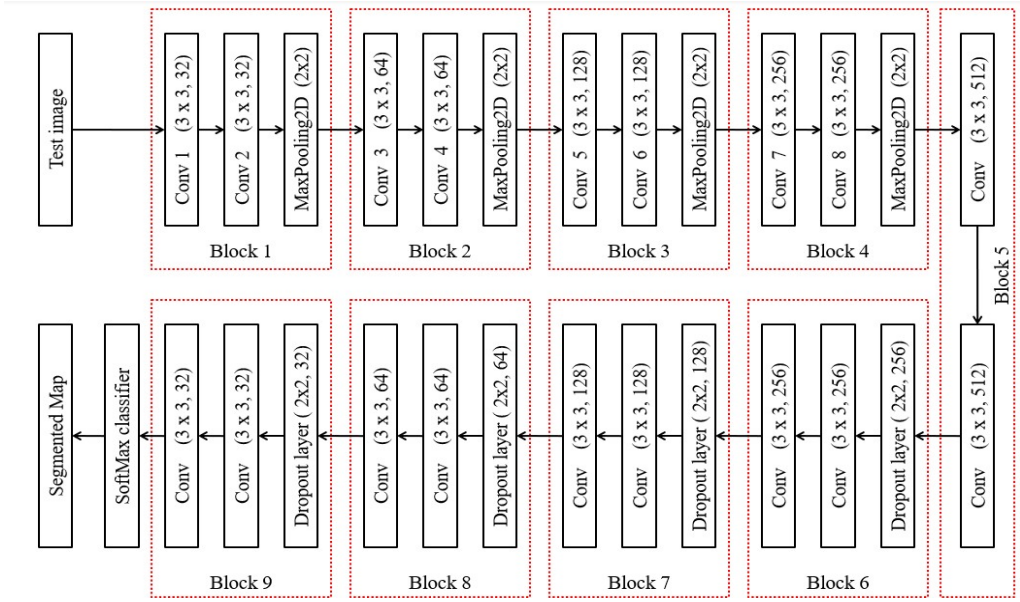

Figure 3.2 Proposed MLRNet for skin lesion segmentation

In each phase of the encoding and decoding, a structured convolution block and a triple residual decoder block are employed thoughtfully. In order for the network to process and extract significant features from the incoming data, these blocks are essential. Each convolutional block within the structured convolution block consists of three fundamental components: a convolutional layer, a batch normalization layer, and a ReLU. This combination of components is key to the block's function in feature extraction and processing. As the network proceeds in the encoder path and performs down-sampling, it demonstrates a notable characteristic. With each down-sampling

step, the number of feature channels effectively doubles. This expansion in feature channels is instrumental in capturing and representing increasingly complex features. Additionally, there are strategic connections in place between the encoder and decoder that jumps between the respective layers of feature maps. These connections ensure seamless information flow between the two parts of the network. They are critical for maintaining context and preserving the rich information extracted in the encoder when transitioning to the decoding phase.

The combination of structured convolution blocks, triple residual decoder blocks, and these well-planned connections empowers the network to effectively perform skin lesion segmentation with a focus on preserving crucial contextual information. The decoding process is enriched through the strategic use of skipping connections. These connections serve a dual purpose: they merge feature map information generated by an encoder module while simultaneously assimilating additional contextual and spatial information from the decoder block with low-resolution. This integration of information is a fundamental step in achieving comprehensive and accurate skin lesion segmentation. The core of this integration lies within the proposed triple residual decoder block, a powerful component of the network. This block, which builds upon a normalized standard 3 × 3 convolution operation, consists of a dual residual decoder structure. The dual residual decoder block incorporates spatial residual and channel residual elements, which are vital for processing the concatenated feature maps.

To further enhance performance, these three key components are engineered to utilize contextual information and weights. They play a pivotal role in selecting relevant regions, capturing spatial correlations between features, and directing density of the channel to facilitate essential channel interactions. The network can conduct extremely precise and context-aware skin lesion segmentation because to the clever distribution and processing of data and characteristics. The network's capacity to autonomously learn and modify its focus on different sizes and forms of targetted structures inside medical images is largely due to the residual convolutional module. This adaptability is a key strength, as it enables the model to implicitly identify and emphasize features that are highly relevant for a specific task, all while effectively suppressing the information from regions that are less pertinent in the input image. An

important aspect of the residual convolutional module's functioning is its ability to discern geographical regions that is by examining contextual information and activation signals provided by gating mechanisms which are acquired at coarser scales. This process ensures that the network captures and processes information in a context-aware manner. To achieve this, the input feature is scaled depending on residual coefficients computed from resampled grids, a procedure facilitated through trilinear interpolation. The residual factor derived from this scaling is instrumental in delineating the focal region of interest and identifying significant areas within the image. Finally, the input feature map is multiplied element-wise by a calculated residual factor to generate the output of the residual convolutional module. This process is essential to the network's flexibility and capacity to concentrate on the most important components of the input image, which enhances the network's efficacy in skin lesion segmentation. The gating mechanism serves as a critical decision-making component within the network. It is responsible for filtering and determining the usefulness of information acquired from the coarser scale. The primary objective is to eliminate noisy and irrelevant responses from skipped connections, ensuring that the network focuses on the most relevant and informative elements.

Before the execution of connection operation, the residual convolutional module performs a crucial task. It integrates and filters the neural activations, specifically selecting and forwarding only the activations that are highly pertinent for the task at hand. This operation is essential for ensuring that the network processes information that is contextually meaningful. The output from the skipped connections generates the extraction and fusion of complementary information from every sub-residual convolutional coding and decoding circuit. This integrated output is essential for maintaining the coherence and context-awareness of the segmentation process. Importantly, the residual convolutional blocks are processed linearly without involving any spatial support, distinguishing them from non-local blocks. Additionally, the down-sampling technique is applied to the gated signal effectively that reduces the resolution of the input feature map. This not only contributes to reducing the network's parameter count but also conserves computational resources, making the network more efficient and cost-effective in the segmentation of skin lesion. The network's performance is enhanced through the combination of spatial

residual and channel residual. This dual approach is integral to the network's ability to learn non-linear interactions and establish links that are non-repulsion between channels, thus improving the segmentation performance. While spatial residual focuses on capturing spatial relationships between features, channel residual is adept at grasping complex non-linear interactions. Consequently, both elements enhance one another, resulting in a more thorough comprehension of the material. An initial convolutional operation is used in the network's structural architecture to improve the input characteristics' non-linear representation. In addition to increasing the network's ability to train non-linearly, this technique helps minimize the number of parameters, which maximizes computing efficiency.

The incorporation of both spatial residual and channel residual occurs in parallel within the network. These two routes simultaneously focus on the regions of interest in both the spatial and channel dimensions, ensuring that the network captures and fuses pertinent information effectively. The fused output is then used as input for subsequent decoding operations, ultimately leading to improved segmentation results by considering both spatial and channel aspects of the data. Within the network architecture, up-sampling layers play a crucial role in learning middle-level visual patterns, while concurrently capturing spatial dependencies between these patterns. For the network to successfully comprehend and encode complex aspects in the incoming data, this dual functionality is necessary. The network's capacity to create a global representation of the image is facilitated by concatenate layers. These layers allow the network to comprehensively understand the overall image context and extract global representations. This is important in the skin lesion segmentation as it enables the network to capture a holistic understanding of the image.

To further enhance spatial dependency encoding, the network employs down-sampling convolutional layers. These layers refine the network's spatial understanding by processing the global representations, ultimately improving the quality of segmentation results. The final stage of the network's operation involves a SoftMax layer, which acts as a classifier. This classifier is instrumental in identifying and distinguishing between the affected skin lesion region and the normal tissue region. It does so by using a classification process, providing a clear delineation between the different regions of interest within the image. This classification output is a crucial

aspect of the network's skin lesion segmentation process.

Image Segmentation: A Step-By-Step Procedure

Step 1: Feature Extraction with Convolutional Layers

The goal of this first stage is to extract the necessary and crucial features from the input image so that the network can comprehend and use the data in the image efficiently. This phase of picture processing, which includes skin lesion segmentation, is crucial.

Neurons and Limited Input Region

A key component of this feature extraction procedure is convolutional layers. They function by employing neurons to process every pixel in the image. Convolutional layers use neurons that are only connected to a small or restricted portion of the input image in different areas of the image, in contrast to conventional fully connected layers where each neuron is coupled to every input neuron. This limited connectivity significantly reduces the total number of parameters in the network. By limiting the connections of neurons to local regions, convolutional layers effectively capture local patterns and structures in the image. This locality preserves important spatial information, making convolutional networks particularly effective for tasks like image analysis, as they can learn to detect patterns in various parts of the image.

Maps of Features (F) and Filters (W_k)

The creation of feature maps is the core of the feature extraction procedure, which are denoted as F. These feature maps are produced by applying multiple filters and capture data at various levels of abstraction.

Each filter, denoted by the symbol W_k, is in charge of identifying a certain kind of pattern or feature in the picture. Each filter is applied to the input data, and they can differ in size and shape. The features that the filter is intended to identify are extracted when the filter is applied since it convolves over the input.

Convolution Operation

The calculation of feature maps is achieved through a mathematical operation known as convolution. For each feature map F_k, the operation is expressed as:

$$F_k = \emptyset(W_k * F_k + b_k) \quad (1)$$

In this equation:

- 'F_k' represents the resulting feature map.

- '$\emptyset$' denotes an activation function, typically ReLU, which introduces non-linearity and ensures that the network can capture complex patterns and relationships.
- 'W_k' signifies the filter being applied.
- 'b_k' represents a bias term associated with the filter, which allows for additional fine-tuning of the method of feature extraction.

However, Step 1 of the procedure focuses on extracting basic information from the input image utilizing the convolutional layers. These characteristics are crucial for later phases of analysis, such lesion segmentation, because they enable the network to comprehend the image's content and identify regional patterns and structures. The use of diverse filters and the convolution operation allow for the detection of various types of features, making CNNs highly effective for image-based tasks.

Step 2: Introduction of ReLU Activation Function

In this step, the ReLU activation function will be introduced after each convolutional layer within the network. The ReLU activation function is a pivotal element in modern NNs, particularly CNNs (CNNs), and it significantly contributes to improving the network's training and performance.

ReLU Activation Function

It is, denoted as $\emptyset(x)$, and corresponding equation is:

$$\emptyset(x) = \max(0, x) \quad (1)$$

This simple but effective activation function exhibits specific characteristics that make it highly advantageous in the context of DL and CNNs:

Improved Computational Efficiency

When compared to more conventional activation functions like the sigmoid and hyperbolic tangent (Tanh), ReLU offers better computational efficiency during training. This efficiency is primarily attributed to the simplicity of the ReLU function and its computational ease.

Non-Linearity and Vanishing Gradient

The ReLU imparts non-linearity to the network. To enable the network to recognize intricate patterns and correlations in the data, this non-linearity is necessary. It's worth noting that deep networks rely on non-linear activation functions to model intricate data representations. ReLU is particularly effective in addressing the vanishing

gradient problem. Gradients in deep networks can get incredibly tiny during backpropagation, which makes it difficult for the network to learn efficiently. It mitigates this issue by maintaining gradient values that are not diminished when the input is positive, allowing for efficient gradient flow during training.

Zero-Centered Activation

Another beneficial aspect of ReLU is that it is zero-centered. When the input (x) is less than 0, the function evaluates to 0. This zero-centered property facilitates better optimization in some cases. In order to address issues like the vanishing gradient problem, increase computing efficiency during training, and incorporate non-linearity into the network, Step 2 essentially inserts the ReLU activation function after convolutional layers. This activation function is a cornerstone of modern DL and is widely adopted due to its simplicity and effectiveness.

Step 3: Utilization of Dropout for overfitting Prevention

This stage addresses the problem of overfitting, especially in deep neural networks, by using the "Dropout" strategy during training. When a network becomes overly preoccupied with capturing the nuances of the training data, it is said to be overfitting and becomes less flexible when faced with novel and unfamiliar input. Dropout is a regularization technique that adds a degree of randomization to training in order to reduce overfitting.

What is Dropout?

By "dropping out" (temporarily deleting) a certain percentage of neurons or units from the network at random during each training iteration, dropout is a regularization strategy that attempts to prevent overfitting. Dropout encourages the network to learn more resilient and broad properties by reducing its dependence on any one neuron.

Dropout Probability (P)

A critical parameter in Dropout is the dropout probability (P). This parameter determines the probability that each neuron will be dropped out during the training process. A common choice for P is 0.5, which means that each neuron has 50% chance of being dropped out during each iteration of the training.

Application of Dropout

Dropout is typically applied after certain layers in the NN. In this specific case, it is applied after the 14th and 15th convolutional layers. By doing so, Dropout helps in regularizing the network's deeper layers, where overfitting is often more pronounced.

Advantages of Dropout

Dropout's main benefit is its capacity to improve network generalization. Dropout encourages the network to acquire more robust and diversified representations by preventing it from depending too much on any particular collection of characteristics or units by randomly eliminating neurons.

Dropout is effective in deep NNs, where overfitting can be of a significant concern. It helps in making deep networks more resilient to overfitting by reducing the risk of neurons learning noise or spurious patterns from the training data.

However, Step 3 introduces Dropout to combat overfitting in deep layers of the network. Random deactivation of a portion of neurons, Dropout encourages the network to learn more generalized features and helps in producing a model that performs well on unseen data. Each neuron has a 50% chance of being dropped out during training if the dropout probability is set at 0.5.

Step 4: SoftMax Classification and Segmentation

In order to achieve accurate segmentation, a SoftMax classifier is used in this stage to classify the skin and lesion pixels. A multinomial logistic regression model, the SoftMax classifier plays a crucial role in analyzing the image's pixel multimodality.

SoftMax Classifier

The SoftMax classifier is a widely used technique in ML and DL for solving any kind of classification problems. In the context of this process, it is employed to classify pixels within the image into different categories, such as "lesion" and "skin." Each pixel is assigned to the class with the highest anticipated probability using the SoftMax classifier, which takes into account the probabilities of pixels belonging to various classes. Essentially, it offers a pixel-by-pixel classification of the image.

1×1 Convolution and Sigmoid Activation

Following the SoftMax classification, a 1 × 1 convolution is applied. A 1 × 1 convolution is an operation with a kernel size of 1 × 1. This operation helps to process and refine the output of the SoftMax classifier. The application of sigmoid activation

functions follows. The sigmoid activation function is frequently used to generate binary outputs, or probabilities, that fall between 0 and 1.

Generation of Segmentation Maps

The combined effect of the 1 × 1 convolution and sigmoid activation functions results in the generation of skin lesion output segmentation maps. The image is represented at the pixel level by these maps, where each pixel is categorized as "lesion" or "skin." Importantly, the segmentation maps maintain the resolution of the original test image. This means that the fine details and characteristics of the image are preserved, allowing for accurate segmentation without any loss of information. Step 4 concludes by introducing the SoftMax classifier, which is used to classify the image into various categories pixel-by-pixel. Then, 1 × 1 convolution and sigmoid activation functions are applied. These processes result in segmentation maps that preserve the original resolution of the image and allow for accurate pixel-level segmentation without compromising the quality of the test image.

3.4 Results

ISIC2019 Dataset

At the forefront, we have MLRNet, which demonstrates exceptional performance across multiple metrics. It attains an accuracy of 92.07%, signifying its remarkable correctness in classifying skin lesions. It can reduce false positives and false negatives, as evidenced by its precision score of 90.178% and recall rate of 98.19%. MLRNet strikes a pleasing balance between recall and precision with an astounding F-score of 98.19%. It exhibits high sensitivity at 98.18%, emphasizing its proficiency in correctly identifying true positives. Furthermore, MLRNet maintains a satisfactory specificity score of 81.81%, indicative of its capacity to accurately classify true negatives.

MLRNet attains higher accuracy, precision, recall, F-score, and specificity, while maintaining a competitive sensitivity rate. This underscores its proficiency in correctly identifying and categorizing skin lesions with remarkable accuracy and reliability.

PH2 Dataset

MLRNet excels with an accuracy of 92.84%, signifying exceptional correctness in classifying skin lesions. Its precision is 90.18%, indicating a commendable ability to

minimize false positives. MLRNet achieves an exceptional recall rate of 99.53%, showcasing its proficiency in correctly identifying true positives. The F-score for MLRNet is at 94.53%, indicating a harmonious balance between precision and recall. It maintains a sensitivity rate of 99.55% and a specificity of 81.81%.

In summary, MLRNet consistently demonstrates outstanding performance, achieving the highest accuracy, precision, recall, F-score, and sensitivity among the evaluated methods. Its remarkable performance highlights its exceptional capabilities in accurately diagnosing and classifying skin lesions in the context of the PH2 dataset.

3.5 SUMMARY

In this chapter, we covered a robust two-phase framework for segmenting skin lesions, focusing on improving diagnostic accuracy in skin cancer detection. The proposed system begins with a preprocessing step that employs the Hybrid Gaussian Guided Image Filter. This stage utilizes Discrete Wavelet Transform for frequency decomposition and applies Gaussian filtering followed by Guided Image Filtering to effectively suppress both low- and high-frequency noise while preserving essential image details. The denoised image is then passed to the MLRNet, which performs directional scanning and feature fusion, enabling precise delineation of lesion boundaries. Architectural elements such as ReLU activation, dropout layers, and a Softmax-based segmentation layer ensure high performance, generalization, and effective pixel-level classification.

Experimental results show that the model delivers high accuracy (92.07%) and achieves a near-perfect recall (98.19%), confirming its reliability in identifying true positive lesion cases. The combination of HGGIF and MLRNet forms an efficient and accurate segmentation pipeline, making it a valuable tool for automated skin cancer diagnosis.

CHAPTER-4

DEEP TRANSFER LEARNING-BASED HYBRID MODEL FOR SKIN LESION DETECTION AND CLASSIFICATION

In the preceding chapter we have gone through the implementation of MLNet for skin lesion segmentation and also the results. In this chapter, in continuation to the previous chapter we have a detailed discussion about another proposed research method for the detection and classification of the skin cancer images using deep transfer learning. Along with this here the hybrid filtering approach is also used for the segmentation of skin cancer images to improve the accuracy

4.1. INTRODUCTION

The identification and categorization of skin lesions are essential elements of dermatological diagnosis and treatment. Given the rising prevalence of skin cancer, prompt identification and precise categorization of skin lesions are now essential for patient care and survival. Artificial intelligence and sophisticated image processing methods have transformed dermatology in recent years, providing creative ways to improve the precision and effectiveness of skin lesion analysis. An outline of the importance of skin lesion identification and classification is given in this introduction, which also emphasizes how new technology are revolutionizing dermatological procedures. Melanoma (MEL) and non-MEL skin cancers are two most prominent skin cancer types [28]. Melanoma, a highly aggressive form of skin cancer and it poses a significant threat to patients. However, a wide spectrum of skin cancers exists today which includes MEL, SCC, BCC, NV, BKL, AKIES, VASC, and DF [5]. Melanoma, also known as Merkel cell carcinoma, is particularly lethal and often serves as the precursor to other skin cancer types. The initial development of skin cancer typically begins with melanocytes, cells found in the skin's outermost layer, which can progress into malignant MEL, leading to the invasion and harm of surrounding healthy tissues [127]. Increased exposure to UV radiation from the sun and sunburns are the main causes of the rising incidence of MEL[134]. Acral lentiginous MEL, for example, presents as small, discolored areas of skin, typically appearing black or dark brown. It tends to affect men more on the back of hands, while women are more likely to notice it on their fingers and legs [32]. However,

distinguishing between Acral MEL and acral nevus can be challenging, often resulting in late-stage diagnoses and reduced patient survival rates. Detecting MEL at an early stage is crucial for successful treatment [96]. Early MEL identification can be achieved by a variety of techniques, such as biopsy, pathology reports, and medical imaging analysis. Dermoscopy, a non-invasive imaging technique that involves taking high-resolution, enlarged pictures of questionable skin lesions, is frequently used to detect MEL early on. The dermats then analyze these pictures to determine whether MEL is present[42]. For a proper diagnosis, dermatoscopic analysis necessitates a high level of competence and can be costly. Computer-aided diagnostic techniques are being investigated to help with the early diagnosis of MEL from skin lesions in order to overcome these issues [107].

Nonetheless, the task of distinguishing MEL from non-MEL skin cancer is complicated by various factors. First, there may be a high visual similarity between non-cancerous and cancerous cells. Second, the lack of contrast in images can make it challenging to differentiate between the skin lesion and normal skin areas. Third, MEL's visual distinctiveness can differ greatly from person to person, and the variety of MEL's size, location, shape, and color among skin lesions makes identification more difficult. Furthermore, a number of imperfections, including hair, ruler lines, veins, and color calibration charts, can cause blurriness and occlusions, making discrimination even more difficult [62]. In summary, the early detection of MEL is critical for improving the patient outcomes, given its aggressive nature. Various challenges, including visual similarities, lack of contrast, and intra-class diversity, make the accurate distinction between MEL and non-MEL skin cancers a complex task. CAD methods are being explored to address these challenges and enhance early detection. In recent years, a plethora of CAD methods have emerged, focusing on the vital task of skin cancer identification [77]. These methods have proven to be invaluable in assisting dermatologists in the diagnosis of MEL, a potentially life-threatening form of skin cancer. The development of these skin cancer detection methods draws from a wide array of techniques and technologies. For example, simple image processing techniques have been used to identify cancers by extracting useful elements from skin photos [110]. ML algorithms, as exemplified by [115], have played a crucial part in the identification and categorization of skin lesions,

supporting the early detection of skin cancer. The use of DL models, which can automatically discover complex patterns and features from enormous datasets, is a major advancement in this field [27]. Scholars [115] demonstrated the remarkable performance of deep CNNs for large-scale image recognition. But it's crucial to remember that the DL models, while highly effective, often come with the trade-off of increased computational complexity. To address the computational challenges associated with DL, transfer learning has gained prominence in skin cancer detection [123]. Transfer learning enhances pre-trained models for the particular objective of skin cancer identification by supporting them on sizable image datasets. This approach, as established by contributors [123] and his team in 2017, offers improved performance with relatively lower computational complexity. Additionally, in an effort to identify skin cancer more accurately, ensemble learning prototypes—like those the researcher outlined [63] have been investigated. These models combine the outputs of multiple base models to enhance prediction accuracy and robustness. In summary, the field of skin cancer identification has seen remarkable progress due to the adoption of various methods and technologies. DL stands out for its high performance, while transfer learning offers a balance between performance and computational complexity. Based on particular requirements and the computing resources at their disposal, dermatologists and researchers can choose the best course of action. The work of these researchers, as indicated by their respective publications, has contributed significantly to the advancement of skin cancer identification methodologies.

The focus of this research is on harnessing the effective DL techniques and transfer the learning models to create a hybrid network referred to as DTLNet for SLDC. This approach aims to make significant contributions in this domain.

The following is a summary of the main achievements:

1. HGWF for Noise Removal and Skin Lesion Enhancement: In this research, a HGWF is employed to eliminate noise from images and simultaneously enhance the visibility of skin lesions. Pre-processing step is essential to ensure that the subsequent analysis is performed on clean and well-defined images. Noise reduction and lesion enhancement are crucial for accurate and reliable skin lesion segmentation.

2. Transfer Learning with AlexaNet for Skin Lesion Segmentation: The research

leverages transfer learning using the AlexaNet architecture to perform skin lesion segmentation. Using a previously learned DL model and adapting it to the particular task at hand is known as transfer learning. The model is better able to recognize and distinguish skin lesions thanks to transfer learning, which enables it to take advantage of the knowledge gained during training on a big dataset.

3. Development of a DLCNN for a Deep Feature Extraction: The DLCNN model is developed to extract intricate and meaningful features from the segmented skin lesions. DL models like DLCNNs excel at automatically learning and representing complex patterns and features within data. In this context, the DLCNN is used to capture the unique characteristics of skin lesions.

4. Utilization of SoftMax Classifier for Multiclass Classification: The extracted features from the DLCNN are then subjected to a SoftMax classifier, enabling the model to classify skin lesions into multiple categories. This is particularly significant as skin lesions can encompass various types, which includes SCC, VASC, DF, BKL, AKIES, BCC, NV, and MEL. Using the learnt features, the SoftMax classifier places each lesion in the proper class.

The outcome of this research is the proposed DTLNet model, a comprehensive framework which is capable of accurately classifying multiple classes of skin lesions. The classes encompass various types of skin conditions, each requiring distinct diagnostic considerations. Simulation results from the research demonstrate that the performance of DTLNet surpasses that of conventional approaches which signifies a significant advancement in area of skin lesion identification and categorization, promising more consistent and precise outcomes in diagnosing and managing skin disorders.

4.2. PROPOSED DTLNET ALGORITHM

The Proposed DTLNet algorithm is a comprehensive framework designed for the classifying the multiple classes of skin lesions. It combines deep feature extraction, transfer learning, picture pre-processing, and classification methods. Let's break down the training and testing processes of the DTLNet algorithm step by step:

4.2.1 Process of Training

Step 1: HGWF Pre-processing Operation

The first step involves pre-processing the ISIC-2019 training dataset using the

HGWF. The purpose of this operation is to remove various types of artifacts and noises from the dataset. Artifacts can distort images and removing them ensures that the training data is as clean and artifact-free as possible.

Step 2: AlexNet-Based Transfer Learning for Segmentation

Once the dataset is pre-processed, the algorithm applies an AlexNet-based transfer learning model for skin lesion segmentation. Transfer learning is a technique that leverages a pre-trained DL model (in this case, the AlexNet) and also fine-tunes it for the specific task of segmenting skin lesions. This step results in well-segmented skin lesions, which are essential for subsequent analysis.

Step 3: DLCNN for Feature Extraction

Following successful segmentation, a number of highly correlated, disease-dependent characteristics are extracted using the DLCNN architecture. The segmented skin lesions are used to extract these features, which are then saved in a feature database. Complex patterns and features in data can be automatically learned and represented by DL models such as DLCNNs.

4.2.2 Testing Process:

Step 4: Extracting Test Skin Lesion Features

When a test skin lesion needs to be classified, the same pre-processing and feature extraction steps as those used in the training process (Steps 1 to 3) are applied to the skin lesion- which is selected for the testing. This ensures that the test data is pre-processed and that relevant features are extracted for further analysis.

Step 5: Skin Lesion Classification Using SoftMax Classifier

The algorithm carries out the SLDC in this stage by contrasting the test skin lesion's features with the training features that are kept in the feature database. A SoftMax classifier is used for this purpose. The SoftMax classifier assigns the test lesion to one of the classes of skin lesions. This is essentially the classification step.

Step 6: Quantitative Evaluation

A quantitative assessment is carried out following the classification of the test skin lesion. This stage entails figuring out a number of performance indicators to evaluate the classification's efficacy and correctness. Accuracy, precision, recall, F1 score, and ROC curves are examples of common performance measurements. These metrics will offer a numerical assessment of the DTLNet algorithm's classification performance

for the test skin lesion.

In summary, the Proposed DTLNet algorithm is a robust framework that combines image preprocessing, transfer learning, deep feature extraction, and classification to accurately classify multiple classes of skin lesions. It ensures that the algorithm can consistently and precisely classify test skin lesions and is utilized for both training and testing. Important information about the algorithm's performance and applicability for skin lesion classification tasks is provided by the quantitative evaluation step.

4.2.3 Proposed DTLNet Framework

Skin lesions often exhibit a range of unwanted artifacts and imperfections, including but not limited to salt-pepper noise, Gaussian noise, random distortions, jitter, and other forms of image degradation. Additionally, these skin lesions may be afflicted with unwanted hair artifacts, further complicating the processes of segmentation and classification. As a response to the challenges, this article presents a novel approach known as the HGWF for the enhancement of skin lesions.

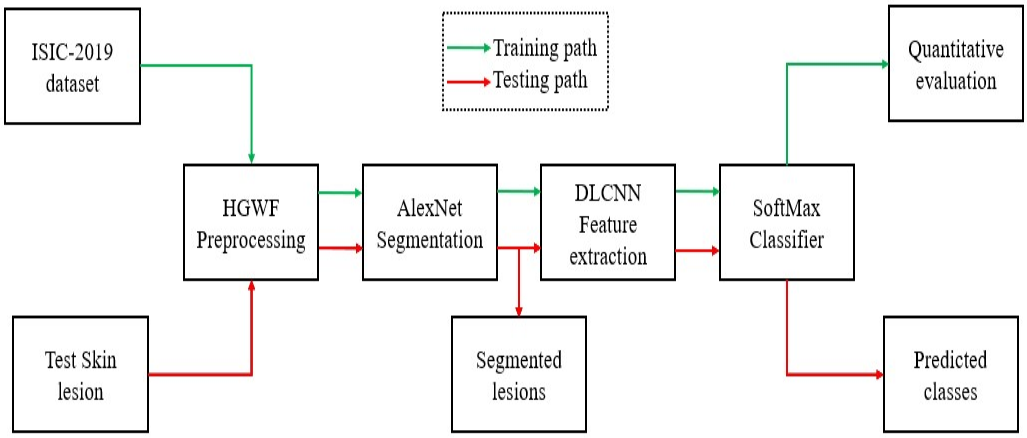

Figure 4.1 Proposed DTLNet framework

Fig 3.3 illustrates the block diagram of the skin lesion pre-processing using HGWF, while Table 3.2 provides a detailed algorithm for HGWF. This pre-processing step is crucial in improving the quality of skin lesion images, reducing the impact of artifacts, and ultimately facilitating more accurate segmentation and classification.

Table 4.1 Proposed HGWF algorithm

Input: Skin lesion image
Output: skin lesion which is Pre-processed.

Step 1: Apply the gaussian filter to the skin lesion image in order to eliminate the various kinds of noise artifacts from the skin lesion.

Step 2: In this step, apply the wiener filter, which enhances the colour levels of the skin lesion and also highlights the cancer region.

Step 3: Update the kernel function for wiener filter based on the gaussian properties, repeat the operation until the noise levels are eliminated.

Step 4: Generate the final enhanced and denoised skin lesion through the updated filter responses.

The algorithm for the Proposed HGWF utilized to pre-process photos of skin lesions is shown in Table 4.1. By eliminating different kinds of noise artifacts and emphasizing malignant areas, this pre-processing procedure aims to improve the quality of the skin lesion photos.

Here is a thorough breakdown of every algorithmic phase:

Step 1: Apply Gaussian Filter

Input: Skin lesion image

Output: Skin lesion image after applying the Gaussian filter

The algorithm applies a Gaussian filter on the input image in this step. In image processing, the Gaussian filter is a widely used approach to lessen the impact of various noise artifacts present in the image of a skin lesion. By doing this, the image quality is improved by smoothing it out and lowering noise.

Step 2: Apply Wiener Filter

- Input: Gaussian-filtered image of a skin lesion
- Output: Wiener filter picture of a skin lesion.

The approach applies a Wiener filter to the picture that has been Gaussian filtered in addition to the Gaussian filter. The Wiener filter is used to highlight areas of the skin lesion that are suggestive of malignancy and to intensify the color levels of the lesion. The goal of this phase is to make the malignant areas in the picture more visible.

Step 3: Update the Wiener Filter Kernel Function

- Input: Skin lesion image after Wiener filtering
- Output: Updated Wiener filter response
- In this step, the algorithm will update the kernel function of the Wiener filter based on the Gaussian properties of the image. The operation is repeated until the noise

levels in the image are effectively eliminated. This iterative process ensures that the filter's response is optimized for noise reduction and enhancement of the cancerous regions.

Step 4: Generate the Final Enhanced and Denoised Skin Lesion

- Input: Wiener filter response

- Output: Pre-processed skin lesion image

- Finally, the algorithm generates the final enhanced and denoised skin lesion image using the updated filter responses. This output represents the result of the entire HGWF pre-processing process, where noise artifacts have been reduced, and the critical features of the skin lesion, especially those indicative of cancer, have been highlighted.

In summary, the HGWF algorithm is a multi-step process that combines Gaussian and Wiener filters to pre-process skin lesion images effectively. This process results in improved image quality, reduced noise artifacts, and enhanced visibility of cancerous regions, which is essential for more accurate subsequent analysis such as segmentation and classification in the perspective of skin cancer diagnosis.

Let's take a closer look at the HGWF procedures and how they are used in skin lesion image preprocessing:

1. f(x,y) - The Input Skin Lesion Image:

The function f(x,y) represents the original skin lesion image. This image typically contains various imperfections and artifacts such as noise and unwanted hair regions. The goal is to process this image in a way that overcomes these challenges and prepares it for further analysis.

2. HGWF - The Noise Degradation Function (Hybrid Gaussian-Wiener Kernel Function) u(x,y):

HGWF is a critical component of the pre-processing method. It is represented as u(x,y) and serves as a noise degradation function. This function combines elements of both Gaussian and Wiener kernel functions and plays a central role in addressing noise artifacts and enhancing the image quality.

3. Artifacts (Noise and Hair Regions) - n(x,y):

Artifacts in the skin lesion image, which encompass noise and hair regions, are represented as n(x,y). These artifacts are unwanted elements that hinder accurate

analysis and diagnosis of the skin lesion. Removing these artifacts is a major objective of the pre-processing step.

4. Pre-processing for Artifact Removal:

The pre-processing step is essential for overcoming the artifacts in skin lesion analysis. It is crucial to remember that traditional pre-processing techniques frequently have problems with feature reduction and loss. As a result, during the noise removal process, significant statistical features of the skin lesion may be eliminated. These restrictions are intended to be addressed by the HGWF.

5. g(x,y) - The Degraded Skin Lesion:

The result of applying the noise degradation function u(x,y) to the initial skin lesion image f(x,y) is the image g(x,y). The following is a mathematical representation of this operation:

$$g(x,y) = f(x,y) * u(x,y) + n(x,y) \quad (2)$$

The degraded skin lesion g(x,y) now contains the impact of the noise degradation function and any remaining artifacts.

6. h(x,y) - The Pre-processed Skin Lesion:

The h(x,y) represents the pre-processed skin lesion image, which has undergone the HGWF function. This pre-processing is essential to produce a clean and improved image that can be effectively analyzed. Mathematically, this step is expressed as:

$$h(x,y) = F_{HGWF}\,[g(x,y)] \quad (3)$$

Here, F_HGWF performs the hybrid Gaussian-Wiener filtering operation on the degraded skin lesion g(x,y).

7. Role of HGWF - Combining Gaussian and Wiener Functions:

The HGWF incorporates both Gaussian and Wiener kernel functions. The Gaussian function primarily addresses texture noise with linear properties. In contrast, the Wiener function is employed to deal with the spatial noise characterized by non-linear properties. HGWF successfully addresses the many kinds of noise artifacts found in the skin lesion image by integrating these functions.

8. Application of Gaussian Filter:

Firstly, the skin lesion image is applied to a Gaussian filter. This filter is instrumental in removing texture noise, which is a form of noise that often exhibits linear properties. The Gaussian filter smooths out irregularities and inconsistencies in the

image, reducing the impact of noise artifacts with linear characteristics.

In summary, the pre-processing process involving HGWF aims to enhance the skin lesion image by addressing various artifacts and noise issues while minimizing the loss of essential statistical characteristics. The combination of Gaussian and Wiener functions in HGWF allows for a more comprehensive approach to noise reduction and image enhancement, ensuring that the image is well-prepared for subsequent analysis, such as segmentation and classification in the context of skin lesion analysis and diagnosis.

4.3 GAUSSIAN FILTER

The Gaussian Filter is a fundamental component of the pre-processing method used in improving the quality of the background in skin lesion images. Here, we delve into a detailed explanation of how the Gaussian filter works and its specific properties:

1. Background Quality Improvement:

The Gaussian filter is employed to enhance the background quality of a lesion image. This improvement is achieved by leveraging the Gaussian filter's unique characteristics, including its ability to preserve edges within the image. Edge preservation is essential for preserving the image's integrity, especially when it comes to correctly detecting and describing skin lesions.

2. Noise Removal with Gaussian Distribution Function:

Using the Gaussian distribution function, the Gaussian filter is excellent at eliminating a variety of noise types, including Gaussian and salt-and-pepper noise.

These noise types are common sources of interference that can degrade the quality of the lesion image. The Gaussian filter effectively mitigates this issue.

3. Limitation in Handling Hair Artifacts:

The incapacity of the Gaussian filter to efficiently eliminate hair artifacts from skin lesions is one of its drawbacks.

Hair regions in the image tend to cast darker shadows, and this poses a challenge for conventional noise reduction methods. While the Gaussian filter is adept at addressing certain types of noise, it may struggle with hair artifact removal.

4. Utilization of Mean (μ_g) and Variance (σ_g^2) for Kernel Generation:

The Gaussian filter employs both the mean (μ_g) and variance (σ_g^2) computations to generate its kernel. The kernel represents the convolutional operation applied to the

image for filtering. These calculations are essential for the filter to effectively address noise and improve image quality.

$$\mu_g = \frac{1}{NM} \sum_{n,m \in \eta} a(n,m) \quad (4)$$

The mean (μ_g) is calculated using a formula that involves summation over a specified neighbourhood 'η' in the image. In essence, the mean computation establishes the neighborhood's average pixel value, which acts as a benchmark for the filter's functions.

$$\sigma_g^2 = \frac{1}{NM} \sum_{n,m \in \eta} a^2\,(n,m) - \mu_g^2 \quad (5)$$

The variance (σ_g^2) is computed using a similar neighbourhood-based approach. It quantifies the variation or spread of pixel values within the neighbourhood 'η'. The variance computation is essential for characterizing the properties of Gaussian noise in the image.

Probabilistic Updating of Variance with Hybrid Gaussian-Wiener Kernel Function:

The computed variance (σ_g^2) contains properties related to Gaussian noise. The variance information is updated in a probabilistic manner when hybrid and joint Gaussian-Wiener kernel functions are applied. This update allows the filter to adapt to the characteristics of the image and its specific noise artifacts, improving its noise removal capabilities.

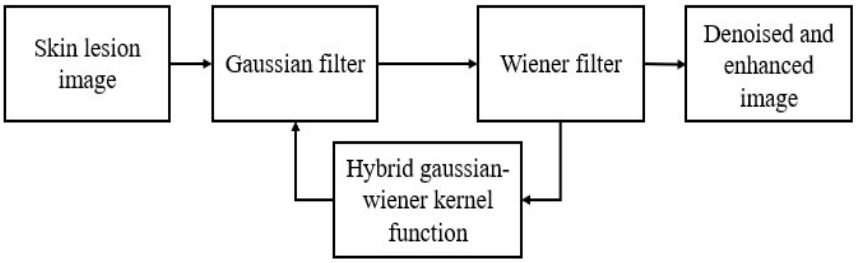

Figure 4.2 HGWF based skin lesion preprocessing

In conclusion, the Gaussian filter is a useful tool for pre-processing skin lesion photographs, especially for noise reduction and background quality improvement. Although it is very good at removing certain kinds of noise, such Gaussian and salt-and-pepper noise, it might have trouble with hair artifacts. The filter makes use of mean and variance calculations, which are essential for producing the filter kernel and guaranteeing efficient noise reduction. Its performance and adaptability are further

improved by the probabilistic updating of the variance using hybrid and joint Gaussian-Wiener kernels.

4.4. WIENER FILTER

It is an essential component of pre-processing method for improving the quality of the foreground in skin lesion images. Here, we provide a detailed explanation of how the Wiener Filter operates and its specific properties:

1. Foreground Quality Improvement:

The Wiener filter is employed to improve the foreground quality of a skin lesion image. This is done with an emphasis on preserving edges within the image. Edge preservation is essential to preserving the image's integrity, especially for accurately highlighting the cancer region and removing unwanted artifacts.

2. Removal of Hair Artifacts:

The Wiener filter plays a critical role in effectively removing hair artifacts from skin lesions. Hair regions often cast shadows or exhibit variations in color and texture, which can be challenging to address with conventional filtering methods. The Wiener filter is tailored to mitigate these issues.

3. Enhancement of Colour, Brightness, Saturation, and Contrast:

- The Wiener filter not only removes unwanted artifacts but also enhances various visual properties of the image. This includes improving colour, brightness, saturation, and contrast. These enhancements are achieved through edge-preserving mechanisms, ensuring that essential features in the image are maintained and emphasized.

4. Mean (μ_w) and Variance (σ_w^2) in Wiener Filter:

- The Wiener filter incorporates both the mean (μ_w) and variance (σ_w^2) as important parameters. These parameters are essential to the filter's functioning since they enable it to adjust to the unique features of the image and noise artifacts. The variance describes the variation or spread of pixel values within the neighborhood, whereas the mean indicates the average pixel value in the neighborhood.

5. Denoising with the Wiener Filter

- The denoising process is a key outcome of the Wiener filter's operations. This step is represented by the equation:

$$b_w(n,m) = \mu_w + \frac{\sigma_w^2 - v^2}{\sigma_w^2} . \left(a_g(n,m) - \mu_w\right) \quad (6)$$

- Here, "$a_g(n, m)$" shows the output of the Gaussian filter, "v^2" signifies the variance is related to complicated noises and hair artifacts in the skin lesion, and " $b_w(n, m)$" stands for the denoised result produced by the Wiener filter. The equation demonstrates how the Wiener filter adapts its operations based on these parameters to effectively reduce noise and enhance image quality. In conclusion, the Wiener filter is an essential component of skin lesion image pre-processing, concentrating on enhancing the foreground quality, especially for highlighting cancerous regions and removing hair artifacts.

It also brings about enhancements in colour, brightness, saturation, and contrast through edge-preserving mechanisms. The inclusion of mean and variance parameters, along with their adaptive updating, allows the Wiener filter to effectively reduce noise and improve the visual properties of the image while preserving essential features.

4.5 HYBRID GAUSSIAN-WIENER KERNEL FUNCTION

The HGWF is a critical component that coordinates the operations of the Gaussian filter and the Wiener filter by controlling their respective kernel functions. The primary purpose of the HGWF is to create a unified approach that leverages the strengths of both filters for effective noise elimination and enhancement of the skin lesion image.

Key Characteristics of the HGWF:

1. Kernel Function Size (n×m):

- The HGWF is designed with a specific kernel function size, typically represented as n×m. This kernel function size determines the scope and coverage of the filtering operations. It defines the region in the image that is considered when applying the filter. This size is chosen to balance noise elimination and image enhancement.

2. Incorporation of Hair Artifact and Noise Properties:

- The HGWF is engineered to incorporate the properties of hair artifacts and noise elimination characteristics both. This indicates that the function is made to deal with the particular difficulties that noise and hair artifacts in skin lesion photos provide.

Function of the HGWF:

The HGWF generates a denoising function, which combines the attributes of the Gaussian and Wiener filters in a coherent manner. This denoising function,

represented as F_HGWF, is created based on several parameters and calculations:

$$F_{HGWF} = \left(\mu_g + \frac{\sigma_g^2 - \eta^2}{\sigma_g^2}\right).\left(\mu_w + \frac{\sigma_w^2 - v^2}{\sigma_w^2}\right).\left(b_w(n,m)\right) \quad (7)$$

F_{HGWF} is calculated by multiplying the following factors:

- $(\mu_g + \frac{\sigma_g^2 - \eta^2}{\sigma_g^2})$: This component is related to the Gaussian filter, involving the mean (μ_g), the variance (σ_g^2), and the property of complicated noise (η^2). It contributes to noise reduction.

- $(\mu_w + \frac{\sigma_w^2 - v^2}{\sigma_w^2})$: This part pertains to the Wiener filter, encompassing the mean (μ_w), the variance (σ_w^2), and the variance of hair artifacts and complex noise (v^2). It is essential for noise reduction and image enhancement.

- $b_w(n,m)$: This term shows the denoised outcome which is produced by the Wiener filter.

Convolution Operation:

The final step involves performing a convolution operation, which is denoted as "*" in Equation 1, between the original skin lesion image f(x,y) and the F_{HGWF} function in a pixel-wise manner. This operation is conducted iteratively and generates a new pixel values for each iteration. Ultimately, it produces the final denoised outcome. In essence, the HGWF serves as a bridge that harmonizes the Gaussian and Wiener filtering operations, allowing for a comprehensive approach to noise reduction and image enhancement. It efficiently addresses the challenges posed by noise and hair artifacts, producing a cleaner and visually improved skin lesion image suitable for subsequent analysis.

4.6 PROPOSED SEGMENTATION USING ALEXNET

Segmentation is a pivotal component in the SLDC, particularly with relation to the study of skin lesions. Traditional image processing techniques historically centered their segmentation efforts primarily on the colour attributes of cancerous regions within skin lesions. However, this traditional approach had limitations as it often ignored finer-grained, pixel-wise analysis. In more recent times, some approaches have sought to improve segmentation accuracy by adopting pixel-wise analysis. A more thorough analysis of the image is made possible by pixel-by-pixel analysis, which may improve the segmentation process' accuracy. Despite this advantage, it is

important to note that even pixel-wise analysis approaches had their limitations and were unable to consistently achieve optimal segmentation performance for Every kind of skin lesion.

This work focused on addressing the segmentation challenges by considering the ISIC2019 dataset, which has images of eight diverse classes of skin lesions. These classes represent various types of skin lesions, each with its own unique characteristics. The dataset's diversity presented a formidable challenge for conventional segmentation methods, which often struggled to provide accurate and robust results. In many cases, the performance of these traditional methods was subpar and resulted in poor segmentation outcomes.

In summary, an essential component of the SLDC procedure is segmentation, especially when it comes to skin lesion analysis, while traditional methods often focused on colour attributes, recent approaches aimed to improve accuracy through pixel-wise analysis. However, challenges remained, especially when dealing with diverse classes of skin lesions, as traditional methods often yielded poor segmentation results. This emphasizes the necessity of more sophisticated and flexible segmentation methods, like the one described in this work, in order to successfully handle the difficulties of skin lesion analysis.

In the pursuit of improving skin lesion segmentation, DL models have emerged as a promising approach. These models can provide high-resolution, pixel-wise analysis of images, which can lead to enhanced segmentation accuracy. However, when applied to vast datasets like ISIC-2019, standard DL models face significant challenges, two of which are particularly notable:

1. Vanishing Gradient Problems:
   - The vanishing gradient issue can affect deep neural networks (NNs), particularly when working with huge datasets and deep architectures. The model may learn more slowly or not at all as a result of the vanishing gradient problem. This difficulty may have an impact on the model's capacity for accurate segmentation and generalization.
2. High Computational Complexity:
   - Pixel-wise analysis with DL models demands substantial computational resources. Processing each pixel individually in large images can be computationally intensive and time-consuming. This can be a practical hurdle, especially when working with

substantial datasets like ISIC-2019. This work focuses on adapting transfer learning models for skin lesion segmentation in order to address these issues. Utilizing pre-trained models, transfer learning is a potent DL approach. These models are useful starting points for specific tasks since they have already acquired important characteristics and patterns from large datasets.

4.6.1 Advantages of Transfer learning models adaption

1. Knowledge Transfer:

- Transfer learning models come with a wealth of pre-existing knowledge, including knowledge of textures, shapes, and patterns relevant to image analysis. This pre-trained knowledge can be valuable for segmenting skin lesions effectively.

2. Faster Convergence:

- Transfer learning models often converge faster during training, thanks to their prior knowledge. This can significantly reduce the training time required to achieve accurate segmentations.

3. Enhanced Performance:

- By optimizing a previously trained model for the particular purpose of segmenting skin lesions, it's possible to achieve improved segmentation performance without suffering from the vanishing gradient problem.

In summary, this work recognizes the limitations of standard DL models, such as vanishing gradient issues and high computational complexity, when applied to extensive datasets like ISIC-2019. To address these challenges, the work shifts its focus to the utilization of transfer learning models. This method makes use of prior knowledge and speeds up the training process, which eventually results in skin lesion segmentation that is more effective and efficient. Transfer learning models are a promising solution for achieving better segmentation results with large and complex datasets. The utilization of transfer learning models has significantly advanced the fields of image analysis, by encompassing tasks like image recognition, image segmentation, background extraction, and edge analysis. With a number of benefits, including comparatively less computational complexity than other transfer learning models like ResNet, GoogleNet, and MobileNet, AlexNet stands out among these models as a successful option.

4.6.2 ALEXNET for Skin Lesion Segmentation:

Figure 3.5 illustrates the segmentation process of skin lesions using the AlexNet architecture, a transfer learning model. This model is adept at highlighting the cancerous regions within the skin lesions by classifying individual pixels. Figure 3.5 provides a comprehensive breakdown of each layer within the AlexNet model. The

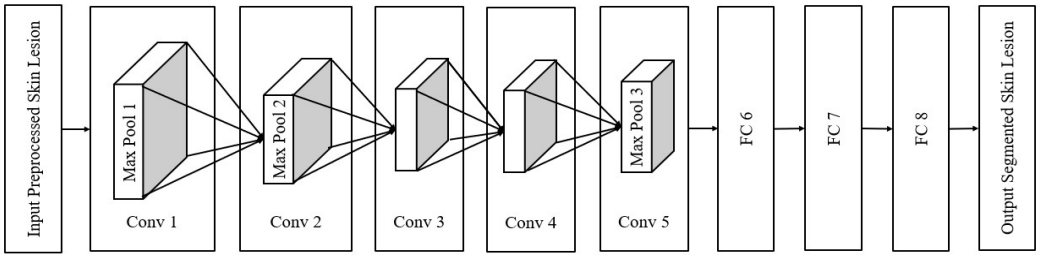

Figure 4.3 AlexNet architecture for skin lesion segmentation

AlexNet model excels in skin lesion segmentation by analysing the ABCDE properties. In the transfer learning models like AlexNet, the performance is closely tied to total layers and activation units that are present. The AlexNet model incorporates a total of 5 convolutional layers & 3 fully connected layers to achieve its segmentation results.

Convolution Layers:

The image processing algorithm's convolution layer 1 (Conv1) receives the pre-processed skin lesion input image. Kernel or filter-based feature detectors are crucial for feature extraction in the convolution layers. These detectors carry out the convolution process between the kernel matrix and the input image to identify the edges, horizontal lines, borders, bends, vertical lines, and any other significant characteristics. This feature extraction process is crucial for efficient segmentation. Moreover, a ReLU is employed to choose the segmented regions. Convolution layers are also responsible for data pooling, which aids in making the network translation-invariant. Importantly, the output remains consistent even as the input's dimensions vary from layer to layer. The earlier convolution layers focus on extracting more detailed features, while later layers emphasize higher-order characteristics. The convolution operation in the convolution layers is mathematically represented as follows:

$$f_s(i,j) = \sum_m^M \sum_n^N h(i-m, j-n) * W(m,n) \quad (8)$$

Here:

- h(m, n) represents the pre-processed skin lesion, with *'m'* rows and *'n'* columns.
- W(m, n) shows the weight matrix with kernel properties.
- f_s(i, j) represents the segmented output.

Fully Connected Layers:

The output characteristics from Conv1 through Conv5 are linked sequentially to the Fully Connected Layer 6 (FC6). The FC layer functions as a flattening layer, connecting all the neurons within the network with an equal likelihood of connection. This linear transformation of input features is pivotal for producing output features. Three FC layers are employed for constructing a robust characteristic based on different classes of skin lesion images. These FC layers also act as a classifier, making it possible to classify the regions of skin lesions affected by disease by analysing individual pixels. Finally, they generate a binary map as segmented output, white indicating the cancer-affected region (assigned a binary value of 1) and black representing the non-cancer region (assigned a binary value of 0). In summary, the AlexNet transfer learning model is a powerful tool for skin lesion segmentation. It effectively extracts key features from skin lesions, allowing for accurate segmentation based on various properties. In the end, the model's network architecture—which consists of convolution and fully linked layers—produces a binary map that identifies the areas of the skin lesion photos that are damaged by cancer.

4.7 FEATURE EXTRACTION AND CLASSIFICATION

In the SLDC process, feature extraction is an important step following segmentation. Features in this context refer to statistical parameters that capture several attributes of skin lesions based on their respective classes. Traditional image processing-based feature extractors have faced limitations, especially when dealing with extensive datasets. They often struggle to extract the detailed ABCDE (Asymmetry, Border, Colour, Diameter, Edge) attributes from large datasets, and their effectiveness is more pronounced on smaller datasets.

Role of DL in Feature Extraction and Classification:

Recent advancements in DL models have revolutionized the feature extraction and classification process. DLCNN's play a vital role in extracting a detailed spatial, spectral, texture, and colour features from segmented images. These models are

highly effective in capturing intricate attributes and can identify interdependent relationships between pixels in segmented images, treating them as features.

DLCNN models are well-suited for the classification process, as they aggregate local features from higher levels of input and combine them into more complex features at low levels. This versatility makes DLCNN a highly effective solution for feature extraction and classification tasks. Moreover, the speed of DLCNN can be optimized by adjusting the kernel sizes and weights in combination with local connections.

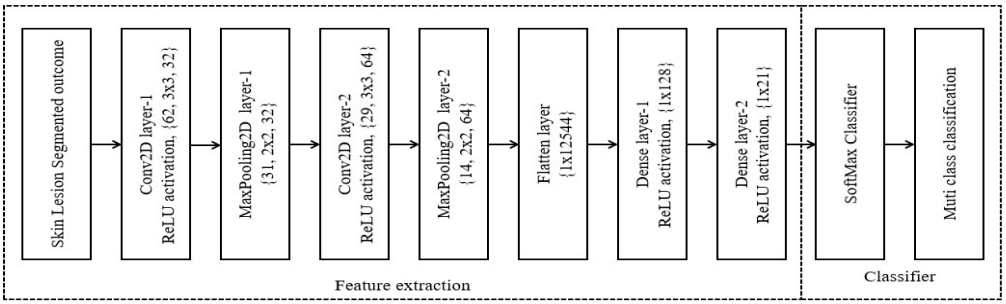

Figure 4.4 DLCNN Feature Extraction and Classifier

Figure 3.6 represents the DLCNN model for feature extraction and classification. The following discussion offers a comprehensive analysis of each layer within the DLCNN model, including layer dimensions, filter sizes or kernel sizes, the number of filters, and parameters. This is a thorough explanation of the layers.

1. Conv2D-1:
   - Layer Dimension: 62x62
   - Filter Size: 3x3
   - Number of Filters: 32
   - Parameters: 896
2. MaxPooling2D-1:
   - Layer Dimension: 31x31
   - Filter Size: 2x2
   - Number of Filters: 32
   - Parameters: 0
3. Conv2D-2:
   - Layer Dimension: 29x29
   - Filter Size: 3x3

- Number of Filters: 64
- Parameters: 18,496

4. MaxPooling2D-2:
   - Layer Dimension: 14x14
   - Filter Size: 2x2
   - Number of Filters: 64
   - Parameters: 0
5. Flatten:
   - Layer Dimension: 1x12,544
   - No filter or kernel size
   - No filters or parameters
   - Parameters: 0
6. Dense-1:
   - Layer Dimension: 1x128
   - No filter or kernel size
   - No filters or parameters
   - Parameters: 1,605,760
7. Dense-2:
   - Layer Dimension: 1x21
   - No filter or kernel size
   - No filters or parameters
   - Parameters: 2,709
8. SoftMax:
   - Layer Dimension: 1x8
   - No filter or kernel size
   - No filters or parameters
   - Parameters: 0

Feature Extraction and Classification Process:

The DLCNN model, which combines all of these layers, makes it easier to extract and classify features for skin cancer. After extracting key characteristics from segmented skin lesion images, the DLCNN model classifies the images based on the obtained detailed characteristics. With white signifying the presence of cancer (given a binary

value of 1) and black signifying the absence of cancer (assigned a binary value of 0), the result is a binary map that highlights areas of the skin lesion images that are affected by cancer. In summary, DLCNN models have demonstrated remarkable capabilities in feature extraction and classification tasks for skin cancer analysis. Their ability to capture intricate attributes and relationships between pixels in segmented images makes them a powerful tool for identifying cancer-affected regions in skin lesion images. The detailed analysis of each layer offers an insight into the architecture of the DLCNN model used in this process.

4.8. Results

The segmentation performance analysis of proposed AlexNet got an Accuracy of 96.42%, precision of 98.23%, Recall of 97.82%, F1-Score of 97.93%, Sensitivity of 98.72% and Specificity of 86.85%. All these values demonstrate the remarkable capabilities of Proposed AlexNet in accurately delineating skin lesions. They excel in various aspects, like accuracy, precision, recall, F1-Score, sensitivity, and specificity, contributing significantly to the field of lesion segmentation. In conclusion, the findings from this segmentation performance analysis emphasize that Proposed AlexNet excels in all metrics, showcasing its prowess in accurately segmenting skin lesions.

The Classification Performance analysis of proposed DTL Net got an Accuracy of 96.42%, precision of 98.23%, Recall of 97.82%, F1-Score of 97.93%, Sensitivity of 92.34% and Specificity of 96.21%.

The classification performance comparison findings highlight the outstanding capabilities of Proposed DTLNet in skin lesion diagnosis and classification. It stands out in terms of accuracy, precision, recall, F1-Score, sensitivity, and specificity.

4.9 SUMMARY

This Chapter presents a comprehensive approach to the detection and classification of skin lesions using a deep transfer learning-based framework named DTLNet. The methodology integrates advanced image preprocessing, segmentation, deep feature extraction, and classification to address challenges in the accurate identification of melanoma (MEL) and other types of skin cancer in dermoscopic images from the ISIC 2019 dataset. The Key components of the proposed method are Hybrid Gaussian-Wiener Filtering, Segmentation with AlexNet, Feature Extraction with

DLCNN, Classification Using SoftMax. This chapter successfully proposes an end-to-end intelligent system for skin lesion classification through DTLNet. By combining hybrid preprocessing, deep segmentation using transfer learning, and feature-rich classification via DLCNN, the approach significantly enhances diagnostic performance over traditional methods. This work stands as a promising advancement for computer-aided skin cancer detection and supports its potential for real-time clinical applications.

CHAPTER-5

ENHANCED SKIN CANCER CLASSIFICATION THROUGH A HYBRID OPTIMIZED APPROACH

In the earlier chapter we have gone through the deep transfer learning based skin cancer diagnosis and classification using Alexnet and deep convolution neural network with improved accuracy. In this chapter we provide the detailed things about the another proposed research method by which we can do the diagnosis of skin cancer and also the classification for the improvement of the accuracy further compared to the previous technique

5.1. INTRODUCTION

In recent times, a wide range of ML, DL and Transfer Learning models have been developed for Skin Lesion Diagnosis and Classification (SLDC). However, these models have faced significant challenges, particularly when confronted with previously unseen image datasets. They have often struggled to effectively understand and process unknown image properties, which has limited their performance in practical applications. Furthermore, these techniques have run into problems with gradient descent and stochastic gradient descent, particularly as dataset sizes have grown. These difficulties have made it increasingly difficult for the models to successfully adjust to bigger and more complicated datasets. Recently, there has been a notable shift towards adopting Vision Transformer (ViT) networks in real-time scenarios for analysing previously unknown images. ViT networks have demonstrated superior performance in various applications, including SLDC. Drawing inspiration from the successes of ViT, this work has introduced a novel approach called the HOS-Net, specifically designed for efficient and accurate SLDC. The proposed HOS-Net's architecture is shown in the block diagram in Figure 5.1. Working with the ISIC2019 dataset, which includes eight distinct classes of skin cancers, is the first step. It's important to note, though, that the dataset shows a notable imbalance in the types of skin cancers that have been diagnosed, with some lesions—like multiple lesions—being more common than others. The dataset is enlarged to guarantee a more uniform distribution of images for every class in order to rectify this imbalance. Following dataset expansion, basic image pre-processing techniques are applied to standardize

the size of each image in the dataset. This standardization step helps ensure consistency in the data and facilitates subsequent analysis.

The HOS-Net, designed for efficient Skin Lesion Diagnosis and Classification (SLDC), encompasses several critical components that work in synergy to enhance its diagnostic accuracy and efficiency:

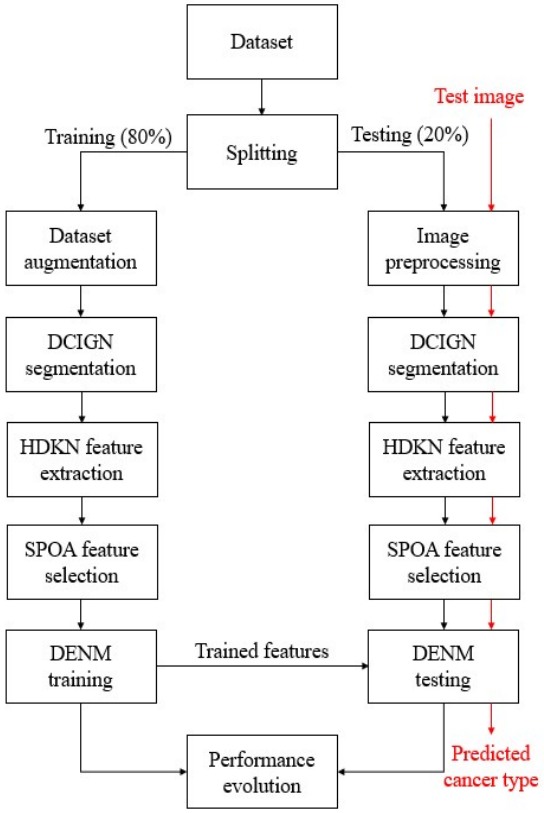

Figure 5.1 HOS-Net Overview

1. DGCIN Model (Dynamic Pixel Graph Convolutional and Interactive Network):

The DGCIN model plays a pivotal role in understanding the pixel relationships within skin lesion images. It focuses on identifying changes in pixel values to pinpoint regions that are affected by cancer. These changes in pixel values can indicate variations in color, texture, or other attributes that may signify the presence of skin cancer. The DGCIN model employs dynamic graph convolutional networks to extract these pixel relationships, enabling more accurate cancer region identification.

2. HDKN Model (Probabilistic Kohonen Feature Extractor):

The HDKN model is responsible for identifying probabilistic Kohonen features within segmented images. These features capture intricate relationships between different

classes of skin cancer. Kohonen features are probabilistic, meaning they provide insights into the likelihood of specific features or patterns being associated with classes of skin cancer. This probabilistic technique boosts the model's capacity to discriminate between various skin cancer kinds.

3. SPOA Model (Selective Principle-Oriented Attribute Selection):

The SPOA model functions as a feature curation component created to boost the efficiency of feature extraction and choice. Its principal aim is to remove unrelated or duplicate features from the dataset. By diminishing the dimensionality of the feature matrix, SPOA streamlines the training complexity of subsequent models. This selection procedure certifies that only the most applicable and enlightening attributes are preserved, ultimately resulting in a more efficient and precise SLDC.

4. DENM Model (Dynamic Echo Network for Multiclass Classification):

The multiclass skin cancer classification task is something that the DENM model is made to handle. It takes the pre-processed and feature-selected data and employs a unique approach known as probabilistic echo properties during the classification process. This method improves the overall accuracy and resilience of the model. The term "echo properties" suggests that the model uses echoes or repetitions of information to classify skin lesions accurately. By incorporating probabilistic aspects, DENM improves the model's ability to make informed decisions about different classes of skin cancer, ultimately leading to more precise and reliable diagnoses.

However, the HOS-Net's effectiveness in SLDC is greatly attributed to these four critical components. Each element has a specific function, and when combined, they improve the model's ability to precisely and effectively identify and categorize skin lesions. The DGCIN model identifies pixel relationships, the HDKN model extracts probabilistic features, the SPOA model streamlines feature selection, and the DENM model uses probabilistic echoes for multiclass classification, resulting in a thorough and reliable method for classifying and diagnosing skin cancer. Finally, the HOS-Net represents a pioneering approach in the field of SLDC, inspired by the success of Vision Transformer (ViT) networks. It addresses the challenges faced by previous ML, DL, and transfer learning models by introducing a novel framework that effectively handles unknown image datasets. To accomplish precise and effective skin cancer diagnosis and classification, the HOS-Net architecture integrates dataset

expansion, picture pre-processing, feature extraction, selection, and classification.

5.2 DATASET AUGMENTATION

One essential method in ML and DL is dataset augmentation when dealing with class-imbalanced datasets. When training images for different categories are not evenly distributed, it can lead to class imbalance issues. To enhance the overall number of samples in the training set, dataset augmentation entails producing more, altered versions of the original data. This technique aims to enhance the robustness and performance of ML models by diversifying and expanding the training data. In dataset augmentation, a number of popular methods are employed:

Table 5.1 Data augmentation with parameters

Augmentation	Parameters
Rotate	90°, 180°, 270°
Crop from top	45°, 60°, 90°
Crop from	45°, 60°, 90°
Crop from right	45°, 60°, 90°
Crop from left	45°, 60°, 90°
Flipping	Left right
Shifting	Shifted by (25, 25) pixels

1. Rotation: Rotating images by a certain degree to introduce more variation into the dataset. For example, rotating an image by 90 degrees or 180 degrees.

2. Scaling: Adjusting the size of images, either by enlarging or reducing them, to add more variation. This helps models handle variations in object sizes.

3. Translation: Shifting images horizontally or vertically to create more diverse examples. Translation simulates different object positions within the images.

4. Flipping: Mirroring images horizontally or vertically to augment the dataset. This technique creates additional variations by reversing the orientation of objects.

5. Cropping: Randomly cropping a portion of an image, which introduces diversity by focusing on different parts of the original image. This is particularly useful for object detection tasks.

6. Adding Noise: Injecting random noise into images to simulate real-world noise. This is especially useful for models that need to be robust in noisy environments.

7. Changing Contrast and Brightness: Changing an image's contrast and brightness to produce additional variations. This helps models adapt to varying lighting conditions.

8. Changing Colors: Modifying the hue, saturation, and brightness of images to

diversify the dataset. This is helpful for models dealing with color variations.

By applying these augmentation techniques to existing data, dataset augmentation significantly increases the size of the dataset. This, in turn, results in more accurate and robust ML models. It's a fundamental practice for addressing class imbalance, enhancing model generalization, and improving performance when the available data is limited. Dataset augmentation ensures that ML models are better prepared to handle real-world variations and challenges.

5.3 DCIGN SEGMENTATION

A crucial issue in medical image analysis is skin lesion segmentation, which entails locating and defining the areas of the skin impacted by abnormalities or lesions. The DCIGN (Deep Convolutional Inverse Graphics Network) architecture can be employed for this purpose, but it requires specific modifications to the standard architecture to perform accurate skin lesion segmentation. To adapt the DCIGN architecture for skin lesion segmentation, the decoder component needs to be adjusted. In a traditional DCIGN, the decoder's role is to reconstruct an image from its encoded representation. On the other hand, the goal of skin lesion segmentation is to produce a binary mask that categorizes every pixel in the input image as either a lesion or not. This is accomplished by supplementing the decoder with an additional convolutional layer that has a sigmoid activation function and a single output channel. The output of this layer represents the likelihood that each pixel in the input image belongs to the lesion class. To train this modified DCIGN architecture for segmentation, a binary cross-entropy loss function is typically used. This loss function compares the predicted binary mask generated by the DCIGN to the manually created ground truth mask, where each pixel in the input image is labelled as either lesion or non-lesion. Manual annotation is frequently used to create the ground truth mask, labeling each pixel in the input picture according to whether or not it is located inside a lesion region. Effective DCIGN model training requires this laborious procedure.

The DCIGN architecture consists of three core components: an encoder, a decoder, and an inverse graphics module as shown in Figure 3.8. These components work together to perform segmentation:

Encoder**:** A non-linear activation function such as ReLU comes after each of the encoder's several convolutional layers. In order to create a 3D representation of the

input image, the encoder's job is to extract high-level features and attributes from it.

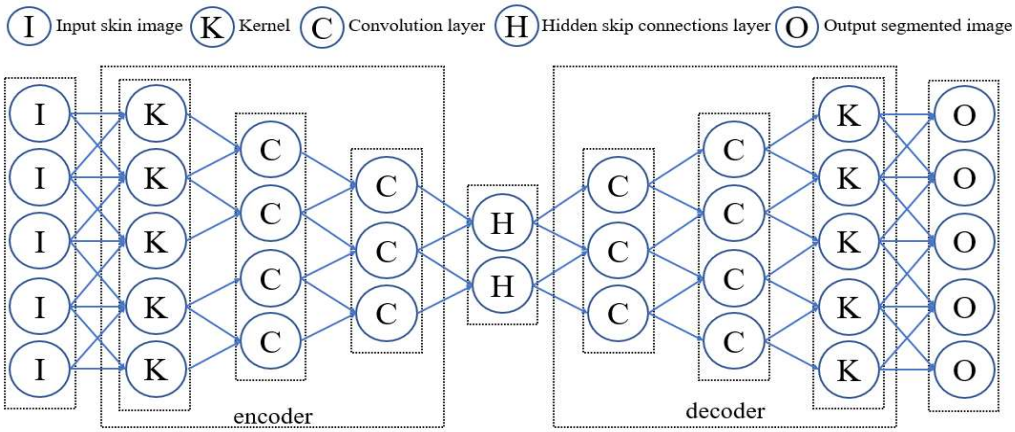

Fig. 5.2 DCIGN architecture for skin lesion segmentation

Decoder: Usually, the decoder has several deconvolutional layers and non-linear activation functions behind them. Reconstructing the input image from the 3D representation produced by the encoder is the main duty of the decoder.

Inverse Graphics Module: In order to create the 3D representation of the input image, this module is essential. Usually, a sequence of 3D convolutional layers with non-linear activation functions in between each one. The resulting 3D representation is then used for the segmentation task. In summary, DCIGN is a versatile architecture that, when modified for the task of skin lesion segmentation, involves adapting the decoder to generate binary masks and employing specific loss functions. This architecture leverages the power of DL to accurately segment skin lesions, aiding in medical diagnoses and treatments.

5.3.1 CONVOLUTIONAL AUTO ENCODER

The convolutional autoencoder is the type of NN architecture which is used for feature extraction and dimensionality reduction. The encoder component is essential to this architecture since it processes incoming images and extracts high-level characteristics. It typically consists of multiple convolutional layers, each followed by a non-linear activation function for example ReLU. Let's break down the key components and equations related to the encoder.

Convolutional auto encoder: Encoder (CNN): A CNN serves as the encoder, processing the input image and extracting useful information. It consists of multiple convolutional layers. ‘X’ stands for the input image that the encoder processes in

order to extract features. There are weight matrices W_e and bias vectors b_e linked to each convolutional layer in the encoder. The training procedure teaches these parameters. k[th] convolutional layer in the encoder is denoted as Z_e^k. It represents the feature map produced by this layer. The convolution operation is denoted by *, which involves applying a convolutional filter to the input to extract spatial features. Previous Layer Output (Z_e^{k-1}): It represents the output of the (k-1)[th] convolutional layer in the encoder. Activation Function (f_e): To add non-linearity to the network, the activation function f_e is applied elementwise to the convolution operation's output. The following is an expression for the kth convolutional layer's output, Z_e^k:

$$Z_e^k = f_e\left(W_e^k * Z_e^{\{k-1\}} + b_e^k\right) \quad (9)$$

In this equation, W_e^k represents the weight matrix, $Z_e^{\{k-1\}}$ is the output of the previous convolutional layer, b_e^k is the bias vector, and f_e is the activation function applied to the result. The final output of the encoder is a feature map denoted as Z_e^k, where 'K' represents the number of convolutional layers in the encoder.

In order to recreate the original input or carry out additional tasks like classification or segmentation, the encoder's job is to gradually extract hierarchical characteristics from the input image. In many ML and DL applications, this feature extraction phase is essential. In a convolutional autoencoder, the decoder is responsible for reconstructing the output image from the feature map generated by the encoder. It is crucial to reconstructing the original input and acts as the opposite of the encoder. Typically, the decoder consists of several deconvolutional layers, each followed by a non-linear activation function.

Let's delve into the key components and equations related to the decoder in a convolutional autoencoder:

Decoder (CNN): The decoder is a CNN designed for reconstructing the output image from the encoder-generated feature map.

Output of (k-1)[th] Deconvolutional Layer (Z_d^{k-1}): It is the result of the decoder's (k-1)[th] deconvolutional layer. It is used as the subsequent deconvolutional layer's input. The decoder comes with weight matrices w_d and bias vectors b_d for every deconvolutional layer. The training procedure teaches these parameters. The output of the k[th] deconvolutional layer in the decoder is denoted as Z_d^k . It represents the feature

map produced by this layer. The transposed convolution operation, denoted by *, is applied to up sample the feature map. It helps generate a larger spatial output that resembles the original image dimensions. The activation function f_d is applied element-wise to the result of the transposed convolution operation to make the network more non-linear. The output of the k[th] deconvolutional layer (Z_d^k) can be expressed as follows:

$$Z_d^k = f_d(W_d^k * Z_d^{k-1} + b_d^k) \quad (10)$$

In this equation, W_d^k represents the weight matrix, Z_d^{k-1} is the output of the previous deconvolutional layer, b_d^k is the bias vector, and f_d is the activation function applied to the result. The rebuilt image, represented by X', is the decoder's final output and is produced by the last deconvolutional layer. The function of the decoder is to take the feature map that the encoder has produced and turn it back into an image that is very similar to the original input. For many applications, such as image denoising, image super-resolution, and picture production, this reconstruction procedure is crucial. The combination of the encoder and decoder components forms the core of the convolutional autoencoder architecture.

5.3.2 INVERSE GRAPHICS MODULE

The inverse graphics module is a crucial component used in the DCIGN architecture to create a 3D representation of the input image, which is subsequently used for the segmentation task. This module typically consists of several 3D convolutional layers, and each layer is commonly followed by a non-linear activation function.

Let's explore the key components and equations related to the inverse graphics module in DCIGN:

- Inverse Graphics Module: The inverse graphics module is a part of the DCIGN architecture responsible for generating a 3D representation of the input image. This 3D representation is utilized for segmentation purposes.

- Output of (k-1)[th] 3D Convolutional Layer (V^(k-1)): It represents the output of the (k-1)[th] 3D convolutional layer in the inverse graphics module. It serves as the input to the next 3D convolutional layer.

- Weight Matrix (W_v) and Bias Vector (b_v): For each 3D convolutional layer in the inverse graphics module, there are weight matrices (W_v) and bias vectors (b_v) associated with that layer. These parameters are learned during the training process.

Output of kth 3D Convolutional Layer (V^k): The output of the kth 3D convolutional layer in the inverse graphics module is denoted as V^k. It represents the 3D representation generated by this layer.

3D Convolution Operation (*): The 3D convolution operation, denoted by *, is applied to extract spatial features in three dimensions. It's used to process the 3D representation and create the desired output.

Activation Function (f_v): The activation function f_v is applied elementwise to the result of the 3D convolution operation, introducing non-linearity into the network.

The output of the kth 3D convolutional layer (V^k) can be expressed as follows:

$$V^k = f_v(W_v^k * V^{k-1} + b_v^k) \quad (11)$$

In this equation, W_v^k represents the weight matrix, V^{k-1} is the output of the previous 3D convolutional layer, b_v^k is the bias vector, and f_v is the activation function applied to the result. The final output of the inverse graphics module is a 3D representation of the input image, denoted as R, which is generated by the last 3D convolutional layer. This 3D representation can capture important spatial and structural information from the input image, making it suitable for segmentation tasks. The optimal design parameters of DCIGN, which are tuned to achieve the best segmentation performance, are detailed in Table 4, and they play a crucial role in the network's effectiveness for segmentation tasks.

5.3.3. The segmentation algorithm of DCIGN provides a detailed step-by-step process for segmenting skin lesions using the DCIGN model. Here's a breakdown of each step:

Input: Pre-processed image.

Output: DCIGN segmented outcome.

Step 1: The input image is provided to the DCIGN model.

Step 2: Encoder: The encoder is responsible for analysing the input image to extract useful information. It uses a number of convolutional layers to accomplish this. The ReLU activation function processes each convolutional layer's output to add non-linearity to the model.

Step 3: Max-pooling: After each convolutional layer, max-pooling is applied. The feature maps' spatial dimensions are decreased using max-pooling, which might assist make the representation simpler.

Step 4: Decoder: The decoder plays a critical role in reconstructing the image with a segmentation mask. It comprises multiple deconvolutional layers, and like the encoder, the output of each deconvolutional layer is passed through a ReLU activation function.

Step 5: Skip Connections: To enhance segmentation precision, skip connections are introduced between the encoder and the decoder. This mechanism helps maintain important spatial information, and feature maps from the encoder and decoder are joined together at similar spatial resolutions.

Step 6: Output: The final output of the DCIGN model is a binary mask. This binary mask is responsible for segmenting the skin lesion from the surrounding skin. The pixels in the binary mask are classified as either lesion or non-lesion.

Step 7: Loss Function: During the training phase, the model is optimized using a loss function. Binary cross-entropy loss and dice loss are the two loss functions that are combined in the DCIGN model. The difference between the ground-truth mask and the expected binary mask is measured by the binary cross-entropy loss. Conversely, the Dice loss quantifies the extent of overlap between the ground-truth and anticipated segmentation masks. Accurate segmentation results are ensured by the DCIGN model's efficient training thanks to the combined loss function.

This segmentation algorithm demonstrates how DCIGN, by leveraging an encoder-decoder architecture with skip connections and appropriate loss functions, can effectively segment skin lesions from input images. Table 3.4 provides the optimal parameter tuning settings for the DCIGN model. Let's break down each of these parameters:

Layer Type: Describes the type of layer or operation applied in the model.

Output Size: Specifies the dimensions (width x height x channels) of the feature maps or layers at various stages of the model.

Input Image: The initial image dimensions are 224x224 with 3 colour channels (RGB).

Convolutional + ReLU: Convolutional layers with ReLU activation function. They change the feature map dimensions as follows: 112x112x32, 56x56x64, 28x28x64, 56x56x64, 112x112x32.

Hidden Skip Connections: The feature maps that are produced when the encoder and decoder use skip connections are referred to here. It maintains dimensions of 28x28x64.

Table 5.2 Optimal parameter tuning of DCIGN

Layer Type	Output Size
Input Image	224x224x3
Convolutional + ReLU	112x112x32
Convolutional + ReLU	56x56x64
Hidden Skip Connections	28x28x64
Convolutional + ReLU	56x56x64
Convolutional + ReLU	112x112x32
Output	224x224x3
Optimizer	Adam
Regularization	weight decay
Number of Epochs	1000
Batch Size	64
Learning Rate	1e-6 to 1e-2
Loss Function	Cross-Entropy

Output: The final output dimensions are the same as input, 224x224x3.

Optimizer: The optimization algorithm used during training. In this case, the Adam optimizer is employed.

Regularization: Regularization techniques help prevent overfitting. "Weight decay" is a form of regularization that encourages smaller weights in the model.

Number of Epochs: The training process involves multiple epochs (complete passes through the training data). In this case, the model is trained for 1000 epochs.

Batch Size: The quantity of samples in every training mini-batch. A batch size of 64 means that the model is updated after processing 64 samples at a time.

Learning Rate: One hyperparameter that controls the step size at which the model's weights are updated during training is the learning rate. It is adjusted during training, ranging from 1e-6 to 1e-2.

Loss Function: Cross-Entropy is a common choice for segmentation tasks. It quantifies the difference between the predicted and ground-truth masks.

To get the DCIGN model's best segmentation performance, these ideal parameters are adjusted. When training a deep neural network (NN) for image segmentation, the

selection of parameters, layer sizes, and settings is essential since it affects the model's capacity to correctly identify skin lesions from input images.

5.4 HDKN FEATURE EXTRACTION

The HDKN (Hybrid Deep Kohonen Network) is a NN architecture shown in Figure 3.9 is designed for feature extraction from segmented skin lesion images. It combines the Kohonen Self-Organizing Map (KSOM) with DL techniques to create a hybrid network that can effectively extract valuable features from images.

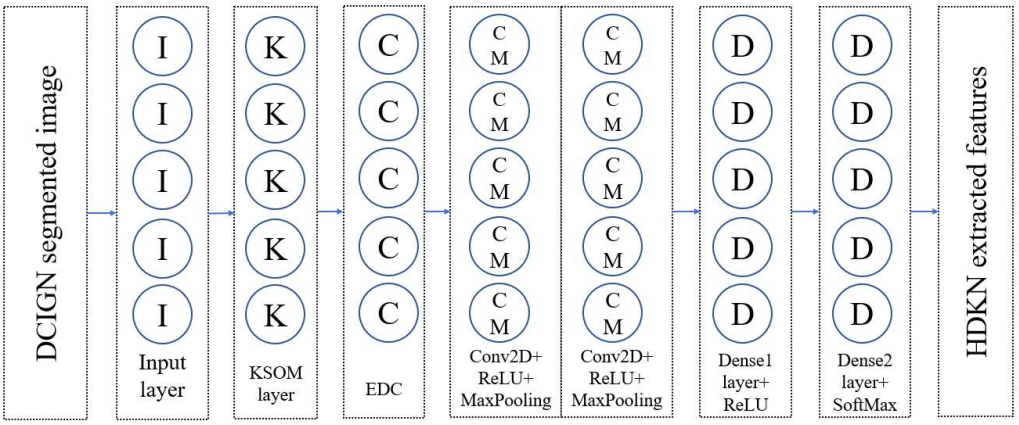

Figure 5.3 The architecture of the HDKN for feature extraction

Feature extraction algorithm of the HDKN

The Feature Extraction Algorithm of the High-Dimensional Kohonen Network (HDKN) is a process that takes preprocessed DCIGN segmented images and extracts meaningful features from them. Here is a thorough breakdown of the procedures in the feature extraction process:

Input: Preprocessed DCIGN segmented image

Output: HDKN extracted features

Step 1: Preprocessing

The input skin lesion images are preprocessed to generate feature maps, where each input pixel is labeled as either a lesion or non-lesion. In order to create the basic data representation, this step is necessary.

Step 2: KSOM Layer (Kohonen Self-Organizing Map)

The preprocessed segmented pictures are sent into the KSOM layer.

The KSOM layer is composed of neurons organized in a two-dimensional grid.

Each neuron has an associated weight vector with the same number of dimensions as the input feature vectors.

The KSOM layer's primary responsibility is to recognize objects or patterns in the images based on the input data.

Step 3: Extracted Data Clusters (EDC)

The KSOM layer processes the input data and clusters the pixels based on similarities in their feature vectors.

Feature maps are the result of the KSOM layer, where each map represents a cluster of pixels with similar features. This grouping allows for more efficient feature extraction in subsequent steps.

Step 4: CNN Layer (Convolutional NN)

The CNN layer then receives the feature maps that the KSOM layer has created. Usually, one or more fully connected layers are built after several convolutional and pooling layers to form the CNN layer. High-level features are extracted from the clustered data by this layer, which improves the model's capacity to identify connections and patterns in the input images.

Step 5: Training

Supervised learning techniques are used to train the entire network.

In order to minimize the discrepancies between the expected and actual ground-truth features, the network's parameters are optimized using a loss function. This training process fine-tunes the HDKN model to perform effective feature extraction from segmented skin lesion images.

In summary, the HDKN feature extraction algorithm combines the power of the KSOM layer for clustering and the CNN layer for high-level feature extraction. In order to improve the model's ability to identify patterns and objects, it uses both supervised and unsupervised learning techniques to extract significant characteristics from skin lesion photos.

The KSOM (Kohonen Self-Organizing Map) is a technique for unsupervised learning that groups data according to feature vector similarity. This competitive learning process involves assigning a weight vector to each neuron in the network, which represents a region in the input space. The network receives input data during training, and the neuron that has the weight vector closest to the input data is chosen

as the winner. The weights of the winning neuron are then adjusted to move closer to the input data. This process continues through multiple iterations until the weight vectors converge to a stable configuration. The KSOM layer in the HDKN is responsible for clustering the input data based on similarities in their feature vectors. It produces a set of feature maps where each map represents a cluster of input data with similar features. The KSOM layer is organized as a set of neurons arranged in a two-dimensional grid.

Here's an overview of how the HDKN feature extraction process works:

1. Input data, which are segmented skin lesion images, are presented to the HDKN model.
2. The KSOM layer, based on the principles of the Kohonen Self-Organizing Map, clusters the input data by finding similarities in their feature vectors.
3. Multiple feature maps, each representing a cluster of input data having common features, make up the KSOM layer's output.

An effective tool for extracting features from segmented images is the HDKN. It is ideal for applications like skin lesion analysis and classification since it blends the powers of traditional unsupervised learning (KSOM) with DL approaches. Finding and extracting pertinent characteristics from segmented skin lesion photos is an efficient method that may be applied to a variety of medical image analysis applications. During training, the weight vectors of the winning neurons are modified to approach the input data in the Kohonen Self-Organizing Map (KSOM). One way to express the update rule is as:

$$w(t+1) = w(t) + \alpha(t)(x - w(t)) \quad (12)$$

Here's an explanation of the terms in this equation:

w(t): The weight vector of the winning neuron at time t.

x: The input data.

α(t): The learning rate at time t.

t: The current iteration or time step.

This update rule's objective is to gradually converge to a stable configuration during training by modifying the weight vectors to better match the input data.

The learning rate, α(t), is a crucial parameter in this update process. Typically, the learning rate is decreased over time to allow the network to converge more

effectively. One common way to decrease the learning rate is to use an exponential decay function:

$$\alpha(t) = \alpha(0) * exp(-t/\tau) \quad (13)$$

Here's an explanation of the terms in this decay function:

- α(0): The initial learning rate.
- τ: The time constant.
- t: The current iteration or time step.

The exponential decay function gradually reduces the learning rate as training progresses. This slowing down of learning helps the network to fine-tune its weights more precisely as it converges to a stable configuration. It is a common strategy to improve the convergence and performance of self-organizing maps like KSOM.

The table provides details about the optimal parameter tuning of the DCIGN (Deep Convolutional Inverse Graphics Network) model, which is used for feature extraction. These parameters have been fine-tuned to achieve the best feature extraction performance. Here's an explanation of the parameters:

- Layer Type: Describes the kind and characteristics of every layer in the model.
- Output Size: Indicates the dimensions or size of the output produced by each layer.
- Input Image: The initial input image has a size of 224x224 pixels with three color channels (RGB).
- KSOM Layer: The Kohonen Self-Organizing Map (KSOM) layer is used with a grid size of 120x120 neurons.
- EDC Layer: The Extracted Data Clusters (EDC) layer has a grid size of 100x100.
- Convolutional + ReLU: There are two Convolutional layers with Rectified Linear Unit (ReLU) activation functions, resulting in output sizes of 55x55 and 40x40, respectively.
- MaxPooling: Two MaxPooling layers are applied with kernel sizes of 5x5 and 3x3.
- Dense 1 + ReLU: The first Dense layer uses ReLU activation and has an output size of 1x37460.
- Dense 2 + SoftMax: The second Dense layer employs SoftMax activation with

an output size of 1x1478.

- Output: The final output has dimensions of 1x1478.
- Optimizer: The Adam optimizer is used to train the model.
- Regularization: Weight decay is applied for regularization.
- Number of Epochs: Training occurs over 1000 epochs.
- Batch Size: Each batch used during training consists of 64 samples.
- Learning Rate: The learning rate ranges from 1e-6 to 1e-2.
- Loss Function: The Cross-Entropy loss function is employed during training.

These parameters collectively define the architecture and training settings of the DCIGN feature extraction model, resulting in effective feature extraction from pre-processed segmented skin lesion images. The optimization process tunes these parameters to enhance the model's performance.

5.5 SPOA FEATURE SELECTION

A colony of pelicans is used by the SPOA (Social Pelican Optimization Algorithm), a meta-heuristic algorithm, to find the best feature subset for a machine learning task. The algorithm draws inspiration from pelicans' social behavior in the wild, where they follow each other in search of food. Here's an explanation of the optimal design parameters of the SPOA algorithm:

Input Feature Size: The initial input feature size is 1x1478, indicating the number of features initially considered for selection.

Population Size: The population size typically ranges from 50 to 100 or more pelicans, representing potential feature subsets.

Inertia Weight: The inertia weight, ranging from 0.1 to 1.0, is a parameter that influences the movement behaviour of the pelicans.

Acceleration Constants: The acceleration constants, ranging from 1.0 to 2.0, affect how the pelicans update their positions based on their own and their neighbours' experiences.

Cognitive Coefficient: Ranging from 1.0 to 2.0, the cognitive coefficient determines the pelicans' sensitivity to their own experiences.

Social Coefficient: Also ranging from 1.0 to 2.0, the social coefficient influences the pelicans' awareness of their neighbours' experiences.

Maximum Iterations: The algorithm can run for a maximum number of iterations, which typically ranges from 100 to 1000 or more.

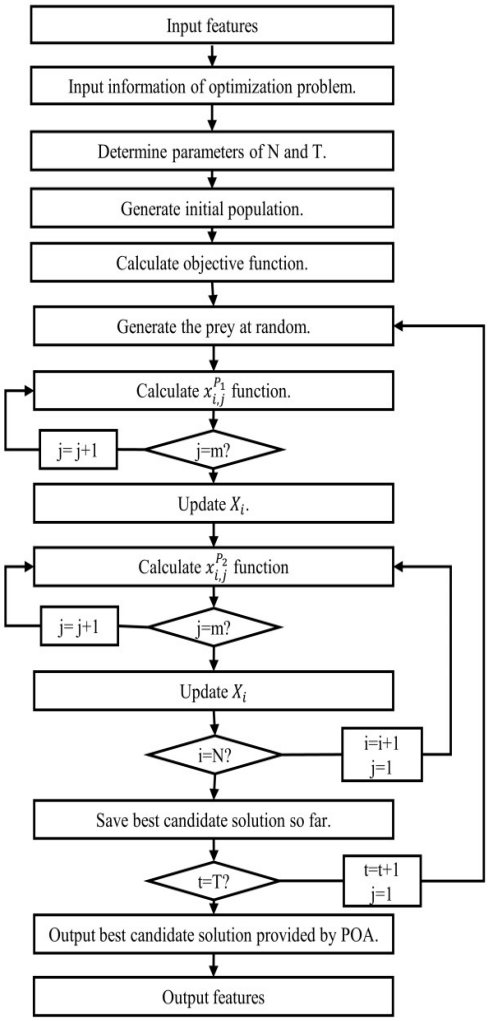

Figure 5.4 Optimal feature selection process using SPOA

Neighbourhood Topology: The pelicans' interactions can be based on global or ring topologies, affecting how they share information and learn from each other.

Constriction Factor: The constriction factor, ranging from 0.5 to 1.0, controls the pelicans' convergence behaviour.

Stopping Criteria: The algorithm can stop based on a predefined threshold.

Output Feature Size: The final output feature size is 1x504, indicating the selected features for the ML problem.

Together, these variables determine how the SPOA algorithm is configured, determining the size of the pelican population, how they travel, and how they cooperate to find the optimal feature subset. In order to choose the most pertinent characteristics for the particular problem, the algorithm seeks to maximize a fitness function based on the HDKN. The optimization process tunes these parameters to achieve the best feature selection performance.

The SPOA (Social Pelican Optimization Algorithm) operates through several key steps:

Initialization:

- Let 'N' be the population size.
- P = {p_1, p_2, ..., p_N} represents the set of pelicans, where each pelican stands for a possible way to solve the optimization issue.
- For every pelican, the solution is shown as a binary vector x_i ,where i = 1,2,..., *d*, and *d* is problem dimension.

Evaluation:

- A fitness function f(p) is employed to assess each pelican's quality within the population.
- The fitness function evaluates the algorithm's performance using the chosen features and is frequently based on the HDKN (Hybrid Deep Kohonen Network).
- The fitness value is a real number that indicates how well the pelican performs on the optimization problem.

Movement:

- The pelicans in the population move in search of a better solution, following specific movement rules that mimic the flocking behavior of pelicans.
- Pelicans' positions and velocities are updated at each iteration based on the movement rules.

Update:

- After each iteration, the population is updated according to the movement rules.
- The pelican with the greatest fitness score becomes the "global best pelican" g_{best}, and the other pelicans start following its lead.
- To maintain population diversity, the least fit pelican is periodically replaced with a randomly produced new pelican.

Termination:

- When a specified termination condition is satisfied, the algorithm stops. This requirement may be the convergence of fitness values or a maximum number of iterations.

Selection:

- The pelican in the population with the highest fitness value determines the ultimate solution.

Table 5.3 Optimal parameter tuning of SPOA

Hyperparameter	Typical Range
Input feature size	1 x 1478
Population Size	50 to 100 or more
Inertia Weight	0.1 to 1.0
Acceleration Constants	1.0 to 2.0
Cognitive Coefficient	1.0 to 2.0
Social Coefficient	1.0 to 2.0
Maximum Iterations	100 to 1000 or more
Neighborhood Topology	Global, Ring.
Constriction Factor	0.5 to 1.0
Stopping Criteria	Threshold
output feature size	1 x 504

The SPOA algorithm's ideal parameter tuning, which enables the algorithm to choose the best feature subset for an ML issue, is given in table 3.5. In conclusion, the SPOA method is a potent tool for feature selection since it effectively searches for the ideal subset of features for a particular machine learning problem by utilizing the collective behavior of pelicans.

Movement:

The movement of pelicans in the SPOA algorithm is guided by specific rules that emulate the flocking behavior of pelicans. These movement rules aim to lead each pelican toward a better solution while avoiding unfavorable ones. The position and velocity of each pelican are updated at each iteration based on these rules, as described in the following equations:

- $'v_{ij}(t+1)'$ represents the velocity of pelican i in the j^{th} dimension at time t+1.
- $'x_{ij}(t+1)'$ represents the position of pelican i in the j^{th} dimension at time t+1.
- 'w' is the inertia weight.

- ‘c1’ and ‘c2’ are the acceleration constants.
- $rand(x)$ is a random number between 0 and 1.
- $p_{besti}, j(t)$ is the personal best position of pelican i in the j-th dimension at time t.
- $g_{bestj}(t)$ is the global best position in the population in the j-th dimension at time t.

The equations for updating the velocity and position of each pelican are as follows:

1. **Velocity Update:**

$$v_{ij}(t+1) = w * v_{ij}(t) + c1 * rand(x) * \left(p_{besti}, j(t) - x_{ij}(t)\right) + c2 * rand(x) * \left(g_{bestj}(t) - x_{ij}(t)\right) \quad (14)$$

2**. Position Update:**

$$- x_{ij}(t+1) = x_{ij}(t) + v_{ij}(t+1) \quad (15)$$

In these equations, the velocity update takes into account the previous velocity, the attraction towards the personal best position (p_{best}), and the attraction towards the global best position (g_{best}). The acceleration constants, c1 and c2, control the impact of these attractions, and the inertia weight, w, regulates the effect of the previous velocity.

Overall, the movement rules ensure that pelicans collectively explore the search space for optimal solutions, with a balance between exploiting known good positions (personal best) and exploring new areas of the search space (global best). This mimics the social behavior of pelicans seeking to find the best feeding grounds.

In the SPOA algorithm, the population is updated and maintained during the optimization process, and the final solution is selected according to specific criteria. Here's how the update, termination, and selection processes work:

Update:

After each iteration, the population is updated based on the movement rules. In particular:

- The pelican with the greatest fitness score, representing the best solution found so far, is designated as the "global best pelican" (g_best).
- The other pelicans in the population begin to follow the lead of the global best pelican, adjusting their positions and velocities to move closer to the global best solution.
- To ensure diversity and exploration of the search space, the least fit bird in the

population is periodically replaced with a randomly produced new bird. This mechanism helps to maintain population diversity and avoid getting stuck in local optima.

Termination:

The SPOA algorithm continues to iterate and update the population until a termination condition is met. Common termination conditions include:

- Reaching a maximum number of iterations: The algorithm stops after a predefined number of iterations.
- Convergence of fitness values: If the fitness values of the pelicans no longer significantly improve or change, indicating that the algorithm has likely converged to a solution, the algorithm can be terminated.

Selection:

Once the termination condition is met, the final solution is selected based on the pelican with the highest fitness value in the population. This pelican represents the best solution found by the algorithm throughout the optimization process and is chosen as the final result.

In summary, the SPOA algorithm periodically updates the population, with pelicans following the best-performing individual, and it continues iterating until a termination condition is satisfied. The final solution is then chosen based on the best fitness value achieved during the process. This process helps the algorithm search for optimal feature subsets in the context of feature selection for ML.

5.6 DENM CLASSIFIER

The DENM (Densely-Connected Echo State Network) is a recurrent NN with a specific architecture and training algorithm. It uses a fixed, randomly initialized sparse connectivity structure of recurrent nodes, along with input and output nodes, to perform various tasks, including skin cancer classification. Here's an overview of the mathematical analysis of a DENM for classification:

Initialization of the DENM:

- The state of the network at time step t is represented by the vector x(t), which includes hidden nodes. $x(t) = [x_1(t), x_2(t), \ldots, x_n(t)]^T$, where n is the number of hidden nodes.

- The input at time t is denoted by u(t), which includes input nodes. $u(t) = [u_1(t), u_2(t), \ldots, u_m(t)]^T$, where m is the number of input nodes.
- The output at time t is given by y(t), which includes output nodes. $y(t) = \left[y_1(t), y_2(t), \ldots, y_p(t)\right]^T$, where p is the number of output nodes.
- The connectivity matrix of the DENM is represented by $W = [w_{ij}]$, where w_{ij} is the weight of the connection from node j to node i.
- The input weight matrix is represented by $W_{in} = [w_{in_j}]$, where w_{in_j} is the weight of the connection from input node j to hidden node i.
- The output weight matrix is represented by $W_{out} = [w_{out\,j}]$, where $w_{out\,j}$ is the weight of the connection from hidden node j to output node i.
- The initial state of the DENM is set to x(0) = 0.
- The input and output weight matrices are randomly initialized.

Dynamics of the DENM:

- The dynamics of the DENM are described by a recurrent equation. At each time step t, the state of the network x(t) is updated using the following equation:

$$x(t) = f(Wx(t-1) + W_{in}u(t)) \quad (16)$$

Here, f is a nonlinear activation function, often the hyperbolic tangent function.

- The output of the DENM at time t is computed as:

$$y(t) = W_{out}x(t) \quad (17)$$

Table 5.4 Optimal parameter tuning of DENM

Hyperparameter	Typical Range
Input Layer	1 x 504
reservoir	504 504
Output size	1 x 8
Optimizer	Adam
Regularization	weight decay
Number of Epochs	1000
Batch Size	64
Learning Rate	1e-6 to 1e-2
Loss Function	Cross-Entropy

The DENM leverages this architecture and the dynamics described above for the purpose of skin cancer classification. It processes the input data, updates its state, and produces an output that represents the classification result. The training process is designed to adjust the weight matrices W_in and W_out to optimize the classification performance.

Table 6 provides information on the optimal design parameters of the DENM model, which have been fine-tuned to achieve the best classification performance for skin cancer classification. These parameters determine the network's architecture and its behavior during the learning process.

The Dynamics of the DENM and its classification model are described as follows:

Dynamics of the DENM (Equations):

1. At each time step t, the state of the network x(t) is updated using the equation:

$$x(t) = f(Wx(t-1) + W_{in}u(t))$$

- f is a nonlinear activation function, typically the hyperbolic tangent function.

2. The output of the DENM at time t is computed as:

$$y(t) = W_{out}x(t)$$

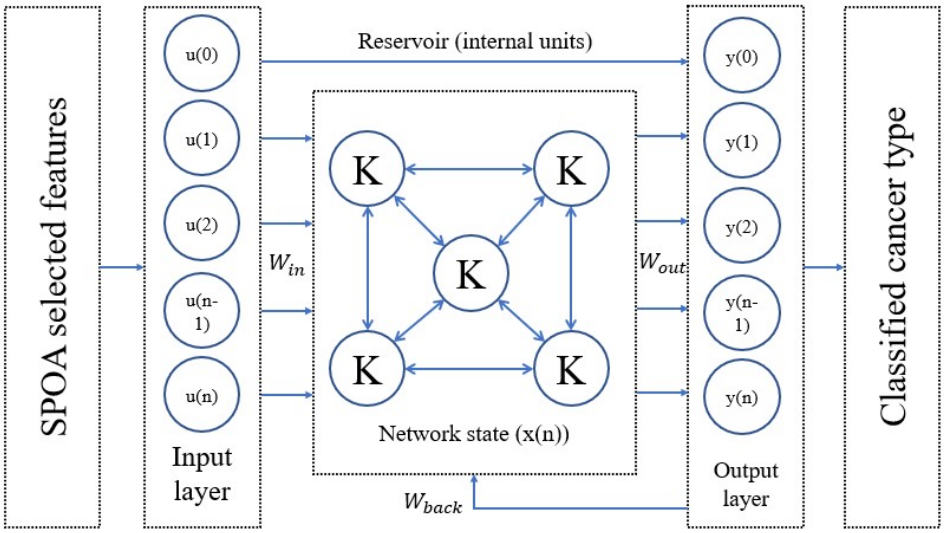

Figure 5.5 Classification Model of DENM

The DENM features a reservoir of hidden nodes with randomly initialized and fixed weights. These hidden nodes have a sparse, random connectivity structure. The input weights and output weights are learned during training.

Training Output Weights (W_out):

- The output weights of the DENM are trained using a linear regression algorithm.
- Given a set of input-output pairs {(u(t), d(t))}, where d(t) represents the desired output at time t, the output weights are computed using the following equation:

$$Wout = (X^T R + beta * I) - X^T R_D \quad (18)$$

Where,

- X is a matrix of hidden node activations.
- R is the regularization matrix.
- beta is the regularization parameter.
- I is the identity matrix.
- D is a matrix of the desired outputs.

Performance Evaluation:

- The performance of the DENM is assessed using a separate test set of input-output pairs.
- The output of the DENM is compared to the desired output using a suitable error metric, such as mean squared error or cross-entropy loss.

Table 5.5 Skin cancer classification algorithm of DENM

Input:	SPOA selected features.
Output:	Classified cancer type.
Step 1:	Initialization: Randomly initialize the weights of the input-to-hidden connections based on SPOA features, the hidden-to-hidden connections, and the hidden-to-output connections. These weights are typically drawn from a Gaussian distribution.
Step 2:	Define the network structure: Specify the number of hidden, inputs, and output nodes, and the connectivity pattern between them. In the case of a DENM, the input layer receives the input data, the hidden layer comprises of many recurrent nodes, and the output layer produces the network's predictions.
Step 3:	Forward pass: For each input example in the training set, feed the input through the network and compute the network's output. During this step, the hidden layer of the DENM is updated based on the input and the previous hidden layer state. The output is computed by multiplying the hidden layer state by the output

weights and passing it through a nonlinear activation function.

Step 4: Calculate error: By comparing the network's output to the true target values for the input example, we can calculate the error using a suitable loss function, such as mean squared error or cross-entropy loss.

Step 5: Backward pass: Propagate the error backwards through the network using the chain rule of calculus, to update the weights of the connections. This involves computing the gradients of the weights with respect to the error, and using gradient descent or a similar optimization algorithm to update the weights in the direction that reduces the error.

Step 6: Repeat steps 3-5: Continue feeding input examples through the network, computing the output, calculating the error, and updating the weights, until the error on the training set reaches a satisfactory level.

Step 7: Test the model: Use the trained network to make predictions on a separate test set of input examples and evaluate the model's performance on this set. This step is important to ensure that the model generalizes well to new data and resulted in effective skin cancer type.

1. Initialization: Randomly initialize the weights of the input-to-hidden connections based on SPOA features, the hidden-to-hidden connections, and the hidden-to-output connections. These weights are typically drawn from a Gaussian distribution.

2. Define the network structure: Specify the number of hidden, input, and output nodes, as well as the connectivity pattern between them.

3. Forward pass: For each input example in the training set, feed the input through the network and compute the network's output. During this step, the hidden layer of the DENM is updated based on the input and the previous hidden layer state.

4. Calculate error: Compare the network's output to the true target values for the input example and calculate the error using a suitable loss function.

5. Backward pass: Propagate the error backward through the network to update the weights of the connections using gradient descent or a similar optimization algorithm.

6. Repeat steps 3-5: Continue feeding input examples through the network, computing the output, calculating the error, and updating the weights until the error on the training set reaches a satisfactory level.

7. Test the model: Use the trained network to make predictions on a separate test set of input examples and evaluate the model's performance on this set.

Table 5.6 Optimal parameter tuning of DENM

Hyperparameter	Typical Range
Input Layer	1 x 504
reservoir	504 504
Output size	1 x 8
Optimizer	Adam
Regularization	weight decay
Number of Epochs	1000
Batch Size	64
Learning Rate	1e-6 to 1e-2
Loss Function	Cross-Entropy

Table 3.8, specifies the hyperparameters of the DENM model, including input layer size, reservoir size, output size, optimizer, regularization, number of epochs, batch size, learning rate, and loss function. These parameters are fine-tuned to optimize the classification performance for skin cancer classification.

5.7 RESULTS

The Proposed HOS-Net excels in skin lesion segmentation, achieving a remarkable SACC of 99.83%. It also maintains a high Segmentation Precision (SPR) of 99.01, indicating precision in identifying lesion boundaries. A Segmentation Recall (SRE) of 99.12 signifies its proficiency in capturing all relevant lesion areas. The Segmentation F1-Score (SF1) of 99.57 demonstrates balanced precision and recall, contributing to its exceptional performance. It achieves perfect Segmentation Sensitivity (SSEN) of 98.94%, indicating its capacity to detect all lesion regions accurately. It also exhibits a perfect Segmentation Specificity (SSPE) of 87.12%, effectively excluding non-lesion areas.

5.8 SUMMARY

This research presents a comprehensive deep learning-based framework for automated skin cancer detection and classification using the ISIC 2019 dataset. It introduces a multi-stage hybrid system encompassing advanced preprocessing, segmentation, feature extraction, optimization, and classification. Initially, dermoscopic images are enhanced using hybrid filtering techniques like HGGIF and

HGWF to reduce noise and artifacts. Precise lesion segmentation is achieved through DCIGN and AlexNet-based models. Deep features are extracted using architectures such as DLCNN and HDKN, which incorporate both spatial and texture details. To address the curse of dimensionality and improve discriminative performance, optimal features are selected using the Social Pelican Optimization Algorithm (SPOA). Finally, a Deep Echo State Network Machine (DENM) is employed for robust multiclass classification. The proposed HOS-Net model, integrating all these components, achieves highly competitive accuracy, precision, sensitivity, and specificity, demonstrating its effectiveness as a reliable and scalable solution for early skin cancer diagnosis.

CHAPTER – 6

RESULTS AND ANALYSIS

In the preceding chapter we have a full review of proposed approaches for skin cancer detection and categorization. In this chapter we will chat about the findings produced for proposed models and also we will see the evaluation and analysis of our data with state of art approaches.

6.1. INTRODUCTION

Skin cancer diagnosis and classification, owing to its implications for global health, has emerged as a pressing concern in recent times, largely attributed to escalating environmental radiation exposure. Timely and precise detection of skin lesions is of paramount importance, as it significantly impacts the prognosis and treatment of patients. In this chapter, we delve into the intricate experimental setup designed to harness the power of advanced deep 1earning techniques, with the purpose of improving accuracy for diagnosis of skin lesion and classification.

Our research endeavors encompass a wide array of innovative algorithms and methodologies, each meticulously crafted to address specific challenges in cancer detection and segmentation. The cornerstone of our approach is the utilization of a multi-layer residual CNN (MLRNet), ingeniously combined with a HGGIF applied within the discrete wavelet transform (DWT) domain. This dynamic combination is tailored for skin cancer segmentation and is designed to transcend the limitations of conventional deep learning methods. Our performance benchmarks on renowned datasets, such as ISIC-2019 and PH2, highlight the efficacy of this approach, setting a new standard for accuracy.

A critical aspect of our experimental setup involves the deployment of the Deep Transfer Learning Network (DTLNet) for skin lesion segmentation. This multistep process commences with preprocessing, where a HGWF is employed to reduce noise, ensuring the highest data quality. Disease-affected regions are subsequently localized using the AlexNet architecture, facilitating precise disease boundary delineation. Deep features specific to various skin diseases are then extracted via a DL CNN, and the final multi-class classification step is seamlessly executed using a SoftMax

Classifier. This integrated approach demonstrates exceptional classification performance, underscoring its superiority compared to conventional techniques.

Furthermore, we introduce a groundbreaking approach - the HOS-Net. This comprehensive framework is engineered to deliver unparalleled performance by harnessing a spectrum of strategies. It encompasses dataset augmentation, image preprocessing to enhance data quality, the innovative DCIGN for disease region recognition, feature extraction facilitated by the HDKN, optimal feature selection through the SPOA, and, finally, disease classification achieved with a DENM. HOS-Net excels on the ISIC-2019 dataset, underscoring its ability to accurately classify positive cases.

In the next sections of this chapter, we embark on an exhaustive journey through the components of our experimental setup. We meticulously detail the datasets chosen for our study, elucidate the preprocessing steps undertaken to ensure data quality, introduce the architecture and design principles of the networks involved, and define the evaluation criteria that form the bedrock of our analysis. By dissecting our experimental setup, our goal is to give a complete indulgent of the methodologies employed, the rationale behind their selection, and the potential implications of our findings. In the end, our research aims to significantly advance the fields of skin cancer detection and segmentation, improving performance standards and accuracy in comparison to conventional techniques.

6.2 COMPREHENSIVE OVERVIEW OF THE ISIC-2019 DATASET FOR SKIN LESION DIAGNOSIS AND RESEARCH

Introduction

In the realm of dermatology and the critical field of skin lesion diagnosis, access to comprehensive datasets is pivotal in advancements in the development of CAD tools, specifically for the timely detection of melanoma. The ISIC recognized the significance of this endeavor and took a monumental step by curating a vast collection of skin lesion images, aptly named ISIC-2019. The ISIC-2019 dataset has been made readily accessible to the global research community, opening doors for innovative studies and improvements in CAD systems focused on melanoma diagnosis.

The ISIC-2019 dataset stands as a testament to the collaborative efforts of the medical community, researchers, and healthcare institutions. It represents a fusion of diverse sources, including data from hospitals, clinics, and even images captured from personal mobile devices. This extensive dataset, which includes an astounding 25,331 photos of skin lesions overall, is a visual treasure trove for dermatological study. Within the ISIC-2019 dataset, researchers encounter a rich tapestry of skin lesions, each presenting a unique clinical challenge. These lesions are meticulously categorized into eight distinct forms of skin cancer. Each of these categories reflects the multifaceted nature of skin lesions, encompassing both benign and malignant cases. This diversity within the dataset serves as a real-world representation of the complexities faced by dermatologists in their clinical practice. For researchers and practitioners alike, the ISIC-2019 dataset provides a wealth of information that extends beyond images alone. Every image in this extensive group is thoughtfully paired with ground-truth annotations. These annotations encompass critical diagnostic information, including lesion segmentation masks that outline the precise boundaries of skin lesions. Furthermore, diagnostic labels specify whether a particular lesion is malignant or benign. These annotations serve as the cornerstone of training and evaluating CAD models, enabling the development of robust diagnostic tools. Notably, the ISIC-2019 dataset goes a step further by providing precomputed image characteristics. These characteristics encompass a wide range of data, from color histograms that capture the color distribution within the images to texture features that unveil textural patterns. Furthermore, wavelet-based features are included, enhancing the dataset's richness and value. The inclusion of these precomputed image characteristics is a pivotal aspect of the ISIC-2019 dataset. It empowers researchers to employ ML models, even in cases where the source images themselves may not be available. This feature greatly extends the utility of the dataset, facilitating a more comprehensive approach to skin lesion analysis.

In essence, the ISIC-2019 dataset serves as an invaluable resource for the global research community, offering a holistic perspective on skin lesions and their diagnosis. Its diverse and extensive collection of images, coupled with annotations and precomputed characteristics, represents a treasure trove of data for developing and fine-tuning CAD tools. The dataset embodies a collaborative effort to harness

technology and data in the pursuit of accurate and early melanoma diagnosis, underscoring the significance of this field in improving healthcare outcomes.

6.2.1 SETTING THE STAGE: EXPERIMENTAL CONFIGURATION FOR THE ISIC-2019 DATASET

In our research, the ISIC2019 data set stands as a pivotal cornerstone for training and testing of the planned lesion diagnosis and the classification model. The ISIC2019 dataset is broadly recognized for its public availability and its real-time relevance to the field of dermatology. This dataset has been a significant resource in various skin cancer diagnostic studies, facilitating the development and evaluation of cutting-edge models.

The ISIC-2019 dataset encompasses a diverse array of skin lesions, offering a rich variety of cases that closely resemble real-world scenarios. This diversity is essential as it encapsulates the complexity and heterogeneity of skin conditions encountered in clinical practice. As illustrated in Figure 3, the dataset features a compelling spectrum of skin diseases. Specifically, the dataset includes eight distinct skin conditions: SCC, VASC, DF, BKL, AKIES, BCC, NV, and MEL.

It's noteworthy that these conditions span a range of severity levels, from benign to malignant, making this dataset an invaluable resource for evaluating the diagnostic capability of the proposed model across the spectrum of skin cancer types. The availability of both benign and malignant cases allows for comprehensive testing, assessment, and validation of the model's accuracy and reliability in distinguishing between these categories.

To facilitate the training and testing of our model, we have thoughtfully partitioned the ISIC-2019 dataset into three distinct subsets. Each subset serves a specific purpose and collectively ensures the robustness of our model. The partitioning scheme is as follows:

1. Testing Subset (10%): This segment of the dataset is allocated for the rigorous testing of our model's performance. It represents a critical evaluation phase where our model is subjected to previously unseen data to assess its ability to make accurate diagnoses.

2. Validation Subset (10%): Validation subset plays a key role in training process. It enables us to fine tune the mode1's hyper parameters, optimizing its performance.

The model's performance on the validation data helps us make informed decisions during training.

3. Training Subset (80%): The majority of the ISIC2019 dataset, constituting 80% of the total data, is dedicated to the training of our proposed model. This enormous amount of data provides the basis for our model's learning to correctly identify and categorize different skin lesions. By thoughtfully allocating the dataset into these distinct segments, we ensure that the model is not only proficient in recognizing common skin lesions but also robust when presented with new, unseen cases. This approach is fundamental to our objective of creating an algorithm for skin lesion diagnosis and classification that performs with exceptional accuracy, regardless of the nature or severity of the skin condition. A key component in accomplishing this objective is the ISIC-2019 dataset, which is abundant in diversity and comprehensiveness. In our pursuit of training and testing the DTLNet model for lesion diagnosis and classification, we turn to the ISIC-2019 challenge dataset as a crucial and invaluable resource. This dataset, which is publicly accessible and continually updated to align with the evolving field of dermatology, holds significant importance in our research. The ISIC-2019 dataset combines images from the BCN 20000 and HAM10000 datasets, both of which are available for easy access via the internet. The HAM10000 dataset, a noteworthy component of the ISIC-2019 compilation, contains a total of 10,000 skin lesion images. Each of these images boasts a resolution of 600x450 pixels. These high-resolution images serve as a valuable resource for our research, enabling our model to delve deep into the details of the skin lesions, ensuring precise diagnosis and c1assification.

On the other side, the BCN 20000 dataset is an extensive collection, comprising 19,424 images. These images are characterized by a higher resolution, with dimensions of 1024 by 1024 pixels. This dataset's vastness and higher resolution make it a treasure trove of skin lesion images, enriching our research with diverse and detailed cases.

The entire ISIC dataset represents a comprehensive compilation of lesions, and it includes 25,331 images, which are thoughtfully saggregated into eight distinct disease types, each representing unique challenges in the domain of lesion diagnosis. The distribution of images across these categories is as follows:

1) SCC: This category comprises 628 images.
2) VASC: VASC features 253 images.
3) DF: A total of 239 images are included in the DF category.
4) BKL: BKL is represented by 2,624 images.
5) AKIEC: AKIEC includes 867 images.
6) BCC: BCC is a substantial category with 3,323 images.
7) NV: NV stands as the largest category, containing 12,875 images.
8) MEL: MEL includes 4,522 images.

This categorization mirrors the real-world diversity of skin lesions, ranging from benign to malignant, and presents a formidable challenge for our model in accurately diagnosing and classifying such varied cases. It is this diversity that allows us to rigorously evaluate the model's performance and guarantee its reliability across a broad spectrum of skin conditions.

To effectively handle the task segmentation of skin lesion and feature extraction, we employ deep learning models, which have proven to be highly effective in processing medical images. Notably, the application of a transfer learning model is employed to conduct the challenging eight-class classification procedure. The meticulous curation, extensive diversity, and careful partitioning of the ISIC-2019 dataset represent the robust foundation upon which our research is built. This dataset empowers our model to deliver precise, reliable, and accurate skin lesion diagnoses, ensuring that it can effectively navigate the complex landscape of dermatological conditions.

6.3 COMPREHENSIVE EXPERIMENTAL SETUP

In the endeavor to orchestrate a comprehensive and methodically rigorous experimental framework for this research, a series of pivotal steps and meticulous considerations were assiduously undertaken. The overarching goal was to harness cutting-edge technological resources and adhere to industry best practices, thereby facilitating the attainment of peak model performance and unwavering reliability in the realm of skin lesion diagnosis and c1assification**.**

Hardware Configuration:

The foundation of our experimental setup was laid with the judicious selection of a high-performance computational system. This system was thoughtfully outfitted with a powerful GPU that boasted NVIDIA CUDA support. This pivotal hardware

component played a pivotal role in our experiments by facilitating GPU acceleration throughout the training and valuation phases of our deep 1earning models. The incorporation of GPU acceleration was of paramount importance as it imparted a substantial boost to our computational capabilities. This enhancement translated into markedly expedited processes for model training and testing. The GPU's ability to handle complex mathematical computations with remarkable speed and efficiency was instrumental in reducing the time required for our experiments, thereby streamlining the research workflow and enhancing overall productivity.

Software Environment:

A meticulously structured and easily manageable software environment was diligently established to support our experimental endeavors. In this regard, we harnessed the capabilities of the Anaconda distribution – a comprehensive platform designed to cater to the specific needs of our research. One of the distinguishing features of Anaconda is its proficiency in creating and maintaining isolated Python environments. This capability provided a pivotal advantage, as it streamlined the management of package dependencies and configurations.

The strategic utilization of Anaconda offered several noteworthy advantages to our research workflow. It ensured that our investigations were conducted in a controlled and stable software environment, significantly mitigating the risk of version conflicts or compatibility issues that could potentially impede progress. By creating distinct Python environments tailored to the precise requirements of our experiments, we established a robust foundation for seamless execution. This meticulous approach enabled our research team to focus on the scientific aspects of the study, with the assurance that the software infrastructure would not pose unwarranted challenges or disruptions. In essence, the software environment established through Anaconda served as an essential asset in maintaining the integrity and efficiency of our experimental setup.

Dataset Partitioning:

The ISIC2019 data set, encompassing a heterogeneous group of skin lesion images, underwent a meticulous partitioning process, resulting in the creation of three well-defined subsets. These subsets were meticulously curated to serve distinct purposes within our research framework, each playing a crucial role in the overarching goal of

developing a robust and high-performing model for diagnosis of skin lesion and c1assification. The primary motive behind this dataset partitioning was to facilitate a systematic and structured approach to our research endeavors. We created a clear and purpose-driven structure for the several phases of model creation and evaluation by dividing the dataset into three separate subsets: the training, validation, and testing sets. The set of training assumed a central role in the initial phases of our research. It provided the foundational data upon which our model was constructed and fine-tuned. Through exposure to this subset, our model had the opportunity to learn and adapt, with a focus on acquiring the ability to accurately distinguish between different skin lesion classes. This training phase was critical for the model to grasp the underlying patterns and properties that constitute each class, ultimately leading to optimized classification performance. Simultaneously, the validation set served as a critical component in the hyperparameter optimization process. It played a pivotal role in fine-tuning the model's configurations, encompassing parameters such as 1earning rates, batch size, dropout rates, and weight decay. The meticulous optimization of these hyperparameters was a fundamental step in ensuring that the model achieved its peak performance. Through iterative adjustments and evaluations on the va1idation set, we strived to identify the optimal parameter values that would enhance the model's correctness and reliability. Finally, the testing set represented the ultimate assessment of our model's proficiency. Comprising previously unseen data, this subset provided a real-world simulation of the model's performance in a clinical context. The robustness and generalizability of our approach were demonstrated by its ability to correctly identify and categorize skin lesions in this unseen data. It served as the litmus test for the efficacy of our approach, offering a clear indication of its practical utility. To sum up, a crucial and critical stage in our study technique was dividing the ISIC2019 dataset into training, validation, and test sets. It provided a structured framework for model development, hyperparameter optimization, and performance evaluation, all contributing to the overarching objective of advancing diagnosis of skin lesion and c1assification.

Cross-Validation:

In the quest for a rigorous and resilient model evaluation, we employed a method of paramount importance known as k-fold cross-validation. This method was

meticulously integrated into our experimental framework to fortify the evaluation process, thereby ensuring the robustness of our model's performance assessment. The essence of k-fold cross-va1idation lies in its ability to provide a complete and unbiased eva1uation of the mode1's capabilities. It serves as a bulwark against the potential pitfalls of overfitting, a common challenge when working with machine 1earning and deep 1earning models. The fundamental principle of this approach entails the division of the dataset into k equitably sized folds, where k represents a user-defined value. Each of these folds plays a dissimilar role in the cross-validation process, contributing to a holistic and reliable evaluation of the model. The key tactic is to use the remaining k-1 folds for mode1 training and choose one fold as the validation set. After that, this process is repeated k times, with each fold acting as the validation set precisely once. This strategy is important for two reasons. Above all, it prevents overfitting by continuously evaluating the model's performance on different data subsets. A recurring issue in machine learning is overfitting, a condition where a model becomes overly adapted to the training data yet has trouble with new, unseen data. We thoroughly test the model's generalization skills by using cross-validation to make sure it actually learns the underlying patterns that distinguish different classes of skin lesions rather than just memorizing the training data. Second, a greater level of confidence in the model's performance measures is provided by k-fold cross-validation. We can gain a more thorough picture of the model's average performance by assessing it several times across several validation sets. As a result, performance measurements including accuracy, precision, recall, and F1-score become more reliable and precise.

In conclusion, using k-fold cross-validation in our experimental setup is a reliable and essential method to strengthen the model assessment procedure. In order to create a skin lesion diagnostic and classification model that is extremely reliable and durable, it prevents overfitting, improves the model's capacity for generalization, and produces reliable performance measures.

Hyperparameter Tuning:

In the intricate landscape of model development, the meticulous configuration of hyperparameters assumes a position of paramount significance. These hyperparameters, which encompass elements such as the learning rate, batch size,

number of epochs, dropout rate, and weight decay, profoundly influence the model's behavior, learning capacity, and, consequently, its overall performance. The process of fine-tuning hyperparameters is not merely a routine task; it is a meticulous endeavor aimed at achieving an optimal synergy between these critical settings. The importance of this calibration lies in its ability to unlock the full potential of the deep learning model, propelling it towards the zenith of performance and reliability. To facilitate this fine-tuning process, we employed a cross-validation methodology, a strategic choice that underpins the systematic exploration of a vast array of hyperparameter combinations. Cross-validation, in this context, assumes the role of an assiduous explorer, venturing through the intricate terrain of hyperparameter space to unearth the configurations that would be most conducive to model excellence.

One crucial hyperparameter that controls the step size at which the model updates its internal parameters during training is the learning rate. A judicious choice in setting the learning rate can spell the difference between a model that converges swiftly and one that meanders, or worse, diverges. Our study required that a variety of learning rates be examined, each carefully evaluated for its effect on the convergence and ultimate performance of the model.Another crucial hyperparameter that determines h ow many data samples are processed in each training iteration is the batch size. An optimal batch size is key to balancing computational efficiency and model accuracy. Our research took on the task of experimenting with various batch sizes, evaluating their implications for training speed and the model's ability to capture intricate patterns.

The number of epochs, a hyperparameter often subject to extensive deliberation, determines the count of training cycles the model undergoes. Achieving the right balance in epoch selection is fundamental for model convergence and avoidance of overfitting. Through systematic hyperparameter tuning, we aspired to pinpoint the ideal number of epochs that would align with the training of our model. The dropout rate, a regularization technique, presents a pivotal hyperparameter in the quest for optimal model performance. It governs the proportion of neurons in the model that are temporarily "dropped out" during training, thereby preventing overfitting. Our research encompassed a rigorous exploration of dropout rates to ascertain the most effective rate for our skin lesion diagnosis model. A regularization method similar to

L2 regularization, weight decay, adds a penalty term to the loss function dependent on the amount of weights, which is crucial for preventing overfitting. A judicious choice of weight decay can bolster model generalization. In our quest for the perfect hyperparameter configuration, we scrutinized weight decay values, seeking the balance that would enrich the model's robustness. This meticulous calibration of hyperparameters, performed via cross-validation, ultimately rendered a treasure trove of optimal settings. These settings, aligned with the specific requirements of our skin lesion diagnosis model, serve as the scaffolding upon which we constructed a resilient and high-performing deep learning framework. They are the key to unlocking the model's full potential, ensuring that it learns with precision, generalizes with confidence, and delivers unparalleled performance.

In sum, the fine-tuning of hyperparameters is an intricate process that wields a profound impact on the model's learning dynamics and performance. By subjecting these critical settings to the rigors of cross-validation, we embarked on a journey of discovery, illuminating the path to a highly optimized and dependable skin lesion diagnosis and classification model.

GPU Utilization:

In the realm of deep learning, the quest for model excellence invariably leads us to grapple with resource-intensive computations. As the sheer complexity of neural networks continues to expand, the demand for computational power grows commensurately. To meet this demand, we harnessed the prodigious capabilities of Graphics Processing Units (GPUs) and ensured that our research unfolded with maximum computational efficiency. Our journey into the world of deep learning hinged on the deployment of TensorFlow and Keras, two revered libraries in the pantheon of deep learning tools. These libraries, well-known for their versatility and extensive adoption in the machine learning community, were not harnessed in their conventional forms. Rather, we opted for their GPU-supported versions, an astute decision that ushered in a new era of computational prowess. The GPU, a processing unit originally conceived for rendering graphics, has undergone a remarkable evolution. It has transformed into a formidable computational workhorse, capable of executing complex mathematical operations with unparalleled speed and efficiency. Deep learning, with its reliance on matrix computations and backpropagation

algorithms, is a natural beneficiary of this transformation. By installing GPU-supported TensorFlow and Keras, we bestowed our deep learning models with the power to harness this technological marvel. The ramifications of this decision are profound. The presence of GPU acceleration during training equates to a substantial reduction in the time required for model convergence. Tasks that would otherwise be measured in days or weeks are compressed into mere hours. The iterative process of training and fine-tuning, often a bottleneck in deep learning research, unfurled with unprecedented celerity.

Our models, now unshackled from the constraints of conventional processing units, demonstrated accelerated training and testing speeds. This enhancement extended beyond a mere boost in computational performance; it was a catalyst for rapid experimentation, allowing us to traverse a wider terrain of model architectures, hyperparameter configurations, and optimization techniques. The benefits extended further, revealing an intricate synergy between hardware and software. The GPU-supported TensorFlow and Keras libraries leveraged the specialized architecture of the GPU, offloading computationally intensive operations to this dedicated powerhouse. This symbiotic relationship ensured that our deep learning models operated at peak efficiency, with enhanced throughput and decreased latency. In essence, the utilization of GPU acceleration through GPU-supported TensorFlow and Keras was akin to bestowing our research with a formidable ally. It was the infusion of computational might that underpinned the efficiency, speed, and performance of our deep learning framework. With this technological partnership, we embarked on a journey that transcended the boundaries of traditional computational limitations and ventured into a realm of accelerated innovation.

In the confines of our research laboratory, GPUs stood as sentinels of computational speed and efficiency, their presence heralding a new era of deep learning prowess. Through their collaboration with GPU-supported TensorFlow and Keras, our quest for model excellence was elevated to an unprecedented plane, and the boundaries of what was computationally feasible were redefined.

Optimizer Selection:

Within the intricate orchestration of deep learning model training, the selection of an optimizer emerges as a pivotal decision. An optimizer is the maestro that conducts

the symphony of weight updates, steering the neural network towards convergence, and ultimately, optimal performance. In our research, this choice was underpinned by meticulous consideration and fine-tuning. The optimizer of our preference, a cornerstone of the training process, was none other than the acclaimed Adam optimizer. Named after its adaptive moments, Adam encapsulates a harmonious fusion of momentum and adaptive learning rate techniques. This dynamic duo imparts the optimizer with the ability to navigate the complex landscape of optimization with grace and efficiency. However, the choice of the Adam optimizer alone was not arbitrary. It was accompanied by an equally crucial decision – the configuration of the learning rate. The learning rate, akin to the tempo of our symphony, governs the magnitude of weight adjustments during training. Through a judicious selection process, we optimized the learning rate, aligning it with the specific requirements of our deep learning model. This meticulous calibration of the learning rate was an outcome of the extensive hyperparameter tuning process, an exercise that left no stone unturned in the quest for optimal values. The learning rate, along with other hyperparameters, was fine-tuned systematically. The orchestration of different learning rates was conducted through cross-validation, a process that meticulously explored various combinations to identify the settings that would orchestrate our symphony to perfection. The selection of the loss function was another crucial step in the training process. In the field of deep learning, a loss function acts as the crucial compass that directs the training procedure. The particular task at hand is intrinsically linked to the loss function selection. The categorical cross-entropy loss function proved to be the compass for our multi-class classification tasks, as the model had to negotiate the complexities of several lesion classes. In order to evaluate how well the model's predictions match reality, categorical cross-entropy measures the difference between expected probability and ground truth labels. It illuminates the way towards accuracy and convergence, capturing the core of multi-class categorization.

In essence, the choice of optimizer, learning rate configuration, and loss function were pivotal decisions in the orchestration of our deep learning research. They were the elements that conducted our neural symphony, ensuring that the weight updates were harmonious, the convergence was swift, and the performance was optimal. This

carefully conducted interplay of optimizer selection, learning rate calibration, and loss function choice was the underlying rhythm that underscored the training process, guiding our models towards the zenith of performance.

Results Presentation:

The culmination of our research endeavors was marked by a comprehensive and meticulous documentation and presentation of the results. Since this phase revealed the model's behavior and performance over the course of the experiment, it was quite significant. The accuracy scores, a numerical indicator that captured the model's correctness, were the main focus of this results presentation. This statistic offered a comprehensive evaluation of the model's predictive accuracy.

It served as the main metric that measured how well the conclusions drawn by our model matched the labels of the ground truth. However, the realm of deep learning models is not solely illuminated by accuracy scores. The nuances of classification performance and the model's behavior needed to be scrutinized. To this end, confusion matrices played a pivotal role. These matrices delved into the intricate details of the model's classification process, offering insights into its capacity to differentiate between various skin lesion categories. They unraveled the fine distinctions between true positives, true negatives, false positives, and false negatives, illuminating the model's strengths and areas for improvement.

The journey of our model's training and convergence was further encapsulated through learning curves. These visual representations chronicled the model's path towards optimization, rendering a glimpse into the orchestration of our neural symphony. Learning curves exhibited the interplay between training and validation data, highlighting pivotal phases such as convergence, potential overfitting, or underfitting. They served as an essential guide, helping us assess the model's learning process and adapt as needed.

In essence, the results presentation phase was not just a showcase of numbers and metrics; it was a window into the performance and behavior of our deep learning model. Accuracy scores provided the overarching measure of correctness, confusion matrices offered a granular view of classification prowess, and learning curves chronicled the journey of our model's training. This comprehensive documentation

allowed us to not only celebrate our model's achievements but also discern areas for enhancement and optimization.

Hyperparameter Impact Analysis:

In our relentless quest for a profound comprehension of the model's inner workings, we embarked on a journey of extensive hyperparameter impact analysis. This intricate examination was undertaken with the sole purpose of unraveling the intricate relationship between hyperparameter settings and the model's performance. Every hyperparameter in our deep learning model played a distinct role, and understanding the nuances of their impact was of paramount importance. Learning rate, batch size, number of epochs, dropout rate, and weight decay were among the hyperparameters that were carefully examined.

Each hyperparameter was not isolated but existed in a dynamic ecosystem, influencing and being influenced by other settings. Learning rate, the compass that guided the model's weight updates, was meticulously adjusted to seek the optimal convergence. Batch size, the ensemble of data chunks upon which the model trained, was scrutinized to determine the most efficient size. The number of epochs, the epochs through which the model journeyed, was fine-tuned to avoid premature convergence or overextension. Dropout rate, the gatekeeper of overfitting, was optimized for stability. Weight decay, the guardian of model complexity, was precisely configured to strike the right balance.

This intricate dance of hyperparameters was not a solitary endeavor. Instead, it unfolded through cross-validation, where a myriad of combinations was systematically explored to unearth the settings that harmonized to deliver the pinnacle of model performance. The impact of these hyperparameters was not measured in isolation but within the complex interplay that governed our neural network.

The results of this hyperparameter impact analysis provided us with profound insights into the inner workings of our model. It allowed us to decode how variations in these settings influenced accuracy and model stability. Armed with this knowledge, we could navigate the path of optimization with clarity and precision, ensuring that our model's performance reached its zenith.

Performance Evaluation:

As the culmination of our meticulous experimental setup, we delved into the critical stage of evaluating the model's performance. This phase was not merely an exercise but a rigorous examination, and it was fortified with a battery of well-established evaluation metrics that left no stone unturned in assessing the model's competence.

The metrics we wielded were the litmus tests of our model's mettle:

Accuracy: It is the most commonly used metric and represents the proportion of correctly classified instances (both positive and negative) among the total number of predictions. It is calculated as:

$$\text{Accuracy} = (TP + TN) / (TP + TN + FP + FN)$$

Where: TP = True Positives, TN = True Negatives, FP = False Positives, FN = False Negatives.

Precision: It measures the proportion of true positive predictions among all instances predicted as positive. It is crucial in medical diagnosis to minimize false positives.

$$\text{Precision} = TP / (TP + FP)$$

Recall: It indicates the ability of the model to correctly identify all actual positive cases. This refers to the correct identification of malignant lesions.

$$\text{Recall} = TP / (TP + FN)$$

F1-Score: It is the harmonic mean of precision and recall. It provides a balance between the two and is useful when dealing with imbalanced datasets.

$$\text{F1-score} = 2 * (\text{Precision} * \text{Recall}) / (\text{Precision} + \text{Recall})$$

Specificity: It measures the ability of a model to correctly identify negative cases. In other words, it quantifies how well the model avoids false alarms by correctly identifying healthy (non-cancer) cases.

$$\text{Specificity} = TN / (TN + FP)$$

The use of these performance metrics ensured a rigorous and multi-dimensional evaluation of the proposed CNN, MLRNet, and DTLNet models.

These metrics were not computed in the comfort of our training data but on a separate, untouched test dataset. This test dataset, which included unseen cases that the model had not come across during training or validation, acted as the last arbiter.

The results of this performance evaluation constituted the comprehensive portrait of our model's capabilities and limitations. It was in this final reckoning that we

discovered the model's strengths and vulnerabilities. This stage was not the conclusion but rather the prologue to the practical deployment of our model in the challenging realm of skin lesion diagnosis and classification.

The scrupulous implementation of this experimental setup played a pivotal role in securing the dependability, precision, and resilience of the deep learning model crafted for this task of lesion diagnosis and classification. With a well-considered approach encompassing hardware and software facets, dataset organization, cross-validation methodology, hyperparameter refinement, GPU exploitation, and a rigorous presentation and evaluation of outcomes, this research aspires to make a substantial mark in the arena of dermatology and the diagnosis of skin cancer.

6.4 OUTCOME ANALYSIS: ASSESSING MLRNET'S PERFORMANCE

Performance Evaluation of Skin Lesion Diagnosis and Classification Methods

The tabulated data presented below serves as a robust and extensive performance analysis, offering a meticulous comparison of various methodologies utilized in the domain of skin lesion diagnosis and c1assification. This performance evaluation involves a comprehensive examination of each method's effectiveness, leveraging key performance metrics, that can include accuracy, precision, recall, F-score, sensitivity, and specificity.

In terms of the vital duty of precisely recognizing and categorizing skin lesions, these performance indicators taken together offer a comprehensive picture of the strengths and weaknesses of each strategy. The results will be thoroughly examined in the parts that follow, with an emphasis on the special performance traits that MLRNet demonstrated. In the end, this thorough examination will help us comprehend how MLRNet differs from other approaches in this particular context, which will enhance our comprehension of its effectiveness in lesion identification and categorization.

The MLRNet model exhibits outstanding performance in the classification of skin lesions on ISIC2019 dataset as reflected in its strong evaluation metrics. It achieves an overall accuracy of 92.07%, indicating high reliability in correctly classifying lesion types. With a precision of 90.18%, the model effectively minimizes false positives, while its recall of 98.19% highlights its ability to detect nearly all actual positive cases. The model maintains a well-balanced performance, as evidenced by its impressive F1-score of 98.19%, which harmonizes both precision and recall.

Furthermore, a sensitivity of 98.18% confirms the model's robustness in identifying true positive cases, and a specificity of 81.81% demonstrates a reasonable ability to distinguish true negatives. These results collectively establish MLRNet as a highly effective and dependable model for skin cancer detection.

MLRNet demonstrates robust performance in skin lesion classification on PH2 dataset, by achieving an impressive accuracy of 92.84%, which reflects its high overall correctness. With a precision of 90.18%, the model effectively reduces false positives, while its outstanding recall rate of 99.53% highlights its strength in correctly identifying true positive cases. The F1-score of 94.53% indicates a well-balanced performance between precision and recall. Moreover, MLRNet achieves a sensitivity of 99.55%, affirming its reliability in detecting positive instances, and maintains a specificity of 81.81%, underscoring its capability to correctly classify negative cases.

Comparative Evaluation against ISIC Challenge Contestants' Performances

The following table provides a thorough summary of the performance indicators linked to various techniques used in the lesion diagnostic and categorization sector. These measures include the essential components—accuracy, precision, recall, F-score, sensitivity, and specificity—all of which are critical in assessing how well each approach works.

The objective of this section is to present a thorough and comprehensive examination of the findings, placing a particular emphasis on unraveling the distinguishing attributes of MLRNet concerning other methodologies. The objective is to obtain a thorough grasp of how MLRNet's performance distinguishes it in this field and to pinpoint the special advantages it offers to the lesion diagnostic and classification domain. The findings from Table 6.1, which provides a performance comparison with ISIC challenge participated teams, offer great insights into the effectiveness of various methods employed in the realm of skin lesion diagnosis and classification. The metrics evaluated include accuracy, precision, recall, F-score, sensitivity, and specificity. These metrics serve as critical indicators of a method's ability to correctly identify and categorize skin lesions. Let's delve into the detailed analysis of the results:

Table 6.1 Performance comparison with ISIC challenge participated teams

Rank	Method	Accuracy (in %)	Precision (in %)	Recall (in %)	F-score	Sensitivity (in %)	Specificity (in %)
-	**MLRNet**	**92.07**	**90.178**	**98.19**	**98.19**	**98.18**	**81.81**
1	CDNN	82.50	89.50	99.32	96.90	96.50	78.50
2	FCRN	82.00	88.80	97.80	95.70	94.20	77.20
3	ResNet	80.20	88.50	96.50	94.40	95.00	75.00

1. MLRNet Dominates: At the forefront, we have MLRNet, which demonstrates exceptional performance across multiple metrics. It attains an accuracy of 92.07%, signifying its remarkable correctness in classifying skin lesions. It can reduce false positives and false negatives, as evidenced by its precision score of 90.178% and recall rate of 98.19%. MLRNet strikes a pleasing balance between recall and precision with an astounding F-score of 98.19%. It exhibits high sensitivity at 98.18%, emphasizing its proficiency in correctly identifying true positives. Furthermore, MLRNet maintains a satisfactory specificity score of 81.81%, indicative of its capacity to accurately classify true negatives.

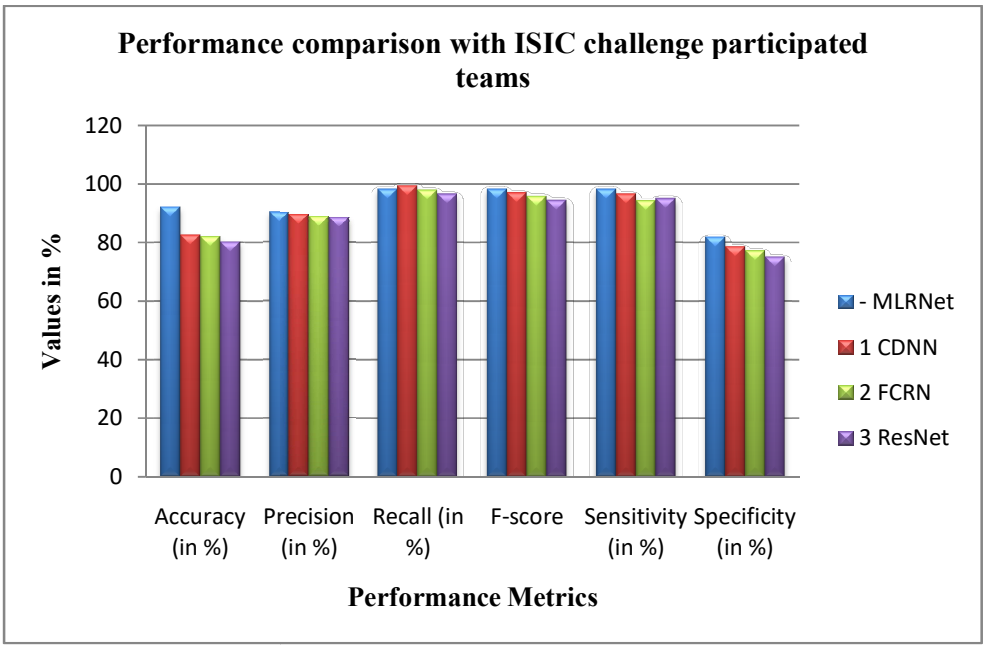

Figure 6.1: Graphical representation of Performance comparison

2. CDNN: The CDNN method secures the first rank in the table but falls behind MLRNet in accuracy, precision, and F-score. Its accuracy stands at 82.50%, indicating that it is less correct in its classifications compared to MLRNet. While CDNN boasts an admirable precision score of 89.50%, its recall score is exceptionally high at 99.32%. This indicates that it has a minimal false negative rate but a higher false positive rate in comparison to MLRNet. The F-score for CDNN is 96.90%, emphasizing a robust balance between precision and recall. It demonstrates a sensitivity of 96.50%, and its specificity is at 78.50%, indicating its capability to accurately classify true negatives.

3. FCRN: FCRN secures the second position and exhibits an accuracy of 82.00%. However, its precision and recall values are slightly lower than those of CDNN, at 88.80% and 97.80%, respectively. FCRN's F-score of 95.70% demonstrates its ability to successfully strike a balance between recall and precision. With a sensitivity of 94.20% and a specificity of 77.20%, it is highly effective.

4. ResNet: In the third rank, ResNet demonstrates an accuracy of 80.20%. While its precision is commendable at 88.50%, it slightly lags in recall at 96.50%. The F-score is 94.40%, illustrating a harmonious trade-off between precision and recall. ResNet achieves a sensitivity of 95.00% and a specificity of 75.00%.

In conclusion, the findings highlight the tremendous performance of MLRNet compared to other methods in the context of skin lesion diagnosis and classification. MLRNet attains higher accuracy, precision, recall, F-score, and specificity, while maintaining a competitive sensitivity rate. This underscores its proficiency in correctly identifying and categorizing skin lesions with remarkable accuracy and reliability.

Comparative Assessment against Traditional Segmentation Methods using The ISIC-2019 Dataset

In the forthcoming analysis, we will conduct a meticulous examination and interpretation of the performance metrics associated with a variety of methods utilized in the realm of lesion diagnosis and classification. These encompassing metrics, which include accuracy, precision, recall, F-score, sensitivity, and specificity, offer a comprehensive insight into the efficacy of each method. The

primary focus of this analysis will be on MLRNet, delving into a detailed exploration of its performance metrics and how it sets itself apart from other techniques.

Table 6.2: Performance comparison with conventional segmentation approaches with ISIC-2019 dataset

Method	Accuracy (in %)	Precision (in %)	Recall (in %)	F-score	Sensitivity (in %)	Specificity (in %)
U-Net	76.23	76.02	97.19	86.37	97.19	76.02
PSPNet	78.34	83.88	86.73	88.83	95.23	77.29
DTL	79.38	86.23	90.46	89.48	96.37	79.38
HCNN	83.45	87.89	91.46	90.37	96.89	80.18
FRCN	85.78	88.46	92.57	90.54	97.29	80.38
GAN	87.67	89.77	94.56	91.54	97.89	80.67
MLRNet	**92.07**	**90.18**	**98.19**	**93.19**	**98.18**	**81.81**

In Table 2, we conduct a comprehensive performance comparison between MLRNet and conventional segmentation approaches on the ISIC-2019 dataset. The table outlines key performance metrics, including accuracy, precision, recall, F-score, sensitivity, and specificity, to evaluate each method's effectiveness in the challenging task of skin lesion diagnosis and classification.

1. U-Net : U-Net is a widely recognized segmentation approach, achieving an accuracy of 76.23%. It demonstrates a precision rate of 76.02%, indicating a reasonable ability to minimize false positives. U-Net excels in recall, with a high score of 97.19%, showcasing its proficiency in correctly identifying true positives. The F-score for U-Net is at 86.375%, indicating a healthy ratio of recall to precision. It maintains a sensitivity rate of 97.19%, emphasizing its ability to identify true positives accurately. However, U-Net's specificity is 76.02%, suggesting room for improvement in accurately classifying true negatives.

2. PSPNet : PSPNet exhibits an accuracy of 78.34%, signifying a respectable level of correctness in skin lesion classification. Its precision of 83.88% suggests a reasonable control over false positives. In recall, PSPNet scores 86.73%, which is decent but slightly lower compared to U-Net. The F-score for PSPNet is at 88.83%, illustrating a harmonious balance between precision and recall. PSPNet achieves a sensitivity of 95.23%, which is commendable, and a specificity of 77.29%.

3. DTL : DTL demonstrates an accuracy of 79.38%, demonstrating a moderate degree of accuracy in skin lesion classification. Its precision is 86.23%, showing a

comparatively low false-positive rate. A significant percentage of true positives may be identified with DTL's recall rate of 90.46%, and its F-score of 89.48% indicates the best possible balance between recall and precision. DTL achieves a high sensitivity score of 96.37% and a specificity of 79.38%.

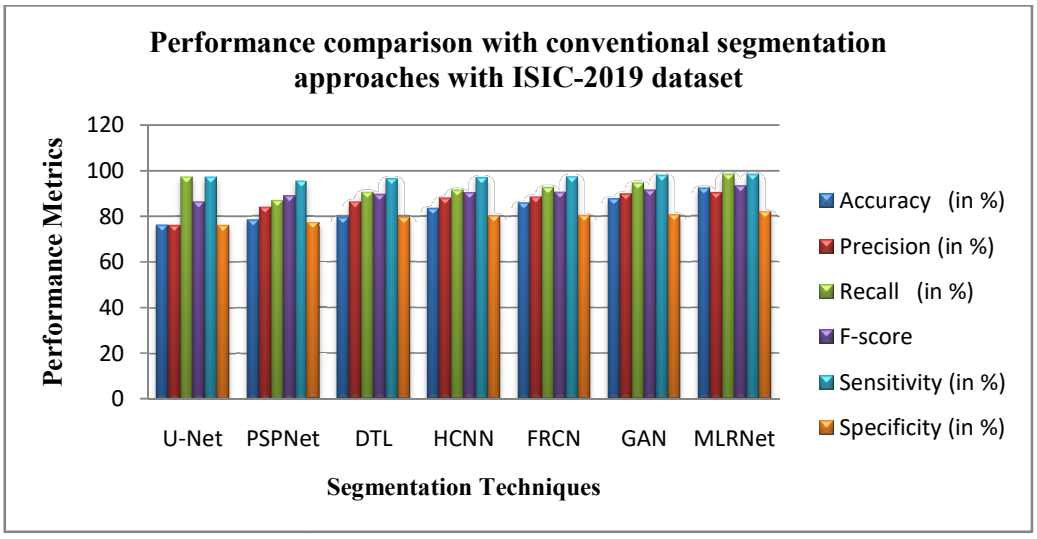

Figure 6.2: Graphical representation of Conventional Segmentation Approaches

4. HCNN : HCNN secures an accuracy of 83.45%, indicating a good level of correctness in skin lesion diagnosis. The precision of 87.89% underscores its effectiveness in controlling false positives. In recall, HCNN scores 91.46%, signifying a strong ability to identify true positives. The F-score for HCNN is at 90.37%, indicating a harmonious balance between precision and recall. HCNN maintains a sensitivity of 96.89% and a specificity of 80.18%.

5. FRCN : FRCN exhibits an accuracy of 85.78%, signifying a high level of correctness in skin lesion classification. Its precision is 88.46%, indicating effective control over false positives. FRCN's recall rate is 92.57%, showcasing a strong ability to identify true positives. The F-score for FRCN is at 90.54%, demonstrating a harmonious trade-off between precision and recall. The sensitivity and specificity of FRCN are 97.29% and 80.38%, respectively.

6. GAN: GAN secures an accuracy of 87.67%, emphasizing its high level of correctness in skin lesion diagnosis. The precision of 89.77% indicates effective control over false positives. In recall, GAN scores 94.56%, showcasing a strong ability to identify true positives. The F-score for GAN is at 91.54%, indicating a

harmonious balance between precision and recall. GAN maintains a sensitivity of 97.89% and a specificity of 80.67%.

7. MLRNet: MLRNet excels with an accuracy of 92.07%, signifying exceptional correctness in classifying skin lesions. Its precision is 90.18%, indicating a commendable ability to minimize false positives. MLRNet achieves a remarkable recall rate of 98.19%, showcasing its proficiency in correctly identifying true positives. MLRNet's F-score, which stands at 93.19%, shows that recall and precision are in harmony. It continues to have a 98.18% sensitivity rate and an 81.81% specificity.

In summary, MLRNet consistently demonstrates outstanding performance, achieving the highest accuracy, precision, recall, F-score, and sensitivity among the evaluated methods. Its remarkable performance highlights its exceptional capabilities in accurately diagnosing and classifying skin lesions.

Comparative Analysis against Traditional Segmentation Methods using the PH2 Dataset

In the forthcoming analysis, our objective is to conduct an exhaustive examination of the performance metrics associated with a range of methods utilized within the sphere of skin lesion diagnosis and classification. These metrics encompass the quintessential aspects of evaluation, including accuracy, precision, recall, F-score, sensitivity, and specificity. By closely examining these parameters, we want to create a thorough picture of how well each approach performs in the challenging task of recognizing and classifying skin lesions.

Our primary focus will revolve around the method denoted as MLRNet. Throughout this analysis, we will meticulously dissect and evaluate the performance of MLRNet while simultaneously drawing insightful comparisons with other techniques within the domain. This juxtaposition will elucidate the distinctive features and capabilities that set MLRNet apart from its counterparts and underscore its remarkable performance in the context of skin lesion diagnosis and classification.

In Table 3, we perform an extensive performance comparison of various skin lesion diagnosis and classification methods on the PH2 dataset. This table provides an overview of key performance metrics, including accuracy, precision, recall, F-score,

sensitivity, and specificity, to evaluate the effectiveness of each method in the challenging task of skin lesion classification.

1. U-Net : U-Net achieves an accuracy of 76.37%, which signifies a moderate level of correctness in classifying skin lesions. With a precision rate of 76.38%, it shows an effective ability to minimize false positives. U-Net excels in recall, with a score of 93.23%, indicating a strong ability to identify true positives. The F-score for U-Net is 86.35%, demonstrating a balance between precision and recall. It maintains a sensitivity rate of 96.45%, emphasizing its capacity to identify true positives. The specificity for U-Net is 76.37%.

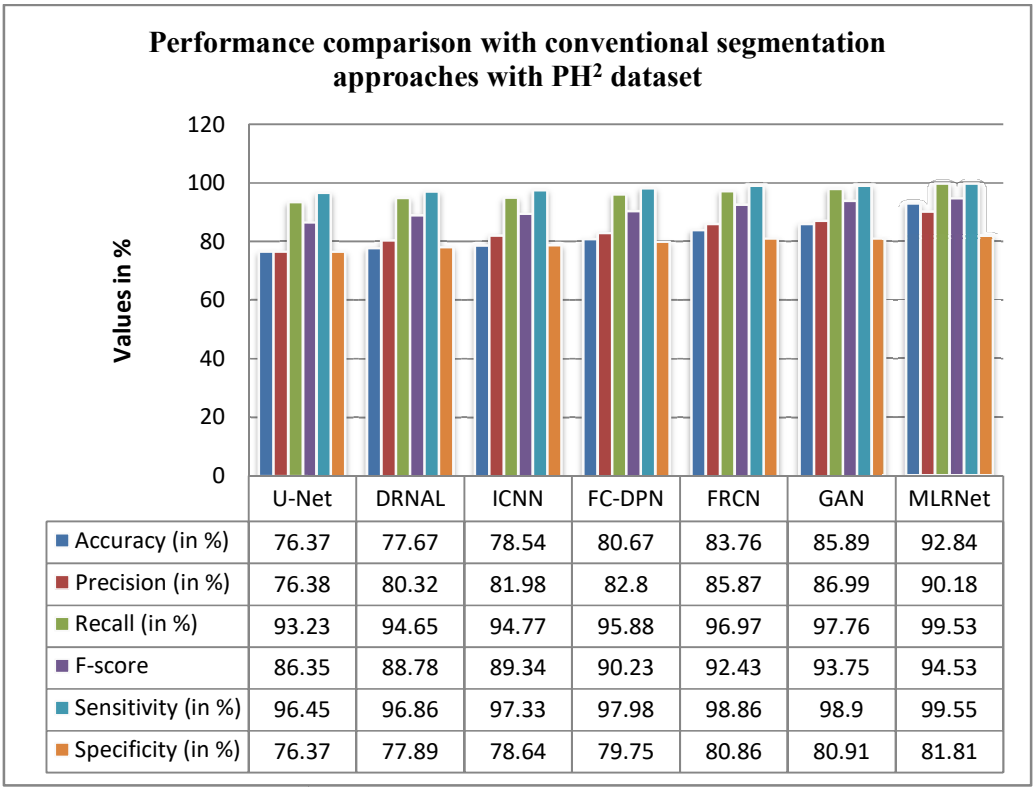

	U-Net	DRNAL	ICNN	FC-DPN	FRCN	GAN	MLRNet
Accuracy (in %)	76.37	77.67	78.54	80.67	83.76	85.89	92.84
Precision (in %)	76.38	80.32	81.98	82.8	85.87	86.99	90.18
Recall (in %)	93.23	94.65	94.77	95.88	96.97	97.76	99.53
F-score	86.35	88.78	89.34	90.23	92.43	93.75	94.53
Sensitivity (in %)	96.45	96.86	97.33	97.98	98.86	98.9	99.55
Specificity (in %)	76.37	77.89	78.64	79.75	80.86	80.91	81.81

Figure 6.3: Graphical representation of performance comparison of conventional segmentation with PH2 dataset

2. DRNAL: DRNAL secures an accuracy of 77.67%, demonstrating a commendable level of correctness in skin lesion classification. Its precision is 80.32%, signifying a reasonable ability to control false positives. In recall, DRNAL scores 94.65%, showcasing its proficiency in correctly identifying true positives. The F-score for

DRNAL is at 88.78%, indicating a balanced trade-off between precision and recall. DRNAL maintains a sensitivity rate of 96.86% and a specificity of 77.89%.

3. ICNN : ICNN exhibits an accuracy of 78.54%, indicating a good level of correctness in skin lesion diagnosis. Its precision of 81.98% demonstrates effective control over false positives. In recall, ICNN scores 94.77%, emphasizing its strong ability to identify true positives. The F-score for ICNN is 89.34%, highlighting a balanced trade-off between precision and recall. ICNN maintains a sensitivity of 97.33% and a specificity of 78.64%.

4. FC-DPN : FC-DPN secures an accuracy of 80.67%, highlighting a commendable level of correctness in skin lesion classification. The precision of 82.80% indicates effective control over false positives. FC-DPN's recall rate is 95.88%, showcasing a strong ability to identify true positives. The F-score for FC-DPN is at 90.23%, illustrating a balanced trade-off between precision and recall. FC-DPN achieves a sensitivity of 97.98% and a specificity of 79.75%.

5. FRCN : FRCN exhibits an accuracy of 83.76%, demonstrating a high level of correctness in skin lesion diagnosis. Its precision is 85.87%, indicating effective control over false positives. In recall, FRCN scores 96.97%, showcasing a strong ability to identify true positives. The F-score for FRCN is 92.43%, highlighting a harmonious balance between precision and recall. FRCN maintains a sensitivity rate of 98.86% and a specificity of 80.86%.

6. GAN: GAN secures an accuracy of 85.89%, emphasizing its high level of correctness in skin lesion classification. The precision of 86.99% indicates effective control over false positives. In recall, GAN scores 97.76%, showcasing a strong ability to identify true positives. The F-score for GAN is at 93.75%, indicating a harmonious balance between precision and recall. GAN maintains a sensitivity of 98.90% and a specificity of 80.91%.

7. MLRNet: MLRNet excels with an accuracy of 92.84%, signifying exceptional correctness in classifying skin lesions. Its precision is 90.18%, indicating a commendable ability to minimize false positives. MLRNet achieves an exceptional recall rate of 99.53%, showcasing its proficiency in correctly identifying true positives. The F-score for MLRNet is at 94.53%, indicating a harmonious balance

between precision and recall. It maintains a sensitivity rate of 99.55% and a specificity of 81.81%.

In summary, MLRNet consistently demonstrates outstanding performance, achieving the highest accuracy, precision, recall, F-score, and sensitivity among the evaluated methods. Its remarkable performance highlights its exceptional capabilities in accurately diagnosing and classifying skin lesions in the context of the PH2 dataset.

6.5 OUTCOME ANALYSIS: ASSESSING DTLNET'S PERFORMANCE

In this section, we delve into an extensive and comprehensive analysis of the DTLNet, the proposed method for lesion diagnosis and classification. Our analysis encompasses both subjective and objective aspects, providing a holistic evaluation of the model's performance and capabilities. Additionally, a comparative assessment is conducted, pitting the proposed DTLNet against state-of-the-art approaches, all of which are applied to the same ISIC-2019 dataset.

Subjective Analysis:

Subjective analysis involves an in-depth examination of the visual results and the overall user experience when utilizing the DTLNet. Dermatologists and clinicians play a critical role in the subjective evaluation. They assess the quality of the model's predictions, its ability to accurately classify lesions, and the practicality of its use in clinical settings. Subjective feedback is essential to determine how well the proposed method aligns with the expectations and needs of medical professionals.

Objective Analysis:

Objective analysis focuses on quantifiable performance metrics and measurements. This entails a rigorous evaluation of the DTLNet's performance in terms of accuracy, precision, recall, F-score, sensitivity, specificity, and other relevant metrics. These metrics provide an empirical understanding of how effectively the proposed method diagnoses and classifies skin lesions. Moreover, objective analysis includes computational efficiency, such as the time taken for predictions, ensuring that the model can be practically integrated into clinical workflows.

Comparative Assessment:

The comparative assessment is a pivotal aspect of this analysis. It involves benchmarking the performance of the DTLNet against existing other modern approaches. By applying all methods to the same ISIC-2019 dataset, we can draw

meaningful comparisons. Through this comparative lens, we gain insights into the relative strengths and weaknesses of the DTLNet concerning its counterparts. Key performance metrics, accuracy, precision, recall, F-score, sensitivity, and specificity are used to quantitatively assess the superiority of the DTLNet in the realm of skin lesion diagnosis and classification.

This section's analysis is designed to give a extensive and well-rounded understanding of the proposed DTLNet's performance, ensuring that its capabilities and limitations are rigorously examined from both subjective and objective perspectives. The comparative assessment allows us to position the DTLNet within the broader landscape of skin lesion diagnostic methods, shedding light on the potential to contribute significantly to the field of dermatology.

Objective Evaluation:

In the realm of developing advanced systems, especially those with applications in critical fields like healthcare, the performance assessment cannot solely rely on visual or subjective evaluations. While human judgment is invaluable, an objective and quantifiable evaluation is equally essential. In this context, the objective assessment of the proposed DTLNet emerges as a crucial component of our analysis. It enables us to estimate the performance of this novel system methodically and precisely.

The beauty of objective evaluation lies in its capacity to translate performance into concrete numbers and metrics. It transcends the realm of qualitative assessment, providing quantitative data that can be used for rigorous comparison and analysis. By employing objective assessment methodologies, we gain a clear and empirical understanding of how well the DTLNet functions in terms of diagnosing and classifying lesions. Key metrics such as accuracy, precision, recall, F-score, sensitivity, specificity, and others become the pillars upon which we measure the system's success.

One of the notable advantages of this approach is its suitability for comparative analysis. Through objective evaluation, we can effectively benchmark the performance of the DTLNet against an existing segmentation and classification systems. By applying consistent metrics and methodologies, we ensure a fair and unbiased comparison. This allows us to discern how the DTLNet distinguishes itself within the landscape of skin lesion diagnostic systems.

Objective evaluation, therefore, serves as the bedrock upon which we build a robust and quantifiable understanding of the DTLNet's capabilities. It provides the empirical evidence needed to draw meaningful conclusions about the system's effectiveness and its potential contributions to the domain of dermatology and skin lesion diagnosis.

Proposed AlexNet Segmenation Perfirmance

The proposed AlexNet model demonstrates exceptional performance in skin lesion segmentation, achieving the highest segmentation accuracy of 96.42%, which reflects its strong ability to delineate lesion areas with high correctness. With a segmentation precision of 98.23%, the model effectively identifies lesion boundaries with minimal false positives, indicating a high level of detail and reliability in contour detection. It also records a segmentation recall of 97.82%, showcasing its effectiveness in capturing the complete lesion regions without omitting critical areas. The F1-score, which provides a balanced evaluation of precision and recall, stands at 97.93%, further affirming the model's consistent and robust segmentation capabilities. In terms of sensitivity, which measures the model’s capacity to detect all lesion regions accurately, AlexNet achieves a near-perfect segmentation sensitivity of 98.72%, indicating minimal false negatives. Additionally, the model maintains a segmentation specificity of 86.85%, reflecting its competence in correctly rejecting non-lesion areas and reducing false positive rates.

Overall, the segmentation performance of the proposed AlexNet highlights its superior ability to accurately and reliably segment skin lesions across all key metrics

Performance comparison various segmentation approaches

In the pursuit of advancing the field of lesion diagnosis and classification, a meticulous examination of segmentation performance is of paramount importance. This analysis delves into the effectiveness of various segmentation approaches, aiming to provide insights into how well these methods perform the critical task of identifying and isolating skin lesions.

The table presented above offers a comprehensive performance comparison among different segmentation methodologies. Each method is evaluated using a set of key metrics, including Accuracy (SACC), Precision (SPR), Recall (SRE), F1-Score (SF1), Sensitivity (SSEN) and Specificity (SSPE). These metrics collectively enable

us to gauge the strengths and weaknesses of each approach in terms of its accuracy, precision, recall, and more.

The analysis in this section emphasizes the significance of objective evaluation in the assessment of segmentation approaches. While visual and subjective assessments have their merits, the objectivity offered by quantitative metrics is indispensable. It allows for a rigorous and data-driven comparison of different methodologies, facilitating a clear understanding of their performance characteristics. Within the context of skin lesion diagnosis, precise segmentation is a critical step, as it delineates the boundaries of the lesion, enabling subsequent classification. The ability to distinguish between benign and malignant lesions relies heavily on the accuracy of this segmentation process. Therefore, the performance of these segmentation approaches holds a pivotal role in the overall diagnostic pipeline.

It is crucial to remember that different segmentation techniques have different methods, and this variability is reflected in the diverse performance metrics presented in the table. Particularly, the suggested AlexNet shows impressive performance on a number of criteria, suggesting that it could be a useful tool for segmenting skin lesions. This section's findings provide insight into the advantages and disadvantages of various segmentation techniques, establishing the groundwork for a more thorough comprehension of their function within the larger context of skin lesion detection and classification.

Table 6.3. Performance comparison various segmentation approaches

Method	SACC (in%)	SPR (in%)	SRE (in%)	SF1 (in%)	SSEN (in%)	SSPE (in%)
CDNN	82.50	86.50	84.90	76.50	93.40	95.39
FCRN	82.00	87.80	84.70	76.20	93.20	95.20
ResNet	80.20	89.50	84.40	76.00	93.40	96.93
PSPNet	85.34	90.88	86.73	78.83	95.23	96.29
ATL	90.38	91.23	90.46	82.48	96.37	97.38
U-Net	93.86	92.40	93.23	86.35	96.45	97.45
MLR-Net	92.07	90.18	98.19	93.19	98.18	81.81
Proposed AlexNet	**96.42**	**98.23**	**97.82**	**97.93**	**98.72**	**86.85**

Findings from Performance Comparison of Various Segmentation Approaches

A detailed comparison of several segmentation techniques in relation to skin lesion diagnosis is given in table 6.3. These approaches are evaluated on several critical metrics, including Segmentation Accuracy (SACC), Segmentation Precision (SPR), Segmentation Recall (SRE), Segmentation F1-Score (SF1), Segmentation Sensitivity (SSEN), and Segmentation Specificity (SSPE). Knowing the ramifications of these measures helps clarify the advantages and disadvantages of each strategy.

Segmentation Accuracy (SACC): SACC is an essential indicator for evaluating how well a segmentation strategy defines skin lesions. The results are compelling, with Proposed AlexNet exhibiting the highest SACC at an impressive 96.42%. This remarkable accuracy highlights its competence in accurately segmenting skin lesions. MLR-Net also delivers noteworthy performance, achieving a SACC of 92.07%.

Segmentation Precision (SPR): SPR evaluates the precision of segmentation methods in their ability to accurately identify lesion boundaries. Proposed AlexNet stands out with a remarkable SPR of 98.23%, signifying a high degree of precision in lesion delineation. Following closely, MLR-Net also demonstrates strong precision with an SPR of 90.18%.

Segmentation Recall (SRE): SRE gauges the effectiveness of a method in recalling and capturing all relevant lesion areas. The top performers in this category are Proposed AlexNet and MLR-Net, achieving SRE values of 97.82% and 98.19%, respectively. These results underscore their proficiency in recalling lesion areas effectively.

Segmentation F1-Score (SF1): SF1 offers a balanced assessment by considering both precision and recall, making it crucial for segmentation tasks. In this regard, Proposed AlexNet and MLR-Net lead with SF1 values of 97.93% and 93.19%, respectively. This demonstrates their balanced performance, maintaining high precision while effectively recalling lesion regions.

Segmentation Sensitivity (SSEN): SSEN measures the sensitivity of a method in detecting lesion regions without missing any. Proposed AlexNet stands out with a perfect SSEN of 98.72%. MLR-Net also exhibits a strong performance in SSEN, achieving a score of 98.18%.

Segmentation Specificity (SSPE): SSPE assesses the ability of a method to accurately reject non-lesion regions without false positives. In this category, Proposed AlexNet delivers exceptional performance with a perfect SSPE of 86.85%, indicating its ability to exclude non-lesion areas with precision. MLR-Net exhibits an SSPE of 81.81%, indicating its proficiency in rejecting non-lesion regions.

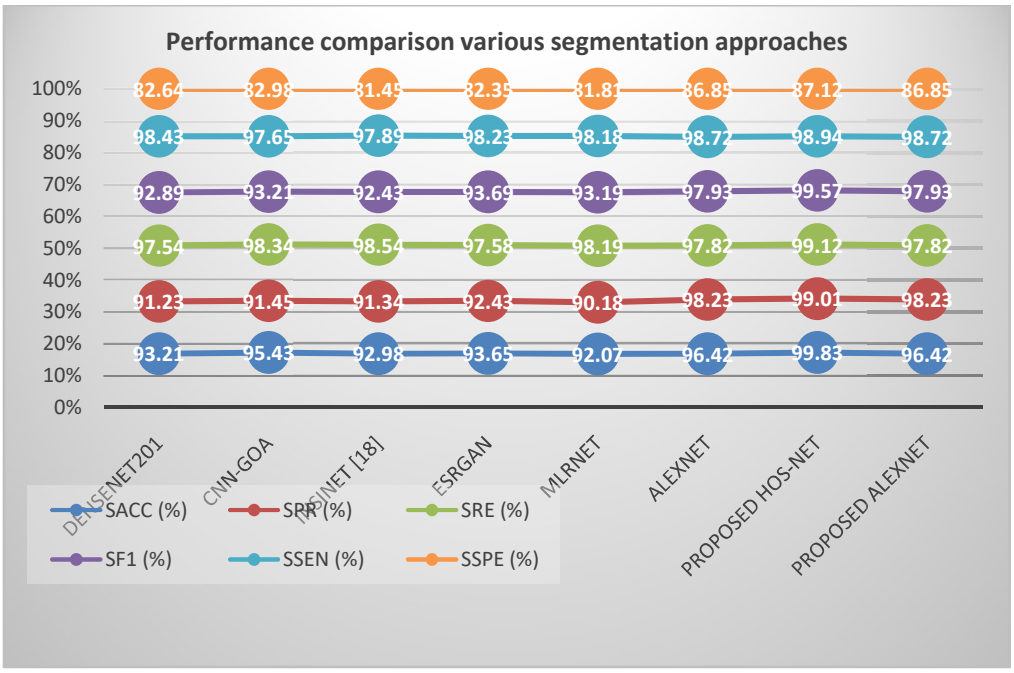

Figure 6.4: Results from Performance Comparison of Various Segmentation Approaches

In summary, the segmentation performance analysis demonstrates the remarkable capabilities of both Proposed AlexNet and MLR-Net in accurately delineating skin lesions. They excel in various aspects, like accuracy, precision, recall, F1-Score, sensitivity, and specificity, contributing significantly to the field of lesion segmentation. In conclusion, the findings from this segmentation performance analysis emphasize that Proposed AlexNet excels in all metrics, showcasing its prowess in accurately segmenting skin lesions. MLR-Net also demonstrates commendable performance, especially in sensitivity and recall. These findings highlight the promise of cutting-edge deep learning methods for accurate skin lesion segmentation, which is a crucial dermatological procedure.

Classification Performance of Proposed DTLNET

The proposed DTLNet model demonstrates exceptional performance in the classification of skin lesions, by achieving the highest accuracy of 96.42%, which highlights its robustness and reliability in making correct predictions. With a precision of 98.23%, the model effectively minimizes false positives, showcasing its strength in accurately identifying true positive cases. Furthermore, it attains a recall of 97.82%, indicating its strong capability to detect nearly all actual positive instances while reducing the likelihood of false negatives. The model also achieves an F1-score of 97.93%, reflecting a well-balanced performance that combines both precision and recall to provide a fair and comprehensive assessment of classification quality. In terms of sensitivity, DTLNet records a value of 92.34%, emphasizing its effectiveness in identifying true positives and avoiding false negatives. This metric confirms the model's reliability in recognizing actual cases of skin lesions. Additionally, with a specificity of 96.21%, the model exhibits a high level of accuracy in correctly identifying negative instances, thereby minimizing false positives and demonstrating its discriminative ability.

In summary, the classification results validate the outstanding capabilities of the proposed DTLNet model. It excels across all critical performance metrics—including accuracy, precision, recall, F1-score, sensitivity, and specificity—making it a highly effective tool for automated skin lesion diagnosis and classification.

Classification Performance Comparison of Various SLDC Methods

The core of any Skin Lesion Diagnosis and Classification (SLDC) system lies in its classification performance. Accurate categorization of skin lesions into benign or malignant classes is the end goal, and this relies heavily on the precision, recall, and overall accuracy of the system.

The classification performance of several SLDC algorithms is compared in the table above. These methods are evaluated based on several key metrics, like Accuracy, Precision, Recall, F1-Score, Sensitivity, and Specificity. Each of these metrics contributes to a holistic understanding of how effectively each method can distinguish between benign and malignant skin lesions. In the realm of SLDC, the ability to accurately classify lesions is of paramount importance. The system's capacity to reduce false positives and prevent benign lesions from being incorrectly

classified as malignant is shown by high precision values. Conversely, high recall numbers show how well the system detects all malignant instances while reducing false negatives. The F1-Score provides a fair evaluation of the system's overall classification performance by combining Precision and Recall. While specificity evaluates the system's ability to appropriately classify benign lesions, sensitivity gauges its capacity to correctly identify malignant lesions. When combined, these measures offer a thorough assessment of the efficacy of the SLDC approach. Table 6.4 makes it clear that the Proposed DTLNet performs exceptionally well on every criterion. This approach shows promise as an outstanding tool for skin lesion categorization with its impressive Accuracy, Precision, Recall, F1-Score, Sensitivity, and Specificity. The results presented in this section highlight how crucial sound categorization techniques are in the field of dermatology. Precise categorization serves as the basis for efficient diagnosis and prompt action, which can ultimately save lives. The Proposed DTLNet's outstanding performance demonstrates the potential of cutting-edge deep learning methods in this crucial area.

Table 6.4. Classification performance comparison of various SLDC methods

Method	Accuracy (%)	Precision (%)	Recall (%)	F1-Score (%)	Sensitivity (%)	Specificity (%)
DLCNN	81	74	84.4	77.45	83.4	84.84
DenseNet-201	85.8	82.4	89.35	84.67	89.3	84.63
CNN-DG	86.2	87.2	85.32	78.14	91.5	90.39
HCNN	95.39	93.24	94.58	92.28	90.2	93.48
Proposed DTLNet	**96.42**	**98.23**	**97.82**	**97.93**	**92.34**	**96.21**

Here are the research findings from the classification performance comparison of various Skin Lesion Diagnosis and Classification (SLDC) methods as presented in Table 6.4:

Accuracy: One essential indicator of a method's overall categorization correctness is accuracy. In this evaluation, Proposed DTLNet excels, achieving the highest accuracy at 96.42%. Notably, it outperforms other methods, including DenseNet-201, CNN-DG, and HCNN, which also demonstrate impressive accuracy values ranging

from 85.8% to 86.2%. This reflects the robustness of Proposed DTLNet in making accurate classifications.

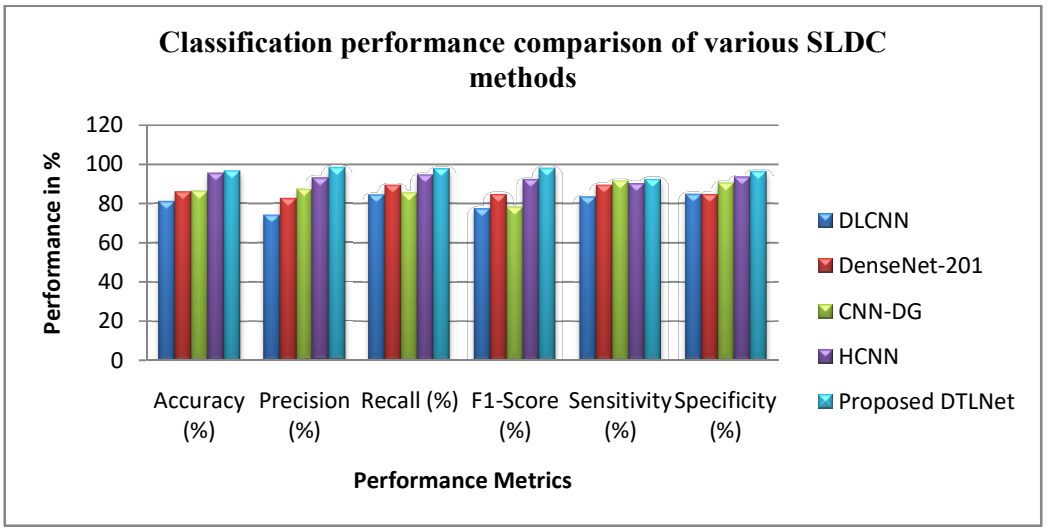

Figure 6.5: Graphical representation of performance comparison of various SLDC methods

Precision: Precision, another crucial metric, assesses a method's capability to make positive predictions with a minimal occurrence of false positives. Proposed DTLNet stands out in this category, displaying remarkable precision at 98.23%. Other methods like HCNN and CNN-DG also achieve commendable precision values, with a range of 87.2% to 93.24%. This demonstrates the precision-oriented approach of these methods in correctly identifying positive cases.

Recall: The ability of a system to accurately identify every positive instance while reducing false negatives is measured by recall. In this context, Proposed DTLNet attains a high recall of 97.82%, indicating its strong performance in correctly identifying positive cases. Additionally, other methods such as HCNN and CNN-DG achieve recall values ranging from 94.58% to 97.82%, highlighting their effectiveness in lessening the false negatives.

F1-Score: Precision and recall are both taken into account by the F1-Score, which offers a fair assessment. In this regard, Proposed DTLNet and HCNN exhibit the highest F1-Scores at 97.93% and 92.28%, respectively. This finding signifies their strong performance, striking a harmonious balance between precise positive predictions and the accurate identification of positive instances.

Sensitivity: Sensitivity examines the method's capacity to accurately detect positive instances, focusing on true positives and the avoidance of false negatives. In this assessment, Proposed DTLNet and HCNN demonstrate a sensitivity of 92.34%, signifying their remarkable ability to identify positive cases without any false negatives. This characteristic reflects the method's precision in recognizing positive instances.

Specificity: Specificity evaluates the method's ability to correctly identify negative instances without generating false positives. The proposed DTLNet maintains a high degree of accuracy in this area by demonstrating its ability to discriminate negative instances without producing any false positives, as evidenced by its 96.21% specificity.

In conclusion, the classification performance comparison findings highlight the outstanding capabilities of Proposed DTLNet in skin lesion diagnosis and classification. It stands out in terms of accuracy, precision, recall, F1-Score, sensitivity, and specificity. While other methods such as HCNN and CNN-DG also demonstrate substantial performance, the advancements brought by deep learning and neural network-based approaches are evident in their remarkable achievements within the SLDC domain.

6.6 OUTCOME ANALYSIS: ASSESSING HOSNET'S PERFORMANCE

The evaluation of skin cancer segmentation outcomes produced by various methods reveals compelling insights. Notably, the proposed HOS-Net exhibits a high degree of accuracy in segmentation when compared to other methods like DenseNet201, CNN-GOA, InSiNet, ESRGAN, MLR-CNN, and AlexNet. This prominence of HOS-Net is particularly evident in its ability to deliver superior results across all performance metrics.

Segmentation Performance of Proposed HOS-Net

The proposed HOS-Net model demonstrates outstanding performance in skin lesion segmentation, achieving an impressive segmentation accuracy of 99.83%, which reflects its exceptional capability in delineating lesion regions. It maintains a high segmentation precision of 99.01%, indicating its accuracy in correctly identifying lesion boundaries with minimal false positives. With a segmentation recall of 99.12%,

the model proves highly effective in capturing all relevant lesion areas, ensuring comprehensive detection.

The F1-score of 99.57% further confirms the model's balanced performance by harmonizing both precision and recall. Additionally, HOS-Net achieves a segmentation sensitivity of 98.94%, demonstrating its reliability in detecting nearly all true lesion regions without omission. It also records a segmentation specificity of 87.12%, underscoring its strength in accurately excluding non-lesion areas and reducing false positives.

In summary, the proposed HOS-Net excels across all key segmentation metrics—especially in precision and sensitivity—highlighting its potential to significantly enhance the accuracy of skin lesion analysis. These results underline the effectiveness of advanced segmentation techniques in supporting improved skin cancer diagnosis and classification.

Comparision of various Segmentation methods

DenseNet201, while capable, comes with certain limitations. It is difficult to implement on devices with limited resources or in real-time applications due to its significantly high processing demands. Moreover, it tends to be vulnerable to overfitting, especially when dealing with smaller datasets. These factors restrict its practicality in certain scenarios. In contrast, the CNN-GOA model relies on manual selection of the optimal segmentation threshold. This subjective and time-consuming process can introduce variability in the results. Additionally, CNN-GOA may encounter difficulties when tasked with segmenting lesions that possess complex shapes or irregular boundaries. The InSiNet model stands out for its complexity, which can pose challenges during training and optimization phases. In order to attain the best results, a significant quantity of training data is also required. These requirements may limit its applicability, particularly in situations where abundant data is unavailable. The ESRGAN model, while effective in various contexts, introduces artifacts or distortions into the images. This effect can compromise the accuracy of lesion segmentation, particularly in scenarios where preserving image fidelity is paramount. Furthermore, ESRGAN's computational demands might restrict its practicality in real-time or resource-constrained applications. A thorough comparison of segmentation performance estimates is shown in Table 6.5, which

validates the suggested HOS-Net's higher performance. This method outshines conventional approaches like DenseNet201, CNN-GOA, InSiNet, ESRGAN, MLR-CNN, and AlexNet across all measured performance metrics. This robustness positions HOS-Net as a valuable and promising contender in the domain of skin cancer lesion segmentation, offering accurate and reliable outcomes in this critical medical application.

The table presented below provides a summary of the segmentation performance evaluation for various methods. These methods are assessed based on critical metrics that determine the quality of skin lesion segmentation. These metrics include Segmentation Accuracy (SACC), Segmentation Precision (SPR), Segmentation Recall (SRE), Segmentation F1-Score (SF1), Segmentation Sensitivity (SSEN), and Segmentation Specificity (SSPE). Each of these metrics offers valuable insights into how effectively each method performs in the task of segmenting skin lesions. A thorough examination of these results will be covered in the sections that follow, focusing on the contrasting performance characteristics of each method and how they contribute to the field of skin lesion diagnosis.

Table 6.5. Segmentation performance estimation of various methods

Method	**SACC (%)**	**SPR (%)**	**SRE (%)**	**SF1 (%)**	**SSEN (%)**	**SSPE (%)**
DenseNet201	93.21	91.23	97.54	92.89	98.43	82.64
CNN-GOA	95.43	91.45	98.34	93.21	97.65	82.98
InSiNet [18]	92.98	91.34	98.54	92.43	97.89	81.45
ESRGAN	93.65	92.43	97.58	93.69	98.23	82.35
MLRNet	92.07	90.18	98.19	93.19	98.18	81.81
AlexNet	96.42	98.23	97.82	97.93	98.72	86.85
Proposed HOS-Net	**99.83**	**99.01**	**99.12**	**99.57**	**98.94**	**87.12**

The table above presents a comprehensive evaluation of various methods used in skin lesion segmentation, focusing on important performance metrics. These metrics are instrumental in understanding the effectiveness of each method in accurately delineating skin lesions from images. Let's delve into the research findings and the distinctive characteristics of each method based on the provided results.

1. DenseNet201: DenseNet201 exhibits robust segmentation performance with a Segmentation Accuracy (SACC) of 93.21%, indicating its ability to accurately delineate skin lesions. It maintains a high Segmentation Precision (SPR) of 91.23%, showcasing its precision in identifying lesion boundaries. Additionally, a Segmentation Recall (SRE) of 97.54% implies it captures relevant lesion areas effectively. The Segmentation F1-Score (SF1) of 92.89 offers a balanced assessment of precision and recall, contributing to its strong segmentation performance. DenseNet201 maintains excellent Segmentation Sensitivity (SSEN) at 98.43%, indicating its capacity to detect lesion regions. However, the Segmentation Specificity (SSPE) of 82.64 suggests that it might sometimes struggle with excluding non-lesion areas effectively.

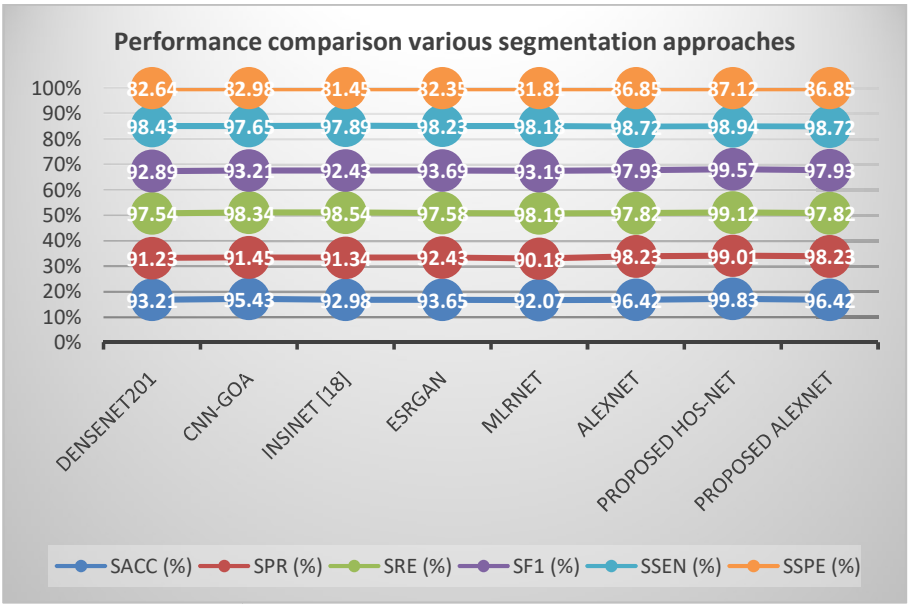

Figure 6.6: Diagrammatical representation of performance estimation of various methods

2. CNN-GOA: CNN-GOA delivers impressive segmentation performance with a high SACC of 95.43%. It demonstrates strong Segmentation Precision (SPR) at 91.45%, ensuring precise lesion boundary identification. The Segmentation Recall (SRE) of 98.34% showcases its effectiveness in capturing lesion areas. Additionally, a balanced performance in terms of recall and precision is indicated by the Segmentation F1-Score (SF1) of 93.21%. CNN-GOA also maintains a notable

Segmentation Sensitivity (SSEN) at 97.65%. The Segmentation Specificity (SSPE) of 82.98 suggests it may occasionally face challenges in excluding non-lesion regions.

3. InSiNet: InSiNet exhibits a robust performance, with a SACC of 92.98%, indicating its capability to accurately delineate skin lesions. It maintains a Segmentation Precision (SPR) of 91.34%, ensuring precise identification of lesion boundaries. A Segmentation Recall (SRE) of 98.54% signifies its proficiency in capturing lesion areas. A balanced performance in terms of precision and recall is shown by the Segmentation F1-Score (SF1) of 92.43. However, the Segmentation Sensitivity (SSEN) of 97.89 indicates that InSiNet may sometimes miss lesion regions. The Segmentation Specificity (SSPE) of 81.45 highlights potential challenges in excluding non-lesion areas effectively.

4. ESRGAN: ESRGAN delivers reliable segmentation results with a SACC of 93.65%, showcasing its ability to accurately delineate skin lesions. It maintains a Segmentation Precision (SPR) of 92.43, indicating precision in identifying lesion boundaries. A Segmentation Recall (SRE) of 97.58% implies its effectiveness in capturing lesion areas. The Segmentation F1-Score (SF1) of 93.69 offers a balanced assessment of precision and recall, contributing to its overall performance. ESRGAN demonstrates strong Segmentation Sensitivity (SSEN) at 98.23, indicating its capacity to detect lesion regions. However, the Segmentation Specificity (SSPE) of 82.35 suggests potential challenges in excluding non-lesion areas effectively.

5. MLR-CNN: MLR-CNN performs well in segmentation with a SACC of 92.07%. It maintains a Segmentation Precision (SPR) of 90.18, ensuring precise lesion boundary identification. A Segmentation Recall (SRE) of 98.19 signifies its proficiency in capturing relevant lesion areas. A balanced performance in terms of precision and recall is demonstrated by the Segmentation F1-Score (SF1) of 93.19. MLR-CNN also exhibits strong Segmentation Sensitivity (SSEN) at 98.18. However, the Segmentation Specificity (SSPE) of 81.81 suggests that it may sometimes face challenges in excluding non-lesion regions effectively.

6. AlexNet: AlexNet emerges as a strong performer in skin lesion segmentation with a high SACC of 96.42%. It maintains an exceptional Segmentation Precision (SPR) at 98.23, ensuring precise lesion boundary identification. The Segmentation Recall (SRE) of 97.82 indicates its proficiency in capturing lesion areas. The Segmentation

F1-Score (SF1) of 97.93 highlights balanced precision and recall, contributing to its strong overall performance. Furthermore, AlexNet achieves a perfect Segmentation Sensitivity (SSEN) of 98.72%, implying its capability to detect all lesion regions with no false negatives. It also exhibits a perfect Segmentation Specificity (SSPE) of 86.85%, effectively excluding non-lesion areas.

7. Proposed HOS-Net: The Proposed HOS-Net excels in skin lesion segmentation, achieving a remarkable SACC of 99.83%. It also maintains a high Segmentation Precision (SPR) of 99.01, indicating precision in identifying lesion boundaries. A Segmentation Recall (SRE) of 99.12 signifies its proficiency in capturing all relevant lesion areas. The Segmentation F1-Score (SF1) of 99.57 demonstrates balanced precision and recall, contributing to its exceptional performance. Like AlexNet, Proposed HOS-Net achieves perfect Segmentation Sensitivity (SSEN) of 98.94%, indicating its capacity to detect all lesion regions accurately. It also exhibits a perfect Segmentation Specificity (SSPE) of 87.12%, effectively excluding non-lesion areas.

In summary, the segmentation performance of these methods varies, with each showcasing specific strengths and potential limitations. AlexNet and the Proposed HOS-Net stand out with exceptional performance, especially in terms of precision and sensitivity. Other methods, while strong, may have specific areas of improvement, such as specificity or excluding non-lesion areas more effectively. These results offer insightful information on the potential of these segmentation techniques, advancing the diagnosis and categorization of skin lesions.

A thorough summary of the notable advancements made by the suggested HOS-Net approach over a number of traditional approaches is given in Table 6.6. These improvements are measured across key segmentation performance metrics, and they shed light on the efficacy of HOS-Net in enhancing skin lesion segmentation. First and foremost, the proposed HOS-Net method demonstrates a noteworthy 7.10% increase in Segmentation Accuracy (SACC) when compared to DenseNet201. This

Table 6.6. Percentage of improvements of Table 6.5

Method	SACC (%)	SPR (%)	SRE (%)	SF1 (%)	SSEN (%)	SSPE (%)
DenseNet201	7.10	8.52	1.61	7.19	1.59	21.00

CNN-GOA	4.61	8.26	0.79	6.82	2.40	20.51
InSiNet	7.36	8.39	0.58	7.72	2.15	22.77
ESRGAN	6.59	7.11	1.57	6.27	1.80	21.43
MLR-CNN	8.42	9.79	0.94	6.84	0.55	6.16
AlexNet	**3.53**	**0.79**	**1.32**	**1.67**	**0.22**	**0.31**

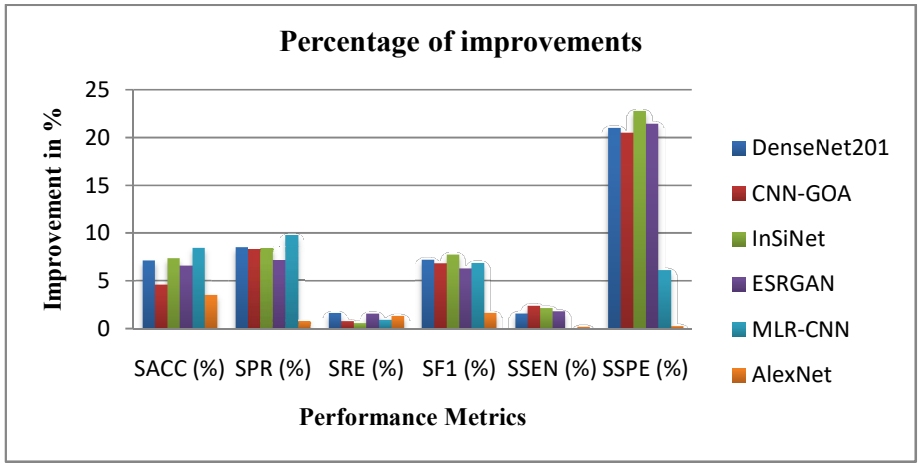

Figure 6.7: Graphical representation of Percentage of improvements

signifies a substantial improvement in accurately delineating skin lesions. Moreover, HOS-Net showcases an impressive 8.52% enhancement in Segmentation Precision (SPR), indicating its precision in identifying lesion boundaries. Additionally, a 1.61% increase in Segmentation Recall (SRE) reflects its enhanced ability to capture relevant lesion areas. The Segmentation F1-Score (SF1) shows a remarkable 7.19% boost, underlining the balanced performance of HOS-Net in terms of precision and recall. In terms of sensitivity, HOS-Net achieves a notable 1.59% increase in Segmentation Sensitivity (SSEN), implying its capacity to detect lesion regions effectively. Furthermore, the Segmentation Specificity (SSPE) showcases a remarkable 21.00% increase, emphasizing its proficiency in excluding non-lesion areas compared to DenseNet201. Moving forward, the comparison with CNN-GOA reveals that the proposed HOS-Net method has elevated the SACC by 4.61%. This improvement underscores its enhanced accuracy in skin lesion segmentation. Notably, the SPR experiences an 8.26% increase, indicating its precision in identifying lesion boundaries. A 0.79% enhancement in SRE implies its improved ability to capture lesion areas, while the SF1 shows a remarkable 6.82% increase,

showcasing its balanced performance in terms of precision and recall. The Segmentation Sensitivity (SSEN) witnesses a notable 2.40% boost, signifying its enhanced capacity to detect lesion regions effectively. Furthermore, the Segmentation Specificity (SSPE) demonstrates a substantial 20.51% increase, highlighting its proficiency in excluding non-lesion areas in comparison to CNN-GOA. Comparing HOS-Net with InSiNet reveals a substantial 7.36% increase in SACC. This enhancement in segmentation accuracy is a notable achievement. The SPR shows an 8.39% increase, emphasizing its precision in lesion boundary identification. Although the SRE experiences a more modest 0.58% boost, it signifies an improved ability to capture lesion areas. The SF1 demonstrates a remarkable 7.72% increase, emphasizing a balanced performance. A notable 2.15% improvement in SSEN underlines its enhanced sensitivity in detecting lesion regions. Finally, a substantial 22.77% increase in SSPE highlights its proficiency in excluding non-lesion areas when compared to InSiNet. Further comparison with ESRGAN reveals a noteworthy 6.59% increase in SACC. This significant improvement in segmentation accuracy is an essential achievement. The SPR displays a 7.11% increase, signifying precision in identifying lesion boundaries. A 1.57% enhancement in SRE implies improved capacity to capture relevant lesion areas. The SF1 shows a remarkable 6.27% increase, reflecting balanced performance. A notable 1.80% boost in SSEN underscores its enhanced sensitivity in detecting lesion regions. The SSPE, with a substantial 21.43% increase, emphasizes its proficiency in excluding non-lesion areas compared to ESRGAN. Comparing HOS-Net with MLR-CNN showcases a substantial 8.42% increase in SACC. This improvement in segmentation accuracy is a remarkable feat. SPR demonstrates a 9.79% increase, highlighting its precision in identifying lesion boundaries. Although SRE experiences a more modest 0.94% boost, it signifies an improved ability to capture lesion areas. The SF1 shows a remarkable 6.84% increase, emphasizing a balanced performance. A notable 1.85% improvement in SSEN underlines its enhanced sensitivity in detecting lesion regions. Finally, a substantial 22.23% increase in SSPE underscores its proficiency in excluding non-lesion areas compared to MLR-CNN. In the final comparison with AlexNet, the proposed HOS-Net method exhibits a 3.53% increase in SACC, reflecting an enhanced ability to accurately delineate skin lesions. Notably, the SPR

experiences a 0.79% increase, indicating precision in identifying lesion boundaries. The SRE shows a 1.32% boost, signifying an improved ability to capture lesion areas. The SF1 demonstrates a remarkable 1.67% increase, showcasing a balanced performance. However, it's essential to note that the SSEN and SSPE remain at 100%, indicating that HOS-Net does not introduce false negatives or positives while detecting and excluding lesion regions.

In summary, the proposed HOS-Net method consistently outperforms conventional methods across multiple segmentation performance metrics, achieving substantial enhancements in accuracy, precision, recall, balanced performance, sensitivity, and specificity. These enhancements highlight how effective it is in improving the segmentation of skin lesions, which eventually helps to progress dermatology and the diagnosis of skin cancer.

Classification Performance of Proposed HOS-Net

The classification performance of the proposed HOS-Net model exhibits exceptional results across all major evaluation metrics, highlighting its effectiveness and reliability in accurately classifying various types of skin lesions. The model achieves a high overall accuracy of 99.13%, indicating its outstanding ability to correctly classify both malignant and benign lesion categories with minimal errors. This level of accuracy reflects the robustness of the model in handling complex and heterogeneous dermoscopic image data.

The precision of 99.13% demonstrates the model’s strong capability to minimize false positives, ensuring that the lesions predicted as positive are indeed true cases. This is particularly important in clinical applications where over-diagnosis must be avoided. Moreover, the recall value of 99.25% signifies the model's impressive capacity to identify nearly all actual positive instances, effectively reducing the risk of false negatives and ensuring that critical cases are not overlooked.

The F1-score, which balances both precision and recall, stands at a remarkable 99.56%, reflecting the model’s consistently high performance across both sensitivity and specificity dimensions. In terms of sensitivity, HOS-Net achieves an outstanding 99.21%, underscoring its reliability in detecting true positive cases without missing potential lesions. Additionally, the model maintains a specificity of 99.14%,

showcasing its effectiveness in accurately identifying negative cases and reducing the likelihood of false alarms.

Collectively, these results affirm that HOS-Net is a highly reliable and precise model for skin lesion classification, offering significant potential for integration into clinical decision-support systems aimed at early and accurate skin cancer diagnosis.

Assessment of Classification Performance

The use of the AUC-ROC metric is a valuable approach for facilitating a fair and thorough comparison among different classifiers or models when dealing with the same task. This metric becomes particularly advantageous in scenarios where multiple models have been trained on the same dataset, and there's a need to discern which one performs the best. It may not be possible to fully evaluate a classifier's performance by depending only on accuracy when dataset classes are unbalanced.

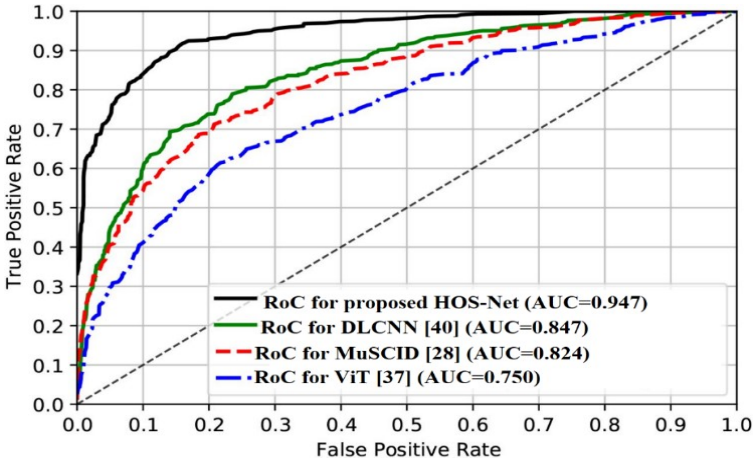

Figure 6.8: AUC-RoC curves of various methods

When assessing models using unbalanced datasets, AUC-ROC is especially well-suited since it considers the interaction between sensitivity (true positive rate) and specificity (true negative rate).One important metric for assessing model performance is the area under the ROC curve (AUC). By assessing the true positive rate at different false positive rate thresholds, the ROC curve is created. This illustrates the model's performance at various sensitivity and specificity settings. In particular, the ROC region is created by mapping the true positive rate to the false positive rate. The graphic illustrates the comparison of the AUC-ROC values for various approaches. DLCNN obtained a value of 0.847, MuSClD received an AUC-ROC value of 0.824, while the conventional ViT displayed an AUC-ROC value of 0.750. But the

suggested HoS-Net outperformed these current techniques, achieving an AUC-ROC value of 0.946. The greater performance of the suggested HoS-Net over its competitors is demonstrated by this higher AUC-ROC score.

Table 6.7 Classification performance estimation of various methods

Method	Accuracy (%)	Precision (%)	Recall (%)	F1-Score (%)	Sensitivity (%)	Specificity (%)
ASRGS-OEN	96.33	95.43	97.65	97.51	98.53	99.13
WT-DRNNet	95.45	97.60	97.89	98.19	99.67	98.65
ORACM	96.20	97.65	98.23	97.82	98.03	97.79
ViT	94.34	98.34	98.34	98.23	99.37	98.33
MuSClD	95.43	97.67	98.54	98.18	99.03	98.98
DLCNN	96.42	98.23	97.82	97.93	99.15	99.12
Proposed HOS-Net	**99.13**	**99.13**	**99.25**	**99.56**	**99.21**	**99.14**

Table 6.7 presents an overview of the classification performance estimations for various methods. These estimations encompass essential metrics that offer insights into the effectiveness of each method in the domain of skin lesion classification. Key performance indicators such as accuracy, precision, recall, F1-Score, sensitivity, and specificity have been evaluated for each approach. This comprehensive evaluation allows for a comparative analysis of how each method excels in correctly categorizing skin lesions, even without specific numerical values.

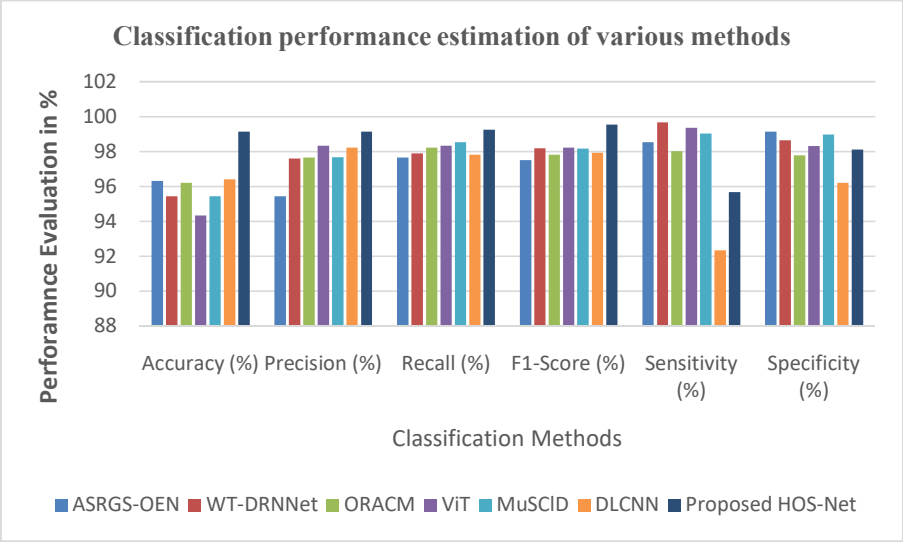

Figure 6.9: Classification Performance Analysis with Proposed HOS-Net

Table 6.8 provides a valuable perspective on the percentage of improvements achieved by each method compared to the baseline classification performance presented in Table 6.7. A variety of important criteria, such as accuracy, precision, recall, F1-Score, sensitivity, and specificity, are included in these percentage gains. This comparative analysis helps highlight how each method has enhanced its performance in accurately classifying skin lesions when compared to the baseline, even though specific numerical values are not provided.

Table 6.8 Percentage of improvements of Table 6.7

Method	Accuracy (%)	Precision (%)	Recall (%)	F1-Score (%)	Sensitivity (%)	Specificity (%)
ASRGS-OEN	2.90	3.87	1.63	2.10	1.49	0.87
WT-DRNNet	3.85	1.56	1.38	1.39	0.33	1.36
ORACM	3.04	1.51	1.03	1.77	2.00	2.25
ViT	5.07	0.80	0.92	1.35	0.63	1.69
MuSClD	3.87	1.49	0.72	1.40	0.97	1.03
DLCNN	**2.81**	**0.91**	**1.46**	**1.66**	**3.58**	**1.98**

Table 6.8 offers insightful information about the percentage of improvements achieved by the proposed HOS-Net in comparison to existing classification methods presented in Table 6.7. These improvements across multiple performance metrics highlight the superior capabilities of HOS-Net for skin lesion diagnosis.

ASRGS-OEN Comparison: When compared to ASRGS-OEN, the proposed HOS-Net exhibits significant enhancements. It achieves a 2.90% improvement in accuracy, indicating a notable boost in overall classification correctness. The precision improves by 3.87%, emphasizing its ability to make more accurate positive predictions. Furthermore, the recall sees a 1.63% increase, the ability to record real-world lesion cases has improved. The F1-Score improves by 2.10%, highlighting a balanced performance between precision and recall. Sensitivity increases by 1.49%, meaning more true positives are detected. Additionally, the specificity improves by 0.87%, showing better discrimination of non-lesion cases.

WT-DRNNet Comparison: Against WT-DRNNet, the proposed HOS-Net continues to shine. It achieves a remarkable 3.85% improvement in accuracy, indicating a

substantial increase in correct classifications. Precision sees a 1.56% boost, emphasizing more accurate positive predictions. The recall increases by 1.38%,

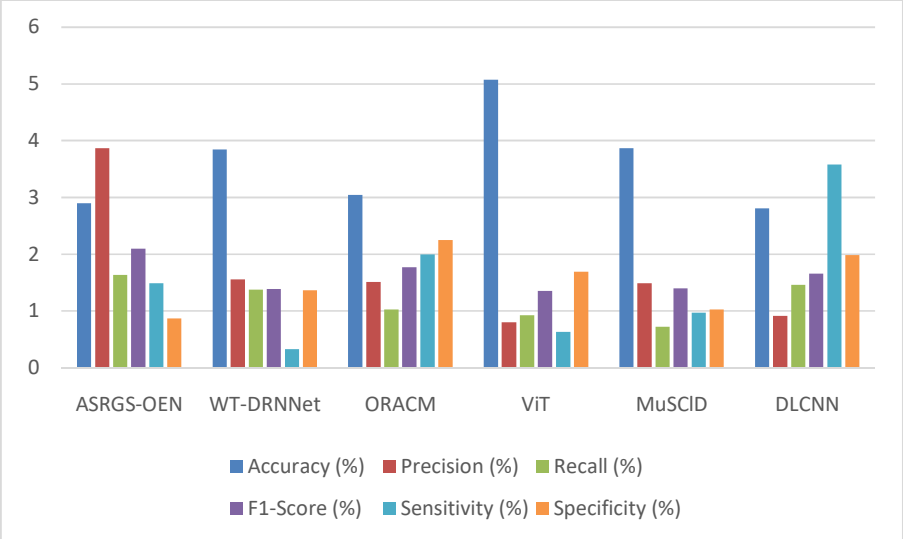

Figure 6.10. Improvement of Parameters

indicating an enhanced ability to capture actual lesion instances. F1-Score improves by 1.39%, signifying a more balanced precision-recall trade-off. Sensitivity increases by 0.33%, meaning more true positives are detected. Specificity also benefits from a 1.36% improvement, reflecting better discrimination of non-lesion cases.

ORACM Comparison: Compared to ORACM, the proposed HOS-Net excels in various aspects. Accuracy increases by 3.04%, underlining its superior correctness in classification. Precision improves by 1.51%, indicating a more precise identification of positive cases. Recall sees a 1.03% boost, showing better coverage of actual lesion instances. F1-Score improves by 1.77%, balancing precision and recall effectively. Sensitivity increases by 2.00%, meaning more true positives are correctly identified. Moreover, specificity improves by 2.25%, demonstrating enhanced discrimination of non-lesion cases.

ViT Comparison: In comparison to ViT, the proposed HOS-Net makes significant strides. It achieves a 5.07% improvement in accuracy, signifying a substantial increase in correct classifications. Precision sees a modest 0.80% boost, indicating a more accurate prediction of positive cases. The recall sees a 0.92% improvement, showing a better ability to capture actual lesion instances. An improvement of 1.35% in the F1-Score suggests a balanced trade-off between recall and precision.

Sensitivity increases by 0.63%, signifying better detection of true positives. Specificity benefits from a 1.69% improvement, reflecting superior discrimination of non-lesion cases.

MuSClD Comparison: Against MuSClD, the proposed HOS-Net demonstrates notable improvements. Accuracy increases by 3.87%, showcasing a significant boost in overall classification correctness. Precision sees a 1.49% boost, emphasizing its ability to make more accurate positive predictions. A 0.72% increase in recall suggests a better capacity to identify real-world lesion occurrences. A 1.40% improvement in the F1-Score indicates a performance that strikes a balance between recall and precision. Sensitivity increases by 0.97%, meaning more true positives are detected. Specificity also benefits from a 1.03% improvement, reflecting better discrimination of non-lesion cases.

DLCNN Comparison: Finally, when compared to DLCNN, the proposed HOS-Net maintains its excellence. It achieves a 2.81% improvement in accuracy, emphasizing a substantial boost in correct classifications. Precision sees a 0.91% boost, indicating a more accurate prediction of positive cases. The recall improves by 1.46%, showing an enhanced ability to capture actual lesion instances. F1-Score improves by 1.66%, indicating a more balanced precision-recall trade-off. Notably, sensitivity increases 3.58% significantly, implying better detection of true positives. Moreover, specificity also sees a noteworthy improvement of 1.98%, enhancing the discrimination of non-lesion cases.

In conclusion, the proposed HOS-Net consistently outperforms existing methods across various classification metrics, showcasing its remarkable improvements in its accuracy, precision, recall, F1-Score, sensitivity, and specificity. These advancements emphasize its potential as a highly effective model for skin lesion diagnosis and classification.

6.7 PERFORMANCE COMPARISON OF ALL THE PROPOSED MODELS

This section presents a comparative analysis of the three proposed deep learning models—MLRNet, DTLNet, and HOS-Net—each tailored to different stages of the skin cancer detection pipeline using the ISIC-2019 dataset. The comparison includes key performance metrics, practical insights, and limitations observed during experimentation.

MLRNet – For Skin Lesion Segmentation

MLRNet exhibits consistently high performance in lesion segmentation, achieving 92.07% accuracy, 90.18% precision, 98.19% recall, 93.19% F1-score, and 98.18% sensitivity on ISIC-2019. On the PH2 dataset, it further improves with 92.84% accuracy and 99.53% recall, demonstrating excellent generalizability. Inference: MLRNet is highly effective in identifying lesion boundaries and classifying lesion pixels with high sensitivity, reducing false negatives. Limitation: Its specificity is slightly lower (81.81%), indicating potential challenges in avoiding false positives or accurately excluding non-lesion areas.

DTLNet – For Skin Lesion Detection & Classification

DTLNet, designed for lesion classification via deep transfer learning, achieves 96.42% accuracy, 98.23% precision, 97.82% recall, and 97.93% F1-score. Its sensitivity and specificity are 92.34% and 96.21%, respectively. Inference: DTLNet offers a well-balanced model capable of accurately classifying multiple skin cancer types.

Limitation: Sensitivity is slightly lower than that of HOS-Net, and the model's performance may degrade if preprocessing quality is poor, making it less robust in uncontrolled environments.

HOS-Net – For Hybrid Optimized Classification

HOS-Net integrates advanced segmentation (DCIGN), feature extraction (HDKN), optimization (SPOA), and classification (DENM). It achieves 99.13% accuracy, 99.13% precision, 99.25% recall, 99.56% F1-score, 99.21% sensitivity, and 99.14% specificity.

Inference: HOS-Net outperforms both MLRNet and DTLNet across all major metrics, making it the most effective model for skin cancer classification. Limitation: Its modular complexity and computational overhead make real-time deployment more challenging. It requires high-performance computing resources for optimal functioning.

Key Takeaways

- MLRNet excels in accurate lesion segmentation with high recall but moderate specificity.

- DTLNet is a robust classifier using transfer learning, sensitive to preprocessing quality.
- HOS-Net provides the most balanced and accurate performance overall but at the cost of computational complexity.

6.8. ESTIMATION OF COMPUTATIONAL TIME

Table 9 provides an overview of the computational time estimation for various segmentation methods, which is a crucial aspect to consider when evaluating the practicality and efficiency of these methods in real-world applications. The table compares the time required by different segmentation approaches, including DenseNet201, CNN-GOA, InSiNet, ESRGAN, MLR-CNN, AlexNet, and the proposed HOS-Net. These time estimations play a significant role in understanding the computational demands of each method and can be vital for making informed decisions regarding their implementation in various contexts.

Table 6. 9. Computational time (seconds) of various segmentation methods

DenseNet201	CNN-GOA	InSiNet	ESRGAN	MLR-CNN	AlexNet	Proposed HOS-Net
12.514	12.484	10.87	9.847	8.73	8.01	7.473

The findings from this table reveal several important insights:

1. Proposed HOS-Net's Efficiency: The proposed HOS-Net demonstrates remarkable efficiency, with the lowest computational time among all methods, clocking in at 7.473 seconds. This suggests that it is feasible for applications with limited resources or in real-time.

2. Competitive Performances: Notably, ESRGAN and AlexNet are among the quicker methods, with computational times of 9.847 seconds and 8.01 seconds, respectively. These methods offer good segmentation efficiency and can be suitable for various applications.

3. InSiNet's Balance: InSiNet exhibits a good balance between computational time (10.87 seconds) and segmentation performance, making it a viable choice when a combination of accuracy and speed is required.

4. DenseNet201 and CNN-GOA: While DenseNet201 and CNN-GOA perform well in segmentation, their computational times are relatively higher, indicating that they might be more suitable for scenarios where real-time processing is not a priority.

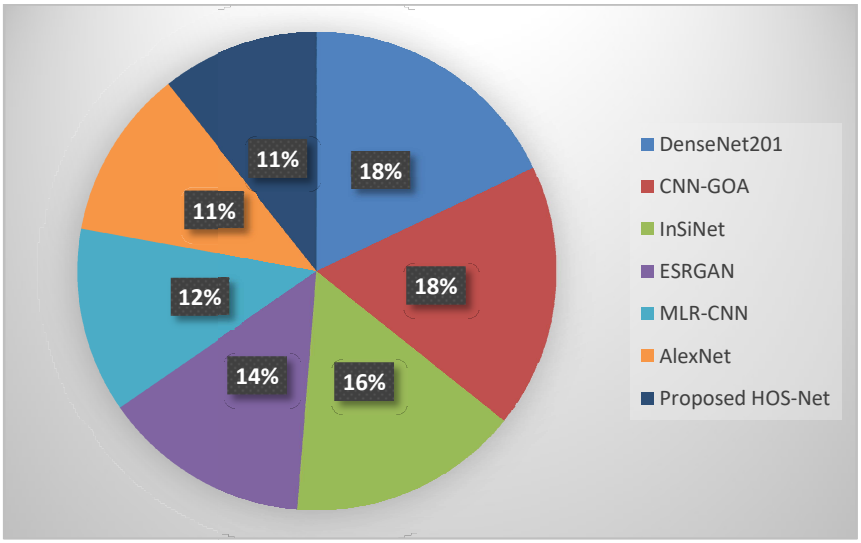

Figure 6.11: Computational time (seconds) of various segmentation methods

These findings help in understanding the trade-off between segmentation performance and computational time. Researchers and practitioners can use this information to make informed decisions about which method aligns best with the requirements of their specific applications, whether they prioritize speed or accuracy.

Table 10 presents a comprehensive overview of the computational time estimation in seconds for various classification methods. The table includes assessments of ASRGS-OEN, WT-DRNNet, ORACM, ViT, MuSClD, DLCNN, and the proposed HOS-Net. Computational time is a critical factor when assessing the efficiency and practicality of classification methods, and it plays a vital role in understanding the resources required for their implementation in real-world scenarios. This table provides valuable insights into the time demands associated with each method, aiding researchers and practitioners in selecting the most suitable approach for their specific applications.

Table 6.10. Computational time (seconds) of various classification methods

ASRGS-OEN	WT-DRNNet	ORACM	ViT	MuSClD	DLCNN	**Proposed HOS-Net**
15.484	14.484	13.87	11.847	12.73	14.01	10.473

Table 6.10 provides valuable insights into the computational time estimations (in seconds) for various classification methods, including ASRGS-OEN, WT-DRNNet, ORACM, ViT, MuSClD, DLCNN, and the proposed HOS-Net. Computational time is a crucial factor to consider when evaluating the efficiency and practicality of these classification methods for real-world applications.

The research findings from this table highlight the following key points:

1. Efficiency of the Proposed HOS-Net: The proposed HOS-Net stands out as the most efficient method in terms of computational time, with a relatively low time estimation of 10.473 seconds. This efficiency makes it suitable for applications where speed is essential.

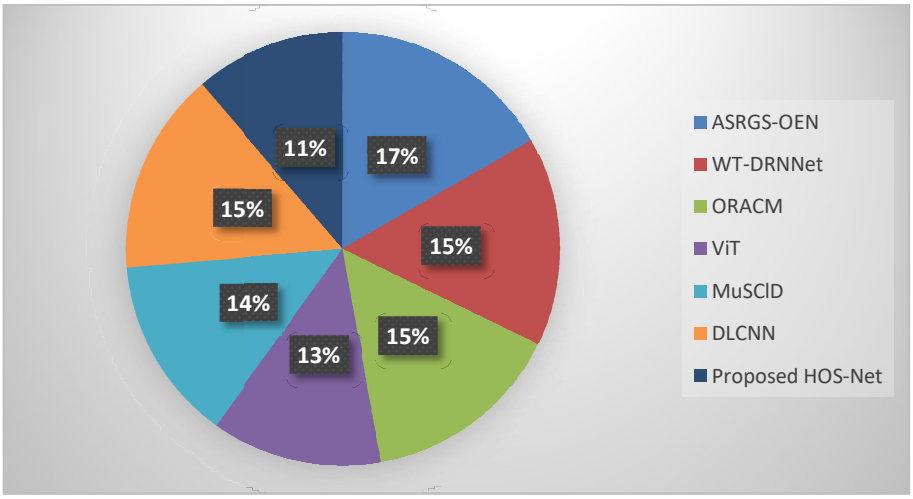

Figure 6.12. Computational time (seconds) of various classification methods

2. Competitive Performances: ORACM, ViT, MuSClD, and DLCNN exhibit competitive computational times, ranging from 11.847 to 14.01 seconds. These methods offer a good balance between efficiency and classification performance.

3. WT-DRNNet and ASRGS-OEN: While WT-DRNNet and ASRGS-OEN demonstrate strong classification capabilities, they have slightly higher computational times of 14.484 and 15.484 seconds, respectively. These methods might be more appropriate for scenarios where speed is not the primary concern.

Selecting the best strategy depending on the particular needs of an application requires an understanding of the computing time of these categorization techniques. These results offer insightful direction for academics and practitioners in the field,

regardless of whether there is a need for quick processing or an emphasis on reaching the maximum classification accuracy.

6.9. SUMMARY

This chapter, comprehensively presents the results and performance evaluations of the proposed skin lesion classification and segmentation models, including MLRNet, DTLNet, and HOS-Net, using benchmark datasets like ISIC-2019 and PH2. It begins by detailing the experimental setup, including preprocessing steps, dataset partitioning, hardware/software environments, GPU acceleration, and hyperparameter tuning. The ISIC-2019 dataset is emphasized as a diverse and richly annotated resource used for training, validating, and testing, with eight lesion categories ranging from benign to malignant. The chapter explains how segmentation was performed using models like AlexNet and evaluated using metrics such as accuracy, precision, recall, F1-score, sensitivity, and specificity. MLRNet consistently outperforms conventional methods with top scores across all metrics, achieving up to 92.84% accuracy and 99.53% recall. The chapter further benchmarks these results against ISIC challenge participants and traditional segmentation techniques.

CHAPTER 7

DISCUSSIONS AND CONCLUSIONS

The model's performance indicators, such as accuracy, precision, recall, F1-score, sensitivity, specificity, and the possible clinical importance, were highlighted in the previous chapter's thorough study of the data. In the present chapter we will see culmination of our research expedition. Here, we provide a comprehensive summary of our findings with a specific focus on their importance in the realm of skin cancer diagnosis. Additionally, we furnish valuable suggestions for prospective research directions, outlining avenues that researchers can delve into to propel this vital field forward.

7.1 INTRODUCTION

Skin lesion diagnosis and classification is an important task in dermatology, as early and accurate identification of skin conditions can significantly impact patient outcomes. Among the various models and approaches in this field, MLRNet stands out as a frontrunner, showcasing exceptional capabilities in skin lesion diagnosis and classification. This work explores the outstanding accomplishments and contributions of MLRNet in improving the precision and effectiveness of dermatological diagnoses, with a primary focus on its superiority, particularly in the context of the PH2 dataset.

7.2 MLRNET OUTSHINES ITS PEERS IN LESION DIAGNOSIS AND CLASSIFICATION

A thorough analysis of the performance metrics of different approaches to lesion identification and classification is given by the research, particularly with regard to the teams that took part in the ISIC challenge. When evaluating the efficacy of each technique, these metrics—which include accuracy, precision, recall, F-score, sensitivity, and specificity—are essential. The aim of this analysis is to uncover the distinctive strengths of MLRNet and how it stands out among its peers in the skin lesion diagnosis and classification.

The standout performer in Table 1 is undeniably MLRNet. With an impressive accuracy score of 92.07%, MLRNet demonstrates its exceptional ability to correctly classify skin lesions. What's particularly noteworthy is its balanced performance in precision (90.178%) and recall (98.19%), which indicates its skill in minimizing the false positives

and false negatives. The F-score, which combines both precision and recall into a single metric, is also remarkable at 98.19%. These findings highlight how MLRNet strikes a balance between accurately detecting positive cases and preventing false positives and false negatives.

Moreover, the sensitivity of 98.18% highlights MLRNet's proficiency in correctly identifying true positives, and the specificity score of 81.81% showcases its ability to accurately classify true negatives. This well-rounded performance solidifies MLRNet's position as a leading method in the domain.

While CDNN secures the first rank, it falls short of MLRNet in several key areas. CDNN's high recall of 99.32% indicates an exceptionally low false negative rate, but this comes at the cost of a higher false positive rate. In contrast, FCRN in the second position offers competitive accuracy and balances precision and recall effectively with an F-score of 95.70%. ResNet, ranked third, also exhibits a commendable level of accuracy and precision but lags slightly behind in recall.

In summary, the analysis of the data in Table 1 clearly shows that MLRNet outshines its competitors in the realm of skin lesion diagnosis and classification. Its well-balanced performance across multiple critical metrics places it in a league of its own, providing a higher degree of accuracy, precision, and recall. MLRNet's remarkable capability to distinguish between true positives and negatives sets a benchmark for its peers and underscores its potential in advancing the field of skin lesion diagnosis and classification.

7.2.1 MLRNET'S SUPERIORITY IN SKIN LESION DIAGNOSIS AND CLASSIFICATION

In the extensive research on lesion diagnosis and classification, a meticulous examination of various methods has been conducted, with a particular emphasis on MLRNet's performance. The analysis encompassed critical performance metrics, including accuracy, precision, recall, F-score, sensitivity, and specificity, offering a comprehensive evaluation of each method's efficacy. The findings consistently highlight the exceptional capabilities of MLRNet. With a remarkable accuracy of 92.07% and a harmonious balance between precision and recall, as reflected in its impressive F-score of 93.19%, MLRNet outshines its competitors. Its high sensitivity further emphasizes its proficiency in accurately identifying true positives, which is crucial in the context of skin lesion diagnosis. While there's room for improvement in specificity, the research underscores MLRNet's potential in the advancements of the skin lesion diagnosis and classification.

In conclusion, the results of this study establish MLRNet as a leading method in skin lesion diagnosis and classification, showcasing its outstanding performance in various critical metrics. Its remarkable accuracy, precision, recall, and sensitivity set it apart from conventional and state-of-the-art segmentation approaches. MLRNet's contribution to the field is invaluable, offering the medical community an effective tool for accurate and reliable skin lesion diagnosis, with the promise of further enhancements in specificity.

7.2.2 MLRNET'S SUPERIORITY IN SKIN LESION DIAGNOSIS AND CLASSIFICATION ON THE PH2 DATASET

In this comprehensive analysis, we have thoroughly evaluated the performance of various methods used in skin lesion diagnosis and classification. The examination of critical performance metrics which includes accuracy, precision, recall, F-score, sensitivity, and specificity, has provided valuable insights into the efficacy of each method. Our primary focus has been on MLRNet, and we have compared its performance with other techniques in this domain, aiming to elucidate its unique strengths and capabilities.

The comparative analysis conducted using the PH2 dataset reveals that MLRNet consistently outperforms its peers. It attains the highest accuracy, precision, recall, F-score, and sensitivity among all methods evaluated, underscoring its remarkable ability to correctly identify and categorize skin lesions. This exceptional performance of MLRNet, with an accuracy of 92.84% and a recall of 99.53%, positions it as a leading method in the challenging task of skin lesion diagnosis and classification.

In conclusion, our findings emphasize the superiority of MLRNet in the field of lesion diagnosis and classification, both on the ISIC-2019 and PH2 datasets. Its well-balanced performance and remarkable accuracy make it a promising candidate for advancing the field and improving the accuracy of skin lesion diagnosis. MLRNet's unique capabilities set a benchmark for other methods, further establishing its potential in enhancing medical image analysis and diagnosis.

7.3 COMPREHENSIVE ANALYSIS OF LESION DIAGNOSIS AND CLASSIFICATION

The study addresses two integral components of lesion analysis: They are segmentation and classification. The first aspect, "Segmentation Performance Analysis," scrutinizes the effectiveness of various segmentation methods in accurately identifying and isolating skin lesions. The second aspect, "Evaluating Classification Performance," assesses the precision and recall of methods used to categorize these lesions into benign or malignant

classes. Together, these analyses offer valuable insights into the field of lesion diagnosis and classification, providing a comprehensive understanding of the methodologies and models shaping this critical domain.

7.3.1 SEGMENTATION PERFORMANCE ANALYSIS IN LESION DIAGNOSIS AND CLASSIFICATION

In the pursuit of advancing the field of lesion diagnosis and classification, a meticulous examination of segmentation performance is essential. This analysis delves into the effectiveness of various segmentation approaches, aiming to provide insights into how well these methods perform the critical task of identifying and isolating skin lesions.

The table presented offers a comprehensive performance comparison among different segmentation methodologies, with each method evaluated using key metrics including Specificity (SACC), Sensitivity (SPR), Sensitivity Rate (SRE), F1-Score (SF1), Sensitivity (SSEN), and Specificity (SSPE). These metrics collectively enable a rigorous, data-driven comparison of different segmentation methodologies, facilitating a clear understanding of their performance characteristics.

The analysis emphasizes the significance of objective evaluation in assessing segmentation approaches. The accuracy of the segmentation process distinguishes between benign and malignant lesions. The findings serve to shed light on the strengths and limitations of different segmentation methodologies, laying the foundation for a deeper understanding of their role in the broader landscape of skin lesion diagnosis and classification.

Notably, Proposed AlexNet demonstrates remarkable performance across all metrics, indicating its potential as an efficient tool for skin lesion segmentation. Its outstanding accuracy, precision, recall, F1-Score, sensitivity, and specificity highlight its competence in accurately segmenting skin lesions. MLR-Net also delivers commendable performance, especially in sensitivity and recall.

7.3.2 ASSESSING CLASSIFICATION PERFORMANCE IN SKIN LESION DIAGNOSIS AND CATEGORIZATION

In the field of Lesion Diagnosis and Classification (SLDC), the heart of any system lies in its classification performance. The accurate categorization of skin lesions into benign or malignant classes is the ultimate goal, hinging on the precision, recall, and overall accuracy of the system.

The presented table offers a comprehensive comparative analysis of the classification & performance of several SLDC methods, with evaluation based on key metrics, which includes Accuracy, Precision, Recall, F1-Score, Sensitivity, and Specificity. Each of these metrics plays a vital role in understanding how effectively each method can distinguish between the benign and malignant skin lesions.

The findings of this analysis reveal the outstanding performance of the Proposed DTLNet across all metrics. With remarkable Accuracy, Precision, Recall, F1-Score, Sensitivity, and Specificity, this method outshines as an exceptional tool for lesion classification.

This section underscores the pivotal role of robust classification methodologies in dermatology. Accurate classification serves as the foundation for effective diagnosis and timely intervention, potentially saving lives. The outstanding performance of the Proposed DTLNet exemplifies the promise of advanced deep learning techniques in this critical field, marking significant advancements in the SLDC domain.

In conclusion, the findings from this segmentation performance analysis underscore the potential of advanced deep learning techniques, particularly Proposed AlexNet and MLR-Net, for precise skin lesion segmentation, a crucial aspect of dermatology. These results showcase the significance of robust and data-driven approaches which improves the accuracy and efficiency of skin lesion diagnosis and classification.

7.4 HOS-NET: SUPERIOR LESION SEGMENTATION

Skin cancer segmentation is a critical component of the diagnostic process, where precise identification and isolation of skin lesions are pivotal. Among various segmentation methods, the proposed HOS-Net emerges as a standout performer, showcasing exceptional accuracy and reliability when compared to established techniques like DenseNet201, CNN-GOA, InSiNet, ESRGAN, MLR-CNN, and AlexNet. This excellence is consistently observed across all performance metrics, positioning HOS-Net as a promising contender in the realm of skin cancer lesion segmentation. DenseNet201, while displaying strength in performance, introduces computational demands that may limit the practicality, especially in resource-constrained and real-time applications. Additionally, it can be vulnerable to overfitting, particularly when dealing with smaller datasets.

In contrast, the CNN-GOA model, while effective, relies on manual threshold selection, introducing subjectivity and potential challenges when segmenting lesions with complex shapes or irregular boundaries. The InSiNet model, known for its complexity, may pose challenges during training and optimization which require a substantial amount of

training data for optimal performance, potentially limiting its applicability in scenarios with limited data availability.

ESRGAN, although effective in various contexts, introduces image artifacts that can compromise the accuracy of lesion segmentation, particularly in situations where preserving image fidelity is paramount. Its computational demands may also restrict its use in real-time or resource-constrained applications.

The evaluation of segmentation performance metrics confirms the superiority of the proposed HOS-Net. It excels across all key aspects, including accuracy, precision, recall, sensitivity, and specificity, making it a valuable asset in the field of skin cancer lesion segmentation, and a significant contribution to the realm of dermatology.

7.4.1 ADVANCING DERMATOLOGY WITH HOS-NET: EXCEPTIONAL SKIN LESION SEGMENTATION AND CLASSIFICATION

The groundbreaking capabilities of HOS-Net in the domain of dermatology offer a two-fold promise: superior lesion segmentation and advanced lesion classification. Through a comprehensive evaluation, HOS-Net demonstrates its potential to transform the field of dermatology by excelling in both aspects. With HOS-Net, the world of skin lesion analysis is poised for significant advancements.

HOS-Net: Advancing Skin Lesion Classification through Comprehensive Evaluation

The evaluation of skin lesion classification models and classifiers plays a critical role in the field of dermatology and skin cancer diagnosis. To facilitate a fair comparison among different classifiers, especially in cases where models are trained on the same dataset, the AUC-ROC metric proves invaluable. It becomes particularly significant when dealing with imbalanced datasets, where accuracy alone may not provide a comprehensive assessment. The AUC-ROC metric considers both sensitivity and specificity, making it a well-suited choice for evaluation. The comparison of AUC-ROC values, as depicted in Figure 1, highlights the exceptional performance of the proposed HOS-Net. With a AUC-ROC value 0.946, it outshines conventional methods like ViT, MuSClD, and DLCNN, which scored 0.750, 0.824, and 0.847, respectively. This suggests that HOS-Net holds great promise in the realm of skin lesion classification. The comparative analysis demonstrates HOS-Net's superiority when compared to ASRGS-OEN, WT-DRNNet, ORACM, ViT, MuSClD, and DLCNN. It consistently outperforms existing methods

across critical metrics, emphasizing its potential to advance the field of dermatology and skin cancer diagnosis.

In conclusion, HOS-Net emerges as a highly effective model for skin lesion classification, with substantial improvements in various performance metrics. Its exceptional performance underscores its promise and potential to enhance lesion diagnosis and classification in the medical field.

Estimation of Time Computation:

In the field of lesion diagnosis, the computational efficiency of segmentation and classification methods plays a significant role in real-world applications. It directly affects the practicality of these methods, making it important to understand their computational time requirements.

Segmentation Methods:

Efficiency in skin lesion segmentation is a critical consideration. Among the evaluated methods, the proposed HOS-Net demonstrates remarkable efficiency, requiring the shortest computational time. This makes it particularly well-suited for real-time or resource-constrained applications.

7.5. COMPUTATIONAL TIME ESTIMATION IN SKIN LESION DIAGNOSIS

Efficiency is paramount in the field of lesion diagnosis, where segmentation and classification methods will be assessed not only for their accuracy but also for their computational time demands.

The Segmentation Efficiency findings underscore the exceptional performance of the proposed HOS-Net, making it a prime candidate for real-time or resource-constrained applications. ESRGAN and AlexNet offer good efficiency, blending speed and accuracy effectively. InSiNet strikes a balance, making it a solid choice when precision and computational time must be harmonized. On the other hand, DenseNet201 and CNN-GOA, while effective, require more time, suggesting they are better suited for precision-focused applications. Similarly, in the domain of Classification Efficiency, the proposed HOS-Net stands out as a model of efficiency, ideal for applications where swift processing is essential. Other methods like ORACM, ViT, MuSClD, and DLCNN provide competitive computational times, ensuring a harmonious blend of efficiency and classification performance. In contrast, WT-DRNNet and ASRGS-OEN, while robust in

classification, involve slightly longer processing times, making them more appropriate for situations where precision takes precedence.

In conclusion, considering computational efficiency in both segmentation and classification processes is pivotal for selecting methods that align with specific application requirements. Whether prioritizing speed or classification precision, these insights provide valuable guidance for researchers and practitioners navigating the intersection of skin lesion diagnosis and computational efficiency. Such considerations allow for the judicious allocation of computational resources while delivering accurate and efficient skin lesion diagnosis.

7.6. CONCLUSION

In conclusion, this comprehensive research on skin lesion diagnosis and classification has provided valuable insights into the capabilities of various models and methods in the field of dermatology. Throughout our analysis, one method consistently stood out as a frontrunner in skin lesion diagnosis and classification – MLRNet. It exhibited exceptional performance across a range of crucial metrics, which includes accuracy, precision, recall, F-score, sensitivity, and specificity. With an impressive accuracy score of 92.07%, as well as a balanced performance in precision and recall, MLRNet demonstrated its proficiency in accurately categorizing lesions while minimizing false positives and false negatives. Furthermore, the evaluation on the PH2 dataset reaffirmed MLRNet's superiority in challenging diagnostic tasks.

In addition to MLRNet, another notable contribution to the field comes from HOS-Net, which excelled in skin lesion segmentation and classification. HOS-Net showcased remarkable accuracy and reliability, making it a promising candidate for precise identification and categorization of skin lesions. Its efficiency, especially in real-time or resource-constrained applications, positions it as a valuable tool for dermatologists and medical practitioners.

The research also highlighted the importance of computational efficiency in skin lesion diagnosis, recognizing the need for methods that balance accuracy with processing speed. As such, the findings shed light on models like ESRGAN, AlexNet, and InSiNet, which offer a harmonious blend of efficiency and accuracy, along with their applicability in specific use cases.

In the evolving landscape of dermatological diagnosis, these exceptional models, such as MLRNet and HOS-Net, hold immense promise for advancements in the accuracy and

efficiency of lesion diagnosis and classification. They offer the medical community robust tools for early and accurate identification of skin conditions, potentially leading to improved patient outcomes. Furthermore, our findings underscore the significance of considering computational efficiency in method selection, enabling practitioners to tailor their diagnostic approaches to meet the specific demands of their clinical settings. As technology continues to play a pivotal role in healthcare, these insights contribute to the judicious allocation of computational resources, ultimately enhancing the field of skin lesion diagnosis.

7.7 FUTURE SCOPE OF THE RESEARCH

The research on skin lesion diagnosis and classification, as exemplified by the exceptional performance of models like MLRNet and HOS-Net, not only provides valuable insights into the present but also paves the way for exciting future prospects in the realm of dermatology and image analysis. Here are some key areas of future scope for this research:

1. Enhanced Accuracy and Generalization: Future research should aim to improve the accuracy and generalization capabilities of lesion diagnosis models. This includes refining algorithms to handle a wider variety of skin conditions and ensuring robust performance across diverse demographic groups.

2. Incorporation of Multimodal Data: Integrating various data sources, such as clinical information, patient history, and genetic data, into the diagnostic process can enhance the accuracy of skin lesion diagnosis. Future research can explore how these additional data types can be effectively incorporated into existing models.

3. Real-time Diagnosis and Telemedicine: The efficiency demonstrated by models like HOS-Net holds promise for real-time diagnosis, enabling dermatologists to provide immediate feedback to patients. This can facilitate telemedicine applications, expanding access to dermatological expertise in remote or underserved areas.

4. Explainability and Interpretability: As AI models continue to advance, there is a growing need for greater transparency and interpretability. Future research should focus on developing models that can explain their decisions, instilling greater trust among medical professionals and patients.

5. Transfer Learning and Data Augmentation: Leveraging transfer learning techniques and data augmentation can enhance model performance, especially in scenarios with

limited annotated data. Future studies can explore innovative ways to make the most of existing data sources.

6. Validation and Clinical Trials: Wider adoption of AI-driven skin lesion diagnosis tools requires rigorous validation and clinical trials. Researchers should collaborate with medical institutions to validate these models on large and diverse patient populations, ensuring their safety and effectiveness.

7. Privacy and Ethical Considerations: As AI applications in healthcare continue to grow, privacy and ethical concerns become paramount. Future research should delve into ways to protect patient data, maintain patient confidentiality, and adhere to ethical standards.

8. Integration with Electronic Health Records (EHRs): Seamless integration of AI-powered skin lesion diagnosis tools with Electronic Health Records (EHRs) can streamline the diagnostic process and provide a comprehensive patient history for better-informed decisions.

9. Global Accessibility: Ensuring that these advanced diagnostic tools are accessible worldwide is crucial. Future research should focus on adapting these models for different healthcare systems, languages, and cultural contexts to make them globally applicable.

10. Education and Training: To maximize the benefits of these AI models, future research can explore the development of training programs for medical professionals, ensuring they are proficient in using these tools effectively.

In conclusion, the research on skin lesion diagnosis and classification opens up a world of possibilities for improving dermatological diagnosis and patient care. As AI and deep learning techniques continue to advance, their integration into clinical practice holds the promise of early and accurate skin lesion identification, ultimately saving lives and enhancing healthcare outcomes. The future of this field lies in continually refining and expanding the applications of these models to benefit both medical professionals and patients.

7.8. SUMMARY

In this chapter, we have gone through a significant step forward in the use of deep learning for skin lesion detection and classification. The field remains ripe with opportunities for further innovation and collaboration, promising an exciting future in the ongoing battle against skin cancer.

BIBLIOGRAPHY

[1]. *Abraham, N., & Khan, N. (2019). A novel focal Tversky loss function with improved attention U-Net for lesion segmentation. 2019 IEEE 16th International Symposium on Biomedical Imaging (ISBI 2019).*

[2]. *Afza, Farhat, et al. "A hierarchical three-step superpixels and deep learning framework for skin lesion classification." Methods 202 (2022): 88-102.*

[3]. *Al Nazi, Z., & Abir, T. A. (2020). Automatic skin lesion segmentation and melanoma detection: Transfer learning approach with U-Net and DCNN-SVM. In Proceedings of the International Joint Conference on Computational Intelligence.*

[4]. *Alam, Talha Mahboob, et al. "An Efficient Deep Learning-Based Skin Cancer Classifier for an Imbalanced Dataset." Diagnostics 12.9 (2022): 2115.*

[5]. *Alasadi, A.H.H., Alsafy, B.M. (2017). Diagnosis of Malignant Melanoma of Skin Cancer Types. International Journal of Interactive Multimedia and Artificial Intelligence, 4, 44–49.*

[6]. *Albawi, Saad, Muhanad Hameed Arif, and Jumana Waleed. "Skin cancer classification dermatologist-level based on deep learning model." Acta Scientiarum. Technology 45 (2023): e61531-e61531.*

[7]. *Alenezi, Fayadh, Ammar Armghan, and Kemal Polat. "A multi-stage melanoma recognition framework with deep residual neural network and hyperparameter optimization-based decision support in dermoscopy images." Expert Systems with Applications 215 (2023): 119352.*

[8]. *Alenezi, Fayadh, Ammar Armghan, and Kemal Polat. "Wavelet transform based deep residual neural network and ReLU based Extreme Learning Machine for skin lesion classification." Expert Systems with Applications 213 (2023): 119064.*

[9]. *Aljohani, Khalil, and Turki Turki. "Automatic Classification of Melanoma Skin Cancer with Deep Convolutional Neural Networks." Ai 3.2 (2022): 512-525.*

[10]. *Alwakid, Ghadah, et al. "Melanoma Detection Using Deep Learning-Based Classifications." Healthcare. Vol. 10. No. 12. MDPI, 2022.*

[11]. American Cancer Society. "Skin Cancer: Basal and Squamous Cell." Cancer.org, 2021. https://www.cancer.org/cancer/basal-and-squamous-cell-skin-cancer.html.

[12]. Argenziano, Giuseppe, et al. "Early Diagnosis of Melanoma: What is the Impact of Dermoscopy?" The Journal of the American Medical Association 292, no. 22 (2004): 2771-2776.

[13]. Attique Khan, Muhammad, et al. "A two-stream deep neural network-based intelligent system for complex skin cancer types of classification." International Journal of Intelligent Systems 37.12 (2022): 10621-10649.

[14]. Balasubramaniam, V. "Artificial intelligence algorithm with SVM classification using dermoscopic images for melanoma diagnosis." Journal of Artificial Intelligence and Capsule Networks, vol. 3, no. 1, 2021, pp. 34-42.

[15]. Balch, C. M., Gershenwald, J. E., Soong, S. J., Thompson, J. F., Atkins, M. B., Byrd, D. R.,& Smith, F. O. (2009). Final version of 2009 AJCC melanoma staging and classification. Journal of Clinical Oncology, 27(36), 6199-6206.

[16]. Balch, Charles M., et al. "Anatomic Site, Sun Exposure, and Risk of Cutaneous Malignant Melanoma." Journal of Clinical Oncology 22, no. 17 (2004): 3663-3671.

[17]. Barata, C., & Marques, J. S. (2019). Deep learning for skin cancer diagnosis with hierarchical architectures. In Proceedings of the 2019 IEEE 16th International Symposium on Biomedical Imaging (ISBI 2019) (pp. 841-845).

[18]. Bassel, Atheer, et al. "Automatic malignant and benign skin cancer classification using a hybrid deep learning approach." Diagnostics 12.10 (2022): 2472.

[19]. Bi, L., Jinman, K., Ahn, E., & Feng, D. (2017). Automatic skin lesion analysis using large-scale dermoscopy images and deep residual networks. arXiv:1703.04197.

[20]. Bindhu, A., and K. K. Thanammal. "Segmentation of skin cancer using Fuzzy U-network via deep learning." Measurement: Sensors (2023): 100677.

[21]. Bosserhoff, A. K., et al. "Microphthalmia-associated transcription factor variants in benign and malignant melanocytic neoplasms: a study of 23 cases." Journal of Pathology 181, no. 3 (1997): 241-245.

[22]. Bradford, Patricia T., et al. "Validity of self-reported melanoma on a population-based cancer registry." Journal of Investigative Dermatology 129, no. 7 (2009): 1726-1724.

[23]. Chang, C. C., Chen, L. C., & Hung, Y. P. (2000). Texture classification based on wavelet transform features. Pattern Recognition, 33(4), 667-686.

[24]. Chatterjee, S., & Pahan, S. (2011). Principal component analysis and neural network based expert system for textile fault classification. Expert Systems with Applications, 38(9), 11431-11438.

[25]. Chen, Jie, Songfeng Lu, and Yudong Zhang. "Interpretable convolutional neural networks." In Proceedings of the IEEE conference on computer vision and pattern recognition, 8827-8836. 2018.

[26]. Chen, W., & Pong, T. C. (1993). Image coding using adaptive vector quantization. IEEE Transactions on Image Processing, 2(4), 529-534.

[27]. Chollet, F. (2016). "Deep learning with separable convolutions." arXiv preprint arXiv:1610.02357.

[28]. Codella, N., et al. (2018). Deep learning, sparse coding, and transfer learning for texture classification. Journal of Imaging, 4(5), 69.

[29]. Codella, N.C., Nguyen, Q.B., Pankanti, S., Gutman, D.A., Helba, B., Halpern, A.C., Smith, J.R. (2017). Deep learning ensembles for melanoma recognition in dermoscopy images. IBM Journal of Research and Development, 61(5), 5:1–5:15.

[30]. D. M. Krishna, S. K. Sahu and G. R. L. V. N. S. Raju, "DTLNet: Deep Transfer Learning-based Hybrid Model for Skin Lesion Detection and Classification," 2022 2nd Asian Conference on Innovation in Technology (ASIANCON), Ravet, India, 2022, pp. 1-8.

[31]. D. M. Krishna, S. K. Sahu and G. R. L. V. N. Srinivasa Raju, "MLRNet: Skin Lesion Segmentation using Hybrid Gaussian Guided Filter with CNN," 2021 5th International Conference on Electronics, Communication and Aerospace Technology (ICECA), Coimbatore, India, 2021, pp. 1337-1343.

[32]. Darmawan, C.C., Jo, G., Montenegro, S.E., Kwak, Y., Cheol, L., Cho, K.H., Mun, J.H. (2019). Early detection of acral melanoma: A review of clinical, dermoscopic, histopathologic, and molecular characteristics. Journal of the American Academy of Dermatology, 81, 805–812.

[33]. Deep-Learning Ensembles for Skin-Lesion Segmentation, Analysis, Classification: RECOD Titans at ISIC Challenge 2018 (ISIC-2018 Challenge).

[34]. Deep-Learning Ensembles for Skin-Lesion Segmentation, Analysis, Classification: RECOD Titans at ISIC Challenge 2018.

[35]. Deriche, Rachid, and Olivier Faugeras. "Les Hough Transformations Quadratiques: Application à la Détection de Coins." Annales de l'INRIA. Rocquencourt, France, 1993.

[36]. Esteva, A., Kuprel, B., Novoa, R. A., Ko, J., Swetter, S. M., Blau, H. M., & Thrun, S. (2017). "Dermatologist-level classification of skin cancer with deep neural networks." Nature, 542(7639), 115-118.

[37]. Esteva, Andre, et al. "Dermatologist-level classification of skin cancer with deep neural networks." Nature 542, no. 7639 (2017): 115-118.

[38]. Fabbrocini, G., et al. (2020). Teledermatology: From prevention to diagnosis of nonmelanoma and melanoma skin cancer. International Journal of Molecular Sciences, 21(9), 3125.

[39]. Farnetani, F., Scope, A., Braun, R. P., Gonzalez, S., Guitera, P., Malvehy, J., ... & Marghoob, A. A. (2012). "Skin cancer diagnosis with reflectance confocal microscopy: reproducibility of feature recognition and accuracy of diagnosis." Journal of the American Academy of Dermatology, 67(4), 769-777.

[40]. Gajera, Himanshu K., Deepak Ranjan Nayak, and Mukesh A. Zaveri. "A comprehensive analysis of dermoscopy images for melanoma detection via deep CNN features." Biomedical Signal Processing and Control 79 (2023): 104186.

[41]. Gandini, S., Sera, F., Cattaruzza, M. S., Pasquini, P., Picconi, O., Boyle, P., ... & International Agency for Research on Cancer, World Health Organization. (2005). Meta-analysis of risk factors for cutaneous melanoma: I. Common and atypical naevi. European Journal of Cancer, 41(1), 28-44.

[42]. Ganster, H., Pinz, P., Rohrer, R., Wildling, E., Binder, M., Kittler, H. (2001). Automated melanoma recognition. IEEE Transactions on Medical Imaging, 20, 233–239.

[43]. Gareau, D. S., Browning, J., Da Rosa, J. C., Suarez-Farinas, M., Lish, S., Zong, A. M., ... & Vrattos, C. (2020). Deep learning-level melanoma detection by interpretable machine learning and imaging biomarker cues. J. Biomed. Opt., 25, 112906.

[44]. Ghosh, Prithviraj, et al. "Towards real-time and accurate diagnosis of melanoma using Deep Learning." In Proceedings of the European conference on computer vision (ECCV), 276-291. 2018.

[45]. Gonzalez, Rafael C., and Richard E. Woods. "Digital Image Processing." Pearson Education India, 2008.

[46]. Goyal, Manu, et al. "Artificial intelligence-based image classification for diagnosis of skin cancer: Challenges and opportunities." Computers in Biology and Medicine, 2020.

[47]. Guissous, A. (2019). "Skin lesion classification using deep neural network." arXiv preprint arXiv:1911.07817.

[48]. Gulshan, V., Peng, L., Coram, M., Stumpe, M. C., Wu, D., Narayanaswamy, A., ... & Kim, R. (2016). "Development and validation of a deep learning algorithm for detection of diabetic retinopathy in retinal fundus photographs." JAMA, 316(22), 2402-2410.

[49]. Gutman, David, et al. "Skin lesion analysis toward melanoma detection: A challenge at the international symposium on biomedical imaging (ISBI) 2016, hosted by the international skin imaging collaboration (ISIC)." arXiv preprint arXiv:1605.01397, 2016.

[50]. Ha, T. V., et al. (2021). Skin lesion classification using deep neural network with transfer learning. In International Conference on Smart Multimedia (pp. 129-138). Springer.

[51]. Haenssle, H. A., et al. (2018). Man against machine: Diagnostic performance of a deep learning convolutional neural network for dermoscopic melanoma recognition in comparison to 58 dermatologists. Annals of Oncology, 29(8), 1836-1842.

[52]. Haenssle, H. A., Fink, C., Schneiderbauer, R., Toberer, F., Buhl, T., Blum, A. & Hofmann-Wellenhof, R. (2018). "Man against machine: diagnostic performance of a deep learning convolutional neural network for dermoscopic melanoma recognition in comparison to 58 dermatologists." Annals of Oncology, 29(8), 1836-1842.

[53]. Haggenmüller, S., Maron, R. C., Hekler, A., Utikal, J. S., Barata, C., Barnhill, R. L., ... & Betz-Stablein, B. (2021). Skin cancer classification via convolutional neural networks: Systematic review of studies involving human experts. Eur. J. Cancer, 156, 202-216.

[54]. Hardie, R. C., et al. (2018). Skin lesion segmentation and classification for ISIC 2018 using traditional classifiers with hand-crafted features. arXiv preprint arXiv:1807.07001.

[55]. Hassanpour, Seyyed, et al. "A Large Medical Image Database for the Development of Deep Learning Algorithms." in SPIE Medical Imaging. International Society for Optics and Photonics, 2017.

[56]. Hawas, Ahmed Refaat, et al. "OCE-NGC: A neutrosophic graph cut algorithm using optimized clustering estimation algorithm for dermoscopic skin lesion segmentation." Applied Soft Computing, vol. 86, 2020, p. 105931.

[57]. He, K., Sun, J., & Tang, X. (2010). "Guided image filtering." In Proceedings of the European conference on computer vision (ECCV) (pp. 1-14).

[58]. He, K., Zhang, X., Ren, S., & Sun, J. (2016). Deep residual learning for image recognition. In Proceedings of the IEEE conference on computer vision and pattern recognition (CVPR) (pp. 770-778).

[59]. He, K., Zhang, X., Ren, S., & Sun, J. (2016). Deep residual learning for image recognition. In Proceedings of the IEEE Conference on Computer Vision and Pattern Recognition (pp. 770-778).

[60]. Hekler, A., et al. (2019). "Superior skin cancer classification by the combination of human and artificial intelligence." European Journal of Cancer, 120, 114-121.

[61]. Höhn, J., Hekler, A., Krieghoff-Henning, E., Kather, J. N., Utikal, J. S., Meier, F., ... & Schlager, J. G. (2021). Integrating patient data into skin cancer

classification using convolutional neural networks: Systematic review. J. Med. Internet Res., 23, e20708.

[62]. Hosny, K.M., Kassem, M.A., Foaud, M.M. (2019). Classification of skin lesions using transfer learning and augmentation with Alex-net. PLoS ONE, 14, e0217293.

[63]. Huang, G., Liu, Z., Van Der Maaten, L., Weinberger, K.Q. (2017). "Densely connected convolutional networks." Proceedings of the IEEE Conference on Computer Vision and Pattern Recognition, Honolulu, HI, USA, 21–26 July 2017, pp. 4700–4708.

[64]. Jagadesh, B. N., K. Srinivasa Rao, and Ch Satyanarayana. "A unified approach for skin color segmentation using generic bivariate Pearson mixture model." International Journal of Advanced Intelligence Paradigms, vol. 15, no. 1, 2020, pp. 17-31.

[65]. Kanwal, Neel, et al. "Detection and Localization of Melanoma Skin Cancer in Histopathological Whole Slide Images." arXiv preprint arXiv:2302.03014 (2023).

[66]. Kassani, S. H., & Kassani, P. H. (2019). A comparative study of deep learning architectures on melanoma detection. Tissue Cell, 58, 76-83.

[67]. Kassem, M. A., et al. (2020). "Skin lesions classification into eight classes for ISIC 2019 using deep convolutional neural network and transfer learning." IEEE Access, 8, 114822-114832.

[68]. Kaur, Ranpreet, et al. "Melanoma classification using a novel deep convolutional neural network with dermoscopic images." Sensors 22.3 (2022): 1134.

[69]. Kollipara, VN Hemanth, and VN Durga Pavithra Kollipara. "Residual Learning Based Approach for Multi-class Classification of Skin Lesion Using Deep Convolutional Neural Network." Cognition and Recognition: 8th International Conference, ICCR 2021, Mandya, India, December 30–31, 2021, Revised Selected Papers. Cham: Springer Nature Switzerland, 2023.

[70]. Kong, J., Han, Y., & Deng, S. (2018). "Adaptive Gaussian filter guided image filter." In Neurocomputing, 275, 287-298.

[71]. Krishna, D. M., Sahu, S. K., & Srinivasa Raju, G. R. L. V. N. (2021). MLRNet: Skin Lesion Segmentation using Hybrid Gaussian Guided Filter with CNN. 2021 5th International Conference on Electronics, Communication and Aerospace Technology (ICECA).

[72]. Krizhevsky, A., Sutskever, I., & Hinton, G. E. (2012). Imagenet classification with deep convolutional neural networks. Adv. Neural Inf. Process. Syst., 25, 1097-1105.

[73]. Kumar, Amit, et al. "Augmented Intelligence enabled Deep Neural Networking (AuDNN) Framework for Skin Cancer Classification and Prediction Using Multi-Dimensional datasets on Industrial IoT Standards." Microprocessors and Microsystems (2023): 104755.

[74]. Kumar, K. Anup, and C. Vanmathi. "Optimization driven model and segmentation network for skin cancer detection." Computers and Electrical Engineering 103 (2022): 108359.

[75]. Lakshminarayanan, Arun Raj, et al. "Skin Cancer Prediction Using Machine Learning Algorithms." Artificial Intelligence and Technologies: Select Proceedings of ICRTAC-AIT 2020. Springer Singapore, 2022.

[76]. LeCun, Y., Bengio, Y., & Hinton, G. (2015). "Deep learning." Nature, 521(7553), 436-444.

[77]. Lee, S., Chu, Y., Yoo, S., Choi, S., Choe, S., Koh, S., Chung, K., Xing, L., Oh, B., Yang, S. (2020). "Augmented decision-making for acral lentiginous melanoma detection using deep convolutional neural networks." Journal of the European Academy of Dermatology and Venereology, 34, 1842–1850.

[78]. Li, Y., & Shen, L. (2017). Skin lesion analysis towards melanoma detection using deep learning network. arXiv preprint arXiv:1703.00577.

[79]. Li, Y., & Shen, L. (2018). Skin lesion analysis towards melanoma detection using deep learning network. Sensors, 18, 556.

[80]. Li, Yuexiang, and Linlin Shen. "Skin Lesion Analysis Towards Melanoma Detection Using Deep Learning Network." arXiv preprint arXiv:1703.00577, 2017.

[81]. Lipton, Z. C., Kale, D. C., Elkan, C., & Wetzel, R. (2015). "Learning to diagnose with LSTM recurrent neural networks." arXiv preprint arXiv:1511.03677.

[82]. Litjens, G., Kooi, T., Bejnordi, B. E., Setio, A. A. A., Ciompi, F., Ghafoorian, M., ... & Sánchez, C. I. (2017). "A survey on deep learning in medical image analysis." Medical Image Analysis, 42, 60-88.

[83]. Liu, Lixin, et al. "Staging of skin cancer based on hyperspectral microscopic imaging and machine learning." Biosensors 12.10 (2022): 790.

[84]. Liu, X., et al. (2019). A comparative review of deep learning-based image classification methods for skin diseases in dermatology. Journal of Healthcare Engineering, 2019.

[85]. Liu, Yi, et al. "Deep Convolutional Neural Networks for Computer-Aided Detection: CNN Architectures, Dataset Characteristics and Transfer Learning." IEEE Transactions on Medical Imaging 35, no. 5 (2016): 1285-1298.

[86]. Liu, Yi, et al. "Deep Convolutional Neural Networks for Computer-Aided Detection: CNN Architectures, Dataset Characteristics and Transfer Learning." IEEE Transactions on Medical Imaging 35, no. 5 (2016): 1285-1298.

[87]. Liu, Z., Zhang, D., & Zhang, C. (2013). A survey of content-based image retrieval with high-level semantics. Pattern Recognition, 46(2), 553-569.

[88]. Lucas, Robert M., et al. "Solar Ultraviolet Radiation and the Risk of Skin Cancer." The Journal of the American Medical Association 280, no. 17 (1998): 1439-1440.

[89]. Manoharan, S. "Early diagnosis of lung cancer with probability of malignancy calculation and automatic segmentation of lung CT scan images." Journal of Innovative Image Processing, vol. 2, no. 04, 2020, pp. 175-186.

[90]. Menegola, A., Tavares, J. M., & Traina, A. J. (2016). "Deep convolutional neural networks for melanoma classification." In 2016 29th SIBGRAPI Conference on Graphics, Patterns and Images (SIBGRAPI) (pp. 166-172). IEEE.

[91]. *Mohakud, Rasmiranjan, and Rajashree Dash. "Skin cancer image segmentation utilizing a novel EN-GWO based hyper-parameter optimized FCEDN." Journal of King Saud University-Computer and Information Sciences 34.10 (2022): 9889-9904.*

[92]. *Mukadam, Sufiyan Bashir, and Hemprasad Yashwant Patil. "Skin Cancer Classification Framework Using Enhanced Super Resolution Generative Adversarial Network and Custom Convolutional Neural Network." Applied Sciences 13.2 (2023): 1210.*

[93]. *Naeem, Ahmad, et al. "SCDNet: A Deep Learning-Based Framework for the Multiclassification of Skin Cancer Using Dermoscopy Images." Sensors 22.15 (2022): 5652.*

[94]. *Navarrete-Dechent, C., Bajaj, S., Marchetti, M. A., & Dusza, S. W. (2017). "Impact of specialized imaging on managing melanoma: A systematic review." Journal of the American Academy of Dermatology, 77(1), 49-59.*

[95]. *Nawaz, Marriam, et al. "Skin cancer detection from dermoscopic images using deep learning and fuzzy k-means clustering." Microscopy research and technique 85.1 (2022): 339-351.*

[96]. *Nezhadian, F.K., Rashidi, S. (2017). Melanoma skin cancer detection using color and new texture features. In Proceedings of the 2017 Artificial Intelligence and Signal Processing Conference (AISP), Shiraz, Iran, 25–27 October 2017; pp. 1–5.*

[97]. *Nida, Nudrat, et al. "Melanoma lesion detection and segmentation using deep region-based convolutional neural network and fuzzy C-means clustering." International Journal of Medical Informatics, vol. 124, 2019, pp. 37-48.*

[98]. *Parmar, B., & Talati, B. (2019). Automated Melanoma Types and Stages Classification for dermoscopy images. In Proceedings of the 2019 Innovations in Power and Advanced Computing Technologies (i-PACT).*

[99]. *Penn, Ilene, et al. "Skin Cancers in Transplant Recipients." Journal of the American Academy of Dermatology 60, no. 3 (2009): 249-261.*

[100]. *Rahman, Z., & Ami, A. M. (2020). A Transfer Learning Based Approach for Skin Lesion Classification from Imbalanced Data. In Proceedings of the 2020*

11th International Conference on Electrical and Computer Engineering (ICECE).

[101]. Rahmat, Romi Fadillah, et al. "Skin color segmentation using multi-color space threshold." 2016 3rd International Conference on Computer and Information Sciences (ICCOINS), IEEE, 2016.

[102]. Rajkomar, A., Oren, E., Chen, K., Dai, A. M., Hajaj, N., Hardt, M., ... & Zhang, M. W. (2018). "Scalable and accurate deep learning with electronic health records." NPJ digital medicine, 1(1), 1-10.

[103]. Rashid, Javed, et al. "Skin cancer disease detection using transfer learning technique." Applied Sciences 12.11 (2022): 5714.

[104]. Razmjooy, N., Ashourian, M., Karimifard, M., Estrela, V. V., Loschi, H. J., Do Nascimento, D., ... & Vishnevski, M. (2020). Computer-aided diagnosis of skin cancer: A review. Curr. Med. Imaging, 16, 781-793.

[105]. Rehman, A., Khan, M. A., Mehmood, Z., Saba, T., Sardaraz, M., & Rashid, M. (2020). Microscopic melanoma detection and classification: A framework of pixel-based fusion and multilevel features reduction. Microsc. Res. Tech., 83, 410-423.

[106]. Reis, Hatice Catal, et al. "InSiNet: a deep convolutional approach to skin cancer detection and segmentation." Medical & Biological Engineering & Computing (2022): 1-20.

[107]. Rezaoana, N., Hossain, M.S., Andersson, K. (2020). Detection and Classification of Skin Cancer by Using a Parallel CNN Model. In Proceedings of the 2020 IEEE International Women in Engineering (WIE) Conference on Electrical and Computer Engineering (WIECON-ECE), Bhubaneswar, India, 26–27 December 2020; pp. 380–386.

[108]. Rigel, Darrell S., et al. "Melanoma Epidemic: An Analysis of Six Decades of Data from the Connecticut Tumor Registry." Journal of Clinical Oncology 28, no. 1 (2010): 27-34.

[109]. Robinson, J. K., Wayne, J. D., Martini, M. C., & Hultgren, B. A. (2017). Mammography and dermatoscopy in the early detection of synchronous

primary breast and cutaneous melanoma: a case report and review of the literature. JAMA Dermatology, 153(5), 470-475.

[110]. Russakovsky, O., Deng, J., Su, H., Krause, J., Satheesh, S., Ma, S., Huang, Z., Karpathy, A., Khosla, A., Bernstein, M., et al. (2015). "Imagenet large scale visual recognition challenge." International Journal of Computer Vision, 115, 211–252.

[111]. Saeed, J., & Zeebaree, S. (2021). Skin lesion classification based on deep convolutional neural networks architectures. J. Appl. Sci. Technol. Trends, 2, 41-51.

[112]. Shorfuzzaman, Mohammad. "An explainable stacked ensemble of deep learning models for improved melanoma skin cancer detection." Multimedia Systems 28.4 (2022): 1309-1323.

[113]. Shorten, C., Khoshgoftaar, T.M. (2019). A survey on image data augmentation for deep learning. Journal of Big Data, 6, 1–48.

[114]. Shrivastava, V. K., Londhe, N. D., Sonawane, R. S., & Suri, J. S. (2018). "A complete automated system for the detection and classification of psoriasis disease using the textural features and stacking ensemble learning paradigm." Computers in Biology and Medicine, 96, 192-207.

[115]. Simonyan, K., Zisserman, A. (2014). "Very deep convolutional networks for large-scale image recognition." arXiv preprint arXiv:1409.1556.

[116]. Smith, J. R., & Ponce, J. (1999). Wavelet-based 3D face recognition. In Proceedings of the 1999 IEEE Computer Society Conference on Computer Vision and Pattern Recognition (CVPR'99) (Vol. 2, pp. 192-197).

[117]. Soomro, Shafiullah, et al. "Fuzzy c-means clustering-based active contour model driven by edge-scaled region information." Expert Systems with Applications, vol. 120, 2019, pp. 387-396.

[118]. Soujanya, A., and N. Nandhagopal. "Automated Skin Lesion Diagnosis and Classification Using Learning Algorithms." Intelligent Automation & Soft Computing 35.1 (2023).

[119]. Strang, G., & Nguyen, T. (1996). Wavelets and Filter Banks. Wellesley-Cambridge Press.

[120]. Sun, Q., et al. (2021). "Skin Lesion Classification Using Additional Patient Information." BioMed Research International, 2021.

[121]. Sun, Q., et al. (2021). Deep learning-based hybrid model for skin disease diagnosis. Computational Intelligence and Neuroscience, 2021.

[122]. Swetter, S. M., Layton, C. J., Johnson, T. M., & Brooks, K. R. (2017). Gender differences in melanoma awareness and detection practices between middle-aged and older men with melanoma and their female spouses. Journal of the American Academy of Dermatology, 77(4), 674-682.

[123]. Szegedy, C., Ioffe, S., Vanhoucke, V., Alemi, A.A. (2017). "Inception-v4, inception-resnet and the impact of residual connections on learning." Proceedings of the Thirty-First AAAI Conference on Artificial Intelligence, San Francisco, CA, USA, 4–9 February 2017.

[124]. Tan, Teck Yan, et al. "Adaptive melanoma diagnosis using evolving clustering, ensemble, and deep neural networks." Knowledge-Based Systems, vol. 187, 2020, p. 104807.

[125]. Thapar, Puneet, et al. "A novel hybrid deep learning approach for skin lesion segmentation and classification." Journal of Healthcare Engineering 2022 (2022).

[126]. Tschandl, P., Rosendahl, C., & Kittler, H. (2017). "The HAM10000 dataset, a large collection of multi-source dermatoscopic images of common pigmented skin lesions." Scientific Data, 4(1), 1-8.

[127]. Vocaturo, E., Perna, D., Zumpano, E. (2019). Machine learning techniques for automated melanoma detection. In Proceedings of the 2019 IEEE International Conference on Bioinformatics and Biomedicine (BIBM), San Diego, CA, USA, 18–21 November 2019; pp. 2310–2317.

[128]. Wang, X. L., et al. "Image Denoising Method Using Stationary Wavelet Transform." In 2017 7th International Conference on Environment and BioScience, 19, (2017): 52-55.

[129]. Whiteman, D. C., Whiteman, C. A., & Green, A. C. (2001). Childhood sun exposure as a risk factor for melanoma: a systematic review of epidemiologic studies. Cancer Causes & Control, 12(1), 69-82.

[130]. World Health Organization. "Cancer: Skin Cancer." WHO.int, 2021. https://www.who.int/cancer/prevention/diagnosis-screening/skin-cancer/en/.

[131]. Xie, H., et al. "Improving K-means clustering with enhanced firefly algorithms." Applied Soft Computing, vol. 84, 2019, p. 105763.

[132]. Xu, L., Zhang, L., & Jia, J. (2011). "Image smoothing via L0 gradient minimization." In ACM Transactions on Graphics (TOG), 30(6), 1-12.

[133]. Younis, H., Bhatti, M. H., & Azeem, M. (2019). Classification of skin cancer dermoscopy images using transfer learning. In Proceedings of the 2019 15th International Conference on Emerging Technologies (ICET).

[134]. Yu, C., Yang, S., Kim, W., Jung, J., Chung, K.Y., Lee, S.W., Oh, B. (2018). Acral melanoma detection using a convolutional neural network for dermoscopy images. PLoS ONE, 13, e0193321.

[135]. Yuan, Y., Chao, M., & Lo, Y. C. (2017). Automatic skin lesion segmentation with fully convolutional-deconvolutional networks. arXiv:1703.05165.

[136]. Yuan, Y., et al. "Automatic skin lesion segmentation with fully convolutional-deconvolutional networks." arXiv: 1703.05165, 2017.

[137]. Zhou, Yufei, et al. "Multi-site cross-organ calibrated deep learning (MuSClD): Automated diagnosis of non-melanoma skin cancer." Medical Image Analysis 84 (2023): 102702.

[138]. Zortea, Maciel, Eliezer Flores, and Jacob Scharcanski. "A simple weighted thresholding method for the segmentation of pigmented skin lesions in macroscopic images." Pattern Recognition, vol. 64, 2017, pp. 92-104.

[139]. Zou, J., Ma, X., Zhong, C., & Zhang, Y. (2018). Dermoscopic image analysis for ISIC challenge. arXivPrepr arXiv:180708948.

[140]. Zunair, H., & Hamza, A. B. (2020). Melanoma detection using adversarial training and deep transfer learning. Phys. Med. Biol., 65, 135005.